The electrical and optical properties of zinc selenide

G. Jones

THE ELECTRICAL AND OPTICAL PROPERTIES OF ZINC SELENIDE

BY

G. JONES, B.Sc.

Presented in Candidature for the Degree of

Doctor of Philosophy in the University of Durham

September 1973

ACKNOWLEDGMENTS

I would like to express my gratitude to my supervisor Dr. J. Woods for his guidance and assistance during the course of the research project. I would also like to thank Professor D.A. Wright for allowing me the use of the laboratory facilities and the S.R.C. for the award of a grant. The help and advice, both technical and otherwise, of the workshop staff headed by Mr. F. Spence are acknowledged as are the interesting and useful discussions with other members of the research group especially Dr. A.N. Rushby, Dr. J.I.B. Wilson and Mr. J.R. Cutter who is also thanked for growing suitable crystals of zinc selenide. Thanks are also due to Mrs. A. Palmer and Mrs. J. Nichols for their patience and care whilst typing the thesis, and Miss C. Guyll for her help with the diagrams.

Last but by no means least I would like to express my gratitude to my parents for their many sacrifices over the years and their constant encouragement.

ABSTRACT

Zinc selenide is a II - VI compound semiconductor with a wide band-gap of 2.67 eV at room temperature, and is therefore capable of emitting visible luminescence. The main purpose of the research reported in this thesis was to study zinc selenide crystals grown in the department with the aim of developing a suitable material for the manufacture of red-emitting electroluminescent diodes. It is hoped that these will eventually be cheaper and easier to produce than gallium arsenide-phosphide devices.

The most satisfactory means of reducing the resistivity of zinc selenide to values consistent with its use as a device (approx. 1 ohm cm.) was to heat nominally undoped crystals in molten zinc. Measurements of the Hall voltage and conductivity over the range 15°K to 400°K revealed a shallow donor level (Ed = 0.012 eV) thought to be associated with unremoved trace impurities of chlorine.

Manganese was introduced into several crystals to provide an efficient luminescent centre. The characteristic manganese emission band at 85°K was found to lie at 5870 Å with a halfwidth of 0.13 eV. Under 3650 Å excitation, however, the manganese emission was swamped by a band at 6400 Å attributed to copper contamination, and a broad band at 6150 Å which appeared to be the self-activated emission of zinc selenide. The manganese emission could be isolated when crystals were excited in one of the two characteristic excitation bands (5040 Å and 5370 Å). A smaller excitation band was also observed at 4660 Å.

All samples, including those containing manganese, heated in zinc to reduce their resistivity, were found to emit the self-activated band only, thought to be the result of chlorine impurity. An Auger process was assumed to account for the disappearance in semiconducting samples of the manganese emission under photoexcitation and yet explain its appearance in the emission from electroluminescent diodes containing manganese.

CONTENTS.

CHAPTER 1

LUMINESCENT PROPERTIES OF THE II - VI COMPOUNDS

1.1 INTRODUCTION

When an electron is excited to a higher energy state in a solid, it can return to its original state by emitting the excess energy in a variety of ways. For example, the energy can be released in the form of phonons or can be used to promote a photochemical change. The energy can also be released in the form of photons, in which case the process is known as luminescence. The term luminescence is confined to radiation within the visible region and is used to describe the emission of all radiation which is not purely thermal in origin, such as incandescence.

Electronic excitation can be achieved in a variety of ways. If high energy particles are responsible for the emission the process is known as cathodoluminescence or radioluminescence. If the process is the result of an applied electric field, either D.C. or A.C., electroluminescence is the appropriate term. Triboluminescenee can occur when a material is subjected to mechanical forces such as scraping or grinding, and chemiluminescence and bioluminescence occur as a result of certain chemical reactions. However, the process with which we shall be mainly concerned in this thesis is photoluminescence. This occurs when the excitation energy is supplied by means of incident photons which can be of various energies ranging from X-rays to infra-red radiation.

Luminescence is usually divided into two broad classes. These are fluorescence and phosphorescence. The main distinction is concerned

with the respective decay rates. Fluorescence is usually associated with decay times of the order of 10^{-8} seconds and phosphorescence with times of several seconds. For intermediate times, however, the distinction is not clear cut and the temperature variation of the decay times must be taken into account.

1.2 EDGE EMISSION

Luminescent emission in compound semiconductors is usually divided into two categories, namely edge emission and deep centre emission. Edge or Ewles Kröger emission (J. Ewles 1938, F. A. Kröger 1940) is the term used to describe the luminescent emission associated with transitions with energy very close to that of the bandgap of the material. Normally such emission is quenched in materials to which activator type impurities have been added to produce deep centre emission (see later). Although edge emission can be observed in most II - VI compounds at $77^{o}K$ it is really necessary to make measurements over a range of temperatures down to liquid helium temperatures in order to obtain useful information.

Hitherto the most extensive studies of edge emission have been made on cadmium sulphide. A typical emission spectrum is shown in figure 1.1, (C. C. Klick 1953). The emission consists of a series of very narrow bands with widths at half height of approximately 0·005 eV. The bands are equally spaced in energy and decrease in intensity and increase in width towards longer wavelengths. There are two series of bands, one at high energy and one at slightly lower energy. This latter series appears as the temperature is lowered towards $4{\cdot}2^{o}K$. Pedrotti and Reynolds (1960) suggested that the most intense peak at $4{\cdot}2^{o}K$ was associated with recombination between an electron bound at a very shallow donor level, E_d = 0·02 eV, and a hole at a neighbouring acceptor level some 0·14 eV above the valence band. This pair recombination model has

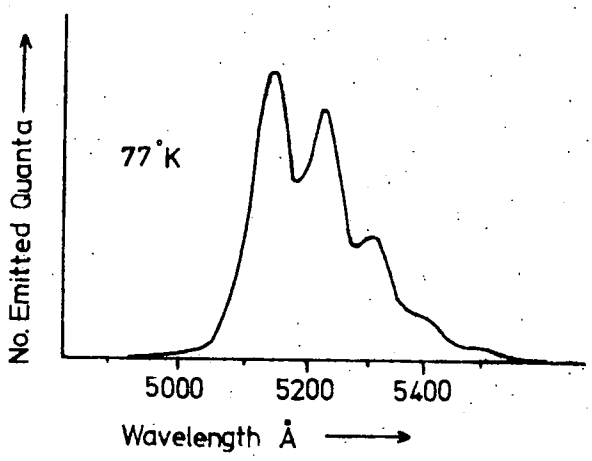

(a).

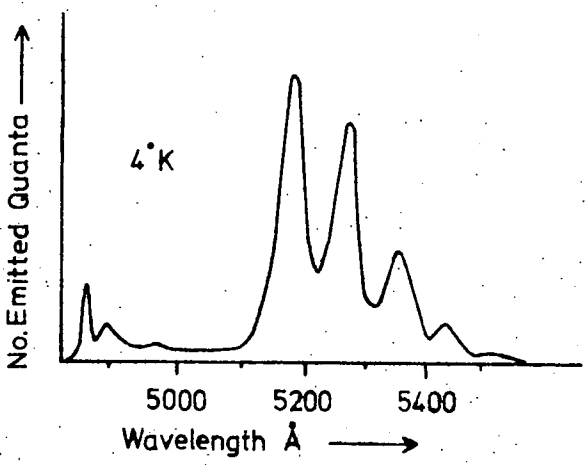

(b).

Fig.1-1. Edge Emission Spectrum of CdS. (C.C.Klick 1953)

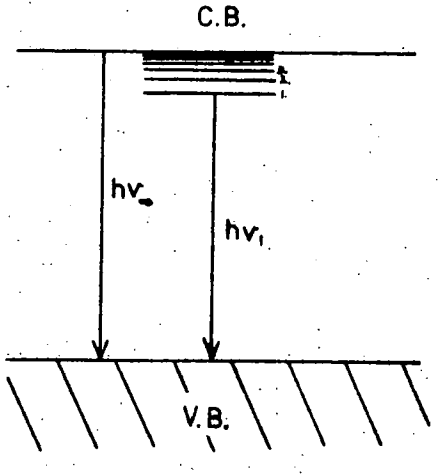

Fig.1-2. Model for Exciton Emission.

since been well established and lines resulting from the recombination of individual pairs have been observed (Henry et al 1969). More will be said about this associated pair model later. As the temperature is raised the high energy series begins to appear (figure 1.1a). This occurs when the donor levels are emptied and the dominant emission results from recombination between free electrons and trapped holes.

The narrow bands in each series are found to be separated by energies equal to those of the longitudinal optical phonon (0·038 eV) so that, with the exception of the zero order band, each band is associated with phonon co-operation and the radiative transition is accompanied by the release of one or more phonons to the lattice. The bands which are members of such a series are known as phonon replicas. Replicas have also been observed at energy separations corresponding to those of transverse optical phonons.

With cadmium sulphide there is still no agreement as to the atomic configuration of the donor centre involved, though sulphur interstitials are thought to play some part in the process (Kulp and Kelley 1960).

1.3 EXCITON EMISSION

The emission spectrum shown in figure 1.1b which was measured at 4·2°K exhibits a further series of very sharp lines which appear on the higher energy side of the edge emission but just below the bandgap energy. The series of lines is hydrogen like and is attributed to exciton recombination. An exciton can be considered to be an electron-hole pair, bound together in a similar manner to components of the hydrogen atom. The allowed energies of free excitons can be represented by a set of levels with a series limit which coincides with the bottom of the conduction band (figure 1.2). The emission energies are given by

$$h\nu_n = h\nu_\infty - \frac{R}{K^2} \cdot \frac{\mu}{m} \cdot \frac{1}{n^2}$$

where μ is the reduced mass of an exciton, K is the dielectric constant of the material, R is the Rydberg constant, m is the free electron mass and $h\nu_\infty \equiv E_g$ the bandgap of the material.

If the valence band of the material is split, as it is for example with the hexagonal II - VI compounds such as cadmium sulphide and cadmium selenide, several series might be expected corresponding to transitions to each branch of the valence band. The reverse transitions have been observed in absorption measurements, for example on zinc selenide (Liang and Yoffe 1967 b).

An exciton can exist either as a free entity or bound to a native defect or impurity level. Bound excitons emit light of lower energy upon recombination, the difference of about 0·01 eV being equal to the binding energy of the free exciton to the defect. Since free excitons are mobile with a range of kinetic energies, the associated emission bands have a half width of approximately 10^{-3} eV, ten times wider than those associated with bound excitons. As the temperature is raised above liquid helium temperatures, free exciton emission tends to dominate as the bound excitons are thermally freed.

It has been suggested that there are four different types of bound exciton in cadmium sulphide which give rise to emission lines known as the I_1, I_2, I_3 and I_4 lines. They correspond respectively to excitons bound to neutral acceptors and donors, and ionized donors and acceptors. However, an I_4 line has not yet been observed. Study of the energy separations of the I_2 series of lines can provide information concerning the donor ionization energies of certain impurities.

1.4 DEEP CENTRE EMISSION

Nearly all phosphors which find practical applications are made luminescent, that is activated, by the addition of certain impurities.

With different impurities phosphors can be prepared to emit light covering a wide range of wavelengths extending from the edge emission region to the infra red. The addition of impurities can also be used to control other properties such as the efficiency, decay rate and long term stability. The emission from II - VI compounds associated with particular impurities or activators is known as deep centre luminescence. It usually consists of broad bands approximately Gaussian in shape with half widths of the order of 0·3 eV.

Models are used in order to simplify the processes occurring in phosphors and we shall now consider those models which can be applied in the case of non-localized transitions.

1.5 NON-LOCALIZED TRANSITIONS

In the majority of phosphors, luminescent emission is accompanied by photoconductivity. This shows that the electron transitions involve the conduction or valence bands of the phosphor as well as the luminescent centre itself. This interaction allows energy to be transferred from point to point in the crystal and the luminescent centre need not be anywhere near the point in space at which the electron is first excited. Other discrete levels within the energy gap such as trapping levels are also involved together with levels associated with native defects which add considerable complexity to the processes involved.

The impurities which produce luminescent emission are known as activators and co-activators. In the II - VI compounds typical activators are copper, silver and gold substituted for the metal atoms. Co-activators can be either elements from group VII such as chlorine or bromine substituting for the group VI atoms, or group III atoms such as aluminium, gallium and indium on group II sites. In most II - VI compounds the name activator is a synonym for acceptor and similarly a co-activator is simply a donor.

The first phosphor to be studied in any great detail was zinc sulphide. It is found that after zinc sulphide powder is heated to about 1000°C with copper and sodium chloride, a bright green luminescence band near 5200 Å is produced. If silver is used instead of copper a blue band near 4400 Å is produced. It was realised that the sodium chloride not only acts as a flux during the firing, but also provides the chlorine ions which are incorporated into the lattice of the zinc sulphide. The function of the coactivator is to ensure charge neutrality. Every Cu^{+} ion on a Zn^{++} site is compensated by the net positive charge of a Cl^{-} ion on a S^{--} site (Kröger and Hellingman 1949). This is further illustrated by the fact that group III elements such as Al^{+++} substituted for the Zn^{++} can be used to provide the excess positive charge (Kröger and Dikhoff 1950). The colour of the resultant luminescence is found to depend mainly on the activator present. If zinc sulphide is fired in the presence of a coactivator only, a blue band near 4600 Å, known as self-activated emission, is produced. Charge neutrality is still maintained and the required negative charge is produced by the formation of zinc vacancies (Prener and Williams 1956 b). Self-coactivated emission is also possible where an activator is compensated by the formation of anion vacancies.

1.6 MODELS FOR NON-LOCALISED TRANSITIONS

Three models have been used as a basis for interpreting non-localised luminescent transitions. These are illustrated in figure 1.1. The Schön-Klasens model was first proposed in 1942 (M. Schön 1942) and elaborated (H. A. Klasens 1953). The initial excitation produces a free electron and a free hole. The Schön-Klasens model assumes that the hole becomes trapped at a localised level above the valence band and the emission is a result of a free electron recombining with the hole at this centre (figure 1.3A).

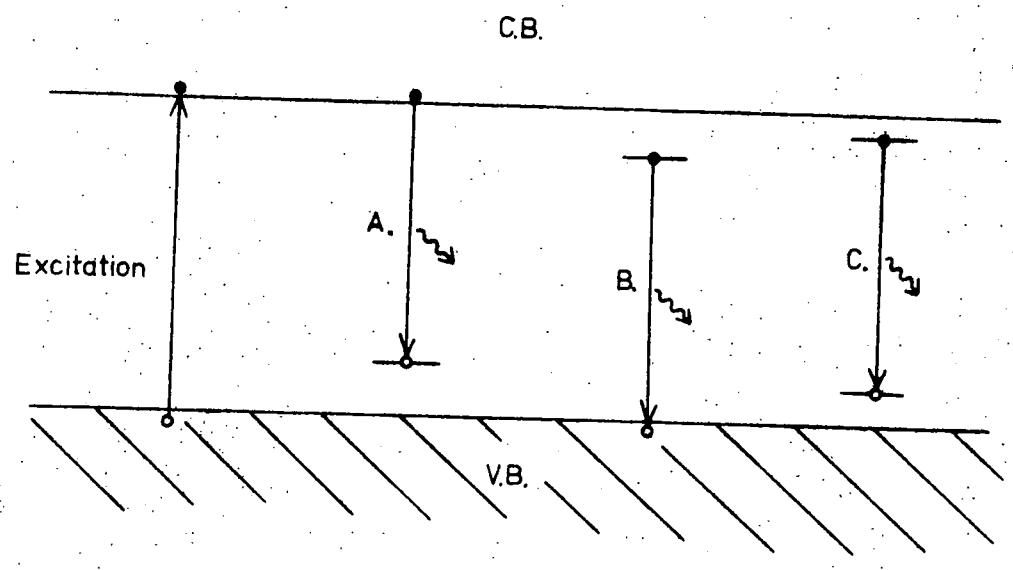

Fig.1-3. Models for Non-Localized Emission Processes.

A. — Schön-Klasens.

B. — Lambe-Klick.

C. — Prener-Williams.

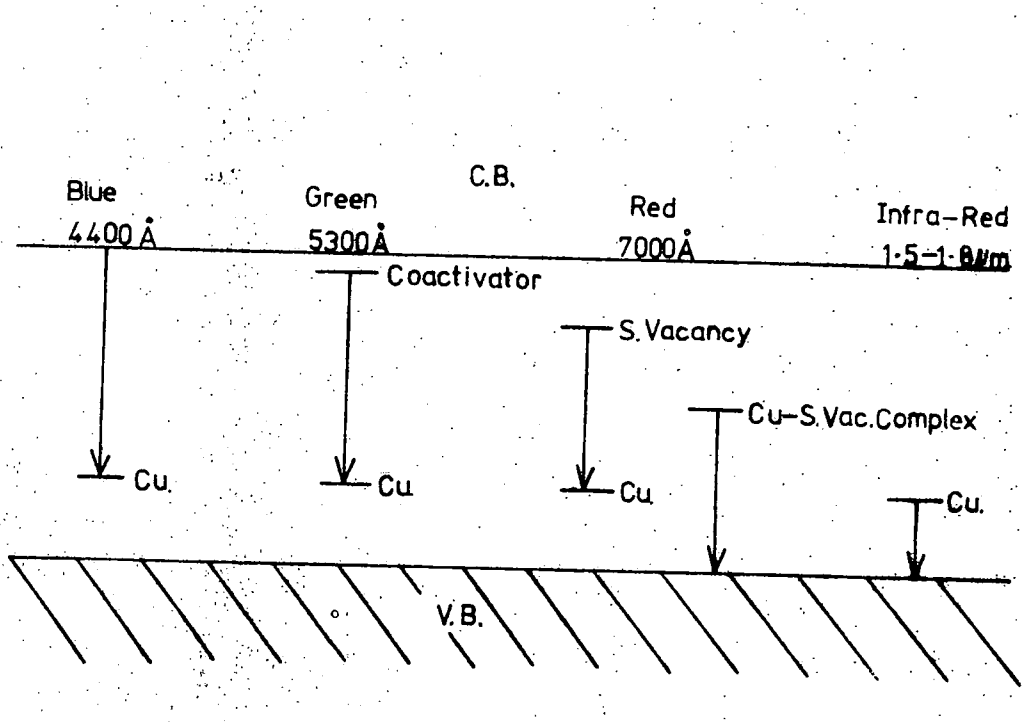

Fig.1-4. Some Models used to explain Emission Processes in ZnS at 77°K.

Lambe and Klick (1955) proposed the model illustrated in figure 1.3B. In this scheme, the free electron is trapped at a level below the conduction band. A free hole then recombines at this level to produce the emission. This model was found necessary to account for the fact that the decay time of photoconductivity in certain materials was greater than the luminescence decay time (Lambe 1955).

Prener and Williams (1956 a) introduced a third model. They considered the emission to result from the recombination of electrons and holes trapped at localised centres in the same region of the lattice (figure 1.3C). This associated pair recombination was first observed in gallium phosphide (Hopfield et al 1963). Fine structure was resolved corresponding to transitions between centres up to 30 Å apart. The low energy edge emission series which occurs in cadmium sulphide and other II - VI compounds can also be explained using this model. Pair recombination can be identified by means of time resolved spectroscopy. In this process the emission spectrum is scanned as it decays and any shift towards lower energy with time suggests pair recombination. This is because more distant pairs take longer to recombine and emit less energetic photons upon recombination.

These three models, with suitable modifications, have been used to describe most of the emission observed in II - VI compounds but with most luminescent systems there is still insufficient evidence unambiguously to assign specific transitions to particular bands and defect levels.

1.7 APPLICATION OF THE MODELS TO ZINC SULPHIDE

In order to illustrate the applications of the three models we shall consider their use with zinc sulphide, partly because zinc sulphide has been studied more extensively than any other II - VI phosphor and also because many of the results are, or should be, of direct relevance to similar luminescent processes in zinc selenide. However, it

will be demonstrated that there is still little unanimity of opinion as to the exact nature of many of the luminescent transitions in zinc sulphide and further work is still necessary to clarify the situation.

When the copper is used as the activator in zinc sulphide, four main emission bands are observed at 77°K. Some of the models which have been used to explain these bands are depicted in figure 1.4.

(a) Copper Blue and Green Emissions

Firstly we shall consider the copper blue and green emissions which are the most distinct and common. At 85°K the blue band is found to have its maximum at some wavelength between 4300 Å and 4440 Å whereas the green has its maximum at a value between 5160 Å and 5250 Å. The actual values depend on whether a group III or group VII coactivator is used. In addition reported values vary from worker to worker. Possible explanations for the lack of agreement on the actual positions of the emission bands are (1) the observed bands may be a superposition of a number of sub-bands or (2) different samples may contain different imperfections within the lattice, such as stacking faults and polytypes, which may alter the detailed band structure of the material. The maxima of both the blue and green copper bands shift towards longer wavelengths on raising the temperature from 77°K to 300°K, the blue by about 30 Å and the green by about 100 Å.

It is found that the green emission dominates when approximately equal amounts of coactivator and activator are present. As the copper concentration is increased, the blue band becomes more pronounced. The green band is sometimes attributed to a Prener-Williams transition between an electron in a coactivator centre and a hole localised at an associated copper centre (G. and D. Curie 1960). This interpretation is supported by measurements of the time resolved spectrum (Shionoya et al 1966). The dependence of the position of the emission peak on

the nature of the coactivator can probably be explained using the model proposed by Prener and Weil (1959) to explain the similar effect on the self-activated band (see later). The blue emission has been considered to result from a Schön-Klasens transition to the same copper level associated with the green band (G. and D. Curie 1960).

Both bands have also been described in terms of Schön-Klasens transitions to different ionization states of the copper centre (Broser and Schulz 1961).

The blue emission has even been attributed to a Lambe-Klick transition although this is unlikely (Birman 1960).

As can be seen, the actual defects and the transitions responsible for the copper green and blue luminescence are still not definitely known after over twenty years of serious study.

(b) Copper Red Emission

Zinc sulphide containing copper also exhibits emission in the red region of the spectrum, which consists of a band with its maximum at 6970 Å at 77°K. In contrast to the blue and green emissions, this band shifts to shorter wavelengths on heating. The emission peak is located at 6740 Å at room temperature. The red emission is usually observed only when the activator to coactivator ratio is extremely high. Shionoya et al (1962) proposed that the emission was due to a localised transition of the Prener-Williams type between a sulphur vacancy and an associated acceptor level due to the copper. However, E.S.R. experiments by Dieleman et al (1964) tend to show that the copper atom and the vacancy act as a complex producing a level below the conduction band, in which case the emission would be associated with a Lambe-Klick type transition. Which of these two mechanisms is correct is still undecided.

(c) Copper Infra-Red Emission

The infra-red luminescence of zinc sulphide is enhanced when copper is incorporated and consists of two main bands located at around 1·46 μm and 1·65 μm at 77°K. There is an additional smaller band at about 1·8 μm. The whole emission is enhanced when the phosphor is prepared under excess sulphur pressure which is thought to reduce the concentration of sulphur vacancies leaving the copper in an uncompensated state. This view is supported by measurements on phosphors containing radioactive ^{65}Zn which slowly decays to ^{65}Cu whereupon the infra-red emission gradually rises (Broser and Franke 1965). Several suggestions have been made to explain the two major peaks. Broser and Schulz (1961) associated them with Lambe-Klick transitions involving the ground and excited states of a hole bound to the copper impurity. Ullman and Dropkin (1961) showed that the excitation responsible for the infra-red emission produced hole photoconductivity, thus supporting this view. A similar model involving transitions from a single copper level to a split valence band was suggested by Bryant and Cox (1965). A completely different mechanism was suggested by Birman (1961) who attributed the emission to internal transitions between the energy levels within the copper ion which result from crystal field and spin orbit splitting. In fact the emission may be due to a combination of internal and free electron transitions.

(d) Self-Activated Emission

So far we have considered zinc sulphide to which an activator, namely copper, has been added. If, however, zinc sulphide is simply fired so as to introduce a coactivator such as chlorine or aluminium, a blue luminescence band with its peak between 4710 Å and 4560 Å at 77°K is produced. The actual value depends on the coactivator group used. The band is very near to the copper blue emission but it can

be easily distinguished since it is found to shift to shorter wavelengths on heating, unlike the copper blue which moves to longer wavelengths. Kröger and Vink (1954) suggested that the centre consisted of a zinc vacancy whose surroundings had lost one electron, to compensate for the coactivator present. A different model had to be proposed however because Bowers and Melamed (1955) failed to observe any paramagnetic resonance. Prener and Williams (1956 b) therefore suggested that a coactivator-vacancy complex was responsible for the ground state of a Schön-Klasens transition. Prener and Weil (1959) showed that a zinc vacancy was involved and also explained the variation in peak position with coactivator group. This variation was considered a function of the different lattice sites at which the two types of atom (group III and group VII) substituted.

E.S.R. measurements on S.A. zinc sulphide have identified a centre which, due to the presence of a trapped hole, becomes paramagnetic when photoexcited. This centre, known as the A-centre, consists of a zinc vacancy associated with the coactivator impurity (Schneider 1965) and appears to be the centre also responsible for the S.A. emission.

The shift in peak position with temperature has been explained in terms of an increasing dissociation of the complex as the temperature is raised. This would lead to increasing transitions from the conduction band to the isolated zinc vacancies.

Clearly the mechanisms used to explain the self-activated emission are very similar to those used to discuss the copper red luminescence, and in fact the latter is sometimes known as the self-coactivated band. Both emission processes can be treated to some extent in terms of the configurational coordinate model which is described later.

1.8 LOCALISED TRANSITIONS

When an impurity such as a transition element or a rare earth

ion is introduced into a II - VI compound, the impurity emission and absorption processes are associated entirely with electronic transitions within the atomic shell of that ion. The crystal lattice plays a relatively unimportant part in the process. The excited electron does not interact with any free electrons or holes and the band structure of the material can be completely ignored. The host lattice, however, affects the transitions via phonon interactions and crystal field splitting of the energy levels of the free ion.

It is very difficult to interpret the broadening and shape of the emission and absorption bands of deep centre luminescence of the type described in the previous section. The shape, width and Stokes shift, that is the fact that the emission usually occurs at lower energy than the excitation, all depend on the interaction of the electronic state of the luminescent centre with localised and non-localised phonons. To take one extreme, for a very shallow donor with a binding energy of 0·01 eV the electron orbital can be considered to extend over many interatomic spacings and only the host lattice phonons will have any effect. However, in the case of deeper levels, which the majority of important activators produce, the electron is fairly localised and tends to interact with several localised phonon modes as well as the lattice. Since these can have widely differing frequencies the matter is severely complicated and no suitable theories have yet been suggested. In the other extreme however, when the electron can be considered to be tightly bound to the centre, as is the case we are now about to consider, it can be assumed that only the localised modes interact. Usually it is assumed that only one type of phonon is involved. This means that the form of the emission and absorption bands can be quite well predicted by means of the configurational coordinate model. Although it has been extended to cover more than one interacting mode, the equations which then result contain so many adjustable parameters that tney are of limited use.

1.9 CONFIGURATIONAL COORDINATE MODEL

The configurational coordinate model was first suggested by Seitz (1939) and has since been modified and improved (F. E. Williams 1953, C.C. Klick 1952). It is a very useful tool for the analysis of absorption and emission bands in localised electronic transitions. A typical configurational coordinate diagram is shown in figure 1.5. Plotted vertically is the potential energy of the system near the impurity ion for the electron in the ground and excited states of the centre, taking into account both electronic and vibrational energy. This is plotted against the configurational coordinate r, which is a parameter specifying the configuration of the ions around the centre. In a diffuse centre the configurational coordinate could specify the positions of a large number of ions around the centre, whereas in the case of a centre with a wave function not extending very far, it might only describe the positions of nearest neighbour ions. For the thallium ion in potassium chloride, for example, the configurational coordinate is simply the displacement in Angstrom units of the Cl^- ions surrounding the thallium ion.

The configurational coordinate curve is assumed to be parabolic, following a classical harmonic oscillation, the frequency of the simple harmonic motion being the same as the phonon frequency ν. In the simplest case the vibration is associated with a breathing mode in which the surrounding ions vibrate radially in phase. According to classical theories, the width of an emission band should be proportional to the square root of the temperature, and at absolute zero the emission band should have zero width. In order to explain the finite width of the bands at absolute zero, quantum mechanical concepts are introduced including a zero point energy of $\frac{1}{2} h\nu$. Allowed energies are thus quantized as shown in figure 1.5.

To help understand the emission and absorption processes we shall

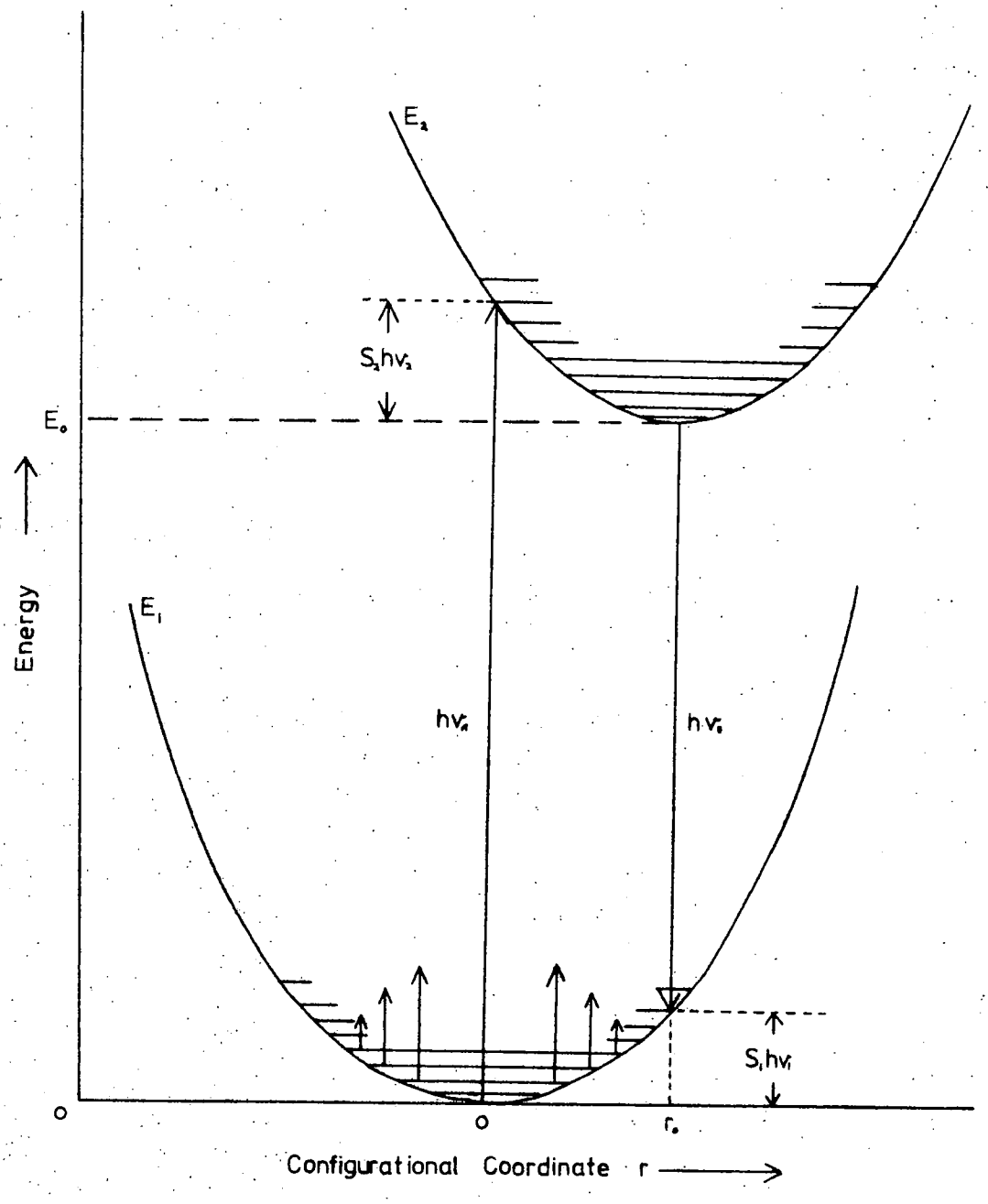

Fig.1-5. A typical Configurational Coordinate Diagram.

use figure 1.5. The electron is initially in its ground state and the combined energy of the electron and vibrating ions is represented by the parabola E_1. The Franck-Condon principle is assumed to hold. This states that an optical transition can occur in a much shorter time than the lattice takes to respond to the change in charge distribution. In other words the absorption of energy and the electron transition can be represented by a vertical line on the configurational coordinate diagram. After the transition the system gradually reverts to its thermal equilibrium position, E_0, in the excited state by interacting with and emitting a number, S_2, of localised phonons of energy $h\nu_2$. In this situation the energy of the system is given by the curve E_2, the minimum of which is usually displaced from 0, the direction depending on the relative movement of the surrounding ions, on excitation. Emission can be represented by a vertical transition which is accompanied by the emission of a photon with energy $h\nu_E$. On reaching the ground state, the ions again revert to their equilibrium positions dissipating their excess energy as S_1 phonons, this time with energy $h\nu_1$. The system then reverts to its equilibrium position 0. S is usually of the order of 40 and the phonon energy is around 0·015 eV. The distance r_o is some representation of the displacement of the surrounding ions produced when the electron is raised to its excited state.

This representation of the emission and absorption processes shows that the emitted energy $h\nu_E$ is always less than the excitation energy $h\nu_A$ because of phonon interaction, thus illustrating Stokes law more clearly than with non-localised transitions. With the latter transitions the energy levels within the forbidden gap are raised in energy in a polar solid when an electron is removed from the centre. Thus when an electron is excited from a centre, the associated energy level is raised and on recombination the energy emitted is less, the excess being emitted as lattice phonons in a similar manner to the localised case.

As the temperature is raised, the amplitude of vibration increases leading to a much wider range of coordinates and hence a wider variation in energy. This means that transitions can occur from either side of the point of minimum energy 0. The distribution of luminescent centres with respect to energy is determined by Maxwell Boltzmann statistics and therefore forms a Gaussian distribution with a maximum number at 0. If E_2 can be considered linear over the range of coordinates involved, the excitation band itself will be Gaussian. If, however, the minima are close together, that is there is little effect on the surrounding ions upon excitation, the resultant band will be distorted towards higher or lower energy. This model applies equally to the emission process. It can therefore be seen that the symmetry of the absorption and emission bands is related to the Stokes shift.

Since the energy of the system is quantized, the emission and absorption bands will consist of a number of discrete lines each associated with a transition between individual levels. Each line will be broadened by Stark field effects and interaction with lattice and localised phonons ignored by the model. The sharp lines making up these broad bands are analogous to the phonon replicas seen in edge emission except that in this case the phonons concerned are localised. The individual lines cannot usually be resolved but at very low temperatures, when the number of lattice and localised phonons is reduced, several lines may be seen. The most intense line normally, is known as the zero phonon line. This appears around liquid helium temperatures when the excitation and emission take place between the zero point energy levels in the excited and ground states. The energies of emission and excitation are therefore the same and this results in the appearance of the zero phonon line at the same energy in both absorption and emission. Lines sometimes also occur at higher absorption energies and lower emission energies at intervals corresponding to the energies of lattice optical and acoustic phonons and of localised phonons.

Using quantum mechanical considerations, the width of the emission band at half height can be calculated and is

$$W_T = Wo \left[\coth \frac{h\nu_2}{2kT} \right]^{\frac{1}{2}} \qquad (1.1)$$

A similar expression is obtained for the width of the absorption band with ν_2 replaced by ν_1.

In equation (1.1) Wo is the width at half height at absolute zero. This is still finite since the system will still possess zero point energy. At low temperatures, when the system has relaxed to the zero point energy, the half width according to equation (1.1) becomes independent of temperature. At high temperatures when $2kT_1 \gg h\nu_2$ the system reverts to the classical approximation and $W_T \propto T^{\frac{1}{2}}$. By measuring the change in half width as a function of temperature it becomes possible to obtain a value for the phonon frequency .

Normally a configurational coordinate diagram is built up from empirical results, for example the temperature variation of half width, the positions of the absorption and emission maxima and the Stokes shift. Then from this configurational coordinate curve, predictions can be made as to other properties of the centre. However, the configurational coordinate curve has been calculated theoretically for the thallium centre in potassium chloride (F. E. Williams 1951). The resulting curve has been used to predict the observed luminescent properties to a reasonable degree of accuracy. Williams considered both the six nearest neighbouring chlorine ions to the thallium ion and the six nearest potassium ions. He then calculated the energy of the system taking into account the energy due to electrostatic, Van der Waals and exchange interactions between the ions when the electron was in its ground and excited states. Although the treatment was necessarily simplified, its predictions were found to be reasonably accurate.

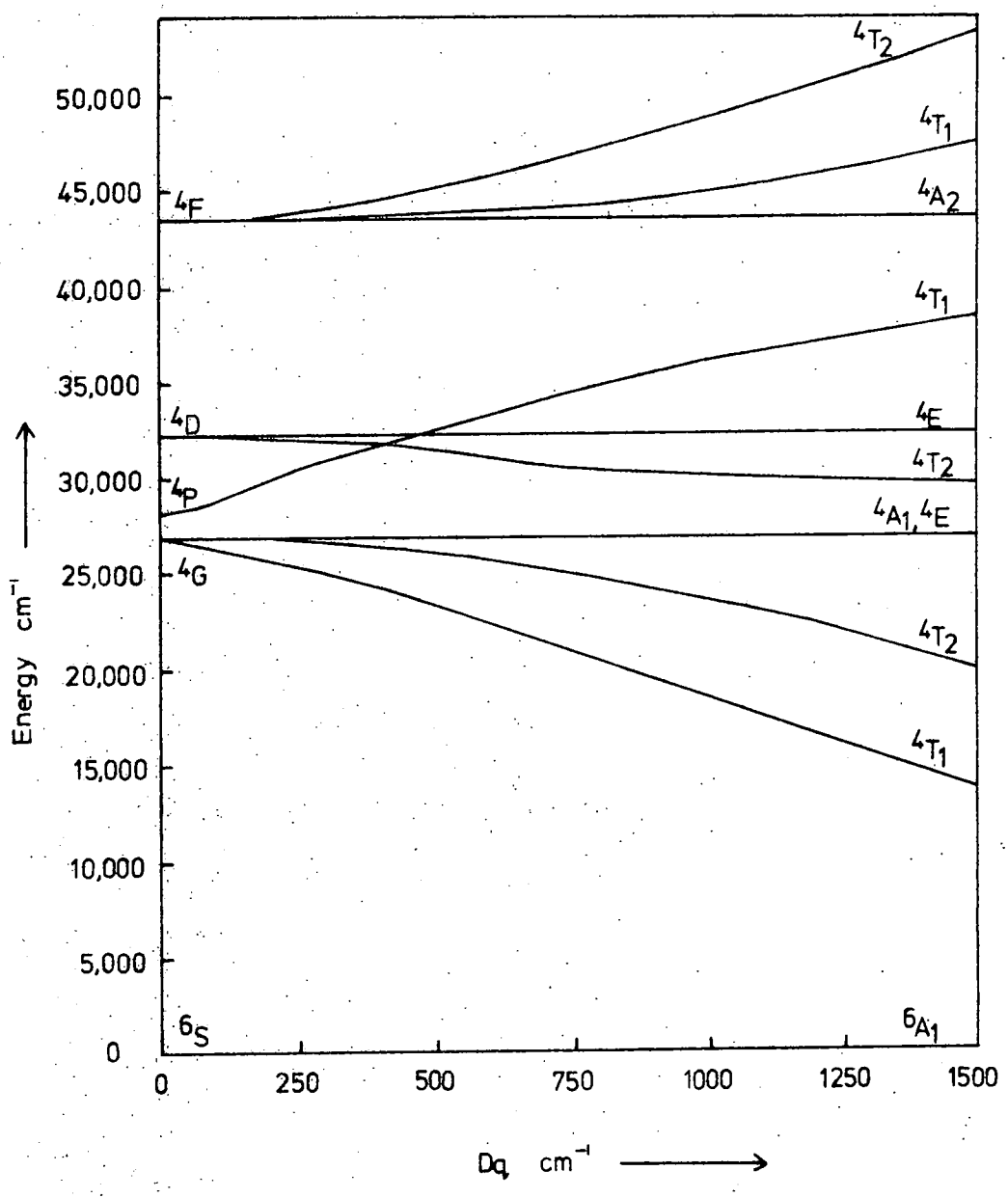

Fig. 1-6. Energy Level Diagram of the Mn^{++} Ion in a Cubic Field relative to the $^6A_1(^6S)$ Ground State as calculated by Orgel (1955).

This model is useful only when the transitions involved are highly localised, and hence it applies to situations where the transitions take place within the impurity atoms themselves. In rare earth atoms such as holmium and thulium, for example, the 4f shell is only partly filled and it is possible for the electron to be excited within this shell. Since the shell lies deep within the atom, there is very little influence from phonons and the emission tends to consist of fairly sharp lines.

Another class of luminescence activators which behave similarly to the rare earths are the transition elements such as vanadium, iron, cobalt, nickel and manganese. However, since the electron transitions in these ions take place in the outermost 3d shell, phonon interaction is more important and as a result the emission bands are broader. So far most effort has been concentrated on manganese which is an effective activator in numerous phosphor systems and is responsible for an efficient orange luminescence in zinc sulphide. In the ground state, ^6S of the Mn^{++} ion, the five 3d electrons are aligned with their spins parallel. On excitation one electron spin is reversed, giving rise to a five fold degenerate level, which is split by spin orbit interaction into the ^4G, ^4P, ^4D, ^4F and ^4S levels, in order of increasing energy. The ^4S level lies approximately 7·2 eV above the ^6S level and is therefore too high to be involved in most optical transitions. Crystal field effects split these levels even further to produce the levels involved in the luminescent transitions. The situation resulting from a cubic field is illustrated in figure 1.6, (Orgel 1955). The observed emission results from the transition from the $4T_1$ (4G) excited state to the $^6A_1$ (^6S) ground state. In most manganese activated phosphors the emitted light is in the yellow to orange spectral region although willemite, because of a different interaction with the crystal field, emits in the green (Vlam 1949). The absorption and emission bands in manganese activated zinc sulphide are illustrated in figures 1.7 and 1.8 (McClure 1963, Langer and Ibuki 1965).

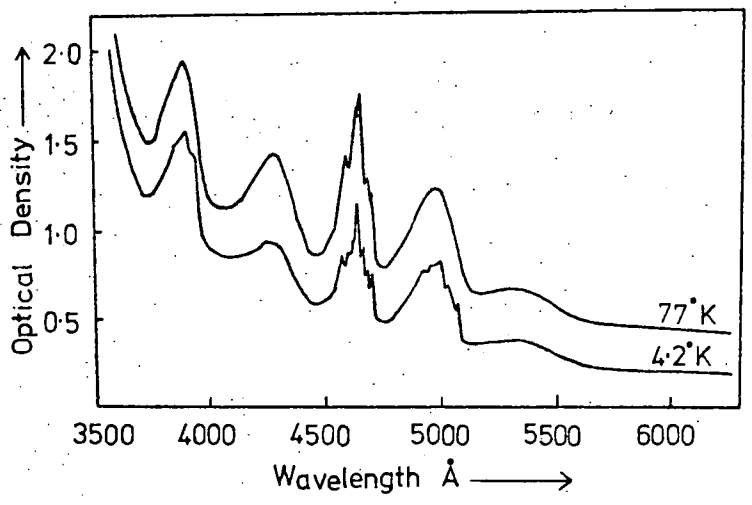

Fig. 1-7. Absorption Spectrum of a ZnS:MnS(4%) mixed Crystal.
(McClure, 1963)

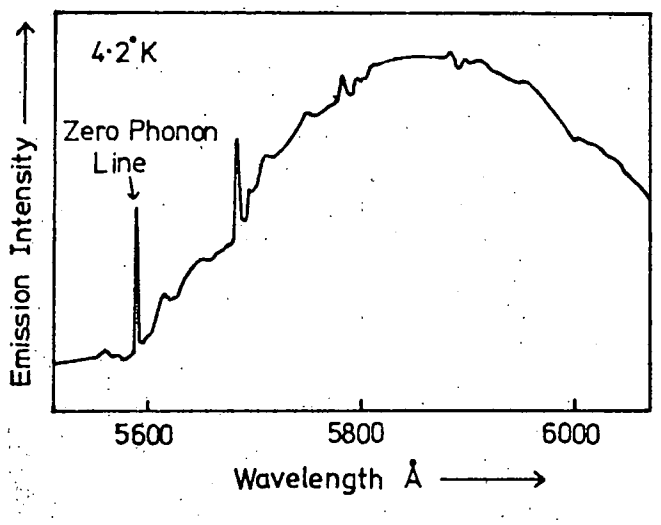

Fig. 1-8. Emission Spectrum of ZnS:Mn. (Langer and Ibuki, 1965)

Although many of the properties of these luminescent activators such as Mn^{++} are well known and the emission and absorption bands are easily explained, the actual locations of the energy levels of the ions with respect to the band edges of the host materials are very difficult to determine and generally not known.

1.10 THERMAL QUENCHING

The luminescent efficiency of a phosphor is found to remain fairly constant as the temperature is raised until a certain temperature is reached at which the efficiency begins to fall exponentially. This process is known as thermal quenching. It is caused by an increase in non-radiative recombination processes which are more temperature dependent than the radiative processes.

With zinc sulphide type phosphors the process is usually interpreted using the model shown in figure 1.9. If the luminescent transition is of the Schön-Klasens type as in A, at sufficiently high temperatures an electron can be excited from the valence band to fill the empty state of the luminescent centre. The excited electron in the conduction band cannot therefore recombine via this centre. The electron will thus migrate until it can recombine via a non-radiative centre. As the temperature is raised further, more centres are filled and the luminescence decreases correspondingly. The luminescence efficiency varies with T as

$$\eta = \frac{1}{1 + C \exp\left(-\frac{w}{kT}\right)} \qquad (1.2)$$

where C is a constant and w is the energy required to excite an electron from the valence band to the luminescence centre. Similarly, with a Lambe-Klick transition, 1.9B, the electron can be excited thermally from the luminescence centre to the conduction band before it has

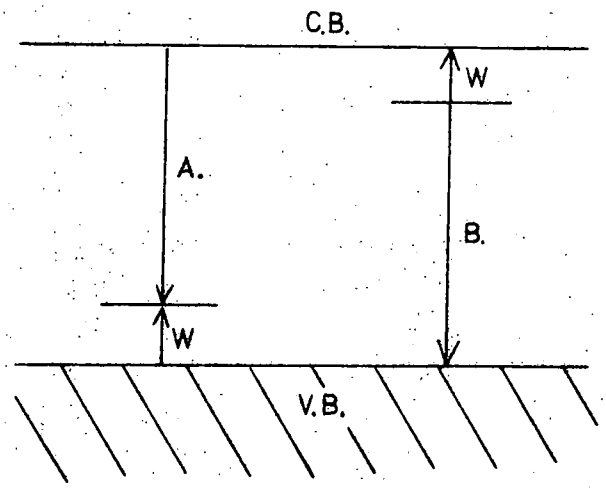

Fig. 1-9. Models for Thermal Quenching of Non-Localized Emission Processes.

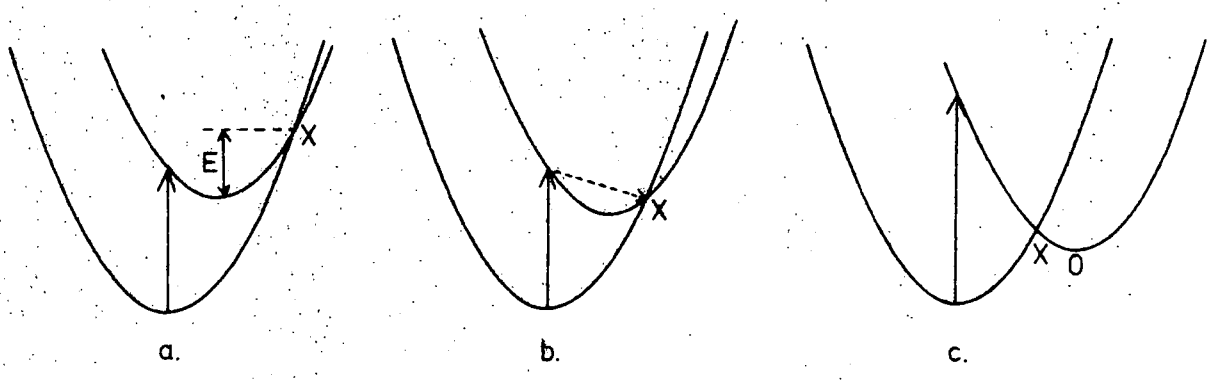

Fig. 1-10. Models for Efficiency Reducing Processes in Localized Emission Centres.

sufficient time to recombine with a free hole. In this case the energy w corresponds to the depth of the luminescent centre below the conduction band. By measuring the variation of the luminescence efficiency with temperature it is therefore possible to obtain a value for w.

The quenching transition produced can also be induced by optical means. Since the energy required is quite low, infra-red radiation is usually required. This process is then known as infra-red quenching. Normally, the measured optical and thermal quenching energies are not identical. This is explained in terms of the Franck-Condon principle which states that there is time for the lattice to adjust itself to facilitate a lower energy transition during thermal excitation, whereas there is insufficient time during an optical transition.

In a localised transition where the configurational coordinate model is applicable, quenching can be explained using the models shown in figure 1.10. Figure 1.10a indicates how quenching is assumed to occur according to Mott (1940). Since the potential energy is more dependent on configurational coordinate when the electron is in the ground state, the ground state parabola crosses the excited state parabola at some point X. As the temperature is raised, the system reaches an energy corresponding to E above the equilibrium position and it becomes possible for an electron to return to the ground state non-radiatively. The luminescence efficiency η is then given by

$$\eta = \frac{1}{1 + C \exp\left(-\frac{E}{kT}\right)} \qquad (1.3)$$

where C is a constant

This equation is clearly the same as that for non-localised transitions. In figure 1,10b a model is shown which was proposed by Dexter, Klick and Russell (1955) to explain the luminescence mechanism in materials with low emission probabilities even at very low temperatures. Immediately

upon excitation the system will possess an energy greater than that at the cross over point X, and hence on relaxation the electron will pass through the point X at which non-radiative recombination will occur.

Finally a non-radiative material can be explained on the basis of the model proposed by Seitz (1939), see figure 1.10c. In this case the minimum in the excited state lies outside the ground state and forms a metastable level. Following excitation the electron will either fall back non-radiatively at X or become trapped with the system in the configuration represented by O. In that case, further energy must be provided to permit the system to reach X and allow the electron to fall back to its ground state. One interesting deduction from the curves of figure 1.10b is that a large Stokes shift is associated with poor luminescent efficiency.

1.11 LUMINESCENCE IN ZINC SELENIDE

Hitherto the compounds zinc sulphide and cadmium sulphide have been investigated mainly and the luminescent properties of zinc selenide have received comparatively little attention. This is partly because of the difficulties which have been encountered in growing crystals reproducibly and of incorporating suitable impurities in known and controlled quantities. Recent improvements in these techniques have resulted in an increase in interest, but results are still complex and their interpretation is still unclear.

(a) Edge and Exciton Emission

The edge emission of zinc selenide crystals lies in the blue region of the spectrum in the wavelength range 4400 Å to 4800 Å. The first important work was carried out by Reynolds, Pedrotti and Larson (1961). They explained their results using the model proposed earlier for cadmium sulphide. Thus the two edge emission series were attributed to a bound

to bound transition involving a donor level 0·015 eV below the conduction band and an acceptor level 0·12 eV above the valence band and a free to bound transition between a conduction electron and a hole bound to the same acceptor. Results on hexagonal material have also been explained with the same model, though with slightly different values for the energy levels involved, (Gross and Suslina 1963, Liang and Yoffe 1967 a). Discrete distant pair recombination lines first seen in gallium phosphide (Hopfield et al 1963) and later in cadmium sulphide (Henry et al 1969) have been observed in zinc selenide (Dean and Merz 1969). Time resolved spectroscopy also supports the suggestion that the low energy series is associated with distant pair recombination (Iida 1968). Exciton emission in zinc selenide has been studied by several workers and the I_1, I_2 and I_3 bound exciton lines have been identified (Park and Schneider 1968, Iida and Toyama 1971, Merz et al 1972). These results all suggest that the edge emission processes in zinc selenide are very similar to those proposed for cadmium sulphide, though the exact positions of the levels and nature of the centres involved are still not generally agreed upon.

(b) Deep Centre Emission

Some of the first work reported concerning the deep centre emission in zinc selenide was by Leverenz (1950). Since then most interest has centred on self-activated and copper-activated material. Tables 1.1, and 1.2, summarize the work done in these fields.

From table 1.1, self-activated material can be seen to emit in the orange region of the spectrum although some uncertainty exists as to the actual position of the band. There is no agreement as to the centre responsible. Several workers suggest a zinc vacancy is present as in self-activated zinc sulphide, whereas others consider excess zinc is responsible.

Table 1.2 shows the results obtained from copper activated material.

TABLE 1-1

Emission bands reported in self-activated zinc-selenide

	Temp. °K	Peak Position Å	Temp. °K	Peak Position Å	Temp. °K	Peak Position Å	Co-Activator	Mechanism Suggested
Leverenz (1950)	300	6500					Chlorine	Excess Zn
Larach (1953) (Cathodolum.)	300	6020					Chlorine	-
Markovskii and Smirnova (1961)	300	6250	170	6000			-	-
Broser et. al. (1961)					4.2	6050	-	-
Gross and Suslina (1963)					4.2	6000	-	-
Aven and Woodbury (1962)	300	6000					-	Zn Vacancies
Asano et. al (1965)	300	6350					-	
Aven and Halsted (1965)			*	6000			Aluminium	Zn Vacancy-Al pairs
Mironov and Markovskii (1965)	300	6450	80	6300			-	Excess Zn
Holton et.al. (1965)					4.2	6240	Bromine, Chlorine	Zn Vacancy-Al pairs
					4.2	6410	Aluminium	
Halsted et.al. (1965)					25	6000	-	-
Lehmann (1967)			80	6230			Chlorine	Schön-Klasens
Stringfellow and Bube (1968)			85	6100			-	-
Iida (1968)	300	6150	77	6100			-	Pair recombination
Asano et.al. (1968a)			77	6150			-	-
				6200				
				6420				
Asano et.al. (1968b)			80	6200			Bromine	-
			80	6300			Chlorine	-
Markovskii et.al (1969)	300	6100	77	6150			-	Excess Zn

* Temp. not specified

TABLE 1-2

Emission bands reported in Copper doped Zinc Selenide

	Temp. °K	Peak Position Å	Temp. °K	Peak Position Å	Temp. °K	Peak Position Å	Co-Activator	Mechanism Suggested
Leverenz (1950)	300	6450					-	-
Larach (1953) (Cathodolum.)	300	6500					-	-
Markovskii and Smirnova (1961)	300	6400					-	-
Morehead (1963)			77	6360			-	Schön-Klasens to doubly ionizable centre
				5390				
Aven and Halsted (1965)			*	6360			Aluminium	Cu-Al pairs
				5250				-
Asano et.al. (1965)	300	6350					-	-
Nakao (1965)	*	6450					-	-
Halsted et.al. (1965)					25	6360	-	-
						5300		-
Fujiwara and Fukai (1966)			78	6200			Chlorine	Cu-Cl pairs
				5350				-
Lehmann (1966)			80	6360			Chlorine	Schon-Klasens
				5300				
			80	6360			Iodine	Schön-Klasens
				5280				
			80	6390-6425			Indium or Gallium	Schön-Klasens
Fujiwara and Fukai (1967)			78	6360			Indium	Cu-In pairs
				5420				-
Stringfellow and Bube (1968)			77	6300			-	Schön-Klasens-Cu^{+}
				5320				Schön-Klasens-Cu^{++}
					<16	(6300)+ 6360		Cu-donor pairs
Iida (1969)	300	6500	77	6400			-	Schön-Klasens Cu-donor pairs
				5700 or 5340				
Markovskii et.al. (1969)	300	6450	77	6400			-	-
				5350				-

* Temp. not specified

The reported positions of the bands are fairly consistent. In general a red and green band are present at 77°K and a single red band occurs at room temperature. However, the natures of the transitions responsible are still unknown. Suggestions include pair recombination to explain the low temperature red band and Schön-Klasens transitions to various charge states of the copper ion to explain both low temperature bands.

Other activators which have received some attention include gold, which produces a band around 7000 Å (Markovskii and Smirnova 1961), lithium (Ibuki et al 1967, Park and Chung 1971), phosphorus and arsenic (Reinberg et al 1971).

The effects of irradiation with high energy electrons have revealed a large number of emission bands in both the green and red regions of the spectrum which can be produced in undoped material simply by introducing native defects (Kulp and Detweiler 1963, Detweiler and Kulp 1966, Watkins 1971). This shows that spectra associated with impurities may be affected by native defects present in the phosphor, and that the conditions of growth, for example, may have an important effect on the resultant emission.

Manganese activation has received very little attention, and the work that has been carried out has produced widely differing results.

Leverenz (1950) first reported a room temperature emission at 6500 Å which he ascribed to manganese. Later, Larach (1953) obtained a room temperature cathodoluminescent band in manganese activated material, centred at 5940 Å, shifting to 6050 Å with chlorine coactivation.

Asano et al (1965) studied the effects of manganese chloride on the photoluminescence of zinc sulphide-selenide powders. They concluded that, at room temperature, the manganese emission band shifted from about 5900 Å in zinc sulphide to around 6400 Å in zinc selenide. A second paper involved measuring the excitation spectra of the phosphors and confirmed their previous results (Asano et al 1968 a).

Langer and Richter (1966) measured the optical absorption and emission of manganese doped crystals at 4·2°K. They observed three absorption bands which they associated with three transitions within the manganese ion. They found the associated emission band at about 5815 A°.

Apperson et al (1967) attempted to correlate the photoluminescence and photoconductivity of manganese doped zinc selenide. They concluded that the ground and first excited states of the manganese ion lay within the bandgap, whereas the higher energy levels were within the conduction band. They attributed a band at 6350 Å, at room temperature, to manganese.

Thus it can be seen that the position of the manganese emission band has been reported to occur at wavelengths ranging from 5815 Å to 6500 Å. Further investigation is therefore needed to clarify the situation.

In conclusion, it is clear that despite the work carried out in the field of luminescence of zinc selenide, especially the considerable effort directed towards copper and self-activation, a great deal of dispute still exists, not only concerning the mechanisms involved but also the positions of the emission bands themselves. This is also true in the case of manganese activation although comparatively little work has yet been done in this field. The problems are partly connected with the difficulties of obtaining sufficiently pure starting material but also with the fact that the emissions due to various impurities tend to occur very close together, rendering the identification of individual bands very difficult. This is especially true in the orange region of the spectrum.

CHAPTER 2

TRANSPORT PROPERTIES OF II - VI COMPOUNDS

2.1 INTRODUCTION

In general the transport properties of a material involve both its thermal and electrical conductivity. This is because both processes are simply concerned with the transfer of energy. Many of the factors involved, such as electron-phonon interactions, are also common to both processes. In this thesis the electrical transport phenomena only will be dealt with. Transport properties provide information concerning many of the basic properties of a material, for example the type and number of carriers involved, the effective scattering processes and the band structure. Some idea of the purity of the material is also obtained.

If mercury and oxygen are ignored, all the compounds formed from groups IIb and VIb of the periodic table are semiconductors or semiinsulators with forbidden energy gaps ranging from about 1·6 eV to 3·8 eV. The presence of impurities forming donors and acceptors, has a profound effect upon the conduction processes. The carrier distribution in both intrinsic and extrinsic semiconductors, and its variation with temperature is described below.

2.2 CARRIER EXCITATION IN AN INTRINSIC SEMICONDUCTOR

The diagram in figure 2.1 represents an intrinsic semiconductor with energy gap Eg. The density of electrons in the conduction band n_c is given by:-

$$n_c = \int_{E_C}^{E_{CT}} S(E)\, F(E)\, dE \qquad (2.1)$$

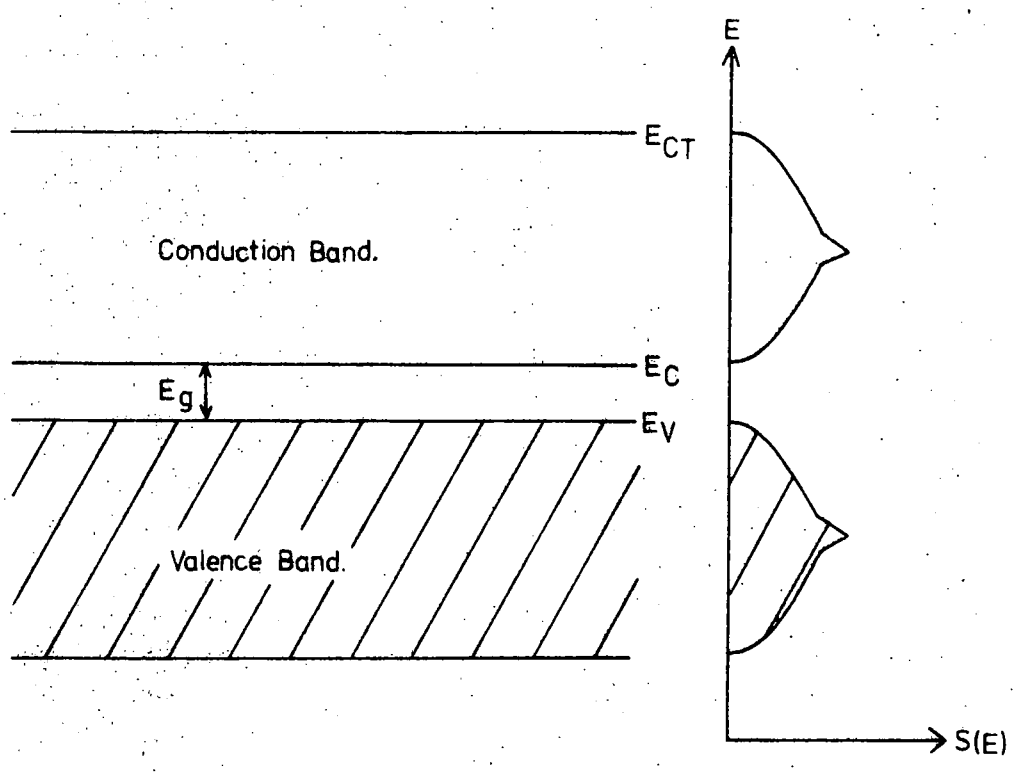

Fig. 2-1. Energy Band Diagram of an Intrinsic Semiconductor.

where S(E) is the density of available electron states in the conduction band and F(E) is the probability that a state will be filled (Fermi function). If it is assumed that the Fermi level E_F lies well within the bandgap, since F(E) falls off very rapidly with energy, E_{CT} can be replaced by ∞. This simply means that there is little chance for an electron to be in a state near E_{CT} and that the important region is very close to E_C.

Close to the bottom of the conduction band the density of states is given by:-

$$S(E) = \left(\frac{4\pi}{h^3}\right)\left(2m_e^*\right)^{\frac{3}{2}}\left(E - E_C\right)^{\frac{1}{2}} dE \qquad (2.2)$$

where m_e^* = effective mass of the electron near the bottom of the conduction band

and h = Planck's constant

The Fermi function is

$$F(E) = \frac{1}{\exp\frac{E - E_F}{kT} + 1} \qquad (2.3)$$

where k = Boltzmann's constant

$$\therefore \quad n_c = \left(\frac{4\pi}{h^3}\right)\left(2m_e^*\right)^{\frac{3}{2}} \int_{E_C}^{\infty} \frac{\left(E - E_C\right)^{\frac{1}{2}}}{\exp\left(\frac{E - E_F}{kT}\right) + 1} \qquad (2.4)$$

It is assumed that $(E_C - E_F) > 4kT$ so that the unity in the denominator can then be ignored and Maxwell-Boltzmann statistics can be used. When the integral is evaluated, it is found that:-

$$n_c = 2\left(\frac{2\pi m_e^* kT}{h^2}\right)^{\frac{3}{2}} \exp-\left(\frac{E_C - E_F}{kT}\right) \qquad (2.5)$$

Similarly it can be shown that the number of holes in the valence band n_h is given by:-

$$n_h = 2\left(\frac{2\pi m_h^* kT}{h^2}\right)^{\frac{3}{2}} \exp-\left(\frac{E_F - E_V}{kT}\right) \qquad (2.6)$$

where m_h^* is the effective mass of a hole at the top of the valence band.

Since n_e must equal n_h, the Fermi level can be obtained from (2.5) and (2.6)

$$E_F = \left(\frac{E_C + E_V}{2}\right) + \frac{3}{4} kT \log e\left(\frac{m_h^*}{m_e^*}\right) \qquad (2.7)$$

Therefore at all temperatures the Fermi level is halfway between the conduction and valence bands, if $m_h^* = m_e^*$. In general, however, m_h^* is greater than m_e^* and the Fermi level rises slightly with increasing temperature.

Substituting equation (2.7) back into (2.5) and (2.6) the carrier densities can be found.

$$n_e = n_h = 2\left(\frac{2\pi kT}{h^2}\right)^{\frac{3}{2}} \left(m_e^* m_h^*\right)^{\frac{3}{4}} \exp-\left(\frac{E_g}{2kT}\right) \qquad (2.8)$$

This can be written as

$$n_e = n_h = \left(N_C N_V\right)^{\frac{1}{2}} \exp-\left(\frac{E_g}{2kT}\right) \qquad (2.9)$$

N_C and N_V are known as the effective density of states in the conduction and valence bands respectively.

$$N_C = 2\left(\frac{2\pi m_e^* kT}{h^2}\right)^{\frac{3}{2}} \qquad (2.10a)$$

$$N_V = 2\left(\frac{2\pi m_h^* kT}{h^2}\right)^{\frac{3}{2}} \qquad (2.10b)$$

Equation (2.9) shows that a plot of $\log_e n$ v $\frac{1}{T}$ would produce a straight line of slope $\alpha - \frac{E_g}{2}$. This assumes that N_C and N_V do not vary rapidly with temperature.

2.3 CARRIER EXCITATION IN AN EXTRINSIC SEMICONDUCTOR

Two situations which result from the incorporation of impurities are shown in figure 2.2. Figures 2.2(a) and 2.2(b) represent a semiconductor containing N_D donor atoms and N_A acceptor atoms respectively. Normally, however, crystals, especially of II - VI compounds, are not as straightforward as this. They tend to contain both acceptor and donor impurities as shown in figure 2.3. If $N_D > N_A$ the acceptor sites are completely filled with electrons from the donor levels, thus producing a lower energy system. Similarly if $N_A > N_D$ all the donor levels are empty. This situation is known as compensation and exists even at absolute zero. The number of carriers actually available for excitation is given by the difference between N_D and N_A. If $N_D > N_A$ the material is n-type. If $N_A > N_D$ it is p-type.

In a compensated n-type semiconductor, the density of filled donor sites at temperature T

= density of donor sites x Fermi function

$$= N_D \times \frac{1}{1 + \frac{1}{g}\exp\left(\frac{E_D - E_F}{kT}\right)} \qquad (2.11)$$

The factor g which is introduced into the denominator, is known as the degeneracy factor and is related to the number of possible ways in which an electron can enter a donor level. For a simple donor level, as in zinc selenide, g has a value of 2.

Since the density of electrons in the conduction band at temperature

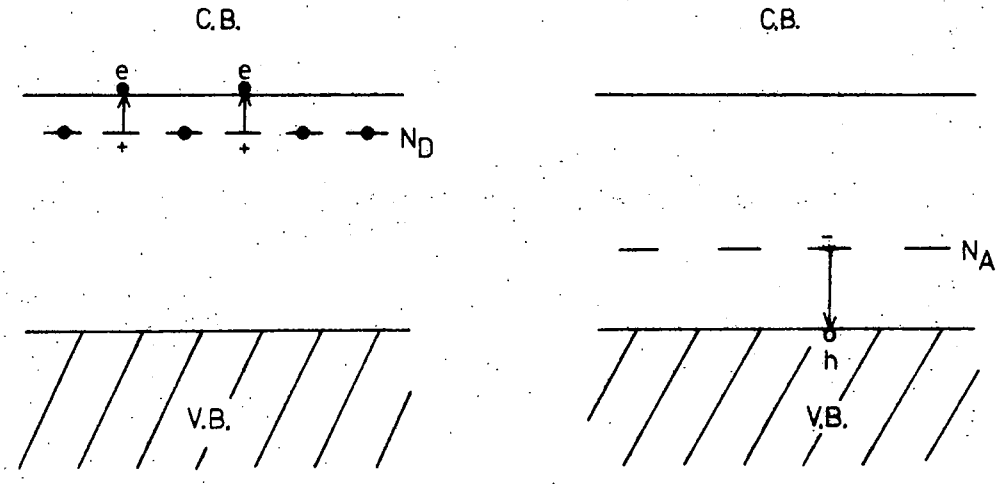

Fig.2-2. Energy Band Diagrams of n-type and p-type Semiconductors.

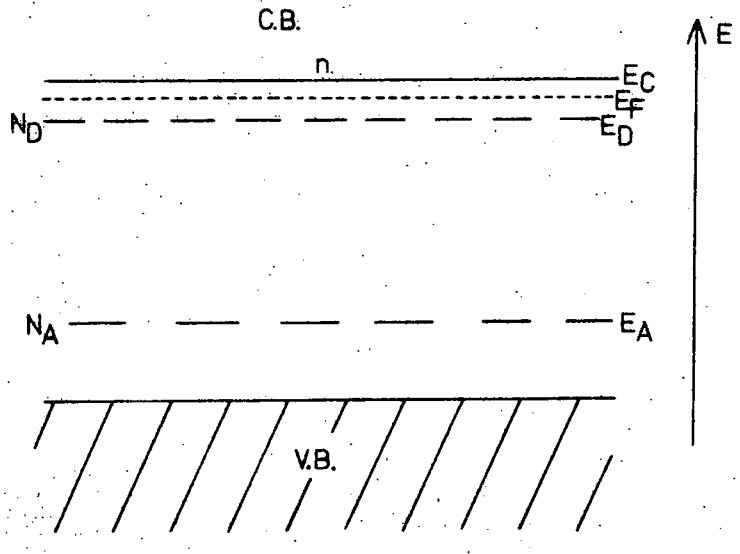

Fig.2-3. Energy Band Diagram of a Compensated n-type Semiconductor.

$$T = n \tag{2.12}$$

and the density of electrons originally in the donor states at

$$0^{\circ}K = N_D - N_A \tag{2.13}$$

Then from (2.11), (2.12), (2.13)

$$N_D - N_A = \frac{1}{1 + \frac{1}{2}\exp\left(\frac{E_D - E_F}{kT}\right)} + n \tag{2.14}$$

$$\frac{N_D}{N_D - N_A - n} - 1 = \frac{1}{2}\exp\left(\frac{E_D - E_F}{kT}\right) = \frac{1}{2}\left[\exp\left(\frac{E_C - E_F}{kT}\right) - \exp\left(\frac{E_C - E_D}{kT}\right)\right]$$

$$\frac{N_A + n}{N_D - N_A - n} = \frac{1}{2}\left[\frac{\exp\left(\frac{E_C - E_F}{kT}\right)}{\exp\left(\frac{E_C - E_D}{kT}\right)}\right]$$

but from (2.5) $n = N_C \exp\left(\frac{E_C - E_F}{kT}\right)$

$$\therefore \frac{N_A + n}{N_D - N_A - n} = \frac{N_C}{2n \exp\left(\frac{E_C - E_D}{kT}\right)}$$

so that

$$\frac{n\,(N_A + n)}{N_D - N_A - n} = \frac{N_C}{2}\exp -\left(\frac{E_C - E_D}{kT}\right)$$

$E_C - E_D$ is the donor ionization energy E_d

$$\therefore \frac{n(N_A + n)}{N_D - N_A - n} = \frac{N_C}{2}\exp -\frac{E_d}{kT} \tag{2.15}$$

In this model it is assumed that there is no thermal excitation from either the valence band or acceptor levels to the conduction band or donor levels. This is usually true over the temperature ranges normally encountered.

At very low temperatures when $n \ll N_D$ and $n \ll N_A$, equation (2.15) reduces to

$$n = \frac{N_D - N_A}{N_A} \cdot \frac{N_C}{2} \exp -\frac{E_d}{kT} \qquad (2.16)$$

If the material is uncompensated, that is $N_A = 0$ then at low temperatures where $n \ll N_D$

$$n = \left(\frac{N_C N_D}{2}\right)^{\frac{1}{2}} \exp -\frac{E_d}{2kT} \qquad (2.17)$$

At high temperatures when all the electrons from the donor levels are ionized, the number of carriers is simply

$$n = N_D - N_A \qquad (2.18)$$

Equation (2.15) shows that if a plot of $\log_e n \vee \frac{1}{T}$ is made for a compensated semiconductor, a straight line of slope $\propto -E_d$ is obtained whereas with a semiconductor containing no compensating levels as described by equation (2.17) a line of slope $\propto -\frac{E_d}{2}$ is obtained. Care must therefore be taken to ensure the correct equation is used. Again in this model N_C is assumed to remain constant with temperature.

2.4 SEMICONDUCTORS POSSESSING LEVELS AT MORE THAN ONE DONOR ENERGY

If a semiconductor contains, for example, two different impurities each producing levels with different ionization energies or an impurity with two or more electrons capable of being ionized, the situation is as shown in figure 2.4. It becomes necessary to modify equation (2.15) so as to sum the effects of each level.

Some typical plots of carrier concentration against temperature are shown in figure 2.5. If $N_{D_1} < N_A$ all the electrons from the shallow

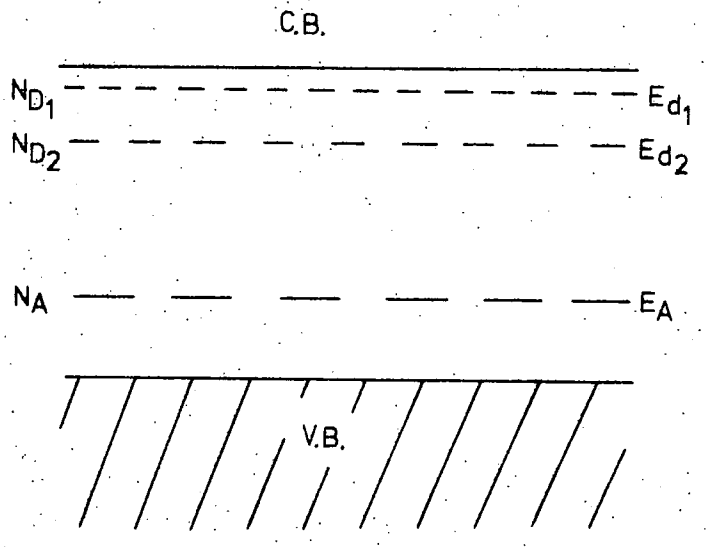

Fig.2-4. Energy Band Diagram of an n-type Semiconductor containing Levels with different Ionization Energies.

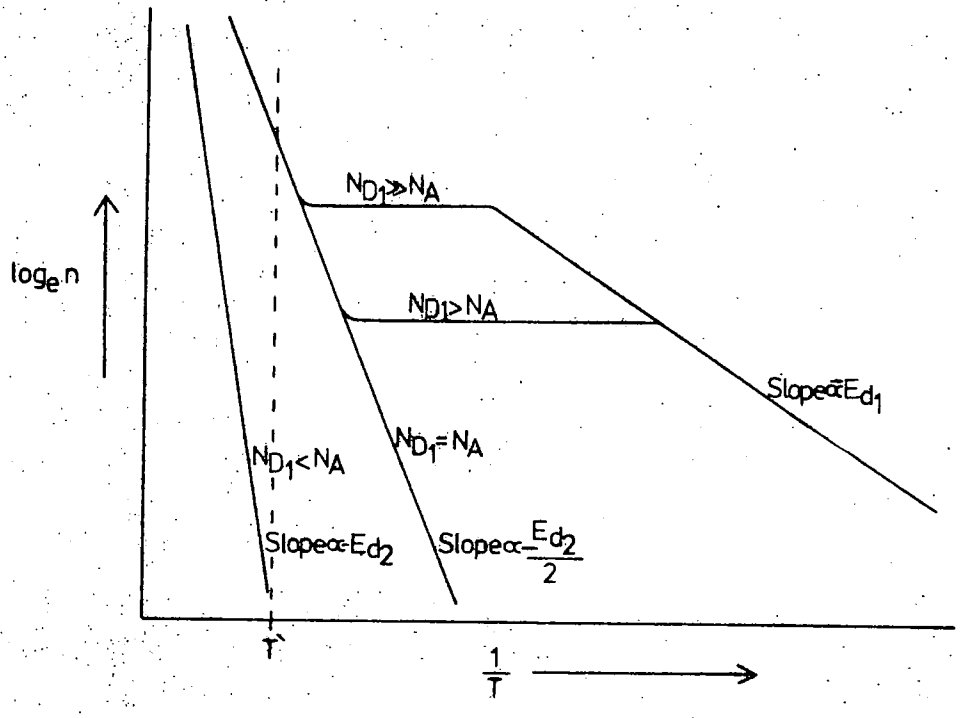

Fig. 2-5. Temperature Variation of Carrier Density n in an n-type Semiconductor as represented by Fig. 2-4.

level and some from the deeper level fill the acceptor centres, the material acts as a compensated semiconductor with a donor ionization energy of E_{d_2} and equation (2.15) can be used. If $N_{D_1} > N_A$ the acceptor levels are fully compensated, the material acts as a compensated semiconductor with a donor ionization energy E_{d_1} and again equation (2.15) can be used. However, as the temperature is raised level 1. is emptied and the electrons are raised from the uncompensated level 2. Now equation (2.17) should be used. If the material could not be cooled sufficiently, for example below the temperature T_0' in figure 2.5, it would be impossible to know whether a shallow donor was present and therefore which equation should be used.

Doubly ionizable impurities can be treated similarly though care must be taken to ensure that the lower level does not act as an acceptor.

2.5 SEMICONDUCTORS CONTAINING A HIGH DENSITY OF DONOR IMPURITIES

Until now it has been assumed that no interaction occurs between impurity atoms. However, when a certain donor concentration is reached the donor wave functions begin to overlap and a donor band, instead of a level, is produced. This band can eventually overlap the conduction band and result in an effective ionization energy of zero. A plot of carrier concentration versus temperature now results in a horizontal straight line. In this case the Fermi level is within the conduction band and the assumptions made earlier do not apply. The material becomes degenerate and Maxwell Boltzmann statistics cannot be used.

2.6 CARRIER MOBILITY

Apart from the carrier concentration, the other parameter which affects the transport properties of a material is the carrier mobility, which is defined as the drift velocity per unit applied field. The mobility is an indication of the extent of the interaction between a carrier

and its surroundings. A factor which must be introduced is the relaxation time τ which is a measure of the time between successive interactions.

In a metal, only electrons near the Fermi level need be considered and hence τ is effectively independent of energy. For a metal, therefore, the mobility μ is given by

$$\mu = \frac{e\tau}{m^*} \qquad (2.19)$$

where e = electronic charge

The effective mass m^* gives some indication of the interaction of the carrier with the regular periodic potential of the lattice. In a semiconductor there are always a large number of empty energy states available in the conduction band, and hence electrons with a wide range of energies can take part in conduction processes. The suitable modification of equation (2.19) will be dealt with later.

There are several means by which carriers can be scattered. A short description of these processes in relation to electrons will now be given. Actual calculations are very complex and only the results are shown. In all equations the e.s.u. system of units is used, and the resulting mobility should be divided by 300 to obtain it in normal units of cm^2/volt.sec.

(a) Acoustic Phonon Scattering

A quantized lattice vibration in a crystal lattice is known as a phonon. Phonons deform the periodic potential of the lattice and hence cause localized changes in the width of the energy gap. These changes produce variations in the kinetic energy of an electron as it passes through the crystal and the resultant interaction is known as acoustic phonon scattering.

Bardeen and Shockley (1950) obtained the following equation for the limiting mobility due to acoustic phonon scattering.

$$\mu_A = \frac{\left(8\pi\right)^{\frac{1}{2}} e \hbar^4 \rho C_L^2}{3E_1^2 m^{*\frac{5}{2}} \left(kT\right)^{\frac{3}{2}}} \qquad (2.20)$$

where ρ = density of the semiconductor

C_L = longitudinal acoustic wave velocity

E_1 = a measure of the change in position of the conduction band edge due to changes in volume of the unit cell.

The most important feature in this equation is the $T^{-3/2}$ variation showing that as the temperature is lowered the mobility should increase as $T^{-3/2}$.

(b) Optical Phonon Scattering

The vibration of adjacent atoms in a unit cell in antiphase produces an optical phonon. In compound semiconductors the fact that the adjacent atoms are oppositely charged allows an electrostatic potential to be associated with an optical phonon. The magnitude of this potential is dependent upon the degree of ionicity of the bonding and is therefore quite important in the II - VI compounds. The effective charges on each ion, and hence the electron-lattice interaction, can be related to the difference between the static and optical dielectric constants. In a covalent material this is zero and there is little interaction.

The theory behind optical mode scattering is complex, especially at low temperatures, because then the energy transferred at each interaction is not negligible in relation to the energy of the electron, and basic relaxation time theories do not hold. However, Howarth and Sondheimer (1953) have obtained an expression for the mobility, μ_{OPT}, limited by optical mode scattering

$$\mu_{OPT} = \frac{1}{2\alpha\omega} \frac{e}{m^*} \frac{8}{3\sqrt{\pi}} \frac{\psi_z}{Z^{\frac{1}{2}}} \left(e^z - 1\right) \qquad (2.21)$$

where ω is the angular frequency of the L.O. phonon

Z = the ratio of Debye temperature to temperature of the crystal = $\frac{\theta_D}{T}$ or $\frac{\hbar\omega}{kT}$

ψ_z = a factor, varying as a function of Z from 0·6 to 1 over the temperature range involved.

α = the polaron coupling constant which is given by

$$\alpha = \frac{e^2}{\hbar} \left(\frac{m^*}{2\hbar\omega}\right)^{\frac{1}{2}} \left(\frac{1}{\epsilon_\infty} - \frac{1}{\epsilon_s}\right) \qquad (2.22)$$

where ϵ_∞ and ϵ_s are the optical and static dielectric constants.

At temperatures above the Debye temperature, θ_D, that is for low Z the exponential term in equation (2.21) can be expanded to $Z + \frac{Z^2}{2} + \frac{Z^3}{6} \cdots$ and Z^2 and the following terms can be ignored. The mobility will then vary as a function of $Z^{1/2}$, that is $T^{-1/2}$. At low temperatures, however, the exponential term dominates and the mobility varies as $\exp \frac{1}{T}$. Since the Debye temperature is approximately 365°K for zinc selenide, the variation of mobility with temperature will depend on a combination of the two terms but will be mainly exponential in the temperature range involved in most studies.

(c) Piezoelectric Scattering

Piezoelectricity is the name given to the electric polarization produced by an applied mechanical stress. Thus an electrostatic potential accompanies an acoustic phonon and this leads to piezoelectric scattering. All the II - VI compounds are piezoelectric although those with the cubic structure are less so than those with the hexagonal phase.

Harrison (1956) gives the mobility limited by piezoelectric scattering as

$$\mu_{PZ} = \frac{0{\cdot}044\ \rho\ C_L^{\,2}\ \hbar^2\ \epsilon_s^{\,2}}{e\ C^2\ m^{*\frac{3}{2}}\ (kT)^{\frac{1}{2}}} \qquad (2.23)$$

where C = Piezoelectric electromechanical coupling constant

ϵ_s = static dielectric constant

C_L = longitudinal acoustic wave velocity

ρ = density of the semiconductor

This equation results in a $T^{-1/2}$ dependence of mobility. Later work by Zook (1964) is in agreement with Harrison's results.

(d) Ionized Impurity Scattering

Ionized impurity scattering results from the interaction of electrons with ionized donor or acceptor centres or native defects, all of which produce a centre of charge. The process can be compared to Rutherford scattering of α-particles. The Brooks-Herring formula (H. Brooks 1955) is given below for a compensated semiconductor.

$$\mu_I = \frac{2^{\frac{7}{2}}\ (kT)^{\frac{3}{2}}\ \epsilon_s^{\,2}}{\pi^{\frac{3}{2}}\ e^3\ m^{*\frac{1}{2}}\ N_I} \cdot \frac{1}{\left[\log_e \frac{6m\ (kT)^2\ \epsilon_s}{e^2 \pi \hbar^2\ n`\left(2 - \frac{n`}{N_I}\right)}\right]} \qquad (2.24)$$

where $n` = n + \left(1 - \frac{n + N_A}{N_I}\right)\left(n + N_A\right)$

N_I = density of ionized impurities = $2N_A + n$

The earlier equation proposed by Conwell and Weisskopf (1950), which did not take into account the screening of the charge centres by conduction electrons, was almost identical except for the logarithmic term which was replaced by

$$\log_e \left[1 + \left(\frac{3\epsilon_s\ kT}{e^2 N_I^{\frac{1}{3}}}\right)^2\right]$$

This SCATTERING effect therefore becomes more important as the temperature is lowered as shown by the $T^{3/2}$ temperature dependence.

Equation (2.24) holds only for singly charged centres. A factor $\frac{1}{Z^2}$ where Z is the charge state of the centre, must be introduced for multiply charged centres such as native defects in the II - VI compounds. As the temperature is lowered N_I becomes smaller as carriers freeze out and the $T^{3/2}$ dependence may not be observed.

Scattering by electron hole collisions, although less important, can be treated in a similar manner to ionized impurity scattering and is found to possess the same temperature dependence.

(e) Neutral Impurity Scattering

As the temperature of a semiconductor is lowered, carriers freeze out into their impurity levels. The amount of ionized impurity scattering decreases and is replaced by neutral impurity scattering. The interaction of the electrons with neutral impurity centres is analogous to electron scattering by a hydrogen atom. Erginsoy (1950) obtained the following equation for the mobility limited by neutral impurity scattering

$$\mu_N = \frac{m^* e^3}{20 N \epsilon_s \hbar^3} \qquad (2.25)$$

where N = number of neutral impurity atoms/unit volume

Defects which are not hydrogen-like produce deeper levels and more localised wave functions. They therefore tend to have less effect than the shallow levels. Scattering due to neutral impurities is independent of temperature and is most important at low temperatures.

(f) Crystal Imperfections

Dexter and Seitz (1952) have shown that dislocations cause the lattice to distort and so alter the band structure. They found that the scattering effect depended on the density of dislocations per unit area

N_X and on temperature according to

$$\mu_X \propto \frac{1}{N_X T} \tag{2.26}$$

Grain boundaries are thought to become important in scattering only at very low temperatures except in extremely poor quality material.

2.7 THE HALL EFFECT

The temperature variation of the carrier concentration and mobility can be seen to provide a great deal of information about a semiconductor. The usual way to study these variations is by measuring the Hall coefficient.

A rectangular block forms a suitable sample, with two current contacts (1, 2), two voltage probes (3, 4) and two Hall voltage probes (5, 6) connected to the edges as shown in figure 2.6. A magnetic field B_Z is applied perpendicular to the large face. This field causes carriers to be deflected horizontally in the Y-direction until an electric field E_Y is set up. This field exactly balances the deflecting Lorenz force and an equilibrium state is then reached.

If the forces on an electron are equated at equilibrium, then

$$B_Z \, e \, v = E_Y \, e \tag{2.27}$$

where v is the electron velocity

The current density J_X is given by

$$J_X = n \, e \, v \tag{2.28}$$

where n is the density of free electrons

$$\text{so that } E_Y = \frac{B_Z J_X}{n \, e} \tag{2.29}$$

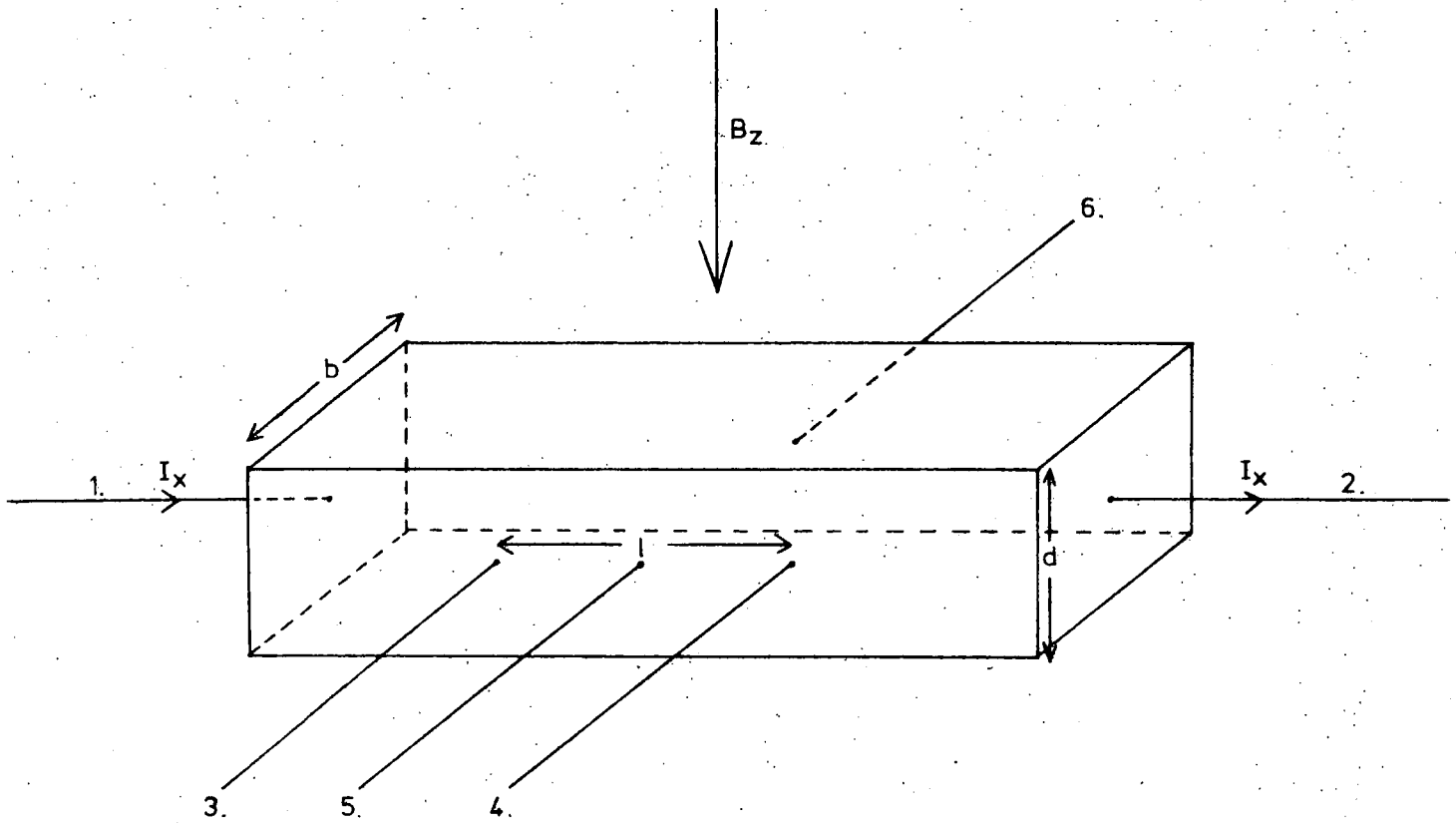

Fig.2-6. Diagrammatic Representation of a typical Hall Effect Sample.

The Hall coefficient R is defined as the ratio of the electric to the magnetic field per unit current density, i.e.

$$R = \frac{E_Y}{B_Z J_X} \tag{2.30}$$

$\therefore$ from (2.29)

$$B_Z J_X R = \frac{B_Z J_X}{n e}$$

$$\therefore \quad R = \frac{1}{n e} \tag{2.31}$$

If e is taken as the magnitude of the electronic charge, the sign of R determines whether electrons or holes are responsible for the conductivity.

From equations (2.29) and (2.31)

$$E_Y = B_Z J_X R$$

$\therefore$ from figure 2.6

$$\frac{V_Y}{b} = B_Z \frac{I_X}{bd} \cdot R$$

$$R = \frac{V_Y d}{B_Z I_X} \tag{2.32}$$

V_Y, the voltage set up between probes 5 and 6 is known as the Hall voltage. Since all four parameters in (2.32) can be measured, R and hence n can be obtained.

By measuring the voltage between probes 3 and 4, V_X, the conductivity σ can be obtained

$$J_X = \sigma E_X$$

$$\therefore \quad \sigma = \frac{l I_X}{V_X bd} \tag{2.33}$$

The conductivity is also given by the expression $\sigma = n e \mu$

$$\therefore \text{ from (2.31)} \quad \sigma = \frac{\mu}{R}$$

$$\therefore \quad \mu = R\sigma \tag{2.34}$$

Therefore by measuring the Hall coefficient of a conducting medium it is possible to obtain both the carrier concentration and its mobility. In equation (2.34) the absolute magnitude of R is used so as to obtain a positive value for μ.

If more than one type of carrier is involved in the conduction process, for example if the material is intrinsic, equation (2.31) must be modified to

$$R = \frac{p - n\left(\frac{\mu_n}{\mu_p}\right)^2}{\left(p + n\frac{\mu_n}{\mu_p}\right)^2} \cdot \frac{1}{e} \tag{2.35}$$

Now the sign of R depends on the ratio of the hole and electron mobilities. If the ratio is unity, R is zero. Normally in the II - VI compounds one type of carrier is always dominant and this problem rarely occurs.

2.8 SCATTERING FACTOR

In equations (2.27) and (2.28) the velocity involved is an average value for all the electrons. However, since different processes are involved in conduction and in magnetic deflection, the average values are not identical. As the velocity depends on the relaxation time τ, it is the averaging of τ which is of interest. It is found that τ varies with energy thus

$$\tau = E^{-S} \tag{2.36}$$

where S = a constant depending on the scattering processes involved.

Therefore the relaxation time must be averaged over a range of energies. In a metal and a degenerate semiconductor, only electrons of a single energy, the Fermi energy, take part in the transport processes and therefore the two averaging processes give the same result. Equations (2.27) and (2.28) are then correct. In a non-degenerate semiconductor electrons with various energies can take part and a factor r, known as the scattering factor, must be introduced. r is the ratio of the relaxation times averaged over energy for the two processes.

$$r = \frac{\langle \tau_{(E)}^{\ 2} \rangle}{\langle \tau_{(E)} \rangle^{2}} \qquad (2.37)$$

where $\langle\ \rangle$ is an average over energy

r is found to be related to S as follows

$$r = \frac{\Gamma\left(\frac{5}{2} - 2S\right) \Gamma\left(\frac{5}{2}\right)}{\left[\Gamma\left(\frac{5}{2} - s\right)\right]^{2}} \qquad (2.38)$$

For more information concerning the scattering factor, see Smith (1961) When the scattering factor is taken into account, equations (2.31) and 2.34) are modified to

$$R = \frac{r}{n e} \qquad (2.39)$$

$$\mu = \frac{1}{r} \cdot R \sigma \qquad (2.40)$$

The mobility given by equation (2.34) is known as the Hall mobility μ_H and that given by equation (2.40) is the conductivity mobility μ_C, which is obtained from conductivity measurements

$$\mu_H = R \sigma \qquad (2.41)$$

TABLE 2.1

Scattering Mechanism	Y ($\mu \propto T^{Y}$)	S ($\tau \propto E^{-S}$)	r ($R = \frac{r}{n e}$)
Acoustic Phonons	$-\frac{3}{2}$	$\frac{1}{2}$	$\frac{3\pi}{8}$
Optical Phonons $T<\theta_D$	exp	complex	complex 1·03 - 1·10
Optical Phonons $T>\theta_D$	$-\frac{1}{2}$	complex	complex 1·00 - 1·20
Ionized Impurities	$+\frac{3}{2}$	$-\frac{3}{2}$	$\frac{315\pi}{512}$
Neutral Impurities	independent	independent	1

$$\mu_C = \frac{1}{r} \cdot R\sigma \qquad (2.42)$$

$$r = \frac{\mu_H}{\mu_C} \qquad (2.43)$$

$$n = \frac{r}{R e} \qquad (2.44)$$

The value of S depends on the scattering process which is dominant. Values of S and r for the different scattering mechanisms are given in table 2.1. together with the temperature dependence of the mobility. It is clear that r is always near unity and quite often it is simply ignored.

2.9 TRANSPORT PROPERTIES OF ZINC SELENIDE

The majority of work carried out on the transport properties of zinc selenide has been that of Aven and his co-workers since about 1962. Because as-grown zinc selenide has a high resistivity which is attributed to compensation effects, all measurements have been made on material heated in molten zinc. This reduces the resistivity by removing compensating impurities such as copper (Aven and Woodbury 1962) and perhaps compensating native defects.

Aven and Woodbury (1962) obtained a value of 530 $cm.^2/v.sec.$ for the mobility at room temperature of 1 ohm.cm. zinc selenide produced by heating undoped material in zinc. In a later paper Aven and Segall (1963) reported measurements on undoped material heated at between 900°C and 1000°C for one or two days in liquid zinc or a zinc plus aluminium melt, and chlorine doped material also heated in zinc. The aluminium doped material was found to be degenerate with a carrier concentration of about 10^{18} $cm.^{-3}$. Both the undoped and chlorine doped samples were found to have carrier concentrations of approximately 6×10^{15} $cm.^{-3}$ at room temperature. However, the donor ionization energies of the undoped

and chlorine doped crystals were 0·008 eV and 0·19 eV respectively. Mobility measurements revealed a maximum of 700 $cm.^2/v.sec.$ at 100°K in the aluminium doped sample. The chlorine doped and undoped samples were not measured below about 200°K but with all samples optical mode scattering was shown to be the limiting factor at temperatures down to about 200°K. In the aluminium doped sample ionized impurity scattering appeared to be dominant at lower temperatures.

Measurements have also been made on zinc selenide irradiated with high energy electrons and the resultant properties have been compared with those of samples fired in zinc under various conditions, (Lorenz, Aven and Woodbury 1963, Woodbury and Aven 1964, Aven 1964). It appears that two donor levels can be produced depending upon the temperature of the firing. A shallow donor level 0·02 eV below the conduction band was observed both in chlorine doped samples heated at 850°C in molten zinc and in crystals pretreated at 1050°C in zinc plus aluminium and subsequently heated in zinc alone at 900°C to 950°C. However, when either the chlorine doped crystal was heated at 1050°C in zinc or the aluminium treated sample was not subsequently heated in zinc, the influence of a level at between 0·1 eV and 0·16 eV below the conduction band became apparent, and the carrier concentration and mobility were approximately a factor of three lower. Once again impurity banding became evident in aluminium doped crystals with a carrier concentration greater than approximately 2×10^{16} $cm.^{-3}$. The deeper level was also observed in samples which had been irradiated with 1·5 MeV electrons. The samples could be alternated between the high and low resistivity states by successive high and low temperature firings, and the properties appeared to be completely reversible. Temporary illumination of the high resistivity crystals at temperatures below approximately 100°K caused both the carrier concentration and the mobility to increase. The level at approximately 0·1 eV below the conduction band was considered to be a very deep

acceptor level produced by a doubly negatively charged native acceptor. A selenium vacancy, which can be taken to act as an acceptor if a covalent bonding scheme is adopted, associated in some way with a halogen ion was believed to be the centre involved.

Recent work (Aven 1971) has shown that after successive heatings in molten zinc at temperatures between 850°C and 650°C for a total of two weeks, the mobility can be increased to a maximum value of 12,000 $cm.^2/v.sec.$ at about 60°K. He concluded that the main reason for the increase was the elimination of the double acceptor defects. Carrier concentrations were of the order of 5×10^{15} $cm.^{-3}$ and a value of 0·021 eV was obtained for the donor ionization energy.

Fukuda and Fukai (1967) studied zinc selenide, heated at 900°C - 1000°C in liquid zinc for several days and obtained a maximum mobility of 3000 $cm.^2/v.sec.$ They explained the scattering as a combination of optical mode, neutral impurity and ionized donor-acceptor dipole scattering. They also suggested that the level they observed 0·011 eV below the conduction band originated from a native defect. Smith (1969), however, carried out Hall Effect measurements on zinc selenide at temperatures between 700°C and 1000°C under various zinc pressures and concluded that the low resistivity, approximately 1 ohm.cm., observed in material subjected to zinc treatment was due entirely to the presence of donor impurities. He suggested that the zinc treatment simply removed compensating acceptors and that the true resistivity of pure zinc selenide after zinc treatment was approximately 10^6 ohm.cm. In a completely different arrangement, Sagar et al (1968b) measured the piezoresistance and piezohall effect in zinc selenide and obtained a donor ionization energy of 0·019 eV.

It therefore seems likely that two donor levels are involved in connection with zinc selenide. One has an ionization energy of between 0·008 eV and 0·023 eV, which is in the region of a hydrogenic donor level,

whereas the other lies deeper at between 0·1 eV and 0·19 eV below the conduction band. The deeper level has been attributed to both chlorine impurity and a native double acceptor level. The lower energy level which appears after low temperature treatment in liquid zinc, has been ascribed to native defects and also to unremoved donor impurities.

The situation concerning the mobility of zinc selenide is much clearer. The room temperature mobility has been reported to have values from about 300 $cm.^2/v.sec.$ to 500 $cm.^2/v.sec.$ by several workers (Aven and Woodbury 1962, Aven and Segall 1963, Woodbury and Aven 1964, Tsujimoto et al 1966, Fukuda et al 1967, Ludwig and Aven 1967, Aven 1971, Heaton et al 1972). The results of Heaton et al are the only ones to have been obtained on material not treated in molten zinc and with a carrier density as low as $10^{12} cm.^{-3}$. The predominant mobility limiting process at high temperatures appears to be scattering by optical phonons whereas below approximately 80°K, ionized impurity scattering and perhaps neutral impurity or dipole scattering begin to become dominant. Aven (1971) has obtained a mobility of 12,000 $cm.^2/v.sec.$ which appears to be the highest yet achieved.

As regards p-type zinc selenide, the few results which have been reported have been mainly concerned with copper doped material. Mobilities of 10 $cm.^2/v.sec.$ at 200°C (Aven 1962) and 28 $cm.^2/v.sec.$ at room temperature (Haanstra and Dieleman 1965) have been quoted together with ionization energies of approximately 0·9 eV and 0·7 eV respectively. Phosphorus doped material was found to be p-type with a mobility of the order of 24 $cm.^2/v.sec.$ and a hole density of 4×10^9 $cm.^{-3}$ at 500°K, (Reinberg et al 1971). The corresponding acceptor energy was approximately 0·7 eV. Park et al (1971) studied p-type lithium doped zinc selenide and again obtained similar values to those of the copper doped material. At room temperature the crystals had a mobility of 23 $cm.^2/v.sec.$ and a carrier concentration of $2·7 \times 10^9$ $cm.^{-3}$. Measurements were made

over the range 260°K - 340°K and an acceptor ionization energy of 0·75 eV was obtained.

It thus appears that the three acceptor type dopants described above behave in a similar manner as regards the height of the acceptor level above the valence band and the mobility, but the resistivities are much too high for most applications, for example in p-n junctions, mainly because of the large ionization energies involved.

CHAPTER 3

CRYSTAL GROWTH AND TREATMENT

3.1 CRYSTAL STRUCTURE

The bonding of the semiconducting elements in group IV of the periodic table such as germanium and silicon is found to be completely covalent. However compounds formed from elements in groups I and VII such as potassium chloride possess almost complete ionic bonding. The shift towards ionic bonding is gradual and in general the ionicity increases as the valency difference between the component elements increases. The compounds formed from elements of groups II and VI can therefore be expected to be partially ionic and partially covalent in nature. Zinc selenide can be considered as either $Zn^{++}Se^{--}$, in which case each ion possesses a completely filled sub-shell and the bond is ionic, or $Zn^{--}Se^{++}$ in which both ions possess four valence electrons and the bonding is covalent. The degree of ionicity increases with the electronegativity difference between the two elements. The electronegativity difference of 0·9 for zinc selenide can be compared with 2·2 for potassium chloride, 0·5 for gallium arsenide and zero for the group IV elements. Although the bonding in the II-VI compounds is mainly covalent, the ionic influence can be seen in the large bandgaps, low mobilities and high melting points relative to the III-V compounds and group IV elements. The covalent nature is seen in the tetrahedral bonding which is a result of the highly directional SP^3 orbitals formed by the shared electrons as in the group IV elements.

The tetrahedral orbital arrangement produces two main crystal structures in the III-V and II-VI groups of compounds. These are the hexagonal

or wurtzite structure and the cubic or zincblende structure. Zinc selenide normally exists in the cubic form. The zincblende structure is very similar to that of diamond which has two interpenetrating face centred cubic lattices. In zinc selenide different ions occupy the points of the two sub-lattices. Zinc selenide has a lattice parameter, that is a cube edge, of 5·67 Å and a nearest neighbour distance of 2·45 Å.

3.2 CRYSTAL GROWTH

There are three important methods of growing crystals of the II-VI compounds, namely growth from the melt, growth from the vapour and growth by chemical transport. Growth of zinc selenide from the melt is difficult as its melting point of 1500°C prevents the use of silica. Moreover the vapour pressure over zinc selenide at this temperature is 1·8 atmospheres and this also introduces problems. Despite these difficulties crystals have been grown satisfactorily from the melt (Fischer 1959, Tsujimoto et al 1966).

Vapour phase transport and chemical transport are much more practicable methods and both have been employed to produce the crystals which were used during the work reported in this thesis. These techniques will now be described.

(a) Preliminary treatment

Zinc selenide powder from one of three sources was used as starting material. B.D.H. Optran zinc selenide was used to produce the majority of crystals although several early crystals were grown from Derby Luminescents material. Latterly some crystals were grown from powder prepared in this laboratory by the direct combination of Metals Research 5N zinc and selenium in the form of vapour at 1150°C.

Each of these zinc selenide starting materials was first purified in a flow run process. The powder was heated in a silica tube in a stream

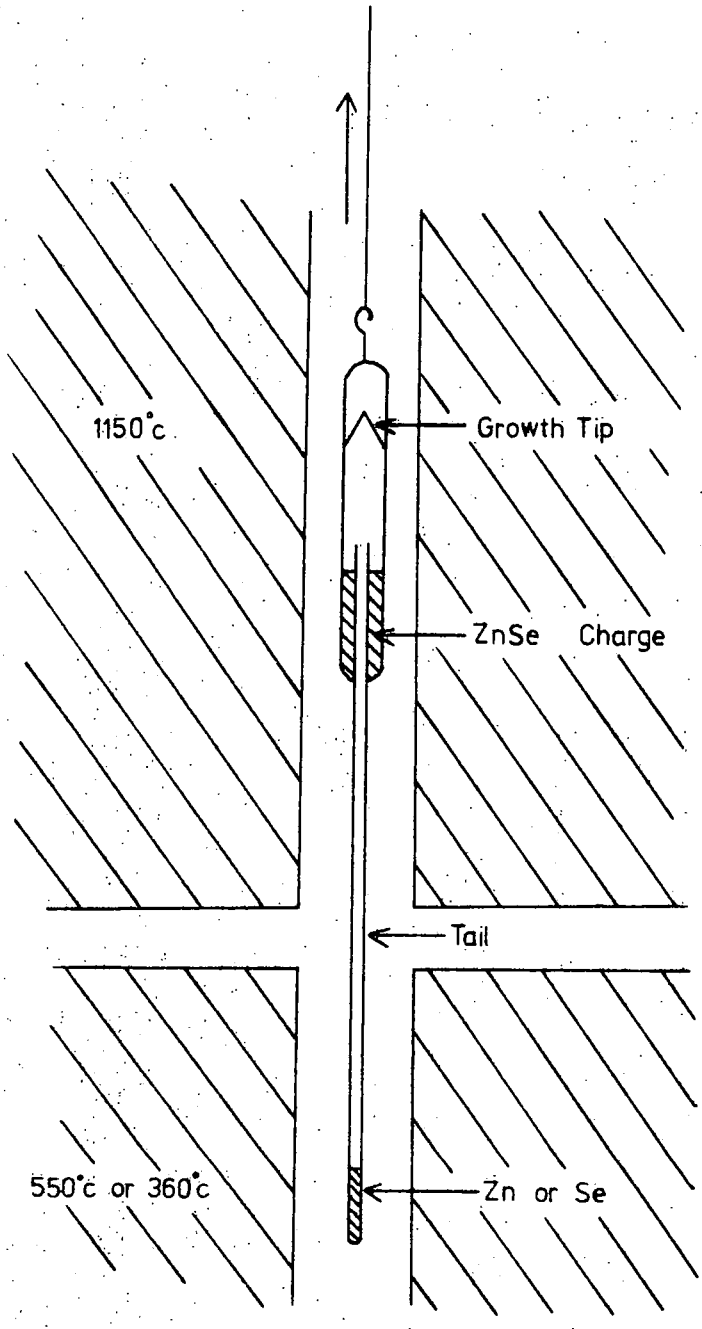

Fig. 3-1. Vapour Phase Transport Crystal Growth System.

of high purity argon at 600°C for twelve hours to remove all volatile impurities. The temperature was then raised to 1160°C for about a week. This caused the powder to sublime along the tube to a cooler region and left any non-volatile impurities behind. The zinc selenide crystallized out in the form of small platelets about 4 mm. square which were used as the basis for the following crystal growth procedures.

(b) Vapour Phase Growth

The crystals were grown by the method developed by Burr and Woods (1971) from the original method of Clark and Woods (1968). A typical growth system is illustrated in figure 3.1. About 20 grams of flow run platelets were used as the charge and about 0·2 grams of either zinc or selenium were held in the tail. The tube was evacuated to 10^{-6} torr and mounted vertically with the charge at 1150°C and the tail at 550°C when using zinc or 360°C when using selenium. The tail charge was necessary to control the pressure of one of the components and maintain a near-stoichiometric composition of the vapour in the growth region of the capsule. The tube was raised at about 3 cm. per day for about a week and 1 cm. diameter crystals between 3 and 4 cm. long were produced. Indium, gallium and aluminium dopants were added directly to the charge, copper was introduced either as the metal or the selenide and chlorine was introduced in the form of zinc chloride. Manganese was introduced as the metal, the selenide or the chloride in the charge or as the chloride in the tail.

Several samples were produced using a horizontal vapour transport method. With this arrangement a 6 mm. sealed tube was held in a 1100°C - 200°C temperature gradient. No tail was used and transport was difficult to control, which led to poor crystal quality. Dopants were added directly to the charge.

(c) Chemical transport

With the chemical transport method iodine was used as the transporting

agent. The technique was based on the method described by Nitsche (1960). Some 4 grams of charge material with 4 milligrams of iodine were placed at the hotter end of a silica tube which was held in a temperature gradient of 830°C - 800°C for seven days. Crystals approximately 5 mm. in diameter and 1 cm. long grew at the cooler end. Manganese was added to the charge as the metal.

Although the boules produced by vapour transport were of good quality and were transparent, they were found to be composed of a number of crystallites. A slice from a particularly poor sample is shown in figure 3.2. A number of twins as shown in figure 3.3 were also present. The crystals grown by iodine transport appeared to beof much higher quality. This is probably because the crystals produced by chemical transport were grown below the unstable phase transition temperature near 1050°C where faulted and mixed cubic-hexagonal crystals tend to form. Thus the crystals studied in this thesis were predominantly cubic although those grown by vapour transport probably contained a small amount of hexagonal component.

3.3 SAMPLE PREPARATION

Experimental samples were cut from most crystals with a diamond saw. Delicate crystals or intricate cuts, however, usually necessitated the use of a reciprocating wire-saw (Rushby and Woods 1970).

After samples had been cut or ground using carborundum powder, reflection electron microscopy showed that the surface was considerably damaged. Surface damage introduces surface states which produce a large number of discrete levels within the forbidden gap. These levels prevent the production of ohmic electrical contacts and also act as non-radiative recombination centres, thus reducing the photoluminescent efficiency. In order to remove this damage an etch must be used.

The etch recommended by Sagar et al (1968a) was used most frequently.

Fig. 3-2. Cross Section through a Boule of ZnSe:Ga showing Polycrystallinity.
(×4·5.)

Fig. 3-3. Area of ZnSe Slice showing Twinned Regions and Grain Boundary.
(×200)

The procedure was to immerse the crystal in an 0·4% solution of bromine in methanol for one to two minutes. The crystal was quickly washed in methanol and then immersed in carbon disulphide for about five minutes to remove the compound of bromine and selenium which tended to form as a red deposit on the surface. If the red deposit persisted it was ground away and the crystal was re-etched. Finally the sample was washed in chloroform to aid drying and prevent drying stains. The etchant was found to produce a slightly matt surface as a large number of pits were formed (Gezci and Woods 1972). The surface was examined by reflection electron microscopy and found to be completely free from surface damage.

A second method of etching used the etchant first described by Hemmat and Weinstein (1967). A concentrated solution of chromic oxide in orthophosphoric acid was prepared. An approximately equal volume of concentrated hydrochloric acid was then added and the sample was immediately immersed in the solution which remained active for about ten minutes. After five minutes of continuous agitation the crystal was removed, washed first in distilled water and then in iso-propyl alcohol to prevent drying stains. This etch produced a highly polished surface rendering the sample transparent. Although the etch did not remove surface damage as well as bromine in methanol, the electrical and optical results obtained were identical irrespective of the etch used.

3.4 INTRODUCTION AND EXTRACTION OF IMPURITIES

Aven and Woodbury (1962) showed that trace impurities of copper and silver could be removed from zinc selenide by heating the crystals in molten zinc. The impurities were more soluble in the zinc than in the crystal and hence segregated out into the zinc. Later Markovskii et al (1969) used the method in reverse to introduce copper into zinc selenide crystals. It was therefore decided that this procedure should be used to purify samples or to introduce a range of dopants. A method

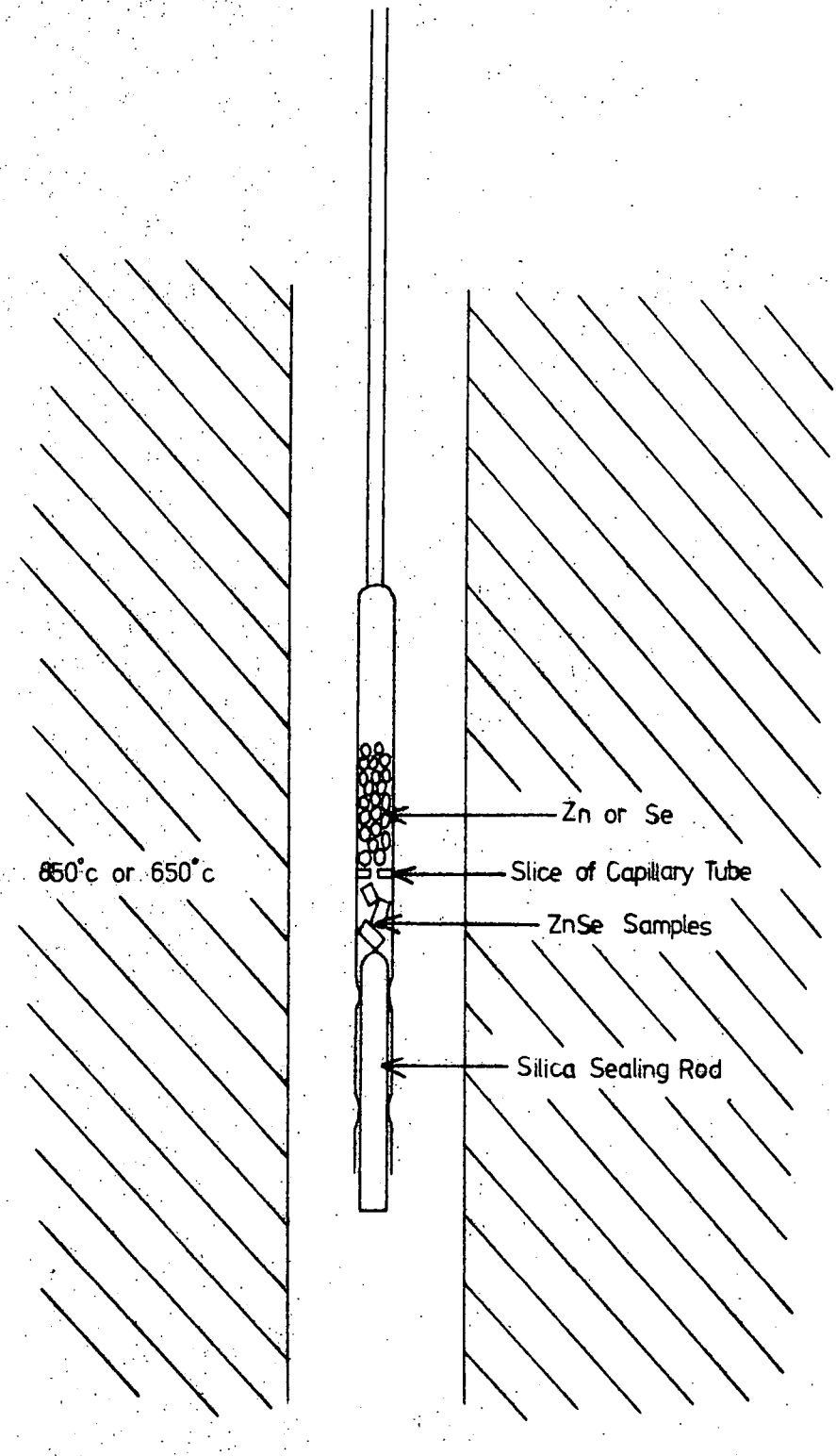

Fig. 3-4. Tube used for heating ZnSe in various molten Elements and Alloys.

was therefore devised by which crystals could be heated in a solvent of liquid zinc, zinc alloys or selenium in order to either purify or dope samples.

The treatment was carried out in a silica tube as illustrated in figure 3.4. Before use all silica was washed in acetone, concentrated nitric acid and then chromic acid. Finally it was washed in acetone and baked for a day at 100°C. A slice from a capillary tube was used to prevent the crystal floating on the melt and also to facilitate the separation of the crystal from the melt after treatment. The tube was evacuated and flushed with argon several times and finally sealed at a pressure of 10^{-5} torr. The seal to the silica rod nearest the crystal was made only after the tube had been evacuated to prevent oxidation of the sample. Either Koch Light or Metals Research 5N zinc or Metals Research 5N selenium was used. Five grams of molten zinc were used to treat about 0·1 grams of zinc selenide. Any metallic dopant such as indium, copper or aluminium was simply added to the zinc charge. The tube was suspended vertically and kept at 850°C in the case of zinc and its alloys, and 650°C when selenium was used. At the end of a week the tube was inverted to separate the crystal from the melt and was cooled to room temperature within about a minute. Prior to this treatment the crystals were either etched or cleaved to remove surface damage and the zinc was found not to stick to the surface on inversion. Samples for electrical measurements were subsequently etched before the contacts were applied whereas the luminescent properties were studied without etching.

When it was necessary to heat a sample alone, exactly the same procedure was followed, apart from the solvent, as regards time, temperature and evacuation of the tube.

CHAPTER 4

EXPERIMENTAL PROCEDURE

4.1 LUMINESCENCE MEASUREMENTS

(a) Apparatus

An Optica 4 NI grating spectrometer was used in conjunction with an Oxford Cryogenics cryostat when measurements were made using liquid helium. The automatic recording spectrometer was equipped with an E.M.I. photomultiplier type 9781 R with an extended S.5 photocathode. The cryostat had a helium capacity of about 1·5 litres and the sample block was directly cooled. The crystal was held in contact with the sample block by means of indium solder and maintained at a pressure of less than 10^{-3} torr.

The majority of the measurements, however, were made using a Barr and Stroud double monochromator type VL.2 fitted with Spectrosil A quality prisms. This was used either to analyse the light emitted from the crystal so as to obtain the emission spectrum, or as a source of monochromatic light to enable excitation spectra to be measured. The experimental arrangements are shown diagrammatically in figures 4.1 and 4.2. At all times the detector was an E.M.I. photomultiplier type 9558 with a trialkali S.20 photocathode. The photomultiplier was run at voltages up to 1000V obtained from a Brandenburg photomultiplier power supply model 472 R. The output from the collector was earthed via a 10 K.ohm load resistor and the voltage across the resistor was taken both to a Philips valve voltmeter type P.M. 2440 and the input of a Brookdeal lock-in amplifier type 401. The reference voltage for the amplifier was obtained by allowing the multibladed chopper across the entrance

slit of the monochromator to interrupt a light falling on a photodiode fed from the internal 9 volt supply of the amplifier. The output from the amplifier was taken to a Honeywell 12 inch chart recorder. The lock-in amplifier was used to obtain all the results. The Philips meter was used to ensure that no strong light was reaching the photomultiplier and for preliminary mirror alignment. Either a 40 or a 2 bladed chopper was driven from a synchronous motor via a flexible drive. The resulting chopping frequencies were either 200 or 10 cps.

The cryostat used for the measurements down to liquid nitrogen temperatures was an open sided copper enclosure with a silica window at one end and a vacuum inlet at the other. Plates holding various filters were used to provide a vacuum tight seal at the side. The sample block was also made of copper and could be rotated about a vertical axis to face any direction. It was directly cooled by liquid nitrogen contained in a nickel-silver cylinder above it. A copper-constantan thermocouple was held in contact with the block and showed that the temperature reached 85 ^{o}K with liquid nitrogen present. Heating was carried out using an external 25 watt heater introduced into the nickel-silver cylinder. Temperatures up to 400 ^{o}K could be obtained. During operation the pressure in this cryostat was reduced to 10^{-1} torr by means of a rotary pump.

(b) Sample preparation

Both cleaved and etched samples were used. Both techniques were found to give identical results. It was necessary for any surface damage to be removed by etching prior to measurements otherwise the luminescence was considerably reduced, probably as a result of the presence of non-radiative recombination centres at the surface. Crystal dimensions were of the order of 4 x 2 x 1 mm. Samples were held in contact with the block by silicone vacuum grease which proved satisfactory at all temperatures encountered. The grease did not itself produce any emission.

Fig. 4-1.

Arrangement for Measuring the Photoluminescent Emission Spectrum of Zinc Selenide Crystals

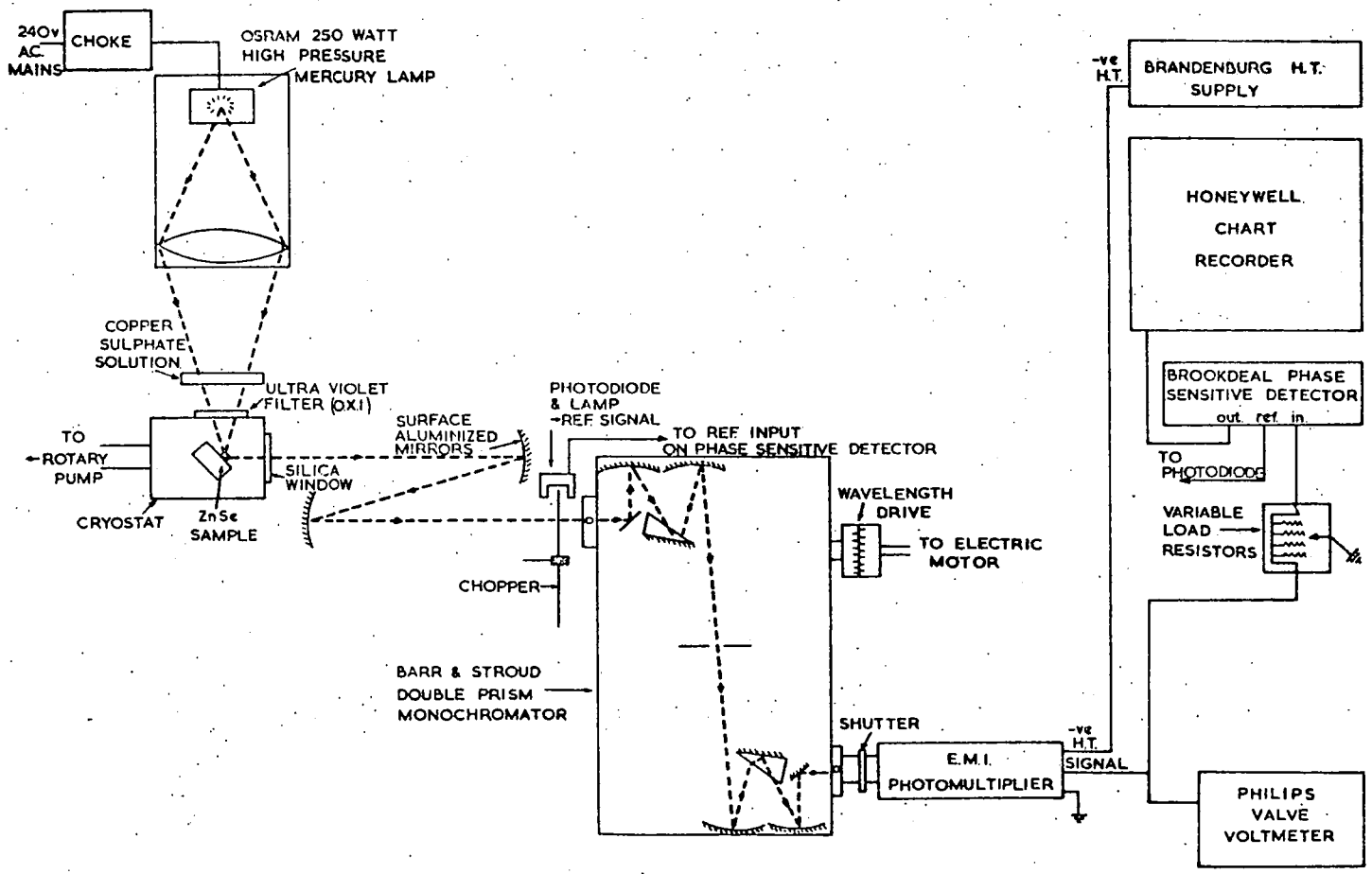

(c) Emission Spectra

Figure 4.1 shows the experimental arrangement used for measuring the emission spectra of the crystals. Light from a 250 watt compact source mercury lamp was focussed onto the sample and a Chance OX.1 filter was used to isolate the 3650 Å mercury line. A 1 cm. path length of 10% copper sulphate solution plus a Chance HA.3 heat absorbing filter were used to remove any infra-red radiation which might have produced quenching or stimulation effects. The emission from the crystal was scanned at about 400 Å per minute in the direction of shorter wavelength. The slits were normally set to admit a bandwidth of about 50 Å. Several spectra were obtained using lower energy excitation. In these cases a suitable interference filter was substituted for the OX.1 filter and the mercury lamp was replaced by a 250 watt 24 volt quartz-halogen projector lamp so as to produce a continuous spectrum. The chopping frequency was always left at 200 cps.

(d) Excitation Spectra

To obtain the excitation spectra the apparatus was rearranged as shown in figure 4.2. The quartz-halogen lamp was used in conjunction with the monochromator to produce a monochromatic beam of light which was directed onto the crystal. In order to isolate the luminescent emission from the excitation a combination of filters was used. This consisted of a Chance glass filter and a circular Barr and Stroud interference filter arranged to have a bandwidth of about 350 Å at 6000 Å and 270 Å at 5300 Å. When observing orange and red emissions an OR.1 Chance filter was used and when the green emission was of interest an OY.2 filter was used. Once the emission band had been excited the interference filter was adjusted to provide a maximum signal.

The chopping frequency was found to have an effect on the resulting excitation spectrum and hence occasionally both frequencies were

Fig. 4-2.

Arrangement for Measuring the Photoluminescent Excitation Spectrum of Zinc Selenide Crystals

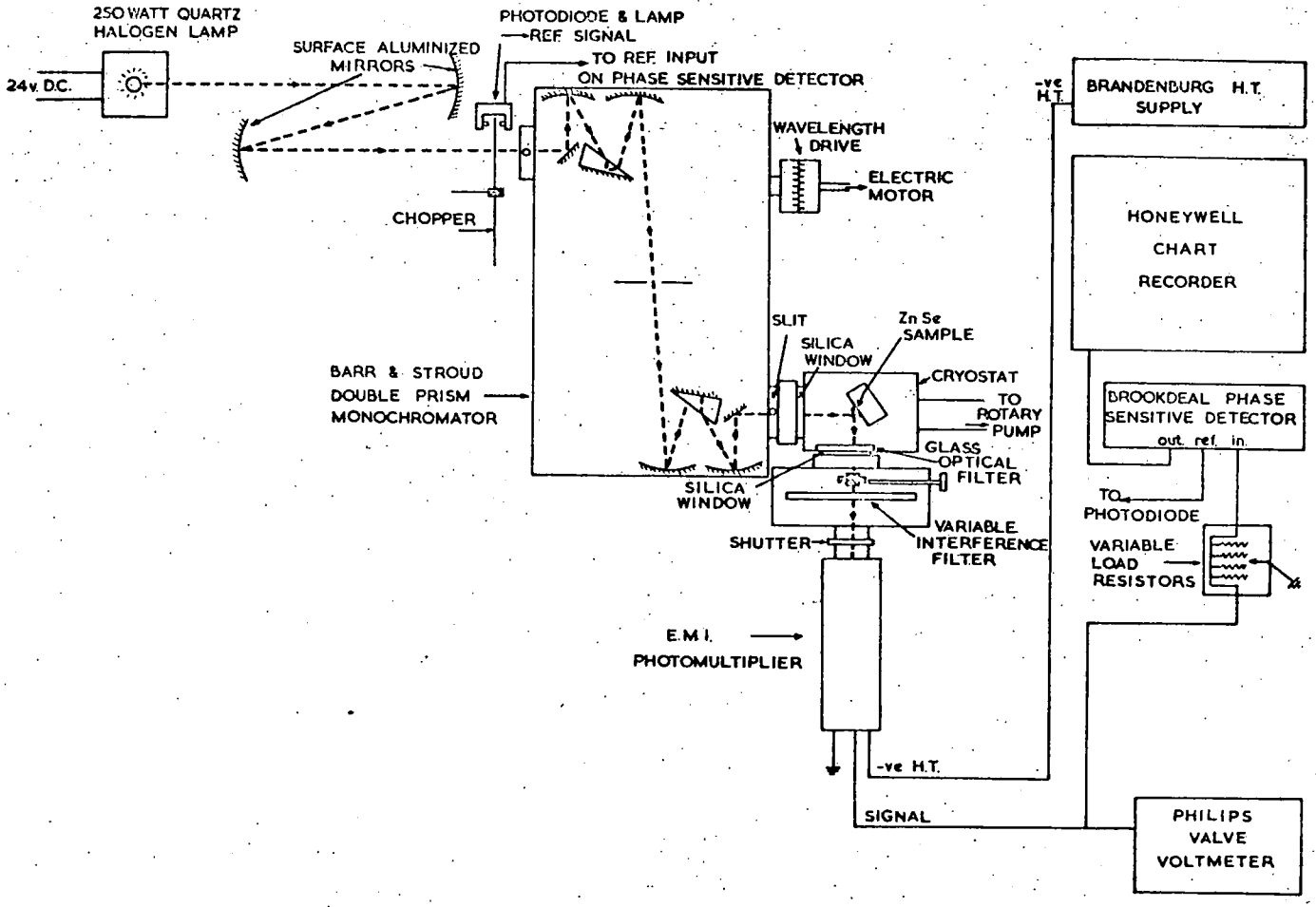

used. The variations and reasons for them will be described later.

In order to provide sufficient intensity to excite the sample, the slits of the monochromator had to be opened resulting in a bandwidth of 200 Å. Again the spectrum was scanned at about 400 Å per minute towards shorter wavelength.

(e) Expression of Results

The shape of an emission curve depends upon the units used to describe the intensity of the emitted light. Almost invariably the intensity is expressed in relative terms since it is extremely difficult and usually unnecessary to know the absolute value. In most experimental data the intensity is expressed as the relative emitted energy per unit wavelength interval I_λ. It can also be expressed in terms of energy per unit frequency interval I_ν, or number of photons per unit energy of emitted photons $I_{h\nu}$. These last two forms are more of theoretical interest and can in fact be related to I_λ.

The units used to describe the emission intensity decide the form in which the abscissa is represented. If $I_{h\nu}$ is chosen, the abscissa will be expressed in terms of energy, usually electron volts. As stated however, I_λ is the most common form in which the intensity is expressed and therefore the abscissa is usually in the form of wavelength, either Angstrom units or microns.

Results in this thesis are expressed in terms of I_λ plotted against wavelength in the form of Angstrom units. How I_λ was obtained from the original data will be explained in section (f).

In all the results quoted in this thesis, the half-width of a particular band is taken to be the full width of the band at half height.

(f) Correction Factors

The experimental results must be corrected for various factors which may be unique to a particular series of experiments. For example, with

the emission spectra two variables existed. They were the spectral sensitivity of the photomultiplier and the dispersion produced by the spectrometer. The former was obtained by comparing the emission from a continuous source seen by the photomultiplier with that seen by a vacuum thermopile. Since the latter measures the emission directly in terms of energy, the true response of the photomultiplier could be obtained. The dispersion of the spectrometer is a function of the prism material and values were supplied by the manufacturer. These values gave the variation in bandwidth with wavelength and thus enabled the signal to be corrected for unit wavelength interval. It was therefore possible to obtain a correction factor to enable I_λ to be found.

With excitation spectra the variable factors were the dispersion of the prism material and the spectral distribution of the exciting light. These were measured together by the photomultiplier to obtain I_λ. The resulting excitation spectra were therefore expressed in terms of emission intensity for equal excitation energy per unit wavelength interval.

4.2 HALL EFFECT MEASUREMENTS

(a) Apparatus

A brass cryostat built in this department was used to house the sample during all measurements which did not involve liquid helium. For the liquid helium measurements a stainless steel, Oxford Cryogenics cryostat was used. However since it was only used occasionally and was based on a similar design to the brass cryostat it will not be described here. The nitrogen cryostat is illustrated in figure 4.3. Liquid nitrogen was held in a container of about 1 litre capacity, connected to the sample block by a 60 cm. nickel-silver tube which formed an exchange space. This space could be evacuated or filled with helium gas when necessary. A silica window was provided opposite the sample and if required the sample could be illuminated via a mirror mounted at 45° to

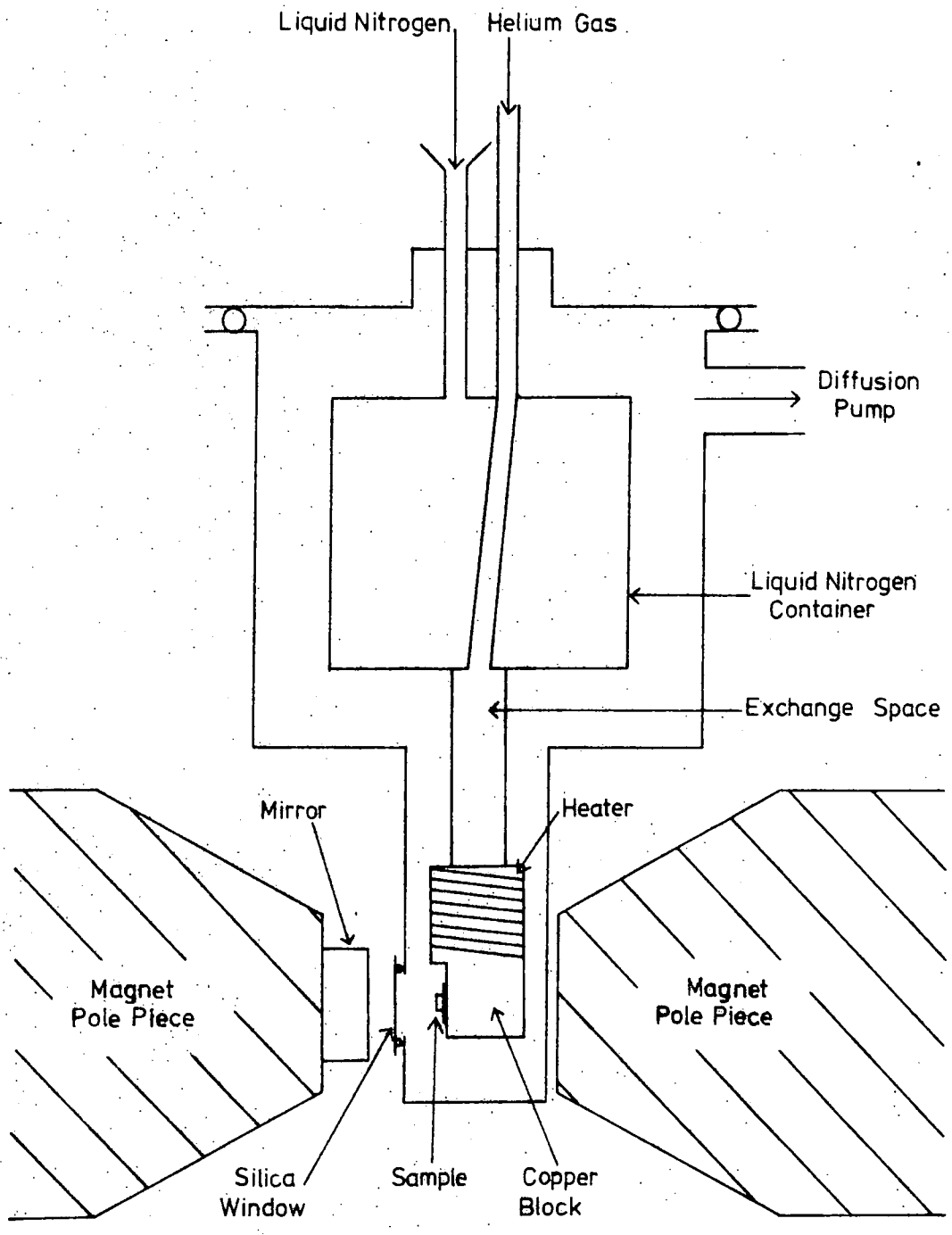

Fig.4-3. Cryostat used for Hall Effect Measurements.

it on one of the magnet pole pieces. The illumination consisted of a 48 watt tungsten lamp focussed onto the sample through a copper sulphate filter. The window was kept covered during measurements unless otherwise stated. A 5 watt heater was wound directly onto the copper sample block as shown, and temperatures of up to 400°K could be readily obtained. Two copper-constantan thermocouples were used to monitor the temperature. One was mounted directly on the block, the other was connected to the sample holder. The reference junction for the thermocouples was held at 77°K in a dewar of liquid nitrogen. The sample holder was held onto the block by a mechanical clamp. Nonaq stopcock grease was found to provide the best thermal contact between the block and the sample even at the lowest temperatures encountered. All electrical connections were made via a 12-way glass to metal seal at the top of the cryostat. The pressure in the cryostat was maintained below 10^{-3} torr by an Edwards 1 inch oil diffusion pump.

When measurements were made in the range 400°K to about 120°K, the intercharge space was filled with helium gas at an excess pressure of about 1 atmosphere. Below 120°K liquid nitrogen was gradually added to the interchange space. If the space was filled with liquid nitrogen and pumped on with a rotary pump, a temperature of 65°K could be attained.

The magnet used was built in the department and possessed 5 cm. diameter tapering polepieces. It was air cooled and produced a field of 2 kilogauss across a 5·5 cm. gap.

The five probe method was used for making measurements (figure 4.4). This was employed as several samples were too small for the more common six probe method to be used successfully. The electrical supply to the sample was virtually a constant current source derived from a 60 volt battery. A Philips voltmeter type G.M.6020 was used to measure the various potential differences. In making the Hall measurements the standing voltage between the probes was backed-off using a Pye portable potentiometer in series with the voltmeter. If backing-off voltages greater

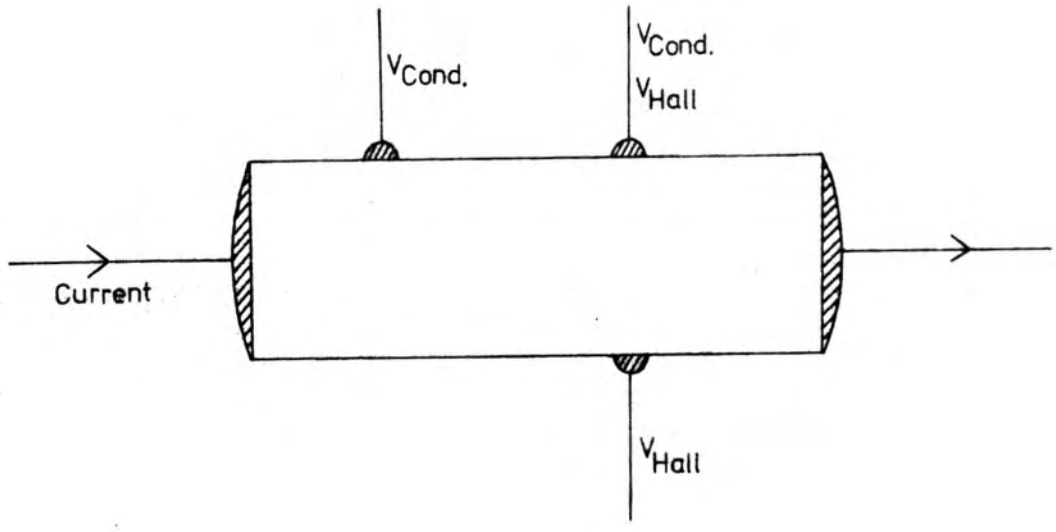

Fig. 4-4. Contact Arrangement used on Samples for Hall Effect Measurements. (5-Probe Method.)

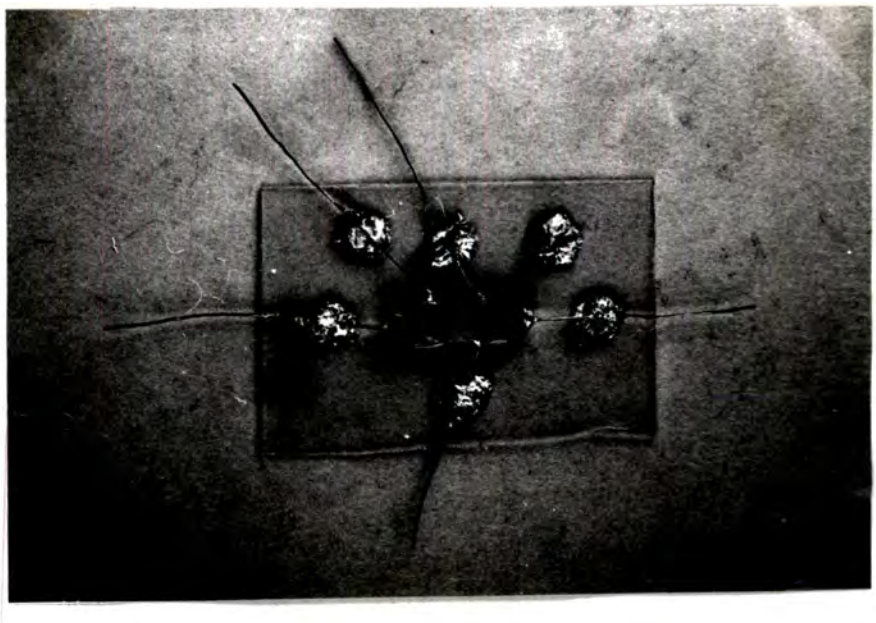

Fig. 4-5. Typical ZnSe Hall Effect Sample. (×2)

than 1·5 volts were needed a 9 volt grid bias battery was added. The current normally used was 5 milliamps and Hall voltages ranging from 30 millivolts to 0·01 millivolts were encountered. Similarly the voltage across the conductivity probes varied from about 15 volts to 10 millivolts.

(b) Sample Preparation

The sample dimensions were of the order of 8 x 2 x 1 mm. The rectangular bar cut from the boule was first ground with 600 grade carborundum powder to obtain flat and parallel sides. It was then etched as described in Chapter 3 to remove surface damage. Contact material was either indium or liquid indium-gallium alloy. Both components were supplied by Johnson Matthey as spectrographically standardized and contained less than 5 p.p.m. metallic impurity. The indium was pressed on to the crystal surface at the required points whereas the alloy had to be brushed on with a fine wire. The crystals were subsequently heated to about 250°C for 3 to 4 minutes in an atmosphere of oxygen-free nitrogen. This process diffused sufficient metal into the crystal to form both an ohmic and mechanically strong contact.

The sample was then fixed to a glass microscope cover slip as shown in figure 4.5, using Durofix cement. The sample was not shorted out as the resistivity of the cement was several orders of magnitude greater than that of the sample. However good thermal contact was made to the cover slip.

Electrical contact to the crystal was made by fine copper wires soldered to the cover slip with indium. The wires were fixed to the contacts simply by insertion when using the alloy. When indium contacts were used the wire was connected with Johnson Matthey air drying silver paste type FSP.51. A further indium dot was soldered on to the cover slip to take a thermocouple during measurements.

The current contacts onto the crystal were made as large as possible

both for strength and uniformity of current flow. The remaining probes were made as small as possible so as not to short out the crystal. A minimum diameter of about 1 mm. was necessary, however, to produce a strong bond. Both indium and indium-gallium were found to produce ohmic contacts on low resistivity material. Crystals with resistivities higher than about 10^4 ohm.cm. began to show slightly non-ohmic current-voltage plots and it seemed impossible to make ohmic contact to undoped material with a resistivity of about 10^{12} ohm.cm. However since almost all the measurements were made on low resistance samples the contacts could be considered ohmic over the whole temperature range studied. Indium was used to contact the majority of samples since it produced a much stronger mechanical bond than the alloy.

(c) Expression of Results

Equations 2.32 and 2.33 were used to calculate the Hall coefficient and conductivity. The material was assumed to be compensated with only one type of carrier present and hence equations 2.31 and 2.34 were used to obtain values for the carrier concentration, n, and the mobility μ. The scattering factor was assumed to be equal to unity unless otherwise stated. The results were plotted in the usual form, that is $\log n$ v. $\frac{1}{T}$ and $\log \mu$ v. $\log T$, so as to identify the donor ionization energy and the scattering processes from the slopes of the resulting curves.

CHAPTER 5

PHOTOLUMINESCENCE RESULTS - NON-LOCALISED CENTRES

5.1 INTRODUCTION

The results of the luminescence studies have been divided into two parts. The present chapter deals with impurities which are known to produce non-localised luminescence centres, for example copper, aluminium and indium while the following chapter is concerned solely with the luminescent properties of the activator manganese. Details of the growth conditions of all crystals described in this chapter are given in table 5.1. In the figures illustrating the emission and excitation spectra of the various crystals, the intensities are in arbitrary units and the spectra obtained at 85°K and room temperature are not shown to scale.

5.2 COPPER ACTIVATION

Copper impurity is considered first since its presence will be shown to have quite important effects upon the luminescence properties of many of the crystals examined during the course of this work.

Copper was introduced into two boules during growth. Crystals 158 and 169 were grown with 1000 p.p.m. copper selenide and 1% copper metal in the respective charges. Crystal 169 was dark green in body colour and appeared to contain a large quantity of precipitate, which was probably copper. Under 3650 Å excitation at 85°K this crystal emitted a single green band at 5300 Å with a half width of 0·21 eV (figure 5.1).

TABLE 5.1 CRYSTAL GROWTH CONDITIONS

Crystal No.	Starting Material	Dopant	Tail Conditions
2	D	-	No Tail
7	D	-	Zn
25	S	-	Zn 555°C
104	D	-	Zn 555°C
122	D	$ZnCl_2$	Zn 555°C
123	D	$ZnCl_2$	Zn 555°C
135	Op	0.05gms$ZnCl_2$+0.2mgmsCuSe	Zn 555°C
136	Op	0.2 gms$ZnCl_2$+0.2mgmsCuSe	Zn 555°C
139	D	In	Zn 555°C
140	D	20 mgms Ga	Zn 555°C
142	D	In	Zn 555°C
150	D	2 mgms In	Zn 555°C
152	D	2 mgms In	Zn 555°C
153	D	2 mgmsMnSe+20mgmsAl	Zn 555°C
158	Op	20 mgms CuSe	Zn 555°C
169	D	0.2 gms Cu	Zn 555°C
171	Op	-	Se 335°C
172	Op	-	Se 360°C
173	Op	-	Se 385°C
177	Op	-	Zn 555°C
181	Op	2 mgms In	Zn 555°C
187	Op	20 mgms Al	Zn 555°C
188	Op	2 mgms Ga	Zn 555°C
197	S	-	Se 310°C
909	Op	16 mgms I	Iodine Transport

Mass of ZnSe Charge = 20 gms for Vapour Phase Transport

4 gms for Iodine Transport

D = Derby Luminescents
Op = B.D.H. Optran
S = Synthesized from Elements.

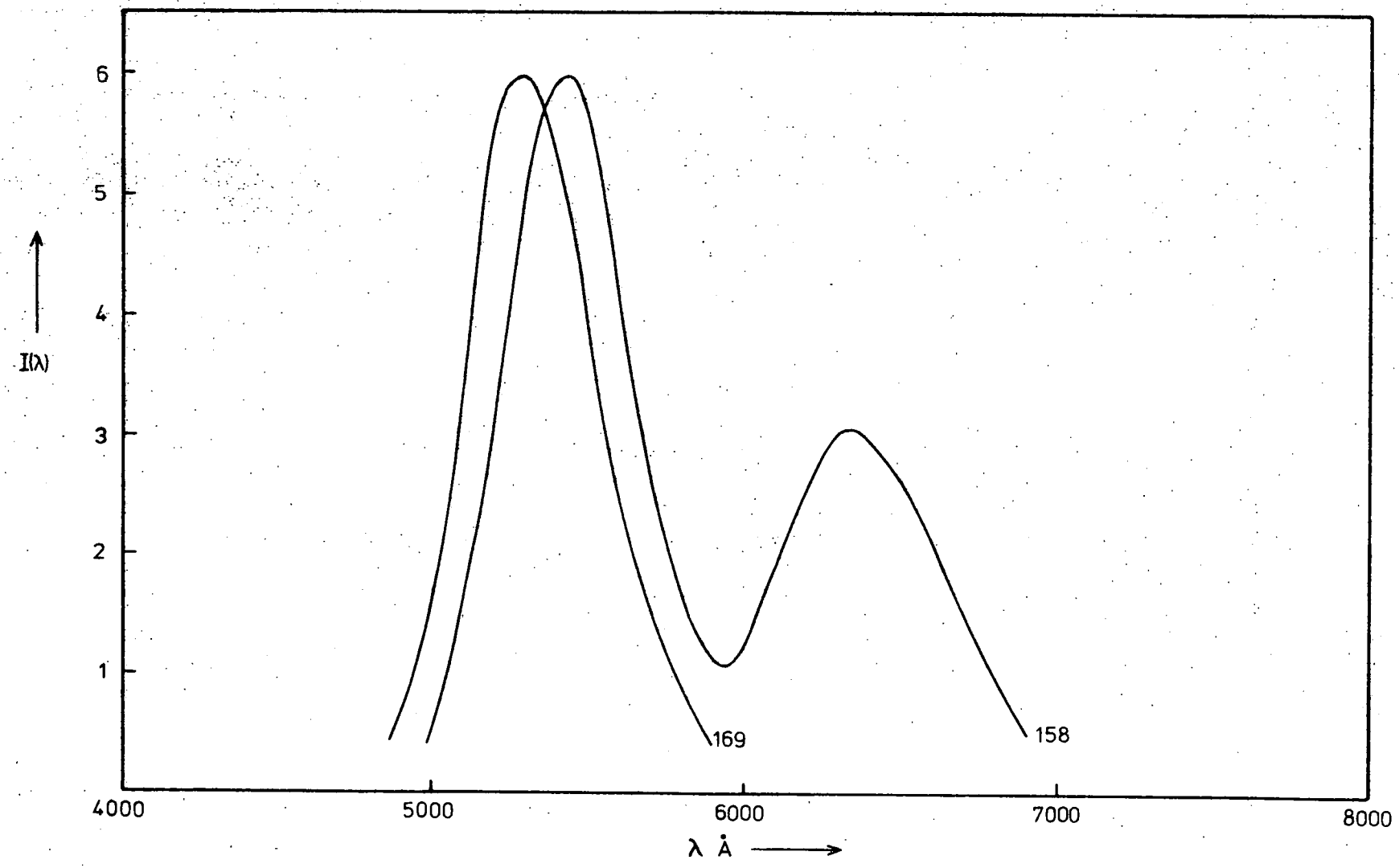

Fig. 5-1 Emission Spectra of ZnSe:Cu 169 and ZnSe:Cu 158 at 85°K under 3650 Å Excitation.

There was no measurable emission at room temperature. Crystal 158 was transparent with a yellow body colour and was found to emit in two bands at 85°K (figure 5.1). A green band was observed at 5450 Å with a half width of 0·20 eV together with a red band with the same half width at 6340 Å. At room temperature a single red band at 6400 Å with a half width of 0·28 eV was observed.

Measurement of the excitation spectrum of the green emission of 169 was only possible at wavelengths shorter than 4750 Å due to the overlap in wavelength of the excitation and the emission being monitored. The only band detected was at approximately 4440 Å and probably corresponded therefore to direct band to band excitation. The bandgap of zinc selenide at 85°K is approximately 2·8 eV which corresponds to excitation radiation of wavelength 4430 Å. At room temperature the band gap decreases to about 2·65 eV with a corresponding excitation wavelength of 4680 Å.

More information was obtained from crystal 158 however. When the red band was monitored at 85°K the excitation spectrum revealed a broad band at about 5100 Å together with a peak at approximately 4500 Å. When the measurement was carried out at the higher temperature of 130°K, the low energy excitation band increased by a factor of about five. This suggests that the low energy band is associated solely with the red emission and decreases when the green band begins to dominate. The green emission was excited by light within a broad band which appeared to be composed of sub-bands at 4600 Å and 4750 Å.

In order to study the effects of copper doping further, several samples from the undoped boule 171 were heated for a week at 850°C in molten zinc containing various concentrations of copper. The excitation spectra of these crystals measured at 85°K can be seen in figure 5.2. The long wavelength band at 5100 Å mentioned previously became quite prominent. It appeared to be built up from two sub-bands in the region of 5100 Å and 4700 Å. The emission spectra of these three crystals measured

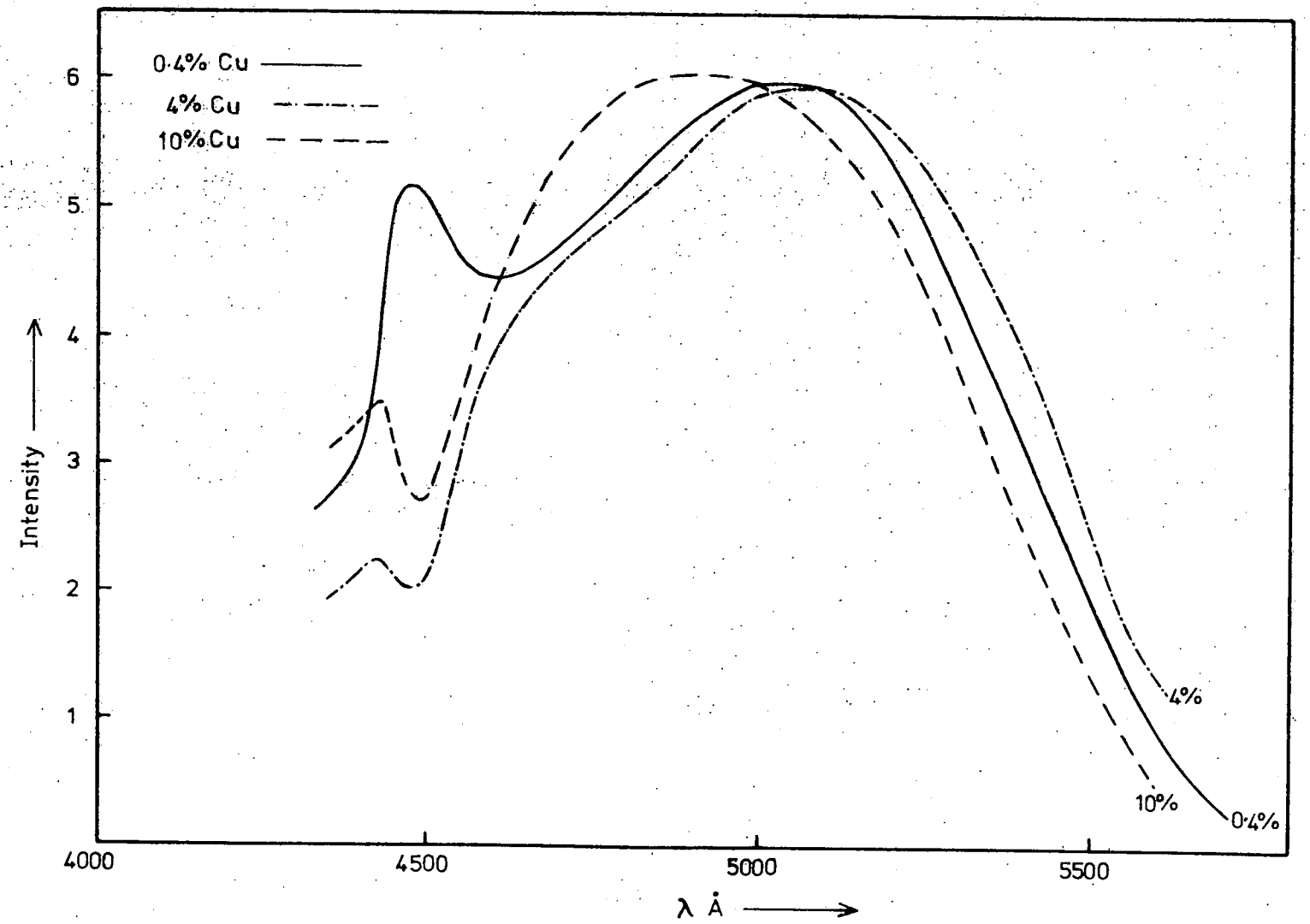

Fig. 5-2. Excitation Spectra at 85°K of ZnSe 171 heated in Zn plus various Concentrations of Cu.

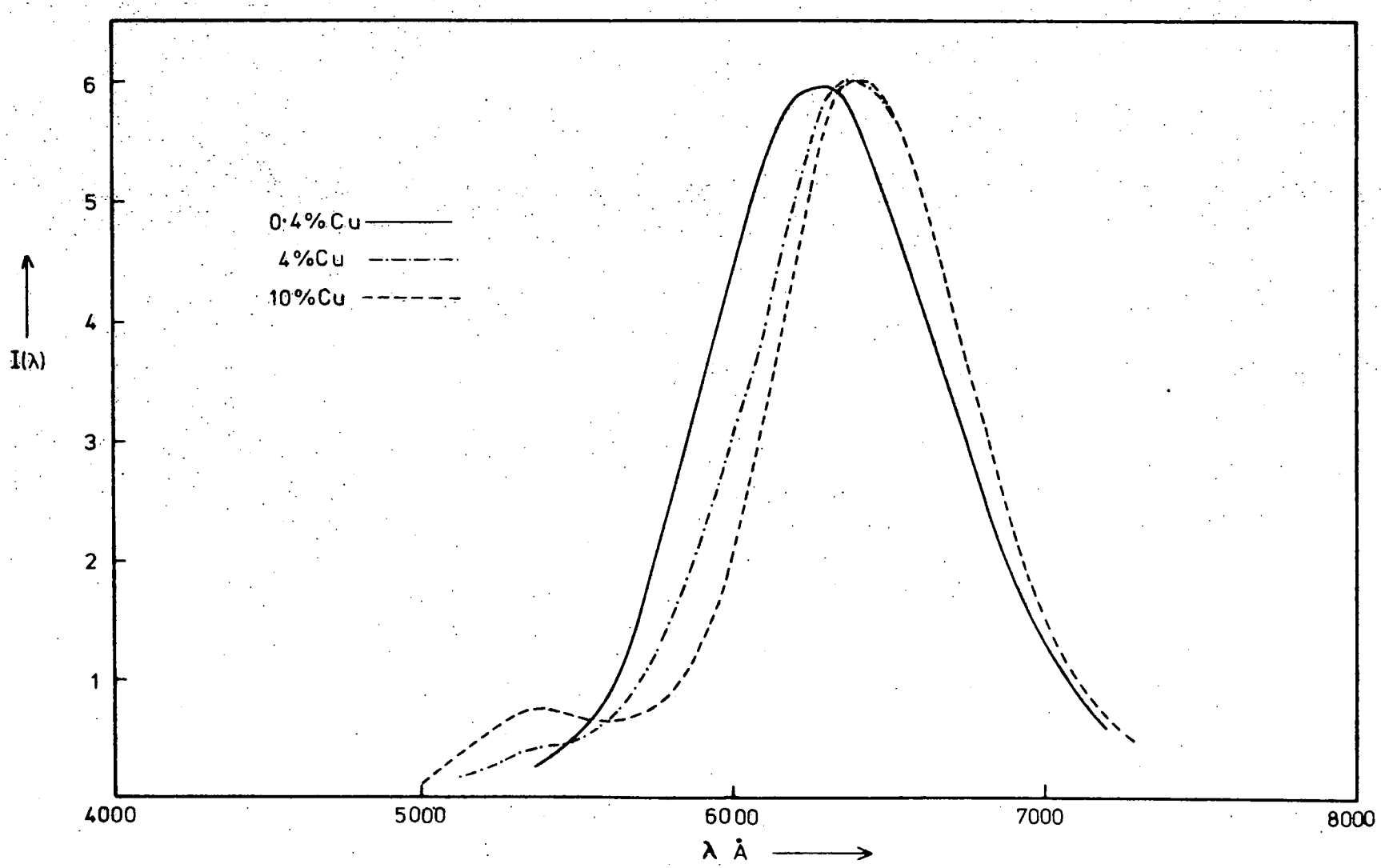

Fig. 5-3. Emission Spectra at 85°K from ZnSe 171 heated in Zn plus various Concentrations of Cu. (3650 Å Excitation)

at 85°K under 3650 Å excitation are shown in figure 5.3. The orange band appeared to shift to lower energy and became narrower as the copper concentration increased. With the crystal heated in zinc plus 10% mole copper the emission peak lay at 6400 Å and had a half width of 0·22 eV. The corresponding half widths of the 4% mole and 0·4% mole crystals were 0·25 eV and 0·28 eV. Evidence will be presented to show that the increase in width and the displacement of the emission to higher energy with decreasing copper content are due to the appearance of a second orange band superimposed on the copper emission. This second band will be shown to be the self-activated emission of zinc selenide. The high energy excitation band observed near the bandgap in the samples heated in zinc plus 0·4% and 4% copper is probably associated with this self activated emission.

The high energy copper emission observed in crystal 158 was also detected in the sample heated in zinc plus 10 at.% copper and also to a lesser extent in the 4% copper sample. The maximum was again found to lie at about 5400 Å.

In an attempt to resolve the low energy emission band, light of wavelength within the low energy excitation band was used to excite the crystals. Light passed by a 5300 Å interference filter was found to isolate and excite the emission most effectively. At 85°K all crystals mentioned so far, except 169, were found to emit a narrow red band at 6400 Å with a half width of 0·20 eV when excited by this filtered light. On heating to room temperature this band shifted to longer wavelength to about 6460 Å and increased in width to about 0·28 eV. This is considered to be the resolved low energy emission band associated with copper and is illustrated later (figure 5.9).

Further details of copper activation will be discussed after the effects observed in some undoped and chlorine doped samples have been considered.

5.3 SELF-ACTIVATION

In order to study the effects of heating zinc selenide in liquid zinc only, samples from the same boule as that used for the copper diffusion studies were heated in liquid zinc for the same time and at the same temperature, that is one week at 850°C. The resulting crystals, which had become green in body colour, were luminescent in the red region again but now the emission consisted of a broad band centred at 6150 Å at 85°K. On heating to room temperature the band increased in width from about 0·28 eV to 0·4 eV and shifted to about 6050 Å (figure 5.4.). This shift towards higher energy with increasing temperature is in the opposite direction to that observed with the low energy copper band and is in the same direction as the shift of the self-activated blue emission in zinc sulphide. It is reasonable to assume therefore that the red band with a maximum at 6150 Å at 85°K is the self-activated (S.A.) emission of zinc selenide. The excitation spectrum of this crystal consists of a band at 4670 Å at 293°K which shifts to 4460 Å when the crystal is cooled to 85°K (figure 5.5). The position and shift of the wavelength of this band with temperature suggest that it is probably associated with a band to band transition.

It is clear that heating in zinc was not responsible for the long wavelength excitation band at 5100 Å observed in the samples heated in zinc plus copper. In fact when a piece of the copper doped boule 158 was heated in liquid zinc, the subsequent emission and excitation spectra were identical to those of the undoped, zinc treated crystal. This agrees with the results of Aven and Woodbury (1962) who extracted copper from zinc selenide using molten zinc. When light with a wavelength of 5300 Å was used to excite the zinc treated crystals, no emission was obtained. The high energy excitation bands near the bandgap energy in the crystals heated in zinc plus 0·4% copper and zinc plus 4% copper are clearly attributable to the presence of S.A. emission which also increased the width of the emission band.

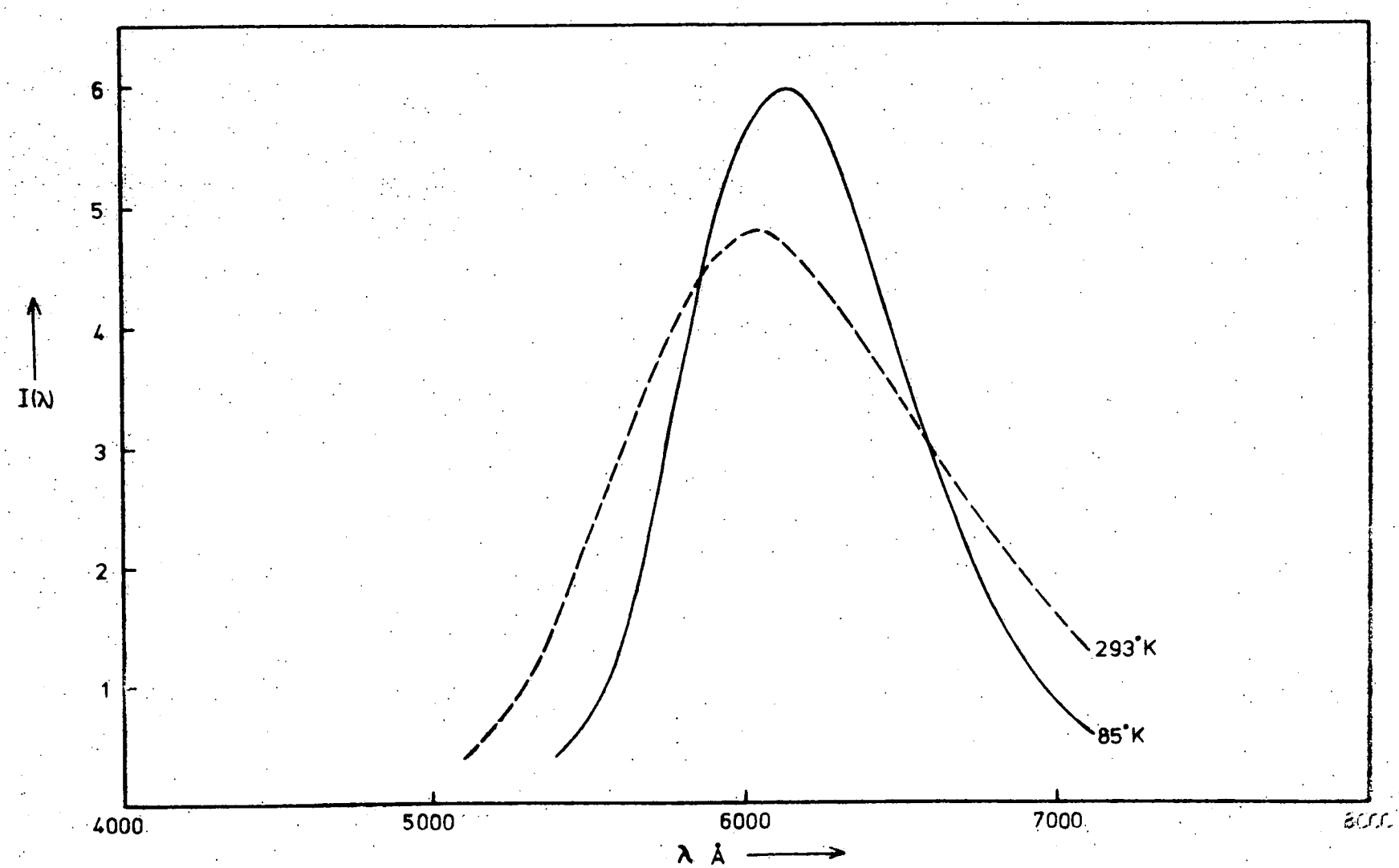

Fig. 5-4. Emission Spectrum of ZnSe 171, heated in Zn, under 3650 Å Excitation. (S.A. Emission)

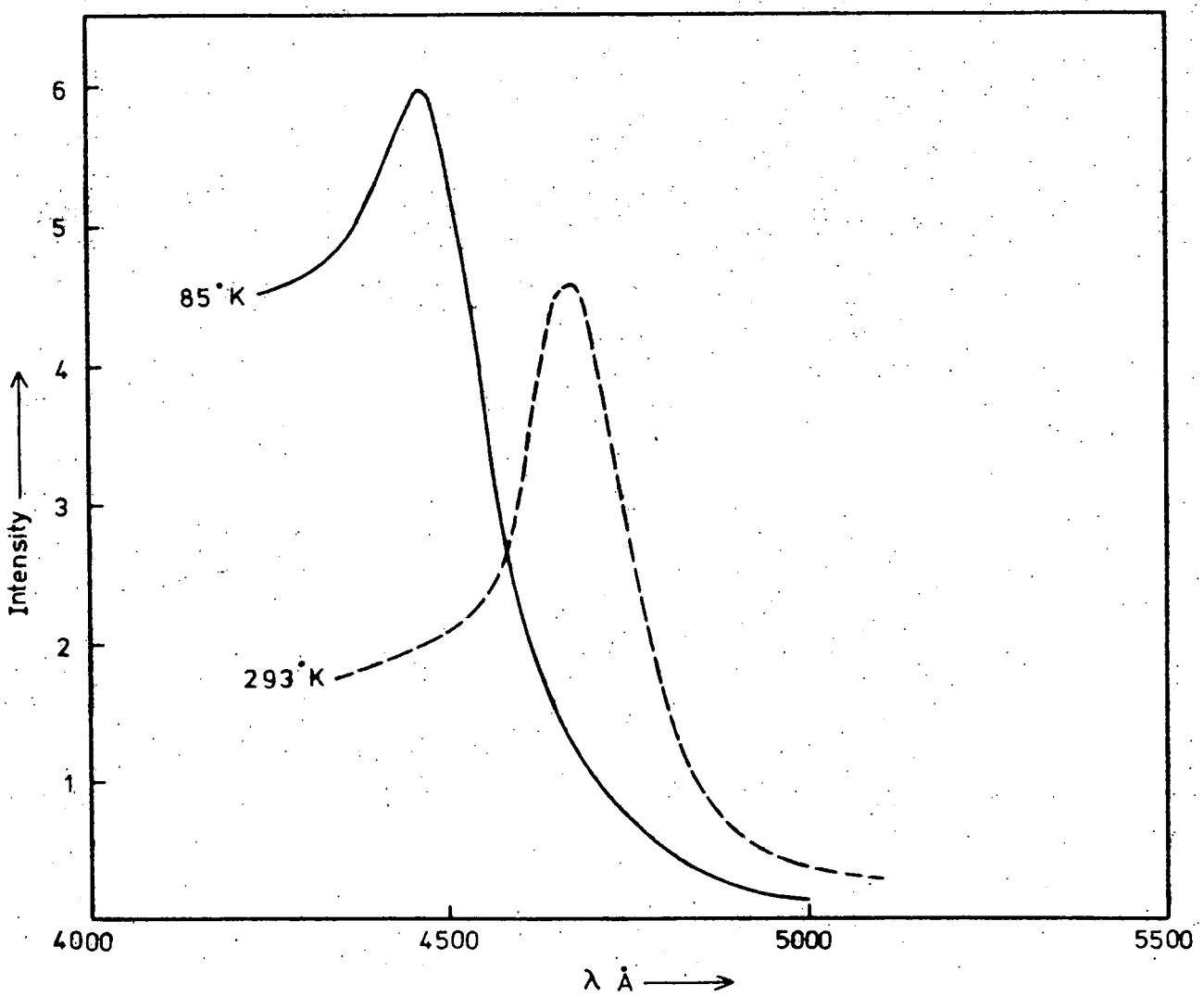

Fig.5-5. Excitation Spectrum of ZnSe 171 heated in Zn. (SA Emission).

The temperature dependence of the position and width of the S.A. band was studied using the undoped crystals 7 and 171 after they had been heated in zinc. The variation in the position of the emission maximum is shown in figure 5.10 together with the results of other crystals which will be dealt with later. The variation of the emission band width with temperature is shown in figure 5.11 with some results from other crystals. The band width changes fairly linearly with temperature by about 6×10^{-4} eV/°K. However, the position of the emission peak is almost independent of temperature until the temperature falls below about 170°K whereupon the band shifts to longer wavelengths.

To summarize the main results so far, it appears that copper activation produces a red emission band at 6400 Å at 85°K with a corresponding excitation band at about 5100 Å. A green emission band associated with copper is sometimes observed at 85°K either at 5300 Å or 5450 Å. When crystals which emit the 6400 Å copper band are heated in liquid zinc, this emission is removed and replaced by a broad band at 6150 Å at 85°K which has an excitation peak at approximately bandgap energy. This 6150 Å emission was found to shift to higher energy on warming and is assumed to be the S.A. emission of zinc selenide.

5.4 CHLORINE COACTIVATION

Chlorine was introduced into several boules during growth by adding zinc chloride to the reservoir attached to the growth capsule. Two crystals were studied, 122 and 123. Both had an orange body colour and under 3650 Å excitation emitted broad bright orange bands (figure 5.6). The bands were identical at room temperature with a maximum at 6460 Å and a half width of 0.295 eV but at 85°K the positions of the maxima differed by about 100 Å. Crystal 123 emitted a band at 6160 Å with a half width of 0.30 eV whereas 122 emitted a narrower band (0.26 eV) at the longer wavelength of 6250 Å. The excitation spectra of the two crystals were very different (figures 5.7, 5.8). The excitation spectrum of crystal 122 at 85°K consisted of a main band at 5150 Å with a shoulder at approximately 4700 Å.

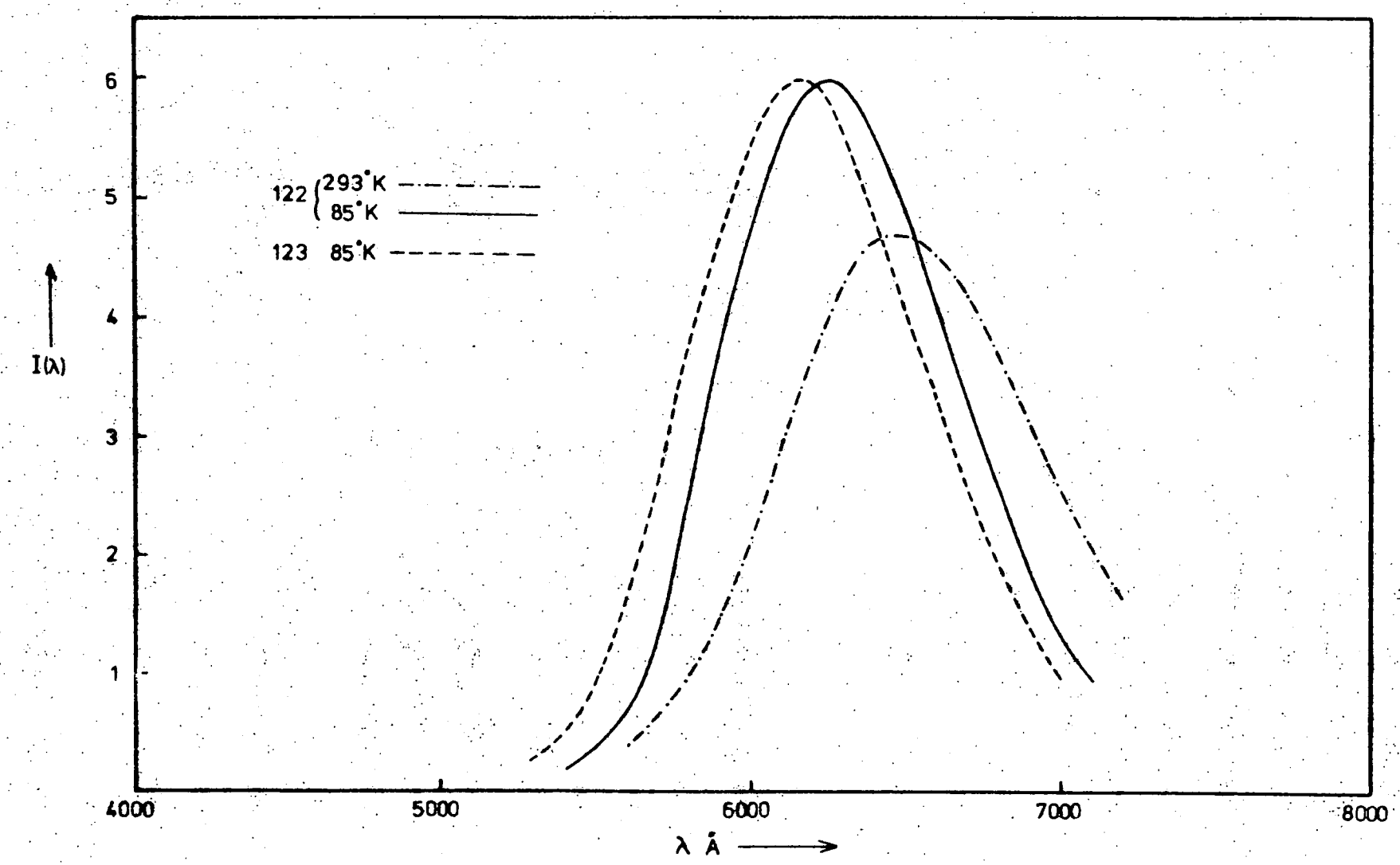

Fig. 5-6. Emission Spectra under 3650 Å Excitation of ZnSe:Cl 122 and ZnSe:Cl 123

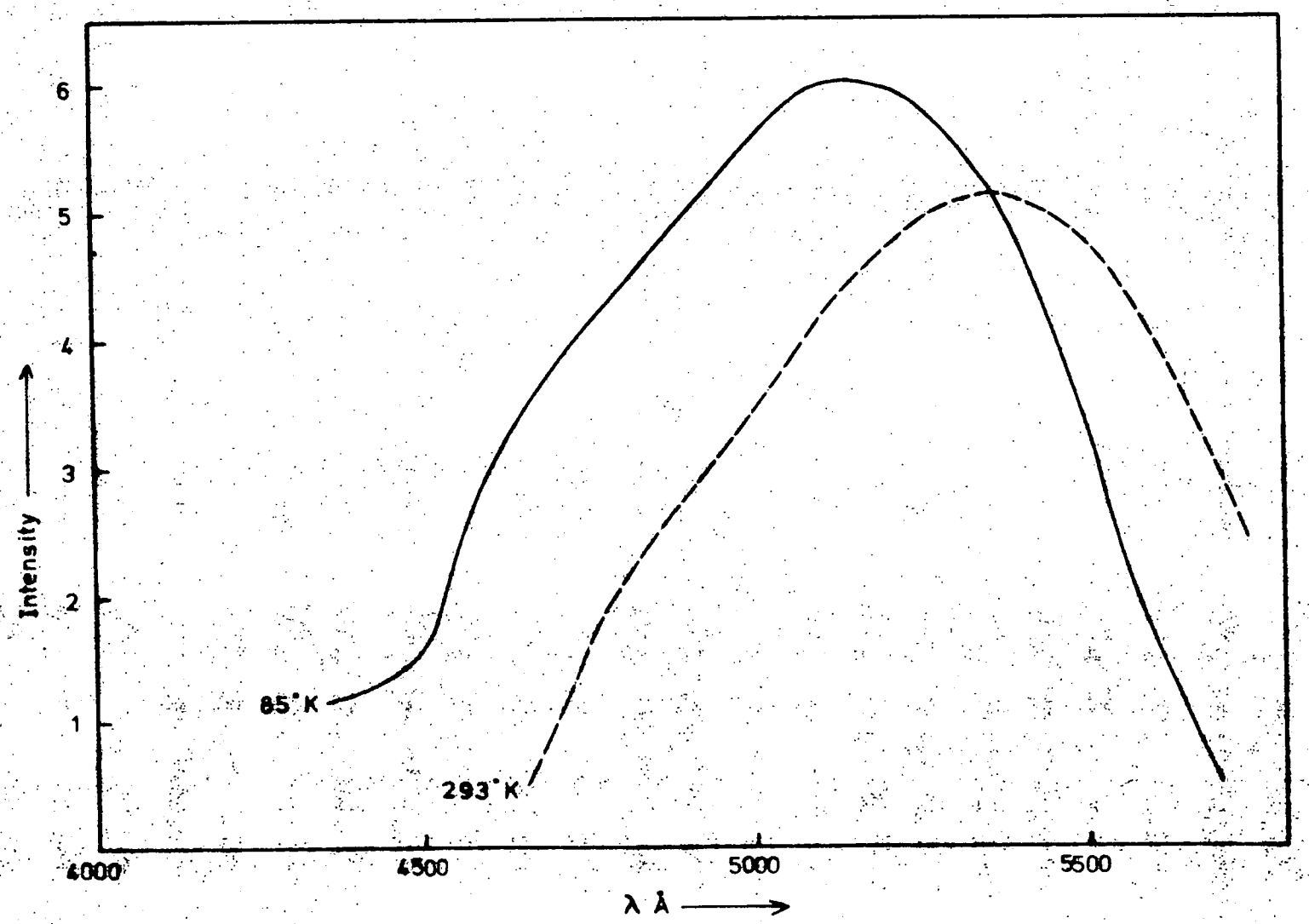

Fig.5-7. Excitation Spectrum of ZnSe:Cl 122.

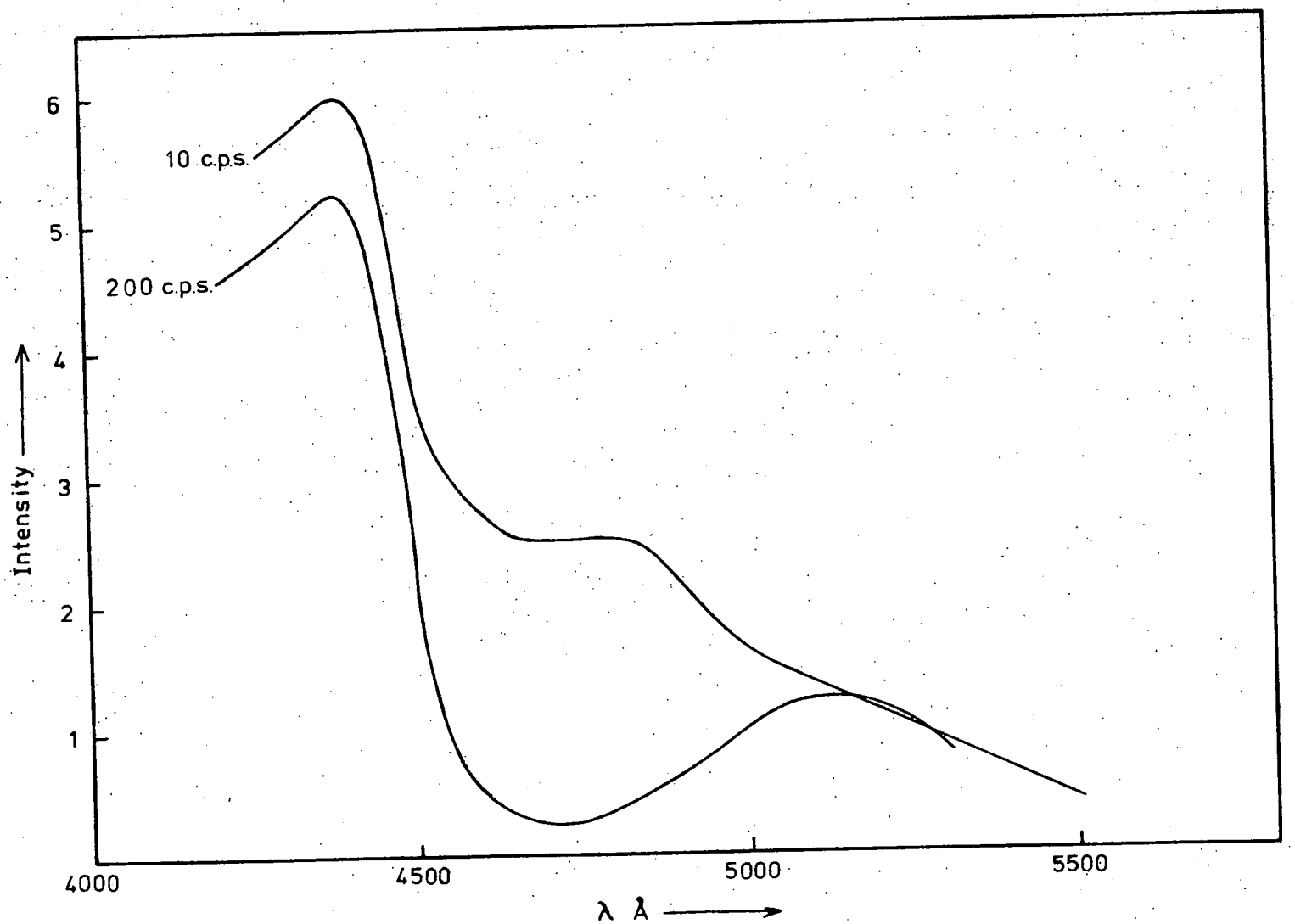

Fig.5-8. Excitation Spectrum at 85°K of ZnSe:Cl 123.

The main feature of the excitation spectrum of crystal 123, however, was a peak at 4400 Å corresponding to bandgap excitation. There was a subsidiary band at 5150 Å together with a band at approximately 4800 Å which was only revealed when the excitation was chopped at 10 c.p.s. This probably infers that that particular excitation process is associated with a recombination process with a long response time. It was not possible to measure the excitation spectrum of crystal 123 at room temperature.

The excitation spectra of crystals 122 and 123 can be explained if it is assumed that copper or a centre with identical properties, is present in both these crystals. This would explain the appearance of the long wavelength excitation band at about 5150 Å at 85°K which was observed previously in both the as-grown copper doped sample and the crystals treated in zinc plus copper melts.

When light with a wavelength of 5300 Å was used to excite the two chlorine doped crystals, a narrow band at 6400 Å similar to the red copper emission, was observed. This was especially prominent in crystal 122 (figure 5.9). The temperature variation of the position of the band maximum and the halfwidth of this red emission is shown in figures 5.10 and 5.11. Results from a number of crystals apart from 122, including some known to contain copper, are also shown. It appears that the behaviour of the red band emitted by crystal 122 is identical to that of the other crystals. It is concluded therefore that this long wavelength band is associated with copper impurity in all cases. The halfwidth of the copper band is much less than that of the S.A. emission and varies by 4×10^{-4} eV/°K. The maximum of the emission shifts from about 6400 Å at 85°K to 6480 Å at 293°K at the rate of $1{\cdot}1 \times 10^{-4}$ eV/°K.

The excitation band at the bandgap in crystal 123 is probably associated with the S.A. band. The presence of the S.A. band in this sample caused the emission measured under 3650 Å excitation to appear to consist of a band at a higher energy than that of 122 which contained a larger

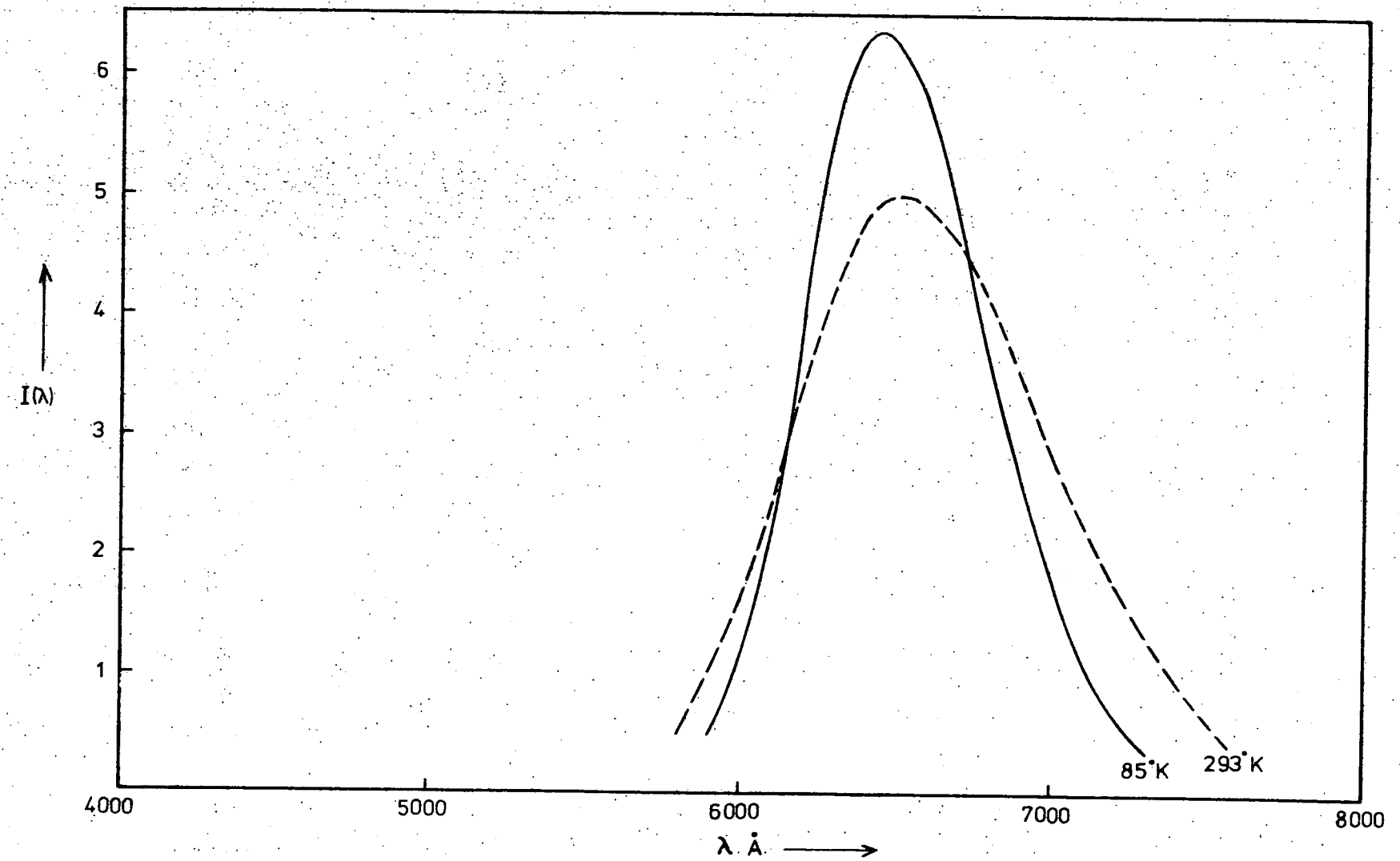

Fig. 5-9. Emission Spectrum under 5300 Å Excitation of ZnSe:Cl 122.

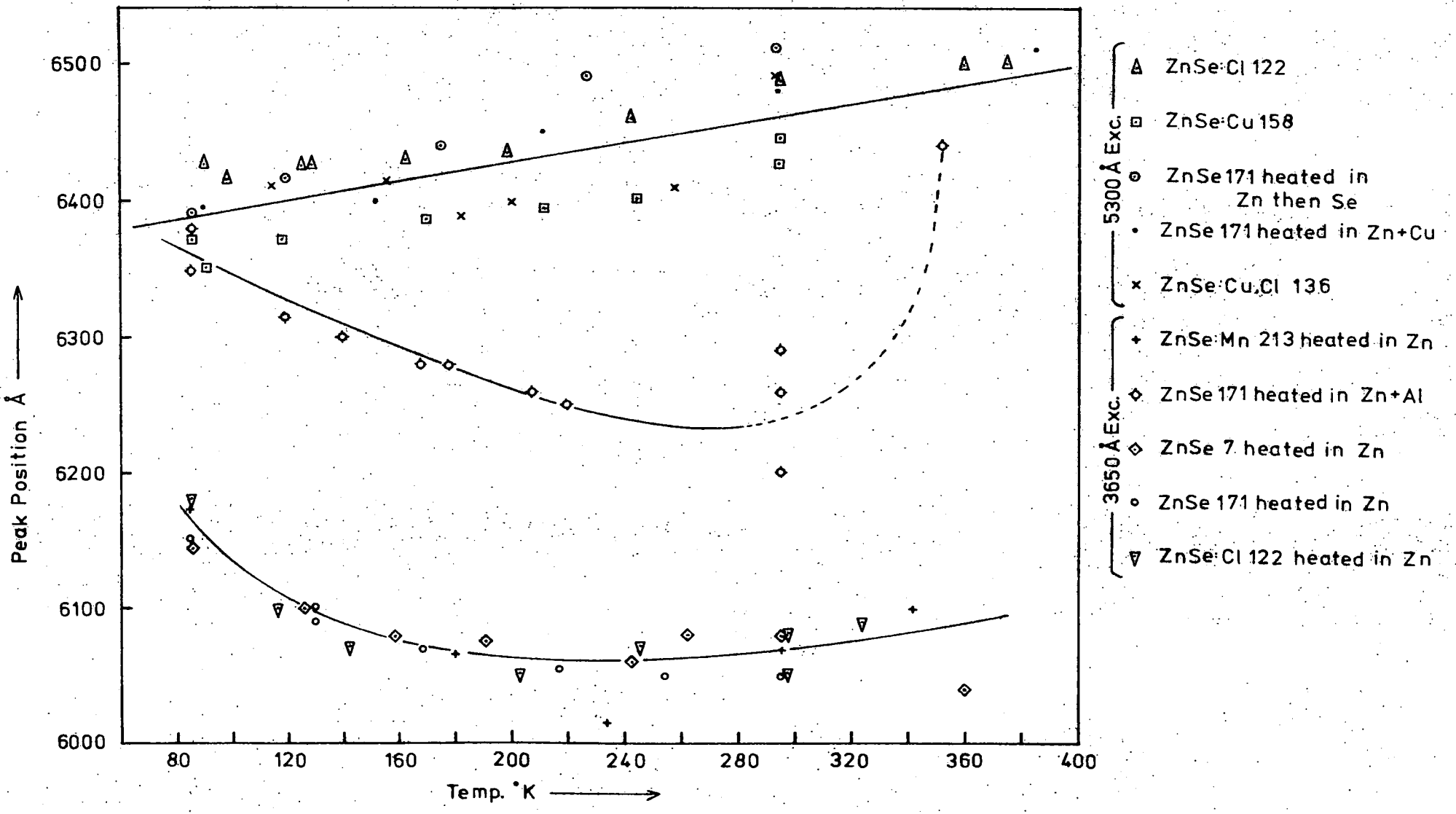

Fig. 5-10. Change in Position of Emission Bands from various Crystals as a function of Temperature.

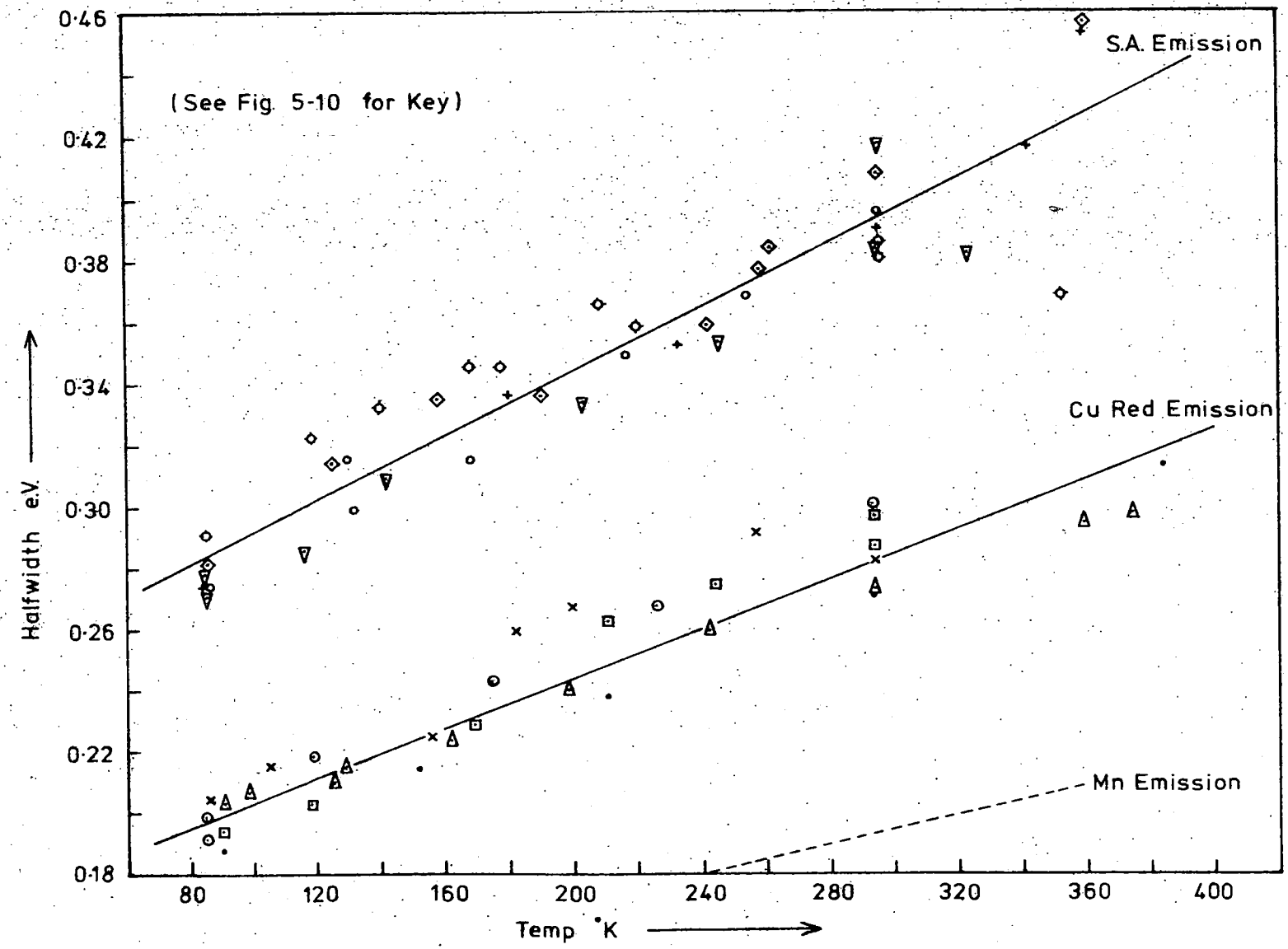

Fig. 5-11. Change in Halfwidth of Emission Bands from various Crystals as a function of Temperature.

copper (6400 Å) component.

After chlorine doped crystals were heated in molten zinc, the emission under 3650 Å excitation was found to be identical to that of undoped, zinc treated crystals which was discussed in section 5.3 (figure 5.4). Thus, the position of the emission band, its halfwidth and the variation of each with temperature (figures 5.10, 5.11) were identical for both chlorine doped and undoped crystals following heating in zinc. However, the excitation spectra were different (figures 5.12, 5.13). That of crystal 122 measured at 85°K after the zinc treatment revealed a prominent band at 4850 Å with a shoulder at approximately 4550 Å. In the excitation spectrum of crystal 123 after the zinc treatment, the 4550 Å band was more prominent with a long wavelength tail in the region of the 4850 Å band. The 4850 Å band, which is probably the same as that observed at about 4800 Å in the untreated chlorine doped crystals, is ascribed to the presence of chlorine. It would appear from the magnitude of the 4850 Å band in figures 5.12 and 5.13, that crystal 122 contained considerably more chlorine than crystal 123. Excitation with light in the region of the 4850 Å band produced exactly the same emission band as excitation at 3650 Å.

In order to investigate further whether copper was introduced along with the chlorine during growth, two crystals were studied which had been grown in the presence of 5 p.p.m. copper, in the form of the selenide, and 1200 p.p.m. chlorine (crystal 135) or 5000 p.p.m. chlorine (crystal 136) in the form of zinc chloride. The excitation spectra of these two crystals (figures 5.14, 5.15) are very similar to the spectrum of the chlorine doped sample number 122, with the 5150 Å band clearly visible, and that at 4850 Å more prominent in crystal 136, which was grown with the higher chlorine concentration. These spectra support the view that copper entered the boule to produce the 5150 Å excitation band, irrespective of whether copper was added to the charge. The emission under 3650 Å excitation at room temperature was almost identical to that of sample 122 for both crystals,

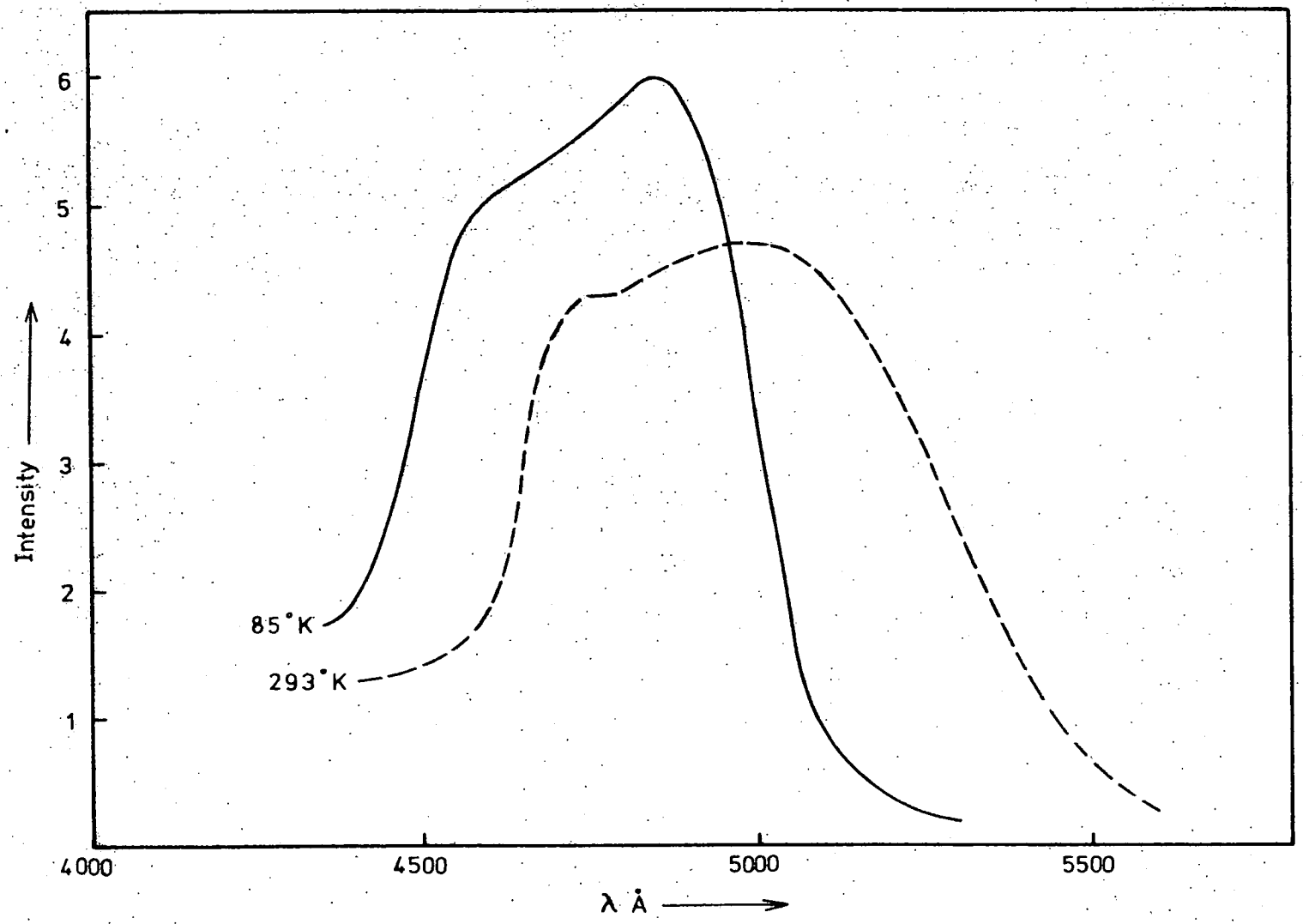

Fig.5-12. Excitation Spectrum of ZnSe:Cl 122 heated in Zn. (S.A. Emission).

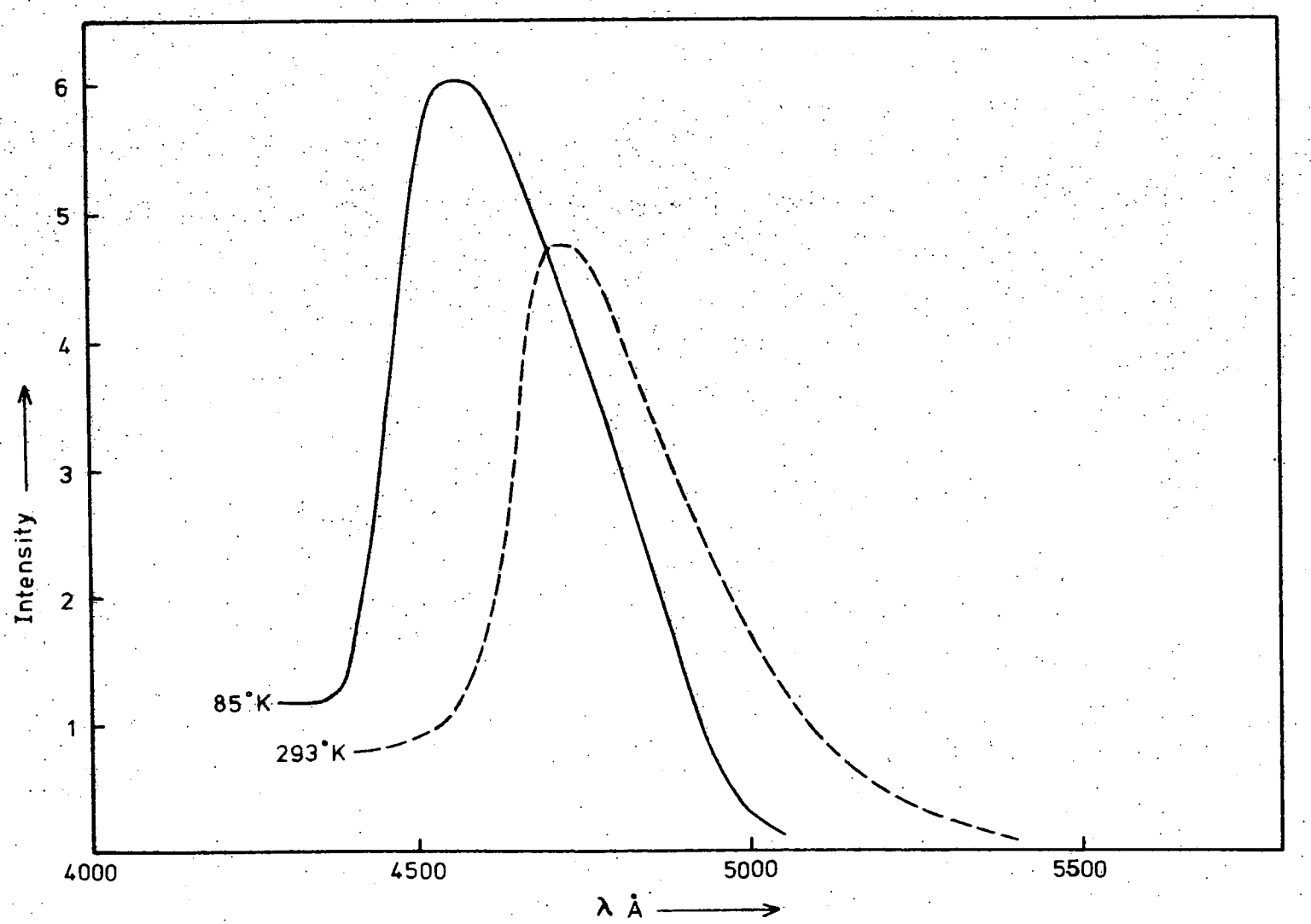

Fig. 5-13. Excitation Spectrum of ZnSe:Cl 123 heated in Zn. (S.A. Emission).

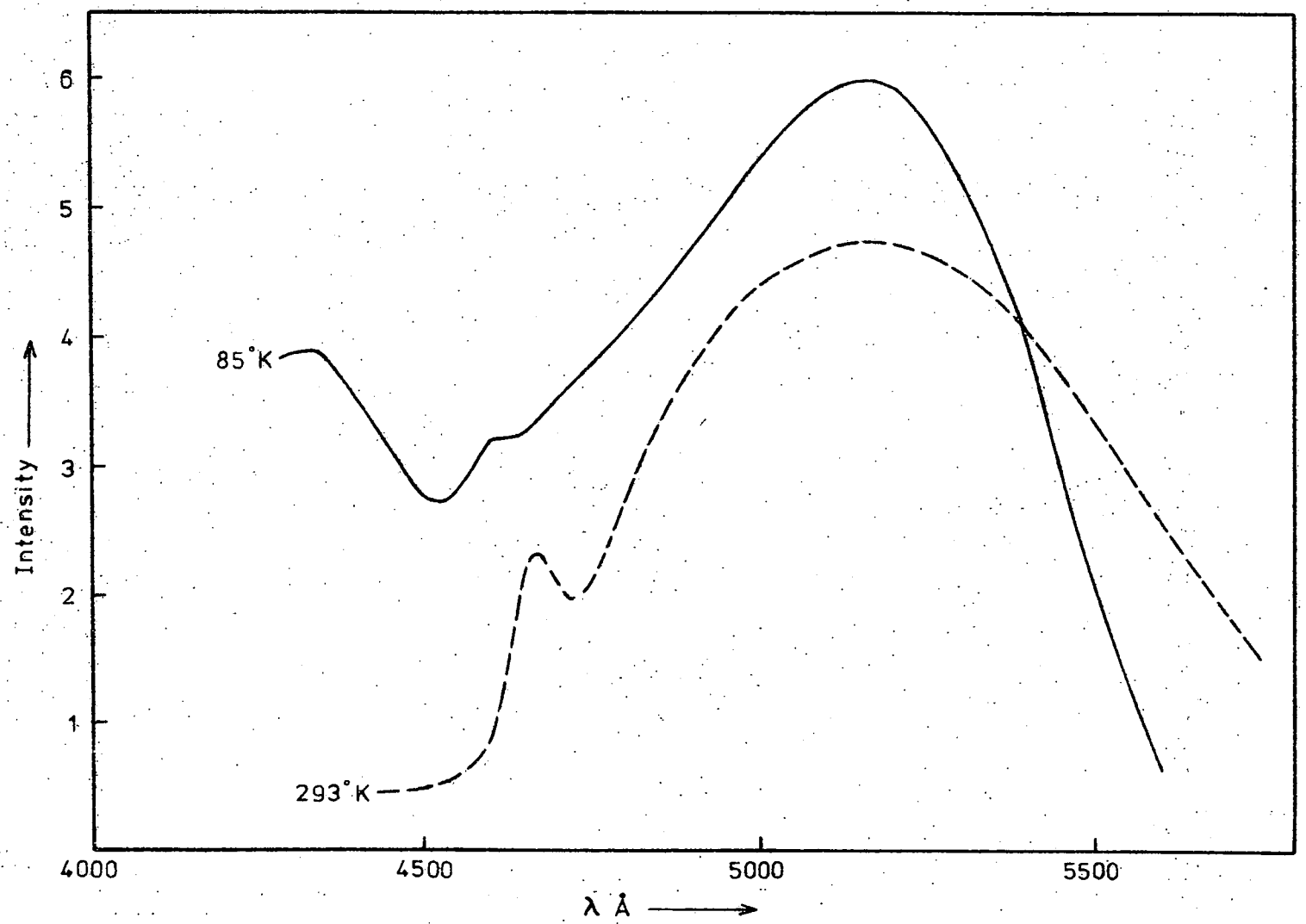

Fig. 5-14. Excitation Spectrum of ZnSe:Cu,Cl 135.

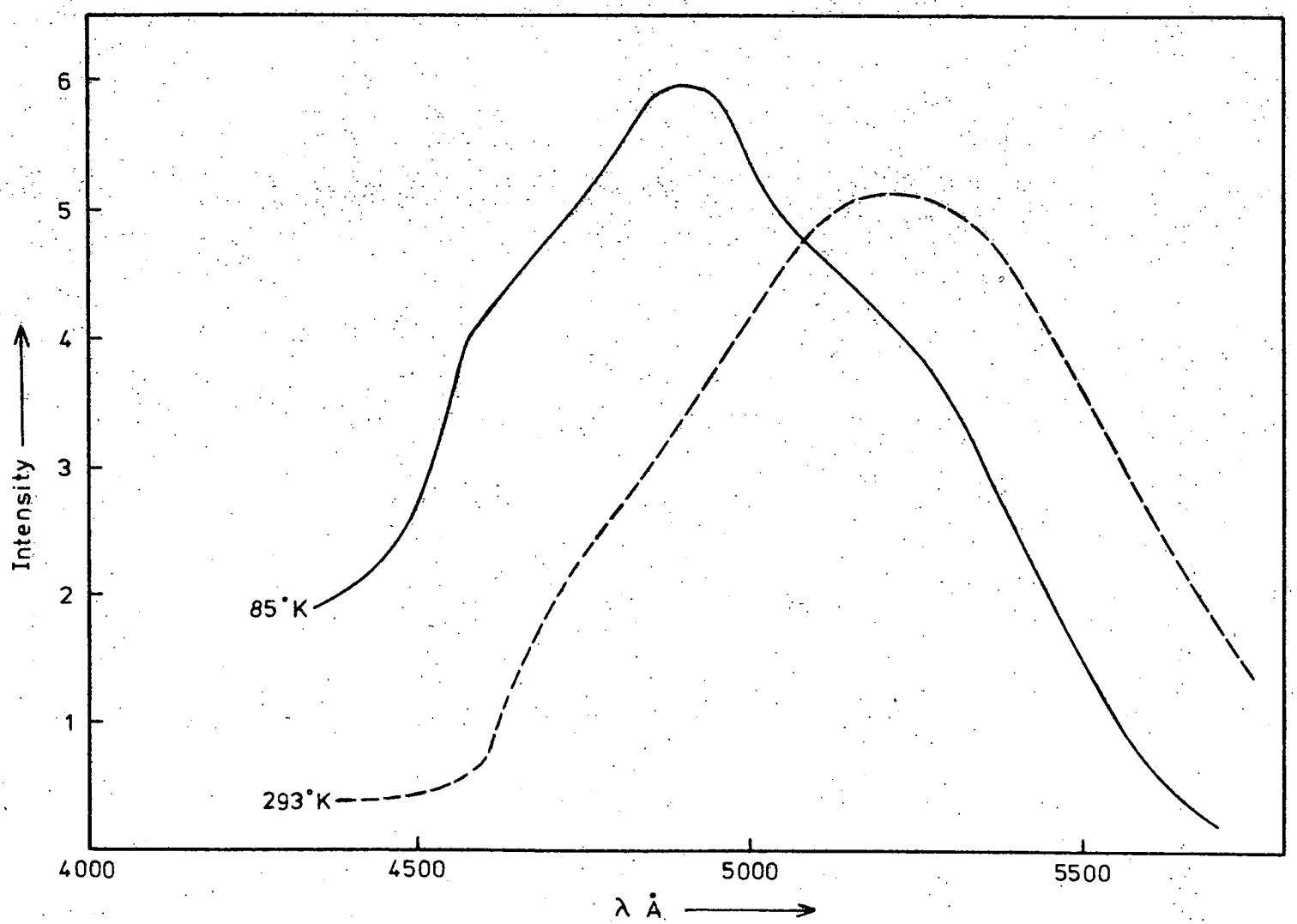

Fig.5-15. Excitation Spectrum of ZnSe:Cu,Cl 136.

but at 85°K crystal 136 emitted a band at 6160 Å in comparison with the 6250 Å band emitted by crystal 122. This is probably due to the influence of the S.A. emission and is connected with the fact that the short wavelength excitation bands are more prominent in the spectrum of crystal 136 than in that of 122. Crystal 135 however, emitted a main band at 5650 Å with a shoulder at approximately 6200 Å. This may have some connection with the band to band and 4600 Å excitation processes which can be seen in figure 5.14, although no excitation spectrum for this emission was obtained.

After heating in liquid zinc, a piece of crystal 136 was again found to emit the usual S.A. band but the excitation spectrum was almost identical to that of crystal 122 after the zinc treatment (figure 5.16).

The emission from crystal 136, excited by 5300 Å light, was found once again to consist of the narrow red band identical to that associated with copper. The variation of half width and peak position is again shown in figures 5.10 and 5.11.

In summary, it appears that when chlorine is introduced into a boule, copper tends to enter simultaneously. The position of the resultant emission band is therefore governed by the relative intensities of the 6400 Å copper band and the 6150 Å S.A. band. Similarly, the excitation spectrum is mainly a combination of the copper band at 5150 Å, a band at 4850 Å associated with chlorine, and the peak near the bandgap energy similar to that seen in undoped material after being heated in zinc. When the copper has been removed by heating the crystal in liquid zinc, the chlorine excitation band at 4850 Å is well resolved and the S.A. emission associated with the chlorine coactivator is observed. This emission band is identical to the S.A. emission described in section 5.3 when undoped material is heated in zinc.

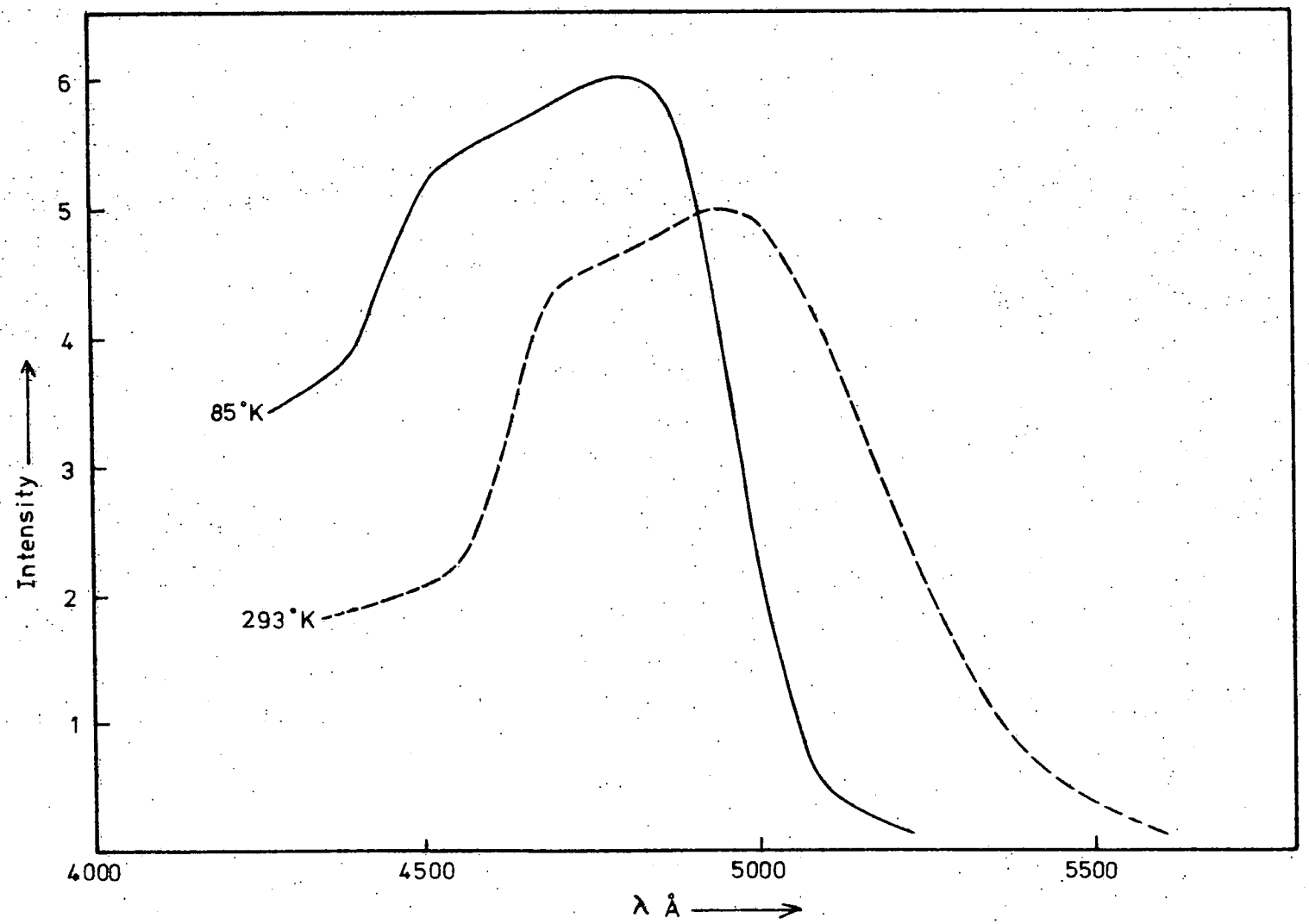

Fig. 5-16. Excitation Spectrum of ZnSe:Cu,Cl 136 heated in Zn. (S.A. Emission).

5.5 IODINE COACTIVATION

Figure 5.17 illustrates the emission spectrum under 3650 Å excitation of crystal 109, which was grown using the iodine transport method. The luminescence at room temperature with its maximum at about 6380 Å was very weak but when the sample was cooled to slightly below room temperature an intense band at about 6050 Å was seen. On cooling further, the band shifted back towards longer wavelengths and at 85°K was located at 6180 Å. This latter behaviour is again characteristic of an S.A. emission band which at 85°K was very similar to that emitted by zinc treated crystals (figure 5.4). The excitation spectrum (figure 5.18) revealed that the long wavelength band at 5150 Å characteristic of the chlorine and copper doped crystals was fairly insignificant compared with the higher energy bands which were similar to the S.A. excitation bands already described. This suggests that the amount of copper in this sample was less than in previous crystals so that the absence of the overlapping copper emission band allowed the S.A. emission to be detected without any treatment in liquid zinc.

After the crystal had been heated in liquid zinc the emission was almost unchanged except at room temperature where a small trace of copper impurity may have been removed leaving the S.A. band even more clearly defined at 6050 Å. The excitation spectrum after the zinc treatment, which is shown in figure 5.19, is almost identical to that of the chlorine doped crystal 122 after zinc treatment (figure 5.12). The low energy copper excitation band is absent and the 4880 Å band is much more prominent. This 4880 Å band seems to be analogous to the 4850 Å band in chlorine doped crystals and is thus attributed to the presence of iodine within the crystal.

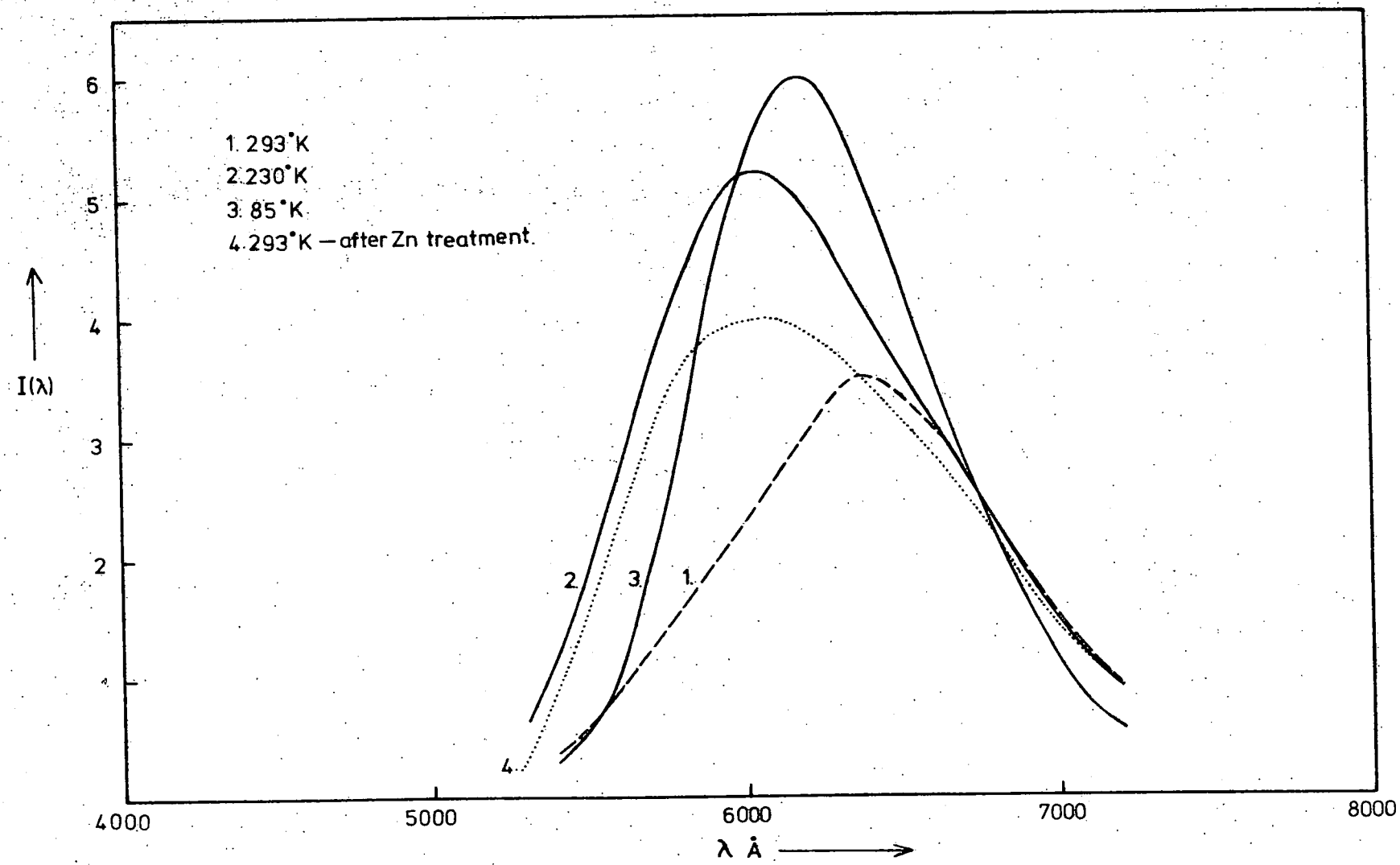

Fig. 5-17. Emission Spectra under 3650 Å Excitation of ZnSe:I 909 before and after heating in Zn.

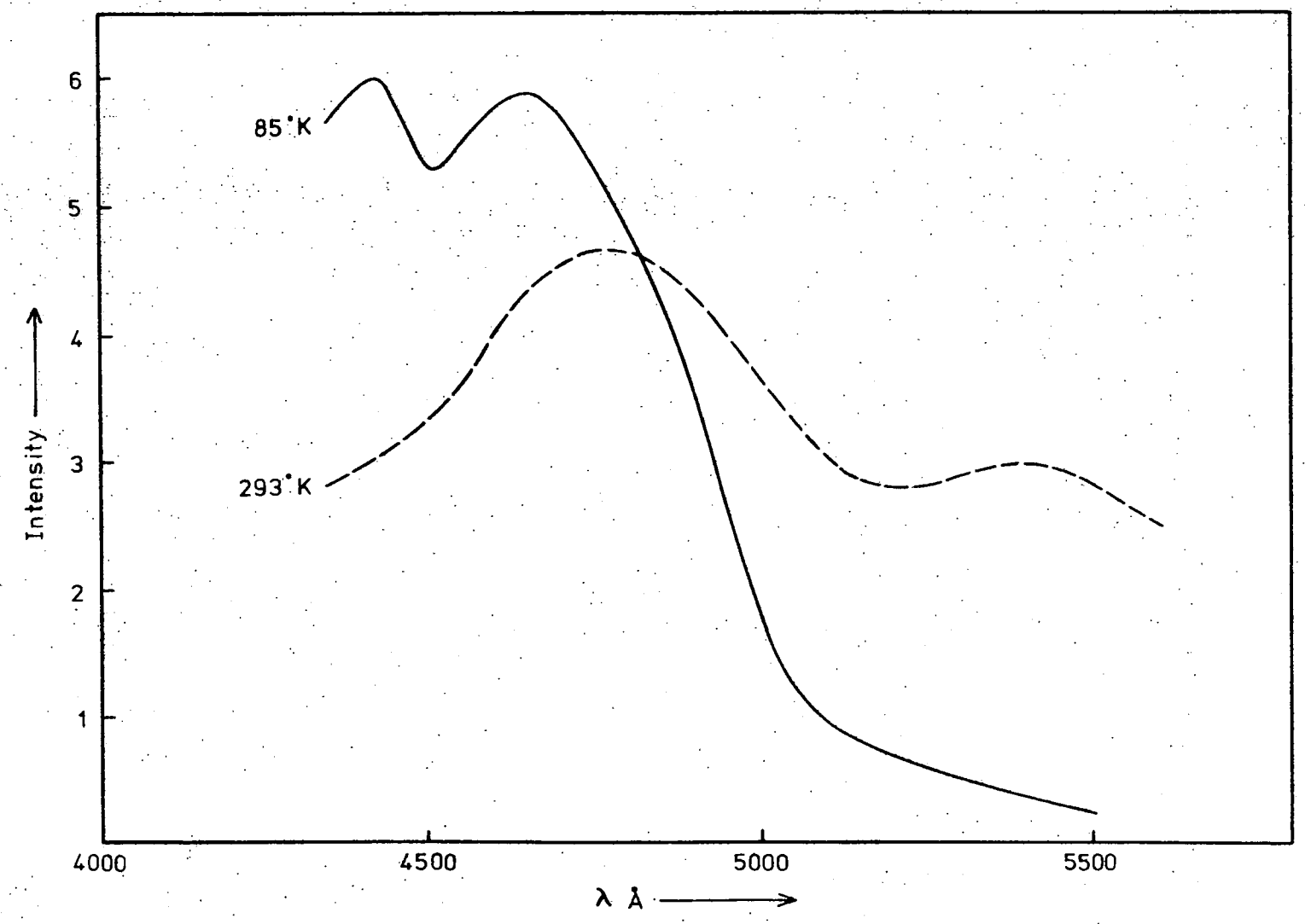

Fig.5-18. Excitation Spectrum of ZnSe:I 909.

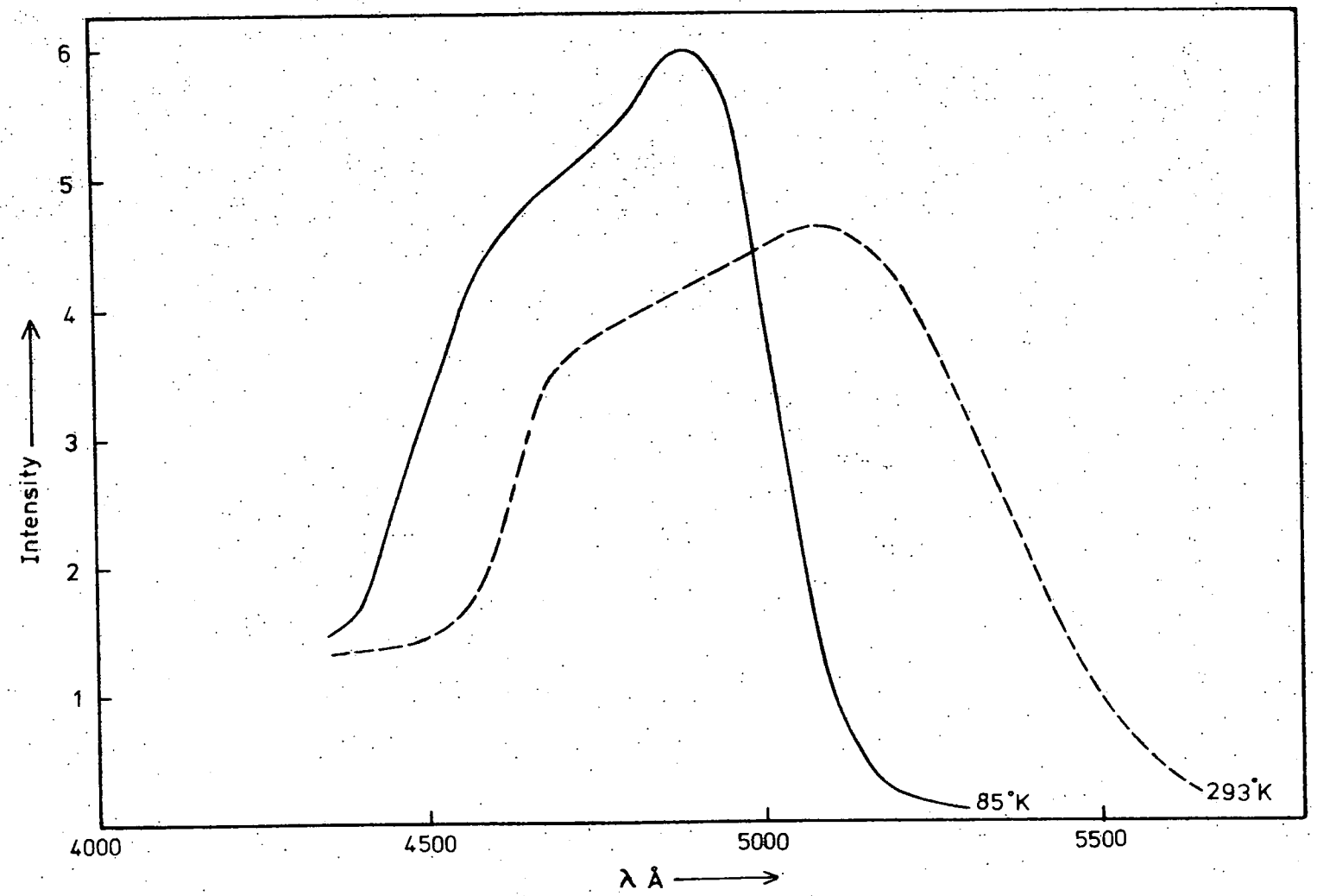

Fig. 5-19. Excitation Spectrum of ZnSe:I 909 heated in Zn. (S.A. Emission).

5.6 ALUMINIUM COACTIVATION

Aluminium was introduced into zinc selenide boules during growth by vapour phase transport, simply by adding aluminium metal directly to the charge. The crystals were normally of orange body colour although there was some tendency for green colouration to occur within a predominantly orange boule. This was probably due to uneven incorporation of the dopant during growth. The red material was found to have a resistivity of approximately 5×10^5 ohm.cm. at room temperature in the dark. This was five orders of magnitude less than that of the green material under the same conditions. It was therefore assumed that since aluminium should act as a donor, the red material must contain the majority of the aluminium. A red piece of crystal 187, grown in the presence of 1000 p.p.m. aluminium, was taken as a representative example. The emission spectrum of crystal 187 under 3650 Å excitation consisted of three main bands at 85°K (figure 5.20). They were the edge emission at 4650 Å, a green band at 5570 Å and a red band at 6320 Å. On increasing the temperature to 293°K the blue and green bands were quenched and the red band shifted to 6400 Å (figure 5.20). The half width of the green and red bands at 85°K were 0·21 eV and 0·22 eV respectively.

The excitation spectrum of the red band at both 293°K and 85°K consisted of a very broad long wavelength band centred at approximately 5150 Å together with a more intense band near the bandgap (figure 5.21). Excitation with 5300 Å light once again revealed the 6400 Å copper emission. This suggests that under 3650 Å excitation the observed emission contained some long wavelength copper component. The excitation spectrum of the green band revealed a small band at about 4750 Å in addition to the main band at the bandgap which was identical to that which excited the red emission with maximum efficiency.

When the crystal was heated in molten zinc the resulting excitation and emission spectra were identical to those of undoped material heated

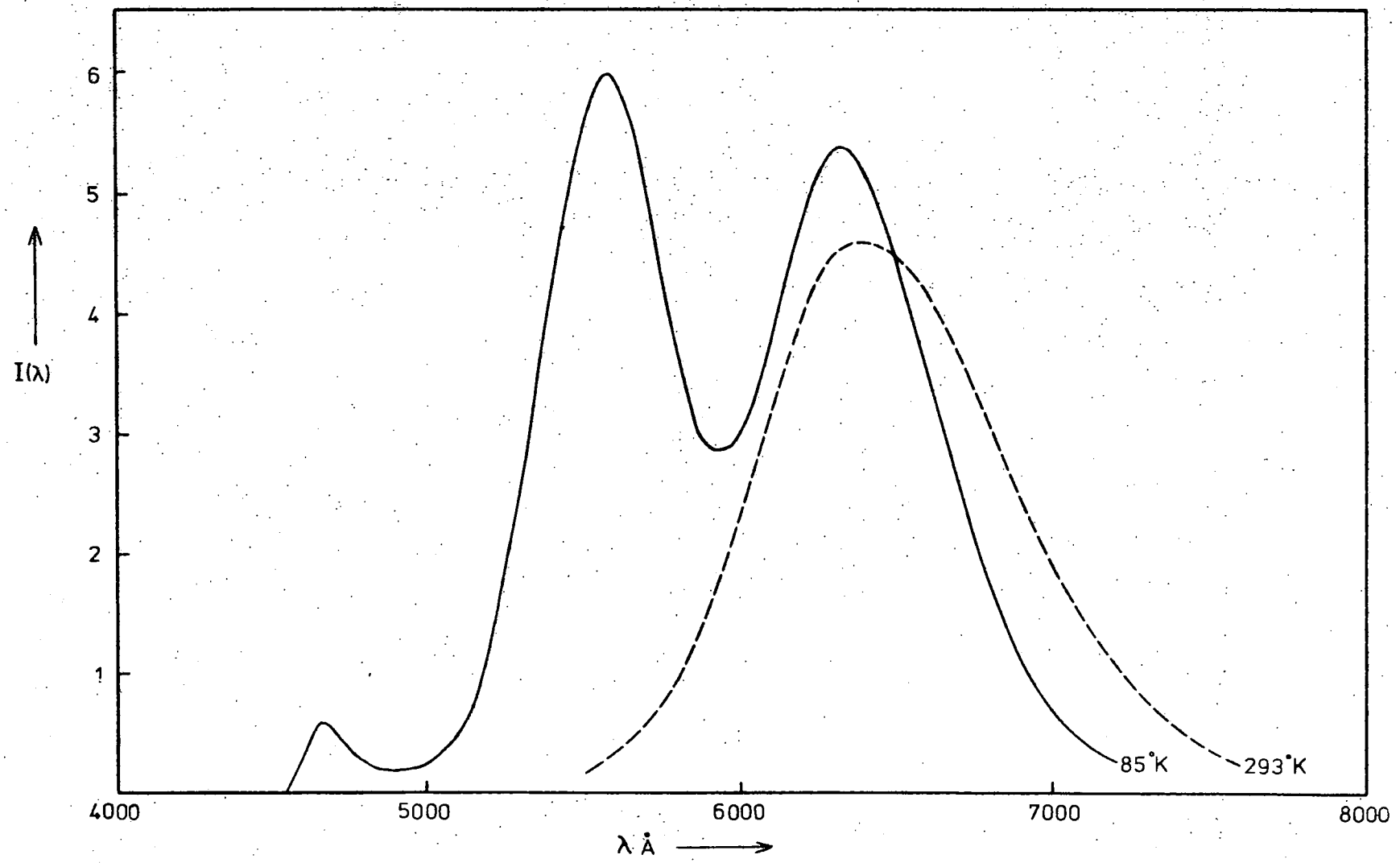

Fig. 5-20. Emission Spectrum under 3650 Å Excitation of ZnSe:Al 187

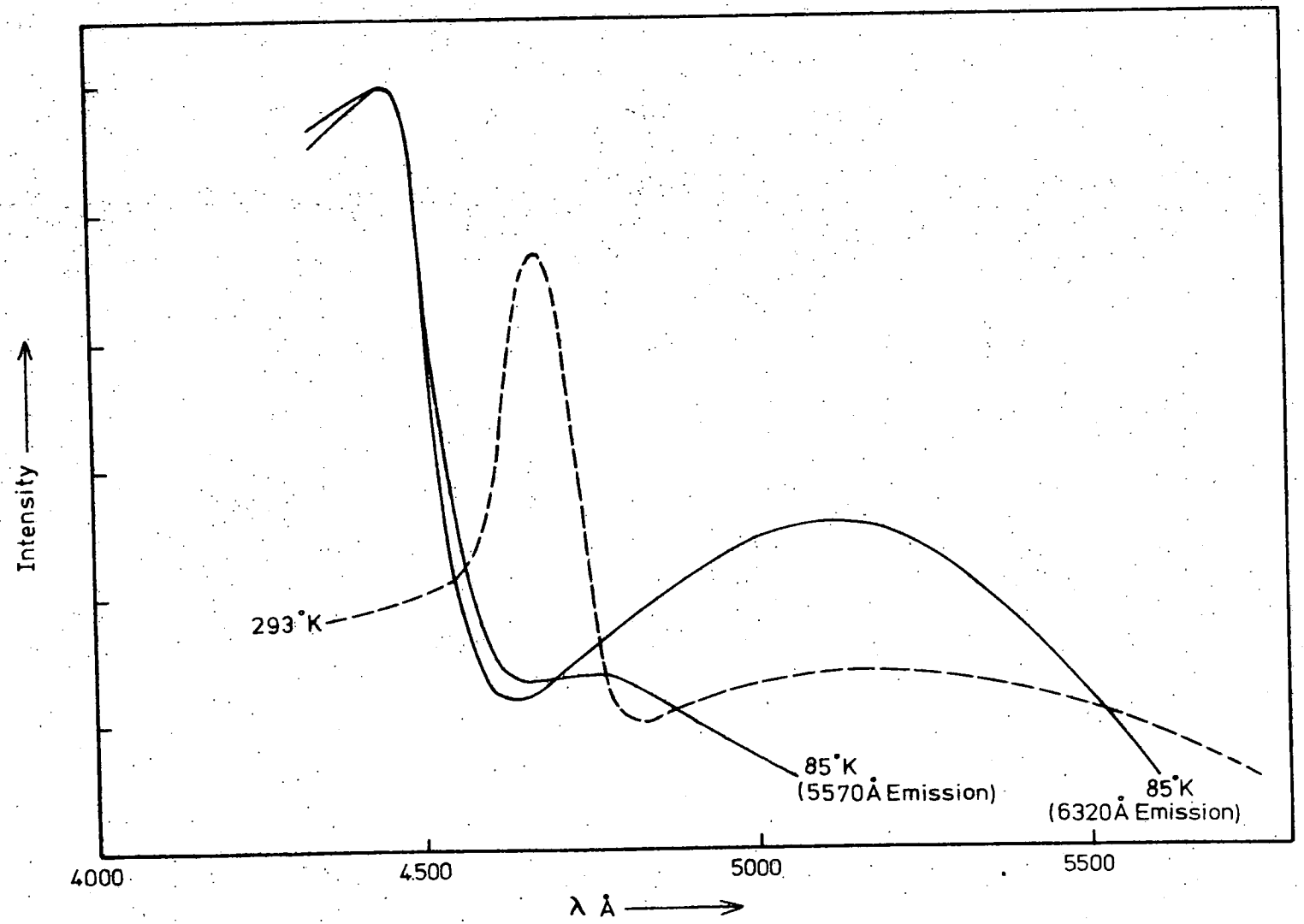

Fig 5-21. Excitation Spectrum of ZnSe:Al 187.

in zinc (figures 5.4, 5.5).

Aluminium was then introduced into a piece of crystal 171 by heat treatment in a solution of 10% mole aluminium in zinc. This procedure proved extremely difficult since the melt always attacked the silica tube and usually caused it to break whilst the zinc was molten. Only one run was concluded successfully and the resulting crystal was found to behave differently from previous samples containing grown in aluminium. The excitation spectrum shown in figure 5.23 can be compared with that of figure 5.5 which was obtained from a piece of the same crystal heated in zinc only. With the post-doped aluminium sample an extra band was observed with its maximum at 4800 Å at 85°K. This was probably the same band seen at about 4750 Å in the excitation spectrum of crystal 187 containing grown in aluminium. The excitation spectrum also exhibited a long wavelength tail which may have been associated with copper contamination. This suggests that not all the copper was removed into the melt, perhaps because of the aluminium content of the melt or because the melt was not in good contact with the sample for a full week. There may have been some other factor which also prevented the tube cracking.

The emission under 3650 Å excitation (figure 5.22) shifted towards lower energy when the temperature was reduced, as did the S.A. emission band. However, the emission band maximum was displaced towards longer wavelengths relative to the previously observed S.A. emission in chlorine or iodine doped samples. The band maximum lay at 6350 Å at 85°K and about 6260 Å at 293°K. There was therefore a displacement to lower energy of about 0·065 eV relative to the halogen doped S.A. crystals. This 6350 Å band is assumed to be analogous to the S.A. band reported at approximately 4700 Å in aluminium doped zinc sulphide. The variation in halfwidth with temperature of the red aluminium S.A. band is shown in figure 5.11 and is clearly very similar to that of the shorter wavelength S.A. emission. The reduction in width at temperatures above 293°K is due

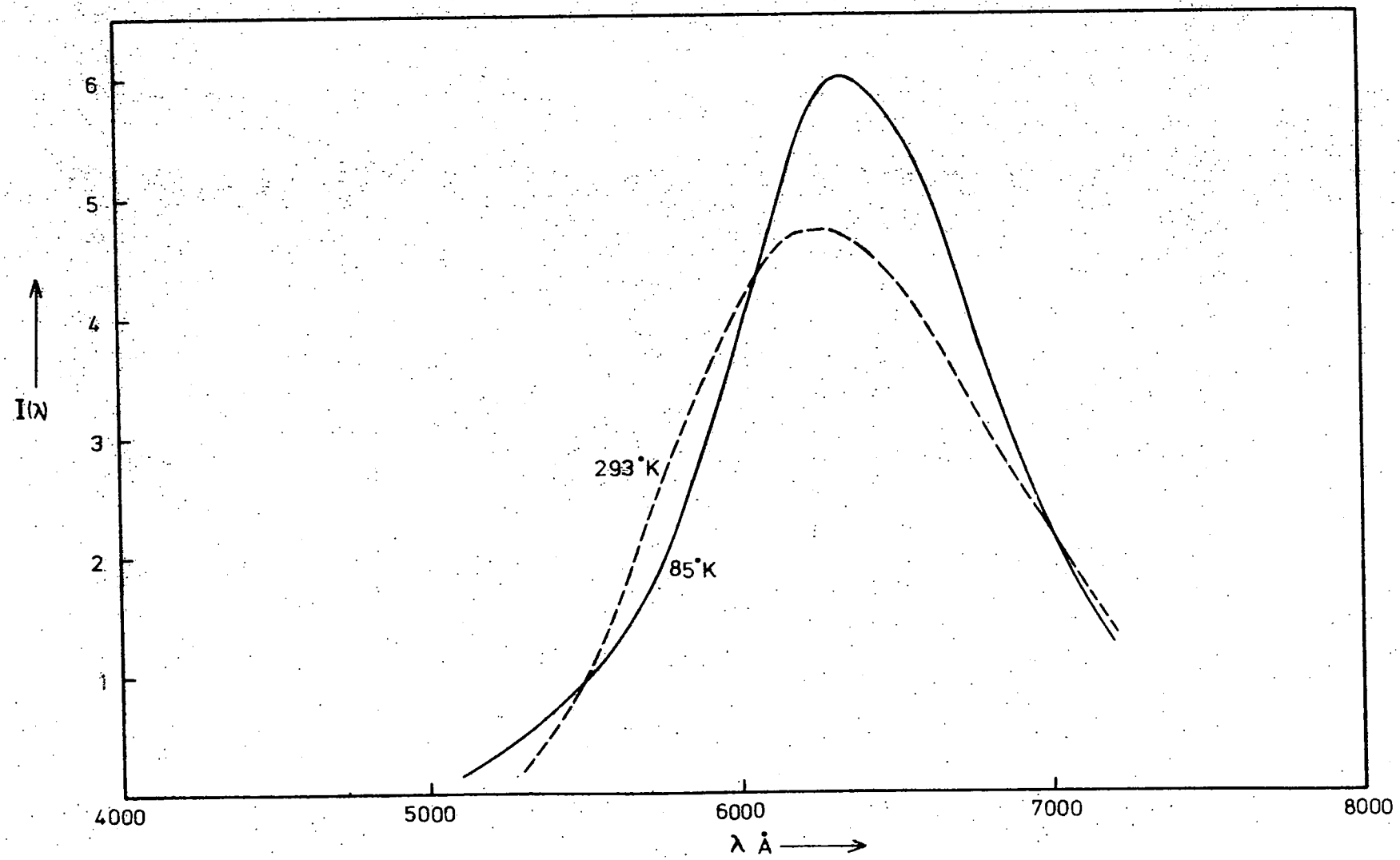

Fig. 5-22. Emission Spectrum under 3650 Å Excitation of ZnSe 171 heated in Zn+Al. (S.A. Emission).

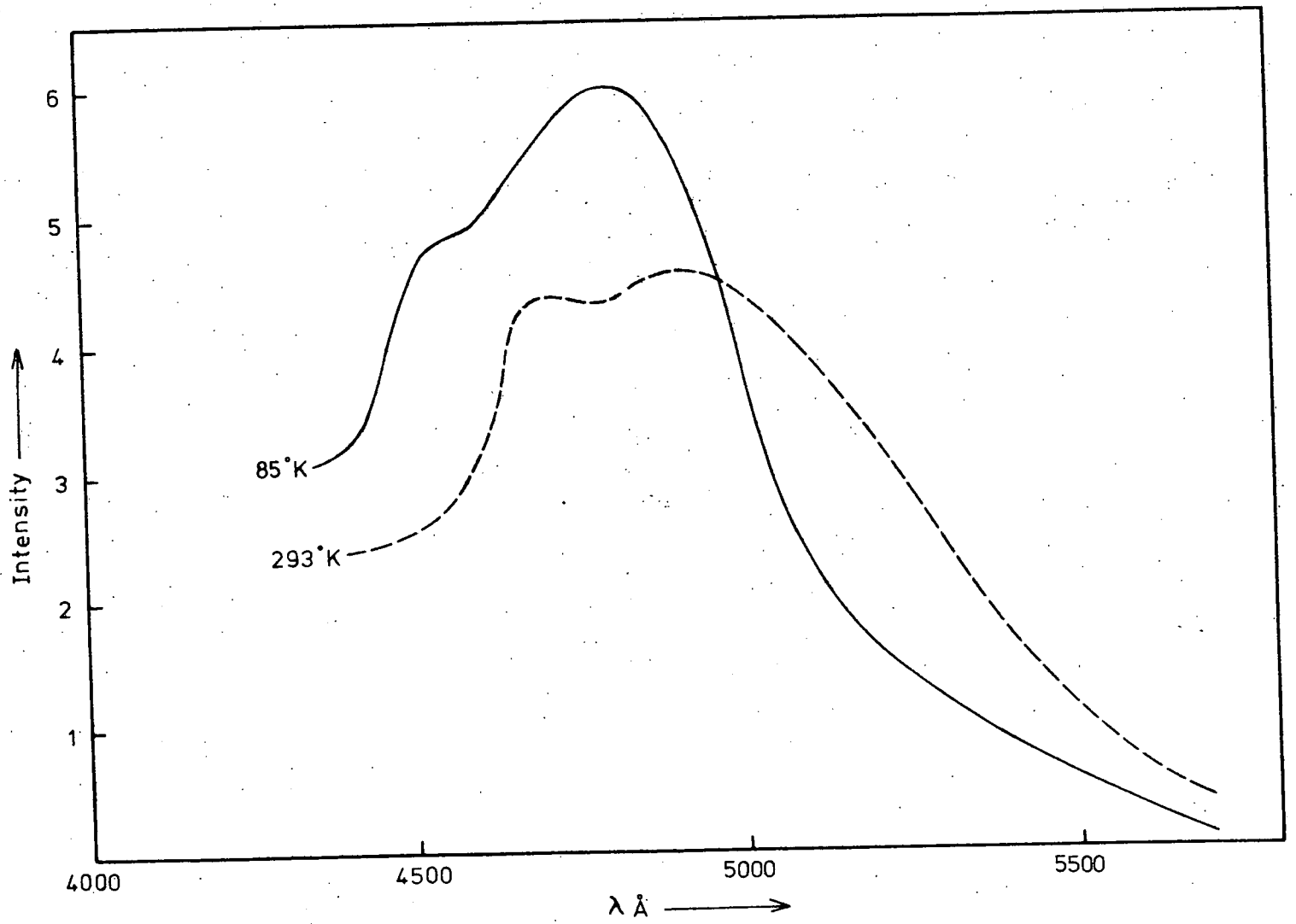

Fig.5-23. Excitation Spectrum of ZnSe 171 heated in Zn+Al.(S.A. Emission).

to the narrower copper band becoming more prominent. This interaction of the copper band is also shown in the plot of peak position versus temperature in which a 6440 Å band is prominent at 350°K and where the band tends to shift towards longer wavelength above about 260°K (figure 5.10).

The emission spectrum of the zinc plus aluminium treated crystal (figure 5.22) also contained a suggestion of a short wavelength tail at 85°K which may have been an indication of the presence of the 5570 Å band which was more prominent in the emission spectrum of 187.

It is concluded that aluminium produces an S.A. emission similar to that of the halogens but displaced by about 200 Å towards longer wavelengths as in zinc sulphide. At 85°K an excitation band at 4800 Å appears which is analogous to the 4850 Å bands in the chlorine and iodine doped crystals. When grown into a crystal of zinc selenide, aluminium produces a green band at 5570 Å, as well as the S.A. and copper bands. This green band appears to be excited primarily by bandgap radiation.

5.7 INDIUM COACTIVATION

Indium was grown into several boules by adding the metal to the charge. All such crystals had a yellow-orange body colour. At 85°K all the crystals emitted both a green and an orange band. Figure 5.24 shows the emission spectrum under 3650 Å excitation, of crystal 181 which contains 100 p.p.m. indium. The green band was centred at 5600 Å whilst the orange band was at approximately 6300 Å. At 293°K a broad orange band, with its maximum at 6200 Å was observed. The position of this room temperature band varied from one crystal to another because of the influence of other sub-bands. Edge emission near 4600 Å was also exhibited by some crystals.

The excitation spectra for the two emission bands of this crystal are shown in figure 5.25. The room temperature spectrum consisted simply of a single, sharp peak at 4670 Å, which is approximately the bandgap

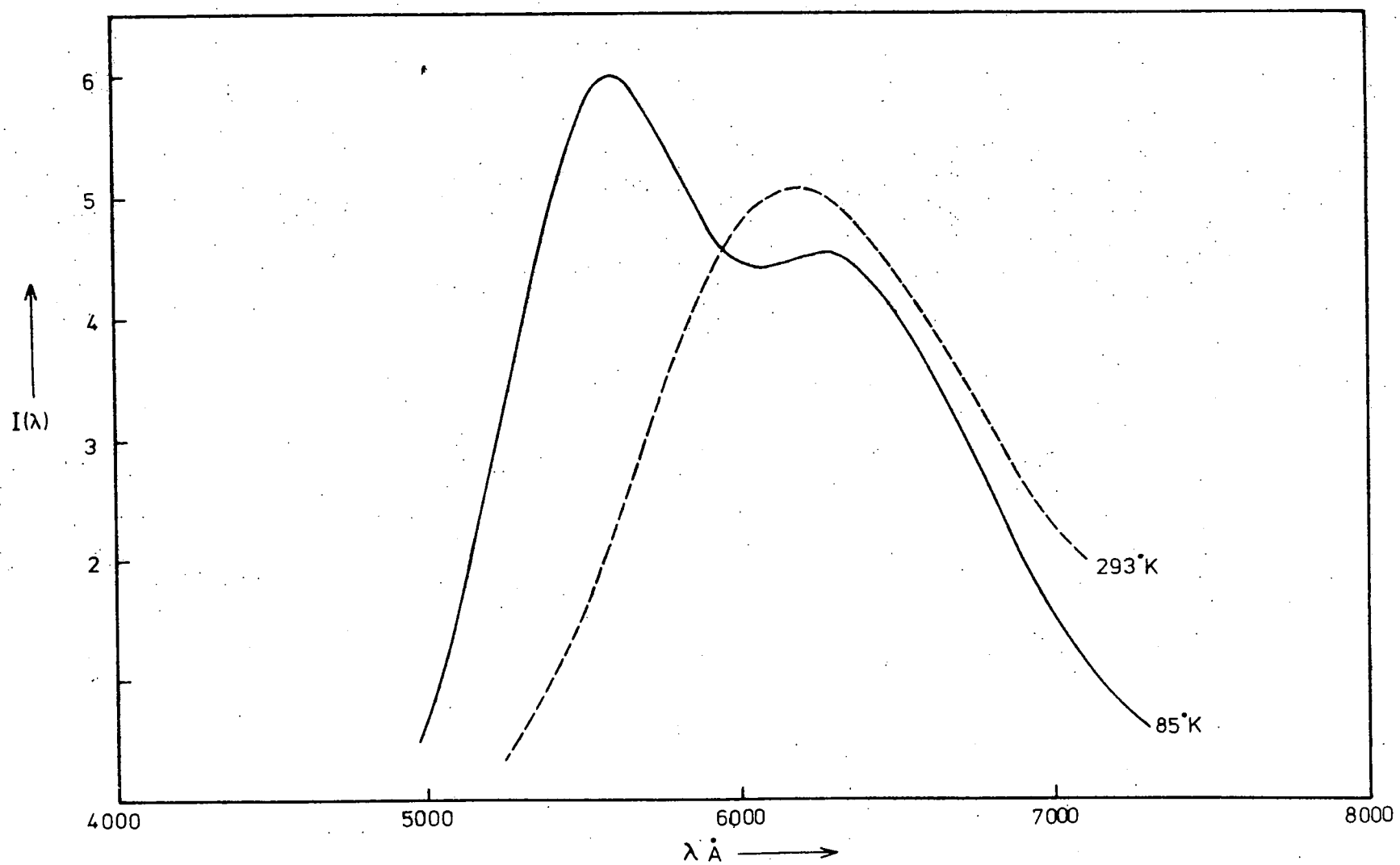

Fig. 5-24. Emission Spectrum under 3650 Å Excitation of ZnSe:In 181.

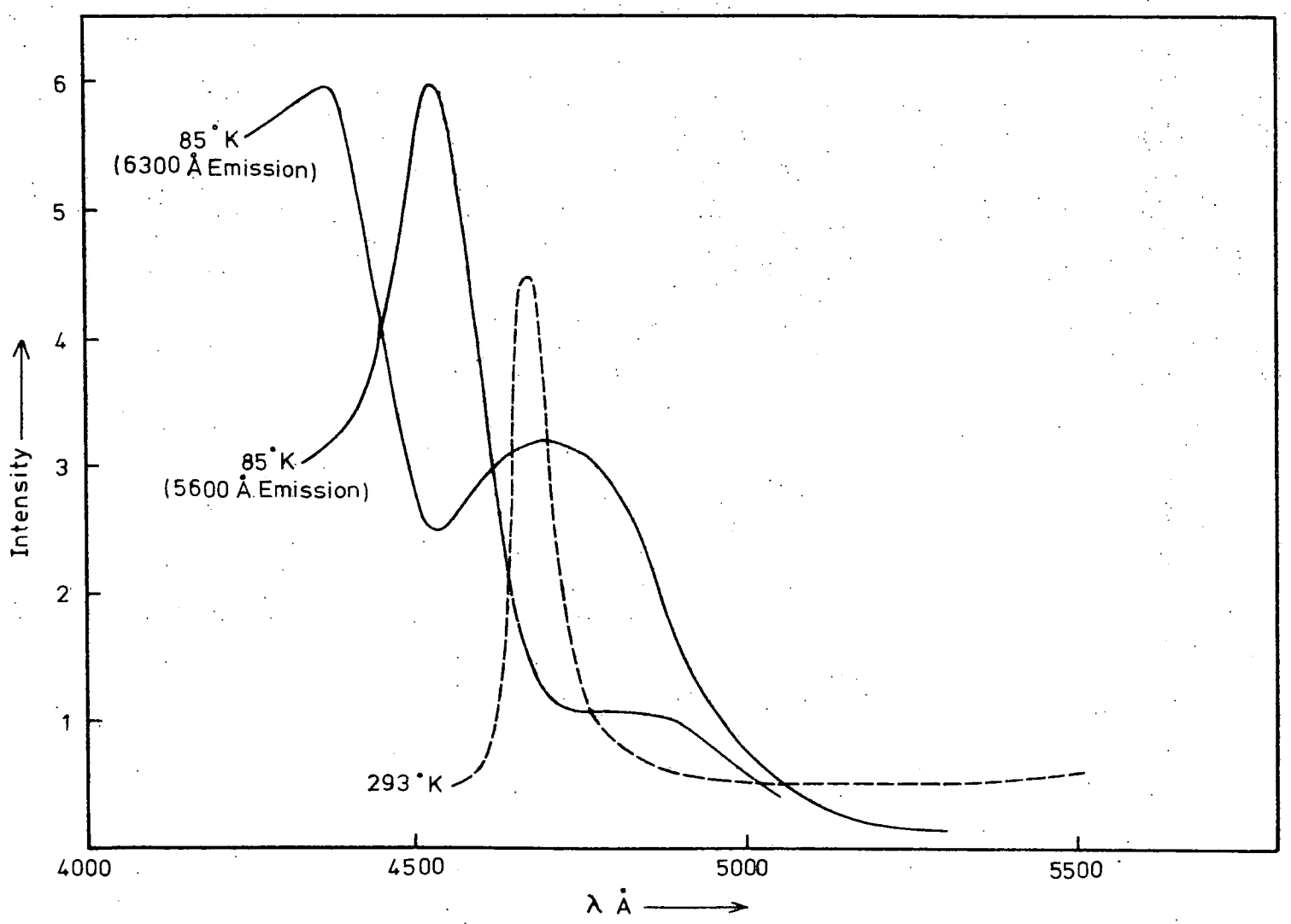

Fig. 5-25. Excitation Spectrum of ZnSe:In 181.

energy at 293°K. At 85°K the broad band centred at about 4700 Å appeared, together with a peak corresponding to bandgap excitation. The 4700 Å band appeared to consist of more than one component. The excitation spectrum of the green band revealed a small band at about 4850 Å, together with a peak at 4530 Å, a little less than bandgap energy.

The red emission band shown in figure 5.24 shifted towards lower energies when the crystal was cooled. This again is typical of S.A. emission but the band was displaced slightly towards longer wavelengths compared with halogen doped crystals as was that associated with the S.A. emission in the aluminium doped sample. Since the copper excitation band was insignificant (figure 5.25), the copper red emission is unlikely to have been responsible for this displacement to longer wavelength. In fact, if substantial copper emission had occurred, it would have tended to displace the room temperature peak to a wavelength longer than that observed at 85°K since the copper red band does not begin to quench until approximately room temperature (see section 5.10). This would therefore oppose the shift which was observed and therefore confirms that in sample 181 the influence of copper was negligible. The band which shifted from approximately 6300 Å at 85°K to 6200 Å at 293°K is therefore most probably the S.A. emission associated with indium.

Although the red and green bands were observed in all crystals, even those containing 1000 p.p.m. indium, the ratio of the two bands was found to vary from crystal to crystal and the red band often appeared only as a shoulder on the green, especially in those samples containing small quantities of indium.

In an attempt to clarify the effects of incorporating indium, several indium doped samples were studied after they had been heated in molten zinc. This, however, led to the formation of a heavy black precipitate, probably of indium. This will be discussed in greater detail in Chapter 7, when the electrical properties are discussed. The precipitate was so

dense in most crystals that the luminescent emission was considerably reduced. However, crystal 139, which appeared to be lightly doped, produced only a small amount of precipitate, and when measurements were made on this sample the emission and excitation spectra were found to be identical to those obtained previously with undoped crystals following heating in zinc (figures 5.4, 5.5). That is an S.A. emission band was produced, but it was not identical to the indium S.A. emission as seen in crystal 181.

Attempts were next made to introduce indium into crystals, after growth, from suitable solutions. Pieces of crystal 171 were heated at 85°K for a week in melts of indium plus zinc containing up to 20% mole indium. This process did not appear to introduce indium, since the resulting excitation spectra were again identical to those of crystals heated in zinc alone. Furthermore, the S.A. emission band which resulted lay at 6150 Å at 85°K, not at the longer wavelength of 6300 Å as would be expected with indium as coactivator (figure 5.24). Subsequently, a crystal was first heated in zinc only to remove any possible copper contamination and was then heated in indium alone at 850°C. This led to the complete solution of the crystal. No crystals doped with indium after growth could be obtained therefore.

Pieces of crystal 139, containing grown in indium, which had been treated in liquid zinc were subsequently heated in either molten selenium at 650°C, or vacuum at 850°C. Both procedures caused the precipitate to disappear, but the emission from such crystals was different from that of the as-grown crystals. Green and red bands were produced, but they occurred at 6360 Å and 5475 Å at 85°K. This is reminiscent of the emission spectrum of the copper selenide doped crystal 158 (figure 5.1). Furthermore, the excitation spectrum at 85°K revealed a prominent band at 5100 Å, which has been assumed to be characteristic of copper impurity. With 5300 Å excitation, the 6400 Å band, which was absent after the zinc

treatment, was once again clearly observed. It appears therefore, that heating both in selenium and in vacuum introduces copper into the crystal. If any indium emission were present, it would almost certainly be masked by the copper emission. More will be said about these results in section 5.9, when undoped material is discussed.

In summary, therefore, indium produces an S.A. emission at about 6300 Å at 85°K (figure 5.24), which is very similar to the aluminium S.A. emission (figure 5.22), although it was not possible to isolate the band from the neighbouring copper band. Similarly, the associated excitation band could not be isolated, but by analogy with the aluminium S.A. band (figure 5.23), may lie within the broad band centred at 4700 Å (figure 5.25). At 85°K a higher energy green band at 5600 Å is also emitted. This, again, is similar to the band emitted by aluminium doped material at 5570 Å, but the corresponding excitation peak now lies at 4530 Å, not at the bandgap. Heating in zinc appears to precipitate the indium as a black deposit and cause it to take no further part in the emission and excitation processes. Although heating in selenium or vacuum leads to the disappearance of the precipitate, subsequent luminescent properties appear to be dominated by copper impurity.

5.8 GALLIUM COACTIVATION

Gallium doped boules were prepared by adding gallium metal directly to the charge. This led to crystals with an orange body colour. The emission under 3650 Å excitation at 85°K from crystal 188, which contains 100 p.p.m. gallium, consisted of green and red bands at 5630 Å and about 6350 Å (figure 5.26). This is very similar to the emission spectrum of the indium doped crystal number 181 (figure 5.24). At room temperature a single red band at 6250 Å was observed. In more heavily doped crystals, the green band was absent at 85°K and only a red band at approximately 6200 Å remained.

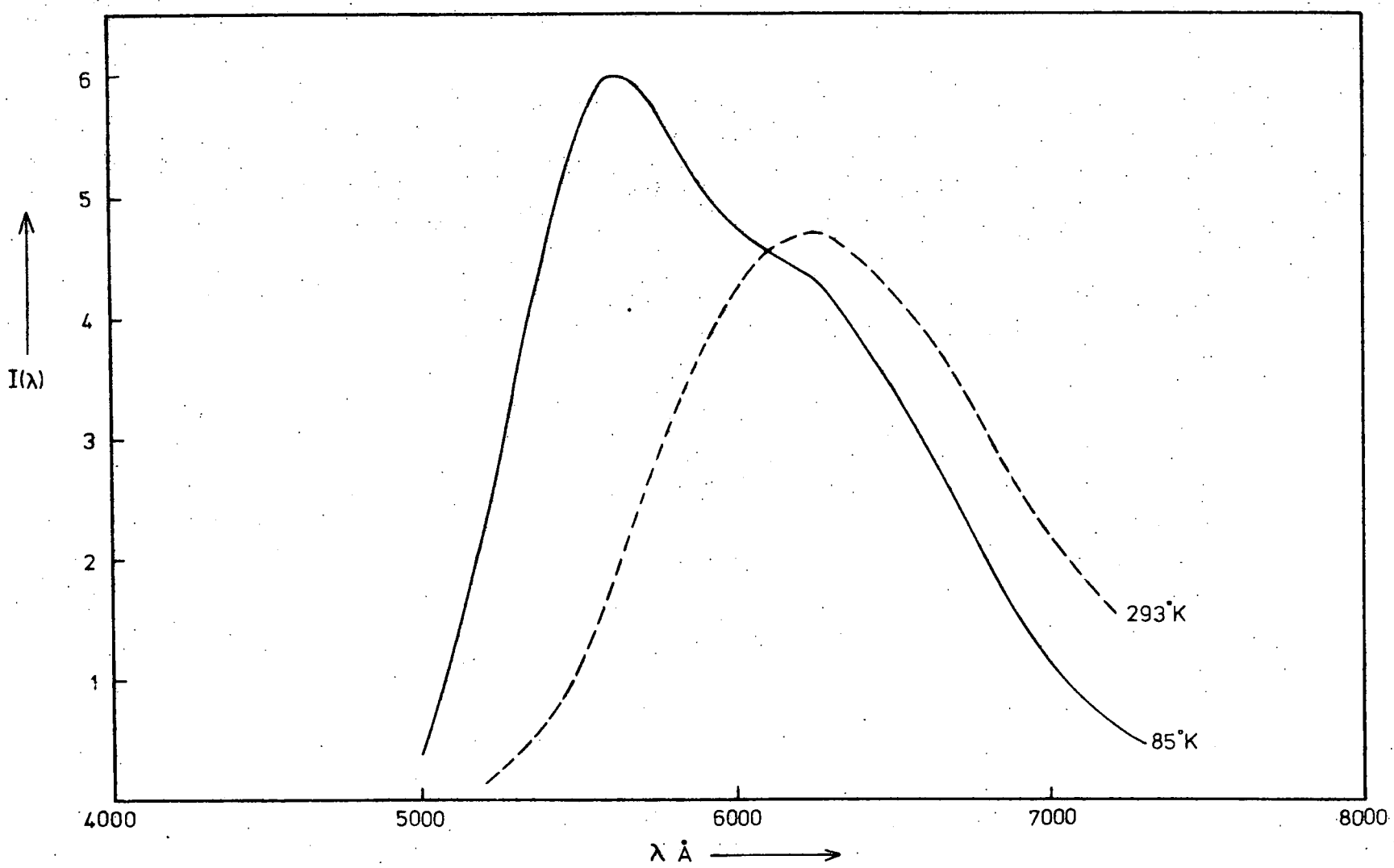

Fig. 5-26. Emission Spectrum under 3650 Å Excitation of ZnSe:Ga 188.

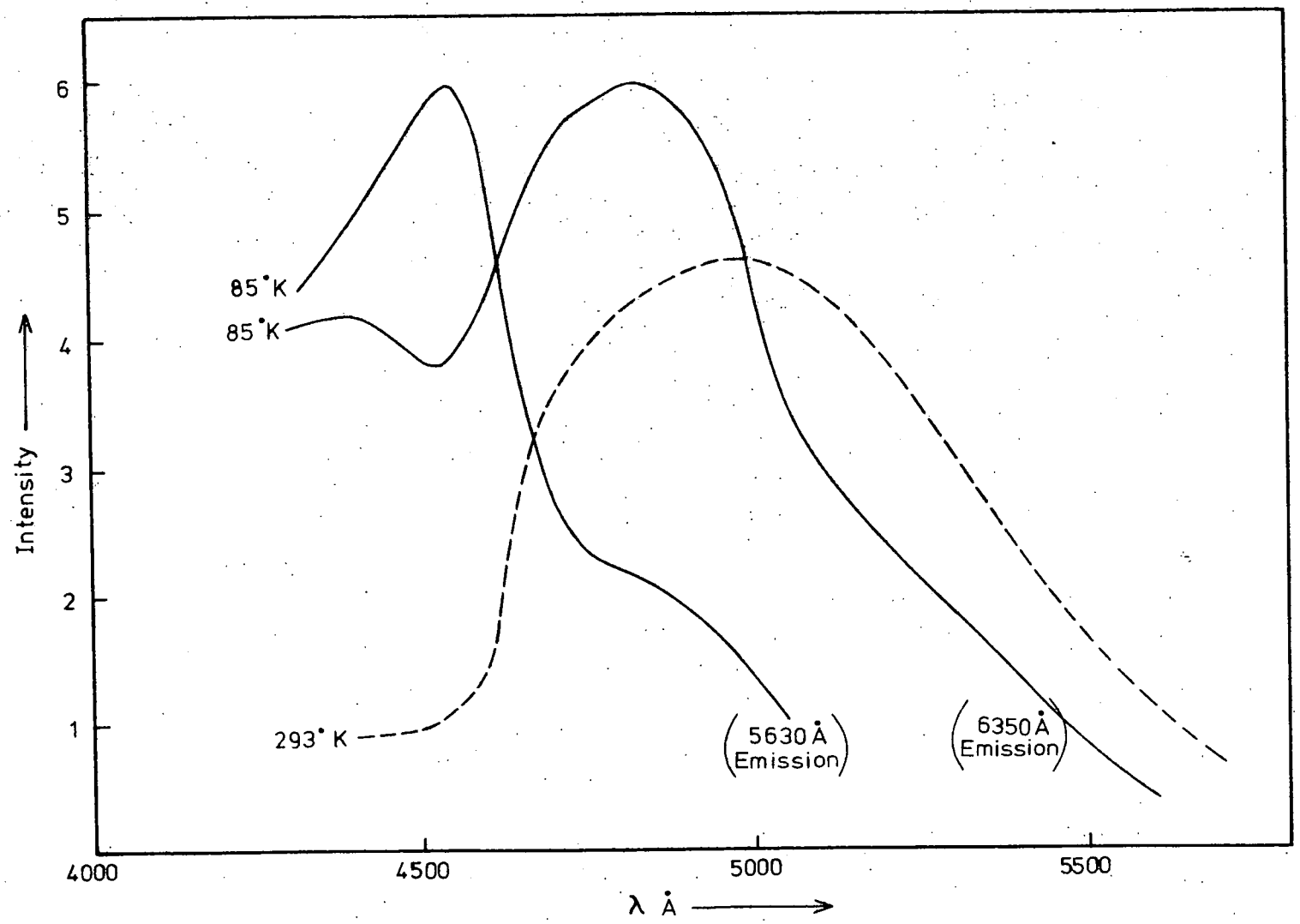

Fig. 5-27. Excitation Spectrum of ZnSe:Ga 188.

The excitation spectrum of crystal 188 at 85°K indicated the presence of the low energy copper excitation which is responsible for the long wavelength tail. However, the main feature was a broad band at 4800 Å, which was probably composed of two sub-bands, together with a peak at 4400 Å corresponding to bandgap excitation. When the green emission was monitored, a sharp peak was seen just below bandgap energy at 4550 Å. There was also a shoulder present at about 4850 Å. Once again this excitation spectrum is very similar to that of the indium doped sample 181 (figure 5.25) apart from an apparently higher copper content.

As in the case of indium doped crystals, zinc treatment produced a dense black precipitate in the crystal doped with 1000 p.p.m. gallium, number 140, and the emission and excitation spectra were again identical to those of undoped crystals following zinc treatment. Subsequent heat treatment in vacuum or selenium removed the precipitate, but caused the luminescence to become dominated by the copper emission as before, although the green emission band was not present at 85°K. The excitation spectrum was identical to that of the indium doped crystal after similar treatment. Excitation by light with a wavelength of 5300 Å, both before heating in zinc and after heating in selenium or vacuum, once again revealed the red emission centred at 6400 Å.

5.9 UNDOPED CRYSTALS

The body colour of undoped crystals varied between boules, from green to orange. Occasionally, this variation occurred within a single boule, the colour gradually changing along the length of the boule. The luminescent emission was also found to vary considerably from boule to boule, but crystals could be grouped into several different classes.

(a) Crystals 25 and 104, which possessed a yellow-green body colour, luminesced only when cooled below room temperature and at 85°K emitted

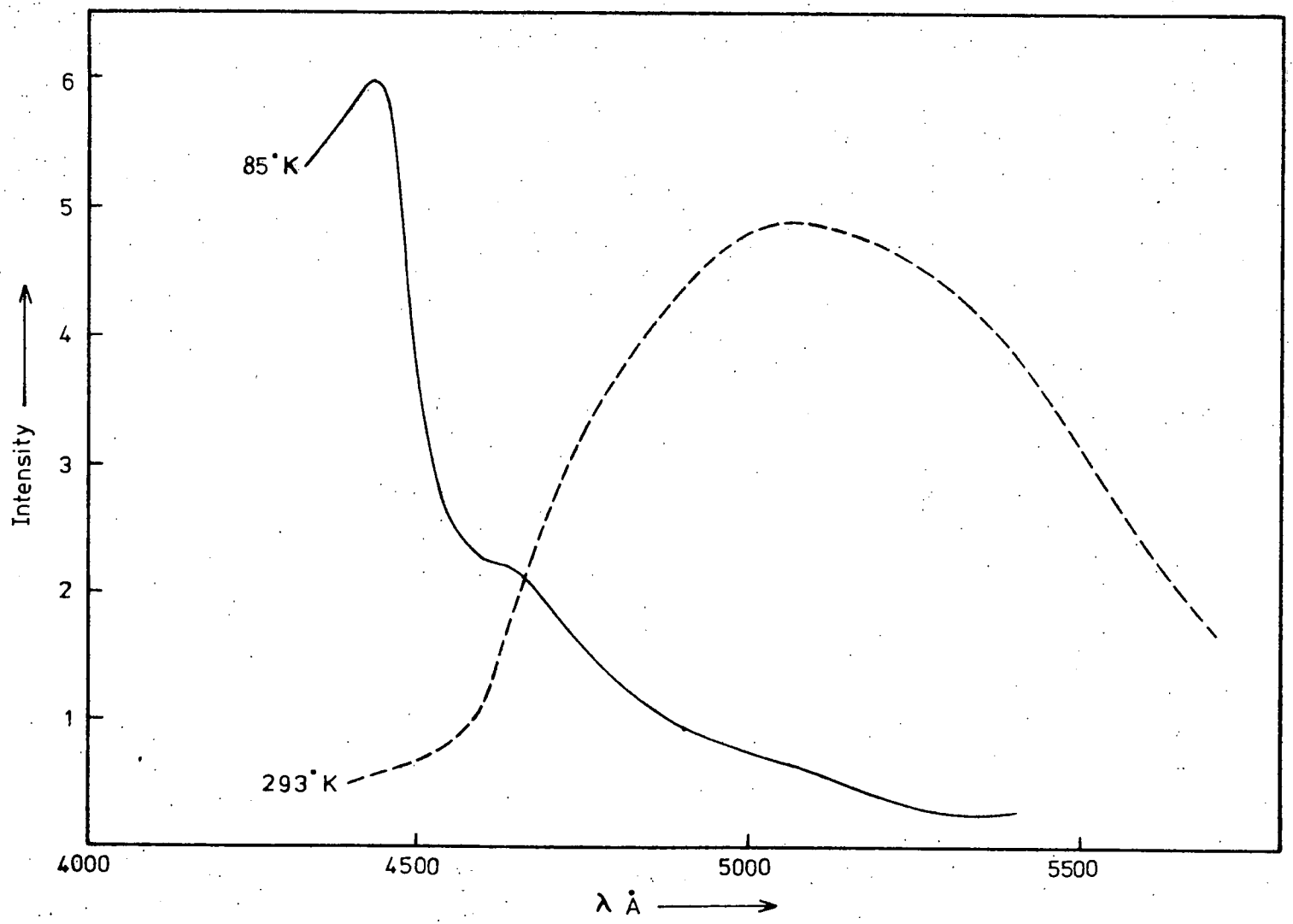

Fig. 5-28. Excitation Spectrum of ZnSe 7.

a single band at 5300 Å with a halfwidth of 0·22 eV. The excitation spectrum of 104 revealed a single band at about 4480 Å which probably corresponded to bandgap excitation.

(b) Crystals 2, 7 and 173 which had an orange body colour emitted a single red band at 6450 Å at room temperature. When cooled to 85°K the band increased in width from 0·28 eV to 0·31 eV, and shifted to about 6150 Å. The excitation spectrum of crystal 7 (figure 5.28) revealed a prominent broad band at about 5100 Å at 293°K and a sharp bandgap peak at 85°K. Excitation by light with a wavelength of 5300 Å again revealed the 6400 Å copper band and the excitation spectrum confirmed that the long wavelength copper emission was the dominant feature at 293°K. When the temperature was reduced the band increased in width as the S.A. emission began to predominate, and at 85°K the main component of the emission appeared to be the S.A. band. The shift in peak position was therefore due mainly to the S.A. band, which swamped the longer wavelength band.

(c) As an indication of the variation between boules, it was found that the end of crystal 7 which was grown last was green in colour and luminesced differently from the orange end. At 293°K this green end again emitted a red band at 6450 Å, with a halfwidth of 0·28 eV, but at 85°K a green band at 5420 Å with a halfwidth of 0·2 eV became dominant, whilst the red band shifted to 6325 Å and narrowed to approximately 0·18 eV. The longer wavelength band was probably again influenced by the presence of copper. The excitation spectrum of the green emission consisted of a broad band composed of sub-bands at approximately 4750 Å and 4550 Å.

(d) Crystal 172 was found to emit identically to 7 at 293°K, but at 85°K, in addition to the red emission, a green band with a halfwidth of 0·21 eV was observed at 5350 Å, instead of at 5420 Å as before.

(e) Crystals 171 and 177, which were yellow-orange in body colour,

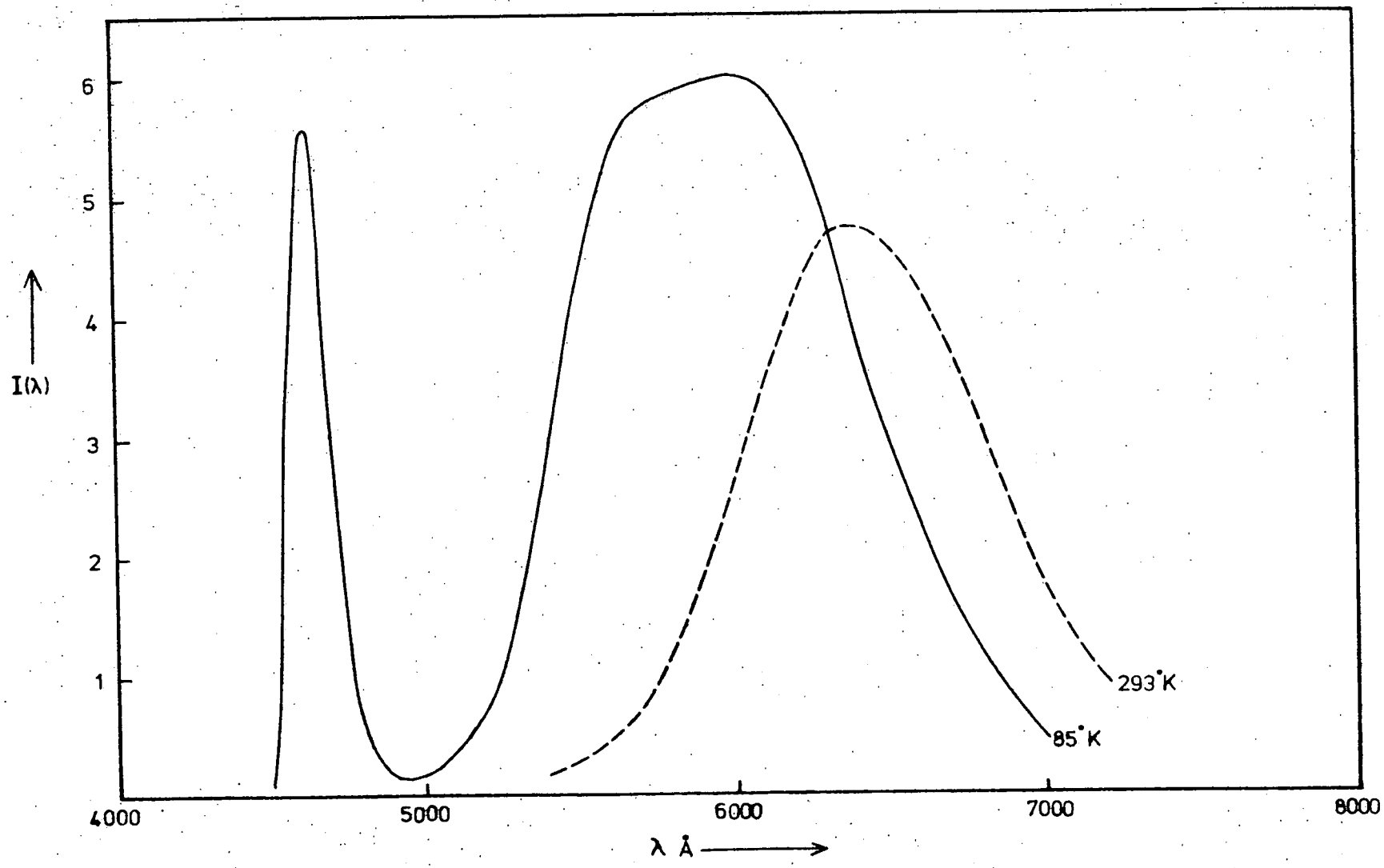

Fig. 5-29. Emission Spectrum under 3650 Å Excitation of ZnSe 171.

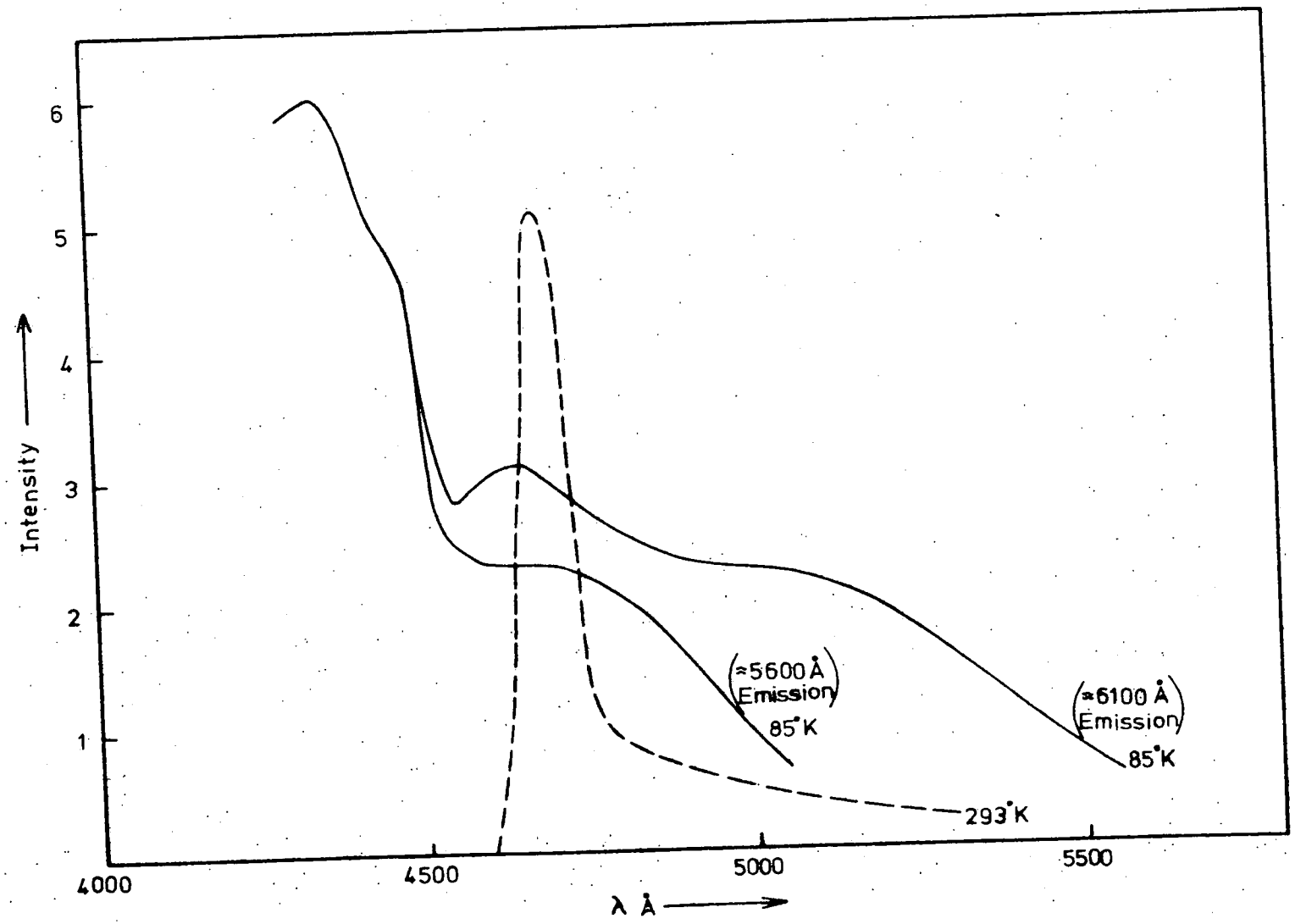

Fig. 5-30. Excitation Spectrum of ZnSe 171.

revealed a different character yet again. The emission at 293°K was again a band at about 6380 Å of 0·27 eV halfwidth. At 85°K two bands which were emitted could not be resolved, but appeared to lie at about 6100 Å and 5600 Å. A very intense edge emission was also produced by 171. The emission spectrum of crystal 171, which was the crystal used in the majority of zinc treatments, is shown in figure 5.29 and this can be compared with the emission after the various heat treatments carried out previously. The corresponding excitation spectrum revealed several bands (figure 5.30). At room temperature it consisted of a sharp peak near the bandgap at 4680 Å which was probably associated with S.A. emission. There was a slight tail towards longer wavelengths, and excitation within this tail at 293°K again produced the 6480 Å emission band. When the crystal was cooled to 85°K the excitation spectrum contained at least three bands apart from the long wavelength copper band. The peaks which occurred near the bandgap were probably associated with the S.A. band although the green emission also appeared to be excited by light of similar energy. The lower energy bands associated with the green emission were probably detected as a result of partial monitoring of the orange band, which was too close to be completely excluded.

(f) Finally, a piece of the yellow boule, number 197 was studied. This was grown from zinc selenide powder synthesized in this laboratory from semiconductor grade elements. The emission at 293°K consisted of an asymmetric broad band of halfwidth 0·32 eV, which had a maximum at 5800 Å. An unresolved orange band also appeared to be present. At 85°K the emission shifted to 5650 Å and narrowed to 0·19 eV. A long wavelength shoulder, caused by a band at about 6400 Å was also observed.

(g) After samples from boules 7, 104 and 171 had been heated in molten zinc, they were found to behave identically, despite the fact that they had emitted completely different bands previously. Each emitted only

the S.A. band (figure 5.4) and the excitation spectra showed the 4650 Å room temperature peak and the 4480 Å peak at 85°K (figure 5.5).

Excitation by light with a wavelength of 5300 Å did not produce the 6400 Å copper emission as it did in all the untreated crystals.

(h) When the undoped crystals were heated in selenium or in a vacuum, the results were similar to those obtained with indium or gallium doped crystals. The emission from samples of 171, treated in various ways, is shown in figure 5.31 and should be compared with the emission from untreated material (figure 5.29). Heating in vacuum at 850°C for one week had the least effect. The long wavelength band was increased and shifted towards longer wavelength whilst the yellow band was unchanged. After heating the sample in selenium for a week at 650°C, the low energy band became even more prominent and moved slightly more towards longer wavelengths, whilst the yellow band shifted towards the green and peaked at 5560 Å. The most obvious results were apparent when a crystal pretreated in zinc was heated in selenium. The emission was very similar to that observed when copper was introduced from the melt (figure 5.3). At 85°K it consisted of a red band at 6400 Å and a green band at 5440 Å. The corresponding excitation spectra (figure 5.32), revealed the prominent band near 5100 Å, previously associated with copper, especially in both the selenium treated crystals. Even in the crystal heated alone, this excitation band was more prominent than in the untreated crystal (figure 5.30). The excitation and emission spectra of crystal 171 heated in zinc and then selenium were identical to those of the indium doped crystal 139 heated in zinc and then selenium. This supports the view that the indium emission is swamped after such treatment. When light with a wavelength of 5300 Å was used to excite a sample from boule 171, which had been heated first in zinc then in selenium, the red band which was emitted was found to behave identically to that observed in crystals known to contain copper

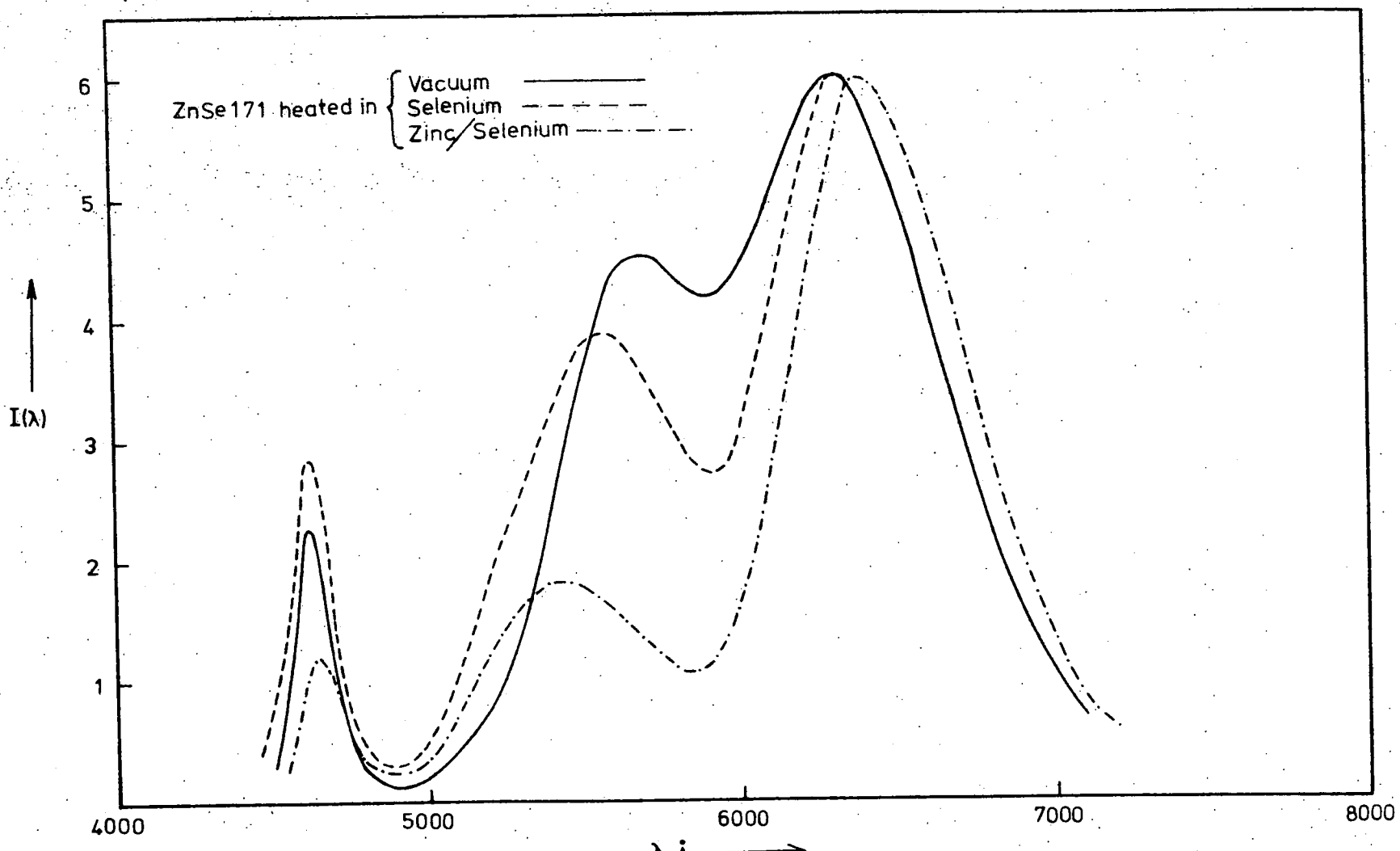

Fig. 5-31. Emission Spectra under 3650 Å Excitation at 85°K of ZnSe 171 after various heat treatments.

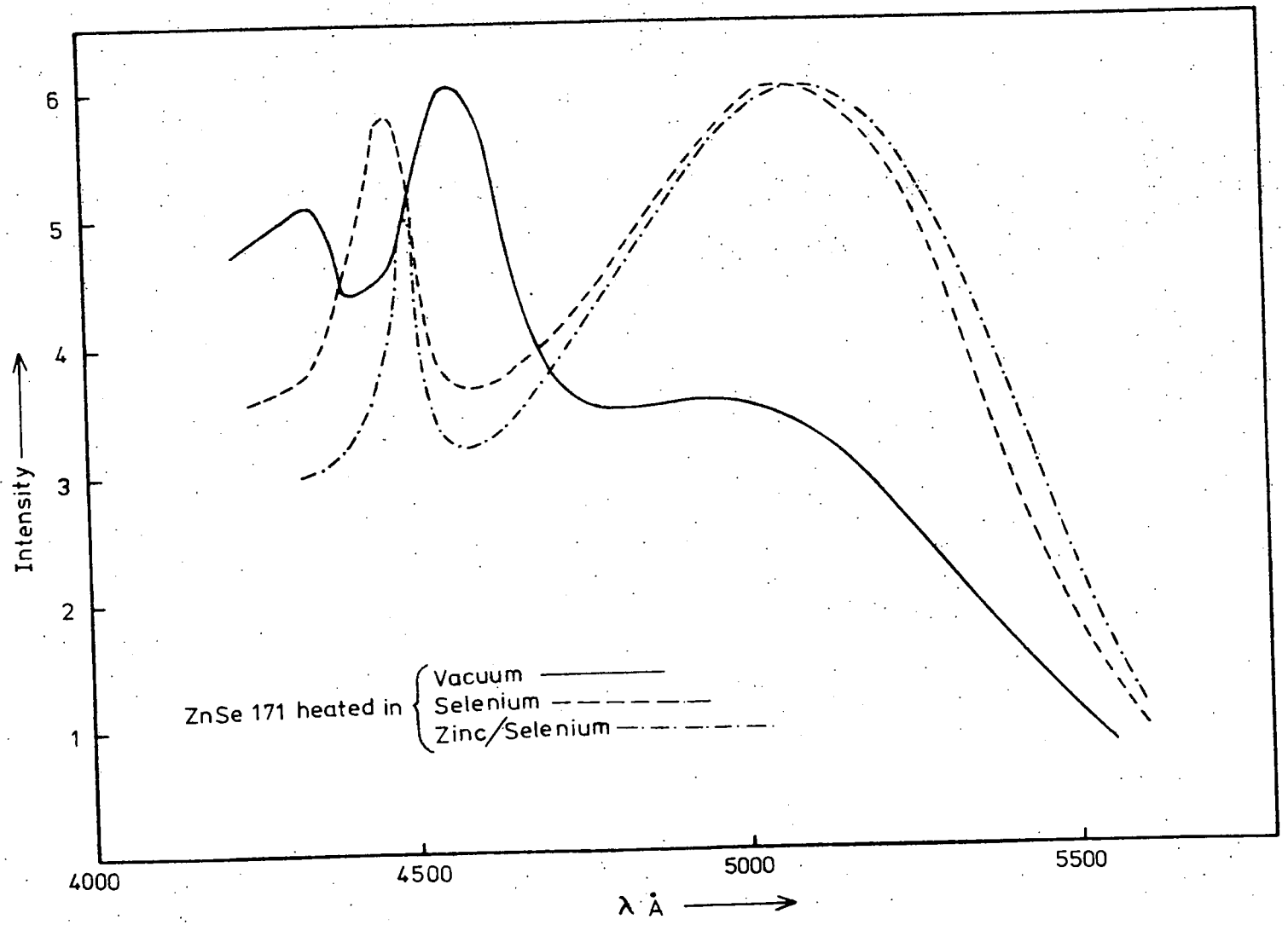

Fig. 5-32. Excitation Spectra at 85°K of ZnSe 171 after various heat treatments.

as regards the variation of halfwidth and peak position with temperature (figures 5.10, 5.11). It must be remembered that before the selenium treatment the crystal emitted only in the 6150 Å S.A. band and that no red emission was observed when 5300 Å excitation was employed. This increase in the copper red band was also observed in a piece of crystal 104, which previously emitted only in the 5300 Å band and then was found to emit an additional 6360 Å band after it had been heated in vacuum. It therefore seems likely that copper is diffused into crystals during heat treatment, especially when heated in selenium. The treatment in selenium also caused the body colour of all the crystals to become orange-red.

(i) To summarise, the emission from undoped material appears complex. Emission in the orange and red regions appears to consist of a combination of S.A. and copper bands, but the various green and yellow emission bands have no such simple explanation. The orange S.A. band, which lay at 6150 Å at 85°K, was produced when undoped crystals were heated in zinc. Heating alone or in vacuum appeared to cause copper contamination.

5.10 THERMAL QUENCHING

It was explained in section 1.10 that from measurements of the quenching of the photoluminescent emission produced when the temperature of a crystal is raised, it is possible to obtain a value for the energy of the luminescent centre relative to either the conduction or the valence band. This technique was used on several crystals and the results will now be explained.

When it is required to monitor the quenching of a particular band it is necessary to ensure that only one emission band is being monitored. This was accomplished by using a suitable wavelength for the excitation. For example, when the copper emission was studied, light with a wavelength of 5300 Å was used, but for the S.A. emission the mercury wavelength of

3650 Å was satisfactory, since there appeared to be only one luminescent emission process present in such crystals.

It is also necessary to ensure that the excitation band does not shift from the wavelength of the exciting light as the temperature is raised, thus changing the excitation efficiency. This was not particularly important for the copper emission, since the corresponding excitation band was fairly wide. With the S.A. emission, 3650 Å light excited the crystal within the short wavelength tail of the excitation peak at both 293°K and 85°K. At 3650 Å there is very little variation in efficiency with wavelength and hence there is very little effect as the excitation band shifts with temperature. If, for example, excitation at 4500 Å were used, there would be a considerable effect when the temperature was raised as the excitation band shifted to 4700 Å.

It is also necessary to ensure that the maximum of the emission band is always monitored as it shifts with temperature. In practice this was a relatively unimportant point because of the large bandwidth of the spectrometer and the comparatively small shifts which were observed. Wavelength corrections were, however, made during measurements. Similarly, the variation in sensitivity of the system with wavelength was negligible over the small wavelength changes involved and no correction factors were necessary.

(a) Self-activated Emission

The thermal quenching curves of the emission from several crystals heated in zinc and which therefore emitted in the S.A. band, are shown in figure 5.33. The crystals behaved identically except for the undoped sample 171 heated in zinc plus aluminium which will be discussed later in this section. The intensity decreased very slowly as the temperature was raised to approximately 240°K and then fell off more rapidly, dropping by about three orders of magnitude by 400°K.

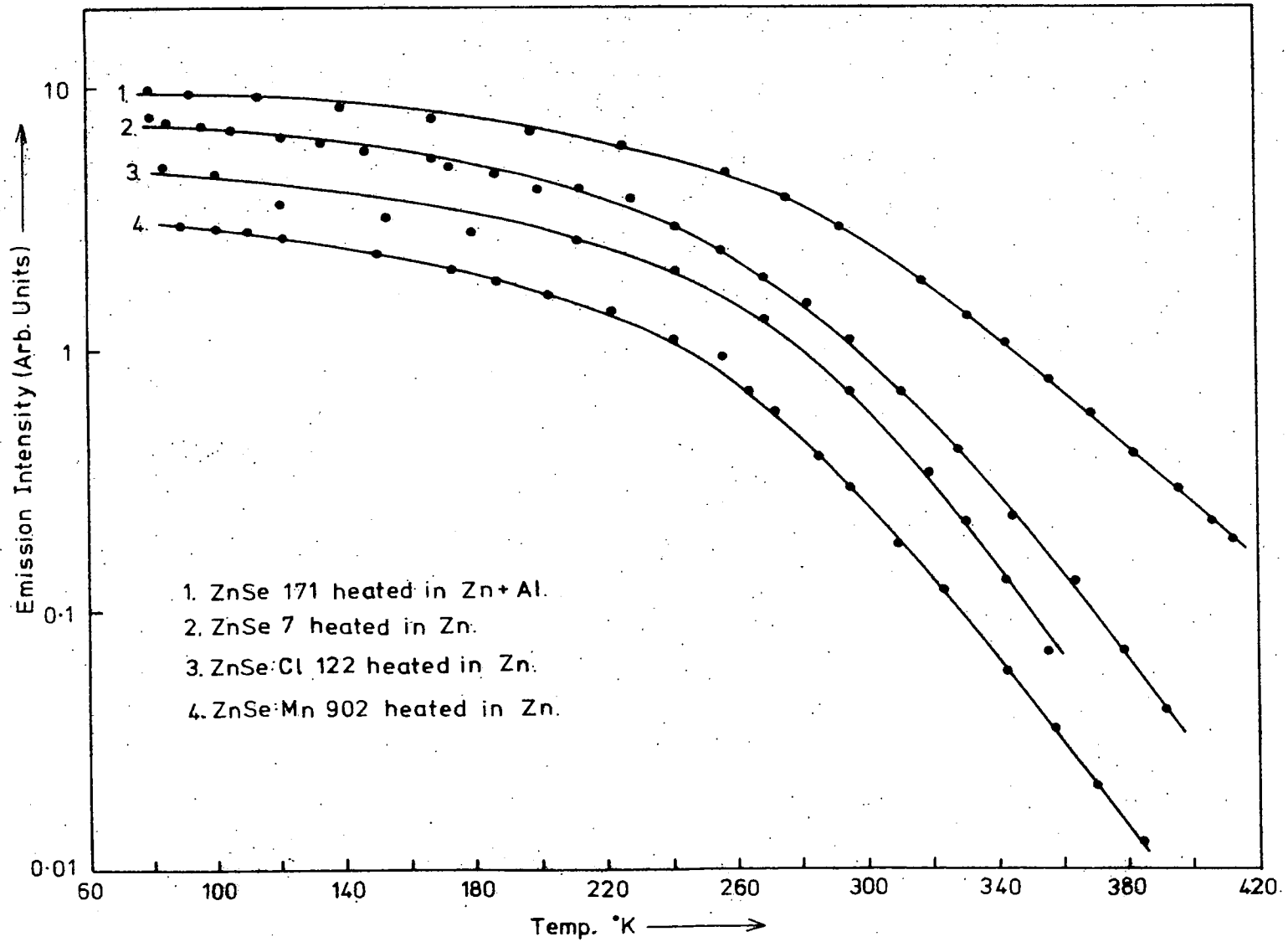

Fig. 5-33. Curves illustrating Thermal Quenching of S.A. Emission for various Samples of ZnSe.

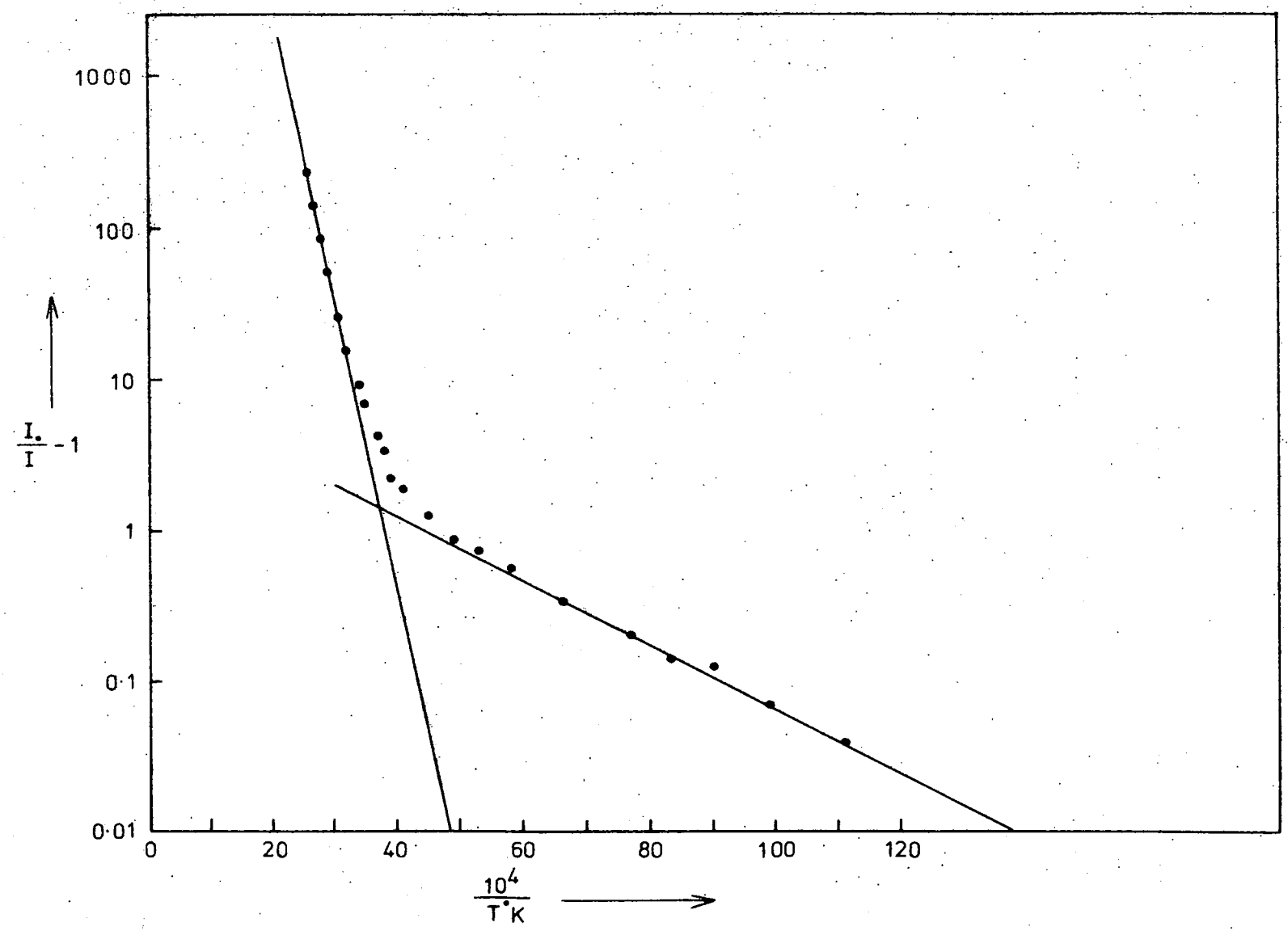

Fig. 5-34. Thermal Quenching Data for S.A. Emission of ZnSe:Mn 902 heated in Zn plotted to allow calculation of Activation Energy.

From equation 1.2 the luminescence efficiency η is given by

$$\eta = \frac{1}{1 + C \exp -\frac{W}{kT}}$$

If I_0 is the emission intensity before quenching occurs and I is the intensity at temperature T, the efficiency is also given by

$$\eta = \frac{I}{I_0}$$

$$\therefore \quad \frac{I}{I_0} = \frac{1}{1 + C \exp -\frac{W}{kT}}$$

$$\frac{I_0}{I} - 1 = C \exp -\frac{W}{kT}$$

$$\log_e \left(\frac{I_0}{I} - 1\right) = \log C - \frac{W}{kT}$$

Therefore a plot of $\log_e \left(\frac{I_0}{I} - 1\right)$ versus $\frac{1}{T}$ ought to produce a line of slope $-\frac{W}{k}$.

When the curves in figure 5.33 were plotted in the form $\log_e \left(\frac{I_0}{I} - 1\right)$ versus $\frac{1}{T}$, as in figure 5.34, the resultant curves appeared to be composed of two straight line regions. The slopes of the high temperature regions gave activation energies of 0·44 eV for 122 (Zn), 0·41 eV for 7 (Zn), and 0·38 eV for 902 (Zn). The low temperature regions gave corresponding energies of 0·031 eV, 0·028 eV and 0·043 eV.

There are two possible explanations for the quenching energies observed. Two quenching processes may be acting. That ~~activated~~ ACTING at the lower temperatures would have low quenching efficiency as well as low energy, whereas the higher energy effect must have a much higher efficiency. The energies obtained for each process are the same for each sample, within experimental error, and the quenching processes appear to be identical irrespective of the initial dopant. The second possibility is

that the slow decrease in efficiency at low temperatures is due to some effect other than quenching, such as the displacement of the excitation spectrum as mentioned earlier and that only one quenching process, that of higher energy, is actually present.

The less pronounced thermal quenching of the luminescence of the crystal treated in zinc plus aluminium is almost certainly the result of interference from the 6400 Å copper emission. This 6400 Å band was found to be present at high temperatures when the halfwidth and peak position of the S.A. emission were studied as a function of temperature (figures 5.10, 5.11). In section (b) it will be shown that the copper emission quenches much more slowly and at a higher temperature than the S.A. emission and thus becomes dominant at high temperatures. Due to the presence of the copper emission, no attempt was made to calculate the quenching energy associated with the aluminium S.A. band.

(b) Copper Emission

Figure 5.35 illustrates the thermal quenching curves for several crystals which exhibited the copper emission at 6400 Å when excited with light with a wavelength of 5300 Å. The samples chosen include both those deliberately doped with copper and those in which the copper had entered the lattice unintentionally, for example the indium and aluminium doped crystals. There is a considerable variation from sample to sample and no pattern seems obvious. However, in none of the crystals did the emission begin to be quenched until above approximately 280°K and most crystals continued to emit even well above room temperature. The red band in the copper selenide doped crystal 158 was quenched very rapidly at just above room temperature whereas the crystal heated in zinc plus copper showed no quenching whatsoever up to 405°K.

When the quenching curve of crystal 158 was plotted in the form of $\log_e(\frac{I_0}{I} - 1)$ versus $\frac{1}{T}$, as for the S.A. emission, a quenching energy of 1·0 eV was obtained. Similar plots for crystals 122 and 171 heated

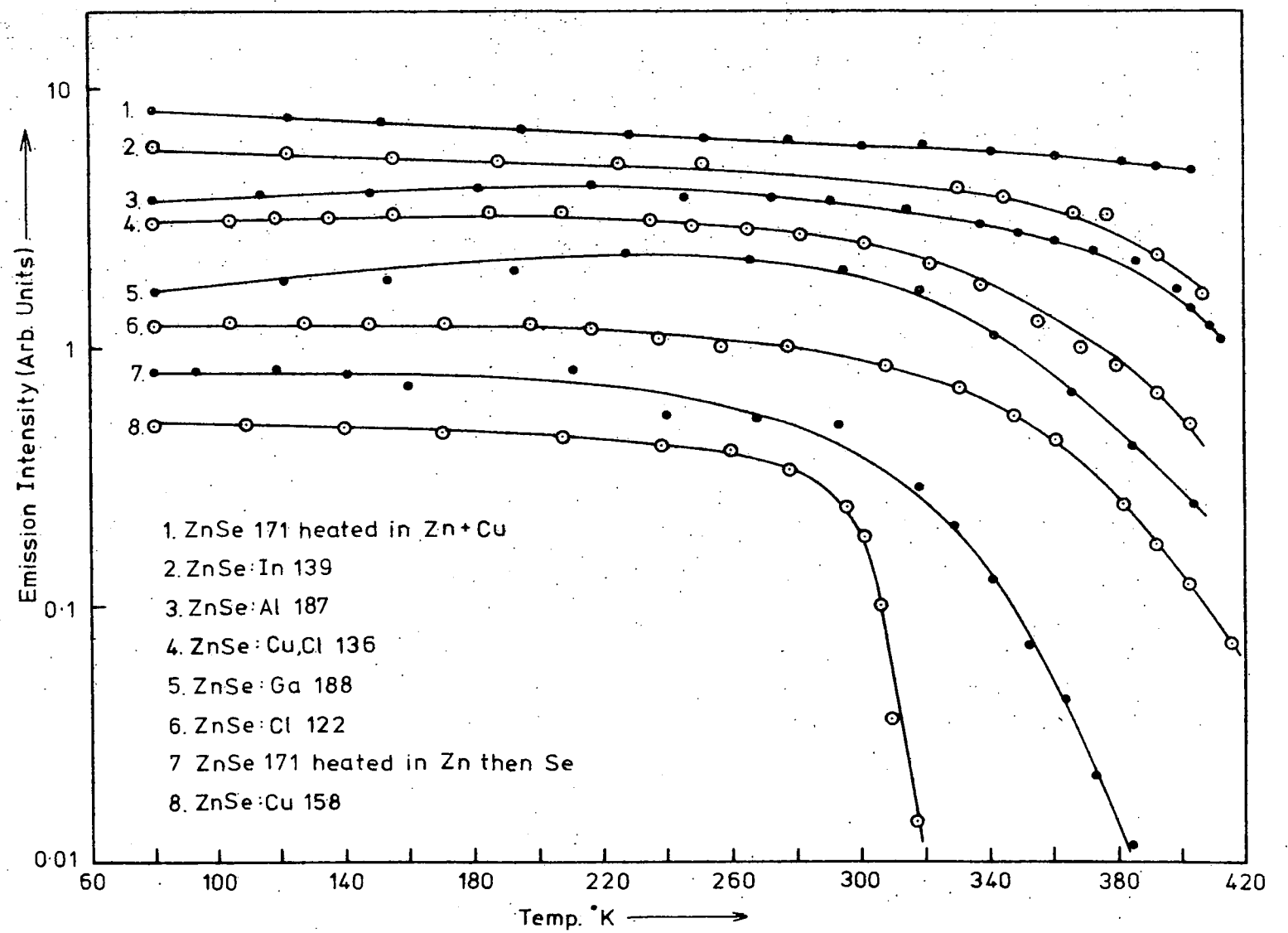

Fig. 5-35. Curves illustrating Thermal Quenching of Copper Red Emission for various Samples of ZnSe.

in zinc then selenium gave energies of 0·55 eV and 0·63 eV respectively. The emission from the majority of crystals quenched at too high a temperature for a complete quenching curve to be obtained. However, it appears that the quenching energy involved must be quite large, partly because of the energy values obtained from the three crystals just mentioned and partly because of the high temperatures at which quenching occurred. It seems that there must be some additional process present which is not taken into account in the simple quenching theory of Chapter 1.

The similarity of the quenching curve of the undoped crystal heated in zinc and then selenium to the other curves in figure 5.35, including those known to contain copper, adds support to the suggestion that heating in selenium somehow introduces copper into the sample.

The high quenching temperature of the 6400 Å band is responsible for the dominance of the copper excitation and emission bands in most crystals at high temperatures. It is also the reason why, with 3650 Å excitation, the emission of the majority of crystals tends to shift towards longer wavelengths when the temperature is raised.

(c) Emission in the Green Region

Very few measurements were made on the quenching properties of the green luminescence bands. Reliable results could not be obtained from those crystals which emitted an adjacent orange band, such as the indium and aluminium doped crystals, due to overlap, but results have been obtained with four green emitting crystals.

The 5300 Å emission band of the copper doped sample 169 quenched very sharply above 130°K with an activation energy of 0·3 eV. The 5460 Å band in the copper selenide doped crystal 158 was however quenched more gradually above approximately 170°K with a corresponding activation energy of 0·37 eV.

Two undoped crystals, 104 and 7, were also studied. The 5300 Å

emission from 104 was found to fall rapidly above 120°K with a quenching energy of 0·22 eV. The 5420 Å band of crystal 7 was not quenched until the temperature exceeded 160°K when an energy of 0·26 eV was obtained.

It thus appears that the green emission bands are quenched, in general, with lower activation energies than the red bands, as would be expected. It also appears that the shorter wavelength 5300 Å band is associated with a lower quenching energy than the 5460 Å and 5420 Å bands.

5.11 SUMMARY

(a) Self-activated Emission

Self activated emission has been observed in the presence of a variety of coactivators, for example chlorine, iodine and aluminium. However, there appeared to be only two distinct emission processes (see table 5.2). Both produced very broad bands which shifted to lower energy upon cooling, the opposite of the usual shift with energy gap variation. A high energy emission occurred at 6150 Å at 85°K and 6050 Å at 293°K, when the coactivator was chlorine or iodine or when the crystal was simply heated in zinc. A low energy emission at 6350 Å at 85°K which shifted to 6260 Å at 293°K was present when aluminium acted as the coactivator and a very similar band was produced as a result of indium coactivation and possibly also gallium. This is a situation similar to that which occurs for the S.A. emission of zinc sulphide where group III coactivators produce lower energy emission than that associated with group VII dopants (Prener and Weil, 1959). The shift to longer wavelengths on cooling is also typical of S.A. zinc sulphide.

Several differences were observed however in the excitation spectra when the various coactivators were present. Zinc selenide simply heated in zinc was found to possess an excitation band at 4480 Å, that is approximately bandgap energy, with a tail towards longer wavelength. However,

TABLE 5.2

EMISSION BANDS OBSERVED IN ZINC SELENIDE DURING PRESENT INVESTIGATION

Emission Band	Dopant	Position of Emission Band Å		Position of Excitation Band Å	
		293°K	85°K	293°K	85°K
Copper- Red	Cu	6480	6400	5350	5150
Copper-Green	Cu		5300		4440
Copper-Green	Cu		5450		≏4600
					≏4750
S.A.	-	6050	6150	4650	4480
S.A.	Cl	6050	6150	4700	≏4550
				4950	4800
S.A.	I	6050	6150	≏4700	≏4600
				5100	4890
S.A.	Al	≏6240	6360	4700	≏4550
				4900	4800
S.A.	In	≏6200	≏6300		
Group III-Green	Al		5570		4450
Group III-Green	In		5600		4530
Group III-Green	Ga		5630		4550
Undoped-Green	-		5650		
Undoped-Green	-		≏5600		
Undoped-Green	-		5420		≏4550
					≏4750
Undoped-Green			5350		
Undoped-Green	-		5300		4480

with iodine, chlorine and aluminium a lower energy excitation process was active resulting in the excitation band at about 4800 Å. An S.A. emission band could not be completely resolved in the indium doped material because of the overlapping copper emission and subsequent zinc treatment caused the indium to be precipitated. However, an S.A. band similar to that produced by aluminium did appear to be present (figure 5.24). It is clear that in all these samples at least two excitation processes contribute to the same emission process. In the impurity coactivated samples the band edge excitation process appears to be of relative insignificance.

The higher energy emission observed after undoped material is heated in zinc is the same as that reported by Aven and Woodbury (1962) to be at 6000 Å at room temperature after purifying zinc selenide by zinc extraction. Markovskii et al (1969) also reported a similar room temperature emission at 6100 Å which shifted to 6150 Å at 77°K in zinc selenide heated in zinc.

Iida (1968) investigated the S.A. band in zinc treated material and attributed the emission to pair recombination involving a level approximately 0·35 eV above the valence band. However, the corresponding excitation spectrum consisted solely of a bandgap excitation peak with no long wavelength tail as observed in the present study.

Holton et al (1965) obtained a broad emission band at 6240 Å at 42°K from zinc selenide coactivated by chlorine or bromine, without zinc treatment. This almost certainly corresponds to the band which is located at 6150 Å at 85°K particularly as they also observed a shift to higher energy when the temperature was raised. They also found the S.A. emission associated with aluminium to be displaced to lower energy by about 200 Å as in the present work. A localised transition between a zinc vacancy and the coactivator was again suggested to be the electronic process involved. However, the corresponding excitation spectrum of chlorine coactivated material at 77°K consisted of a band at approximately 4660 Å

together with a bandgap peak and Holton et al considered the S.A. emission to be associated with the lower energy excitation. Their excitation spectrum is similar to the excitation spectrum of chlorine doped material obtained after zinc treatment (fig 5.12) except that the positions of the long wavelength bands differ by 150 Å. They postulated that the low energy band was associated with excitation between donor and acceptor pairs, a mechanism which is not employed in the present study. No excitation spectra of bromine or aluminium doped material were illustrated.

The majority of so-called S.A. emission bands observed by other workers, for example Leverenz (1950), Markovskii and Smirnova (1961), Asano et al (1965) and Mironov and Markovskii (1965), are almost certainly influenced by the long wavelength copper band and are similar to the emission observed in the present work from several undoped crystals prior to zinc extraction.

Table 1.1 shows that most work has been carried out on undoped material. Where zinc extraction has not been employed the results appear to be influenced by the longer wavelength copper emission. Chlorine has received the most attention of the impurity coactivators but once again the results seem to be influenced by copper. The results of Holton et al (1965) and Iida (1968) agree quite well with the present results although there are some differences with respect to the long wavelength excitation band. Aluminium coactivation has received little attention apart from the work of Holton et al and Aven and Halsted (1965) whose emission bands differ in position by approximately 400 Å. The present results are more nearly in agreement with those of Holton et al. Although bromine coactivation has been mentioned by Holton et al, there have been no reports of S.A. emission with other coactivators, for example iodine and indium.

Since the mechanism of the S.A. emission from zinc sulphide is reasonably well understood and has been attributed to zinc vacancies

associated with coactivator atoms, it seems highly probable that a similar process should occur in zinc selenide. Both undoped and chlorine doped zinc selenide produce the same emission band after zinc treatment and so it would seem that either the chlorine is playing no part in the process or it is present in both types of material. However, since group III and group VII impurities produce different emission bands it is clear that the coactivator does play an important part in the luminescent process and is not simply acting in a compensating role. Therefore the most likely explanation is that trace impurities of chlorine or similar group VII elements in the undoped material are responsible for the S.A. emission observed. The energy level diagram shown in figure 5.36 can be used to explain the excitation and emission processes quite well. The coactivator level C is probably identical to the donor level observed in the region 0.1 eV to 0.3 eV during Hall effect measurements on samples containing various donor impurities (see chapter 7). In undoped material the number of coactivator levels would be quite small and the main electronic excitation would occur across the bandgap or to the shallow donor levels observed during Hall effect measurements on crystals heated in zinc and attributed to the hydrogenic donor level associated with chlorine. A free electron would tend to migrate within the lattice until it reached a coactivator atom where it would fall into the level C. Similarly the free hole would migrate until it became trapped in the zinc vacancy level, whereupon radiative pair recombination would occur. The excitation spectrum would therefore tend to possess a maximum at energies close to the energy gap with perhaps a tail towards longer wavelengths due to excitation directly to the C level (see figure 5.5). As the number of coactivator centres increased however, excitation directly to the level C would tend to increase in opposition to direct band to band excitation and the longer wavelength excitation would become more important (figure 5.13) and would finally become the dominant

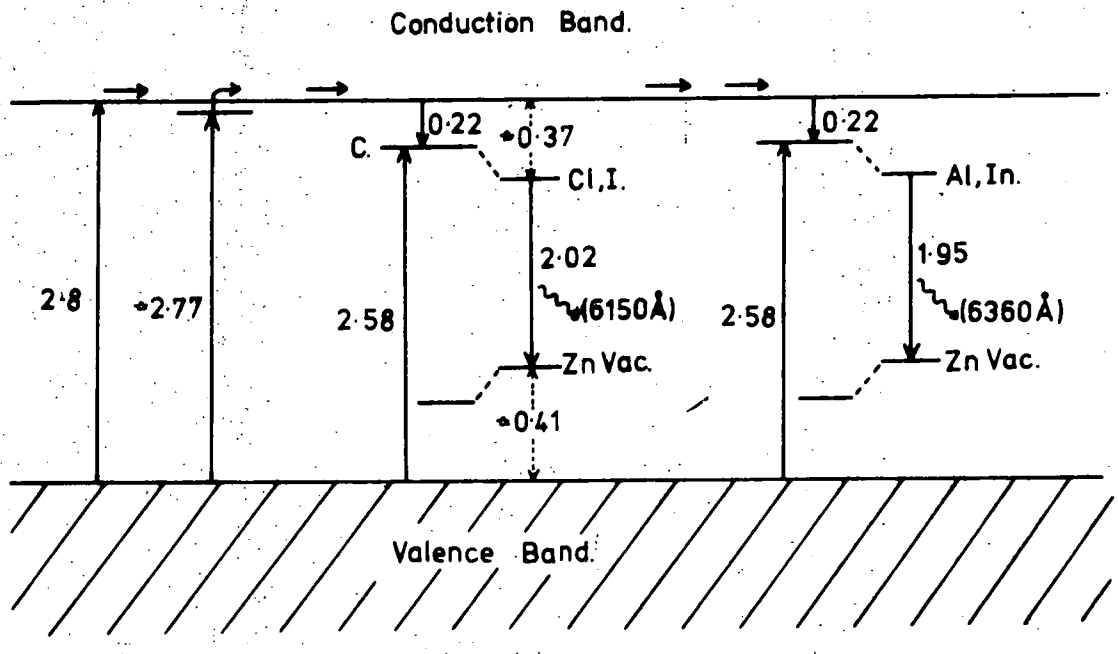

Fig. 5-36. Excitation and Emission Processes present in S.A. ZnSe at 85°K.
(Energies in eV.)

process (figures 5.12, 5.16). Despite the change in the excitation process the emission would be expected to remain the same, as indeed it is observed to do. Doping with iodine led to similar results (figure 5.19). The lower energy emission band produced by aluminium coactivation can be explained using the same process postulated for the S.A. emission in zinc sulphide, that is on a basis of the different lattice sites on which the group III and group VII elements enter the crystal (Prener and Weil 1959). A similar model to that used to explain the chlorine S.A. emission can also be used to explain the aluminium S.A. emission (figure 5.36). Indium also caused the emission to occur at lower energies and can therefore be considered to act in a similar manner to aluminium, which is once again in agreement with the model proposed by Prener and Weil for zinc sulphide.

Several factors must be considered in order to obtain the various energy values shown in figure 5.36 and the following energy level diagrams. In figure 5.36 the energies of the electron transitions to the conduction band and the shallow donor level were arrived at by assuming the bandgap of zinc selenide to be 2.8 eV and the hydrogenic donor ionization energy to be approximately 0.03 eV. The value of 0.22 eV for the depth of the level C below the conduction band prior to excitation was obtained by considering the maximum of the low energy excitation band (4800 Å) observed in chlorine doped crystals heated in zinc to correspond to the transition from the valence band to this level. The energies of the radiative transitions in both the chlorine and aluminium samples were obtained simply from the wavelengths at which the maxima of the respective emission bands occurred although a coulombic contribution which is not known ought to be included. The energy of the zinc vacancy level relative to the valence band was obtained from the thermal quenching data and the depth of the chlorine donor level after relaxation was therefore obtained simply from knowledge of the bandgap energy. However the depth of the

donor level was also compared with the value of 0.33 eV obtained for the donor ionization energy of chlorine using Hall effect measurements. Similar methods involving energies obtained from both excitation and emission spectra and thermal quenching data were used in conjunction with any other relevant information in order to construct the remaining energy level diagrams.

The main necessity for heating zinc selenide in zinc to produce the S.A. emission is to remove the copper impurities responsible for the 6400 Å emission which tends to swamp the S.A. band. This is clear since various samples exhibit S.A. emission even without zinc extraction because of their low copper content (figures 5.17, 5.24). The treatment may however tend to increase the number of zinc vacancies, and hence S.A. emission centres, by removing the copper from zinc sites. The zinc vacancies appear to remain in the crystal in equilibrium with the zinc solvent as was found by Aven and Halsted (1964). It would therefore seem likely that the proposal by Mironov and Markovskii (1965) and Markovskii et al (1969) that excess zinc is responsible for S.A. emission is incorrect.

As the temperature is raised there are three possible explanations for the shift of the emission band towards higher energy. The first is that suggested by Iida who considered that the electron can move from one chlorine ion to another more readily at higher temperatures and since the probability of recombining via neighbouring centres is higher than that between more distant centres, more of the short distance transitions should occur at the higher temperatures. Since the latter produce higher energy emission, the emission band should shift to higher energy upon warming. Alternatively the electrons may recombine whilst they are in the conduction band, utilising their kinetic energy to produce higher energy emission. This is similar to the model proposed by Holton et al. The third explanation is that of Shionoya et al (1964) who explained the

shift on a basis of the configurational coordinate model. Their model seems unlikely since it predicts that the excitation band should shift in the opposite direction to the emission band and this effect was certainly not observed with manganese activation which can undoubtedly be analysed in terms of the configurational coordinate model (chapter 6). Furthermore, the work of H.J. G. Meyer (see Goede and Gutsche 1966) leads to an equation which predicts a shift to lower energy of both the emission and excitation bands upon warming and thus contradicts Shionoya's suggestion. It therefore seems more probable that the shift is due to a combination of the first two mechanisms and that the variety of recombination processes, involving variously spaced donor-acceptor pairs with some contribution from free electrons, contributes towards the large halfwidth observed.

The thermal quenching energy of approximately 0.4 eV almost certainly corresponds to excitation of valence electrons into the zinc vacancy levels although the nature of the lower quenching energy in the region of 0.03 eV does not appear clear and it may well be spurious.

(b) COPPER EMISSION

(i) Three emission bands, thought to have been the result of copper activation have been observed here in zinc selenide (see Table 5.2). With the red emission at 6400 Å, although it is possible that two different centres may be responsible for identical emission bands, it seems more likely that the emission was the result of copper in all crystals, even where it had not been intentionally introduced. For example, with the undoped sample of zinc selenide heated in zinc and then selenium, interstitial selenium or zinc vacancies could produce an acceptor level. However the properties of the emission band as regards its halfwidth, peak position, and temperature variation together with its excitation spectrum are so similar to the properties of the copper emission band that the centre is either identical or, more likely, is in fact due to copper entering the crystal during the heat treatment. Since it has

been shown by Markovskii et al (1969) that the low energy copper emission is produced by as little as 0.1 p.p.m. copper it would seem that if copper is to be avoided, zinc selenide must be heated in the presence of liquid zinc which then acts as a getter and dissolves any copper in preference to the zinc selenide. It was not possible to detect copper chemically in samples thought to contain small quantities because of the limits of the atomic absorption spectroscopic technique which was approximately 20 p.p.m. From the measurements on the chlorine and the indium doped boules it would appear that the amount of copper entering the lattice depends on the amount of donor impurity added. For example, boule 122 which possessed a prominent low energy copper excitation band, was found to contain more chlorine than crystal 123 which was relatively unaffected by copper impurities, the S.A. band being much more prominent and not swamped by the copper red band. This tendency of the copper to enter the lattice with donor impurities is probably associated with the compensating nature of zinc selenide.

There are at least two possible models to explain the copper red emission. They are analogous to the two models used to describe the copper green emission in zinc sulphide and are illustrated in figure 5.27. The first is a Schön-Klasens model involving the copper level approximately 0.86 eV above the valence band whilst the second is based on a pair recombination model involving a shallow copper acceptor level, due to a different charge state of the copper ion, and a donor level. Both models have previously been proposed (Table 1.2) but no definite choice can be made since time resolved spectroscopy has shown a shift typical of pair recombination in one case (Fujiwara and Fukai 1967) and no shift in another (Iida 1969). The Schön-Klasens model would appear to be more probable because the high thermal quenching energies obtained would be associated with the excitation of valence electrons into the deeper 0.86 eV level. Furthermore the red emission was unchanged

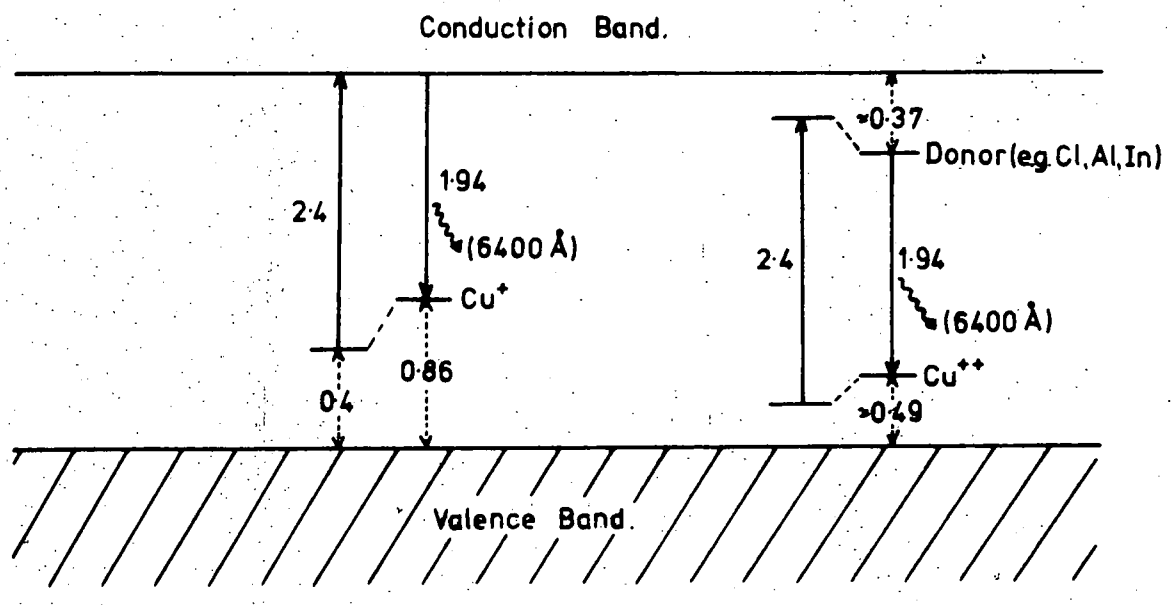

Fig. 5-37. Two Possible Mechanisms to Explain the Cu-Red Emission from ZnSe at 85°K. (Energies in eV.)

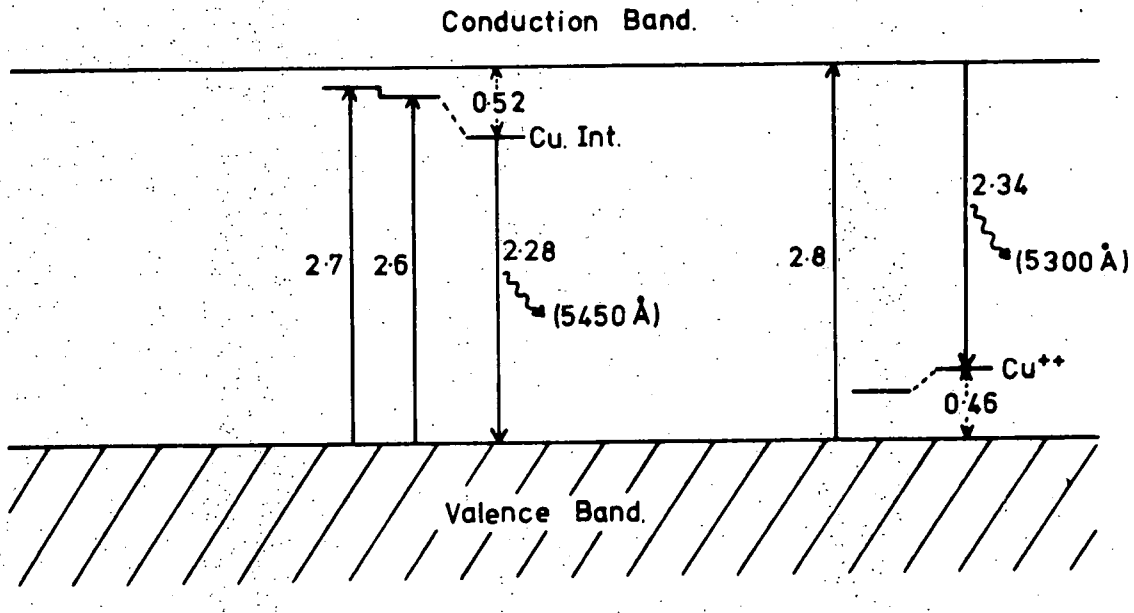

Fig. 5-38. Excitation and Emission Processes responsible for the Cu-Green Emission Bands in ZnSe at 85°K. (Energies in eV.)

regardless of which donor, chlorine or indium for example, was present. This observation differs from that of Kröger and Dikhoff (1950) on zinc sulphide coactivated with elements of groups III and VII. The deep copper level, 0.86 eV above the valence band, is probably the same as that reported by Stringfellow and Bube (1968) as the Cu^{+} level. They placed the level 0.72 eV above the valence band but assumed an energy gap of only 2.7 eV. The photoconductivity measurements reported in the following chapter, which can be explained on a basis of the Schön-Klasens model, might tend to support a pair recombination model. More experiments of this type however are necessary before one mechanism can be preferred to the other. The shift to lower energy with increasing temperature is almost certainly a result simply of the reduction of the energy gap.

(ii) The high energy green emission, which is excited by bandgap radiation may be produced by a Schön-Klasens transition to a copper level approximately 0.46 eV above the valence band (figure 5.38). This is the same model as that proposed by Stringfellow and Bube although they placed the copper level, suggested to be due to a substitutional Cu^{++} ion, 0.35 eV above the valence band. Once again their value of 2.7 eV for the bandgap may be responsible for this difference. If a pair recombination model were assumed to be responsible for the copper red emission this shallow copper level would be the ground state of the transition. However if this were so, the copper red and green bands would be expected to be seen simultaneously and this does not occur. Furthermore the quenching energies would be expected to be identical whereas in fact they differ by at least 0.5 eV. This adds further support for the Schön-Klasens model in explaining the copper red emission.

(iii) The 5450 Å emission is less easy to explain. The excitation energies of both 2.7 eV (4600 Å) and 2.6 eV (4750 Å) appear to produce this emission band. If these excitation transitions transfer electrons

from the valence band to the donor levels, the ground state copper level would need to be less than 0.3 eV above the valence band. This would appear to be much too shallow an acceptor level and would not agree with Cu^{++} level responsible for the 5300 Å emission. Also if the Cu^{++} level were involved in both the 5300 Å and the 5450 Å emissions both bands might be expected to be observed simultaneously and this did not happen. The most likely possibility is that the copper entered the lattice interstitially in a similar manner to that described by Shionoya et al (1965) for zinc sulphide, where it would act as a donor. This would then allow a Lambe-Klick type transition (figure 5.38) from a deep copper donor level approximately 0.5 eV below the conduction band. The higher energy excitation would then be to an excited state of the interstitial copper ion. This interstitial introduction of copper might explain the fact that the 5450 Å band appeared when zinc selenide was heated in zinc containing large quantities of copper and also appeared simultaneously with the copper red band (figure 5.1). The zinc vacancy sites may have been completely occupied by copper atoms after treatment in zinc melts containing a high concentration of copper, the excess necessarily entering interstitially.

The thermal quenching data agree reasonably well with the models proposed to explain the two green bands although the values are slightly less than would be expected. It must be remembered however that the band-gap and energy depths alter considerably at the higher temperatures at which quenching occurs. Furthermore the measured thermal quenching energies are normally less than the corresponding optical energies because of the Franck - Condon effect.

(c) GROUP III GREEN EMISSION

The green emission bands of crystals containing the group III coactivators which occurred in the region of 5600 Å (see Table 5.2) do not appear to have been reported previously. They were usually more prominent in the

lightly doped boules since the more heavily doped boules tended to be dominated by the usual S.A. and copper red bands. The corresponding excitation consists of a transition almost at the bandgap for indium and gallium doped material and at the bandgap with aluminium. The situation is complicated because several green bands can occur in the region of the group III emission in undoped crystals. The 5600 Å emission, therefore, might simply be the result of the group III elements producing some form of native defect following their entry into the lattice although the influence of a donor level associated with the group III elements cannot be ruled out.

(d) UNDOPED MATERIAL

Often undoped zinc selenide was found to emit a green band at 85°K. The position of this band varied from 5300 Å to 5650 Å and sometimes occurred together with emission in the orange to red region. Since measurements were not made specifically on these green emission bands and their corresponding excitation spectra were not always monitored, it is not possible to give any models for the processes involved. Three of the bands involved, those at 5300 Å, 5420 Å and 5600 Å may correspond to bands already observed in copper doped samples and material containing group III impurities and it is possible that copper may again be influencing the emission or alternatively native defects may be responsible. However there is really insufficient information to ascribe the emission bands to any specific process and more work is necessary before this can be done.

CHAPTER 6

PHOTOLUMINESCENCE RESULTS - MANGANESE ACTIVATION

6.1 INTRODUCTION

Attempts were made to introduce manganese into zinc selenide in the hope that it would act as an efficient activator in electroluminescent diodes subsequently fabricated from such material. Manganese was chosen since it is well proved as an efficient photoluminescent activator in such materials as willemite, the halophosphates and zinc sulphide and has also been used successfully in zinc sulphide electroluminescent panels (Vecht 1970). It was expected that the emission would occur in the yellow to red spectral region, partly by analogy with the position of the emission band produced in zinc sulphide and partly as a result of the orange and red bands reported to be emitted by zinc selenide containing manganese (section 1.11b). Since there is no agreement whatsoever as to the true position of the manganese emission from zinc selenide and since the majority of reported results have been obtained using powder samples, the present work should also help to clarify the situation.

Once again, in the figures illustrating the emission and excitation spectra the intensities are in arbitrary units and the spectra obtained at 85^{o}K and room temperature are not shown to scale. Details of the growth conditions of the crystals described in this chapter are given in table 6.1.

6.2 DOPING TECHNIQUES

(a) Two boules, 141 and 160 were grown by vapour phase transport in

TABLE 6.1

CRYSTAL GROWTH CONDITIONS

Crystal No.	Starting Material	Dopant	Tail Conditions
141	D	20 mgm MnSe	Zn 555°C
160	D	0·2 gm Mn	Zn 555°C
165	Op	0·2 gm $MnCl_2$	Zn 555°C
170	Op	0·1 gm $MnCl_2$	Zn 555°C
213	Op	$MnCl_2$ + 20 mgm Mn	Zn 600°C
SS.3	Op	3 mgm $MnCl_2$	Sublimation
SS.4	Op	30 mgm $MnCl_2$	Sublimation
902	Op	2 mgm I + 40 mgm Mn	Iodine Transport

Mass of ZnSe Charge = 20 gm for Vapour Phase Transport
3 gm for Sublimation Runs
4 gm for Iodine Transport

D = Derby Luminescents

Op = B.D.H Optran

the presence of 1000 p.p.m. manganese selenide and 1% manganese metal respectively. The emission from both crystals under 3650 Å excitation at 293°K was found to consist of a single, weak red band. Crystal 141 emitted a band of halfwidth 0·30 eV at 6420 Å and crystal 160 a band of halfwidth 0·27 eV at 6475 Å. These bands appeared to be very similar to those found in the majority of crystals described in the previous chapter and were probably a superposition of both the copper and the S.A. bands. When cooled to 85°K, crystal 141 emitted a green band at 5280 Å (0·21 eV halfwidth) together with an orange band at 6300 Å (0·20 eV halfwidth). The emission from crystal 160 at 85°K consisted of two very weak bands at 5470 Å (0·26 eV halfwidth) and 6340 Å. Because of the relative insignificance of the orange bands and the presence of the green bands at 85°K it was thought probable that very little or no manganese was present in these crystals. Later neutron activation analysis of crystal 160 showed it to contain only 0·5 p.p.m. manganese. It was therefore concluded that the manganese cannot be introduced into a vacuum sublimed boule from either the metal or its selenide.

(b) An attempt to introduce manganese by diffusion into an undoped crystal from a zinc plus manganese melt, as was accomplished with copper and aluminium, also proved unsuccessful. A black deposit was formed on the surface of the zinc selenide. This was probably manganese selenide or some similar compound.

(c) Several boules were grown by vapour phase transport with manganese chloride present in either the reservoir or the charge. The resultant boules possessed an orange body colour and were found to emit a bright orange band at both 293°K and 85°K. The emission from crystal 165, grown with 1% manganese chloride in the reservoir, had its maximum at 6350 Å whereas that from crystal 170, grown with ½% manganese chloride in the tail, lay at 6250 Å. Two other crystals, grown with 1% manganese chloride in the reservoir and charge had maxima at 6460 Å and 6440 Å

respectively. Halfwidths were of the order of 0·3 eV. When cooled to 85°K the bands became slightly narrower, approximately 0·28 eV wide, and shifted to higher energy. The emission from crystals 165 and 170 at 85°K lay at 6150 Å whilst that from the other two crystals occurred at 6200 Å. Although the crystal with the lowest manganese content emitted at shorter wavelengths than the others, this was probably the result of its lower chlorine content and hence a lower copper content. This effect was observed previously when chlorine doped material was studied.

In most respects manganese chloride doped crystals behaved identically to crystals grown in the presence of zinc chloride. However, when the excitation spectrum of the orange emission was measured a major difference was observed. At 85°K, in addition to the peak corresponding to bandgap excitation there were two well-defined excitation peaks at about 5050 Å and 5350 Å. These peaks were much more pronounced for crystal 165 than for 170 (figure 6.1) and are thought to be associated with manganese.

In order to study the manganese excitation and emission spectra more easily, crystal 213 was grown with a higher manganese content. This was achieved partly by raising the reservoir temperature to 600°C and therefore producing a higher partial pressure of manganese chloride in the growth region, and partly by adding manganese metal to the charge material. The resultant crystal again had an orange body colour and emitted a bright orange band under U.V. excitation at both 293°K and 85°K as before. However the band was shifted slightly towards longer wavelengths, its maximum occurred at 6250 Å, with a halfwidth of 0·29 eV at 85°K. When the excitation spectrum at 85°K was measured (figure 6.2) it was found to consist of a small peak at the bandgap at approximately 4400 Å plus the two manganese bands at 5030 Å and 5370 Å. The two sharp peaks were found to be more pronounced than those of crystal 165, and atomic absorption analysis showed that crystal 213 contained 1700 p.p.m.

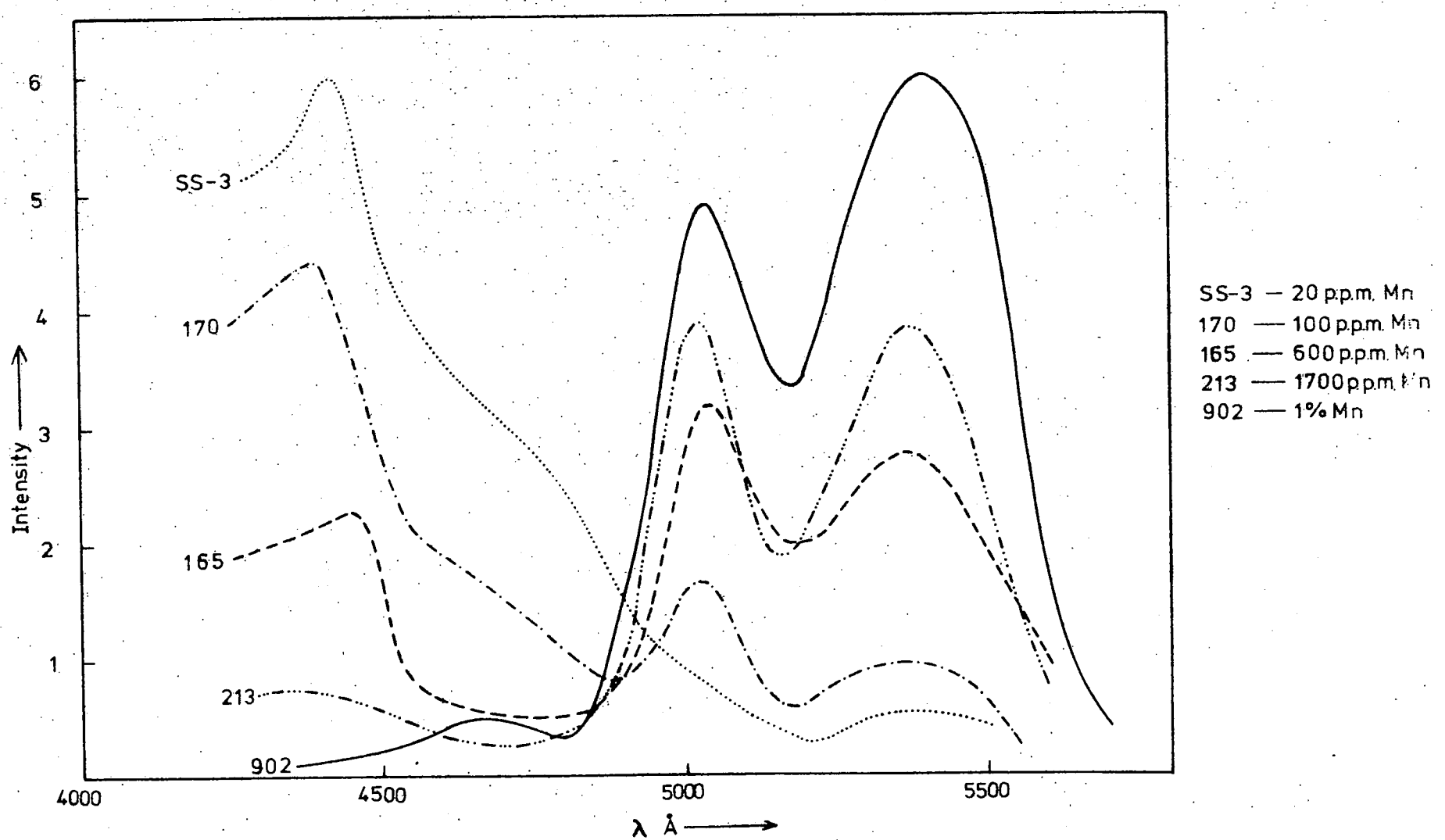

Fig. 6-1. Excitation Spectra at 85°K of various ZnSe:Mn Samples.

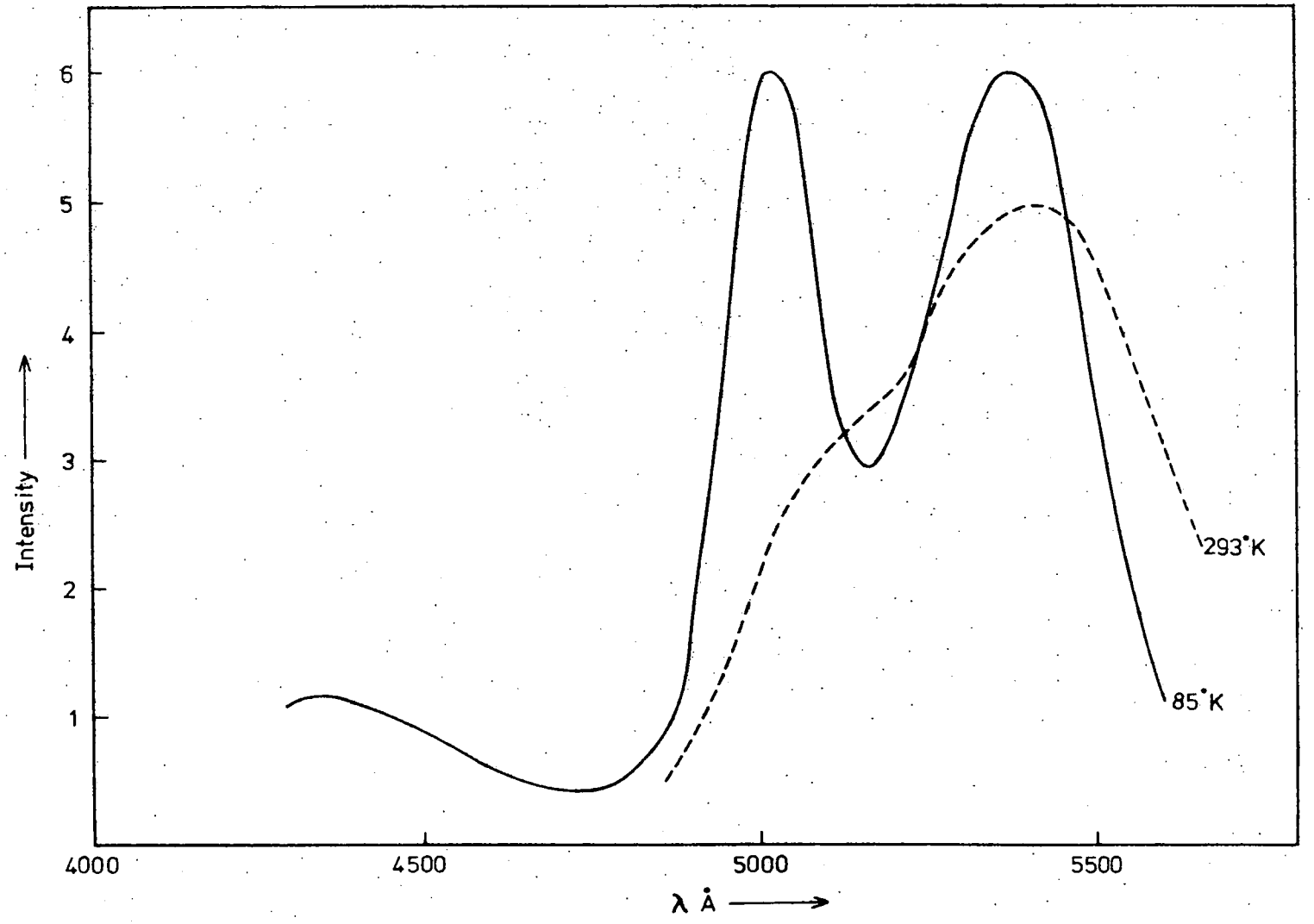

Fig. 6-2. Excitation Spectrum of ZnSe:Mn 213.

manganese compared with 600 p.p.m. in crystal 165 and 100 p.p.m. in crystal 170. At room temperature the excitation peak at the bandgap disappeared and the manganese bands broadened so that they could not be resolved (figure 6.2). At 85°K the halfwidths of the high and low energy manganese excitation peaks were 0·11 eV and 0·13 eV respectively.

When light with a wavelength of 5300 Å was used to excite crystal 213 the spectral emission distribution shown in figure 6.3 was obtained. At 85°K, in addition to the broad red band at 6400 Å observed previously in the majority of crystals, there was a narrower band at 5870 Å. When the wavelength of the exciting light was changed to 5200 Å, the 5870 Å band was reduced considerably and became of comparable intensity to the 6400 Å copper band. The two excitation wavelengths correspond approximately to the maximum of the low energy manganese excitation band (5300 Å) and the minimum between the two excitation bands (5200 Å). It can therefore be assumed that excitation within the manganese excitation band was responsible for the production of the 5870 Å emission, which would appear to be the characteristic manganese emission. In the preceeding chapter an excitation band at 5200 Å associated with copper, was reported. Copper was probably also present in crystal 213 and excitation within this band led to the 6400 Å emission. Excitation with light with a wavelength of 5000 Å also produced the 5870 Å manganese emission band, suggesting that the two excitation bands are associated with the same manganese emission process. The emission spectrum obtained when 3650 Å excitation was employed was apparently a combination of the copper emission, the manganese emission and the S.A. emission, which is strongly associated with the bandgap excitation.

(d) In an attempt to introduce even more manganese into zinc selenide, several further crystals were grown by rapid sublimation in a sealed tube with manganese chloride present. Zinc selenide platelets mixed

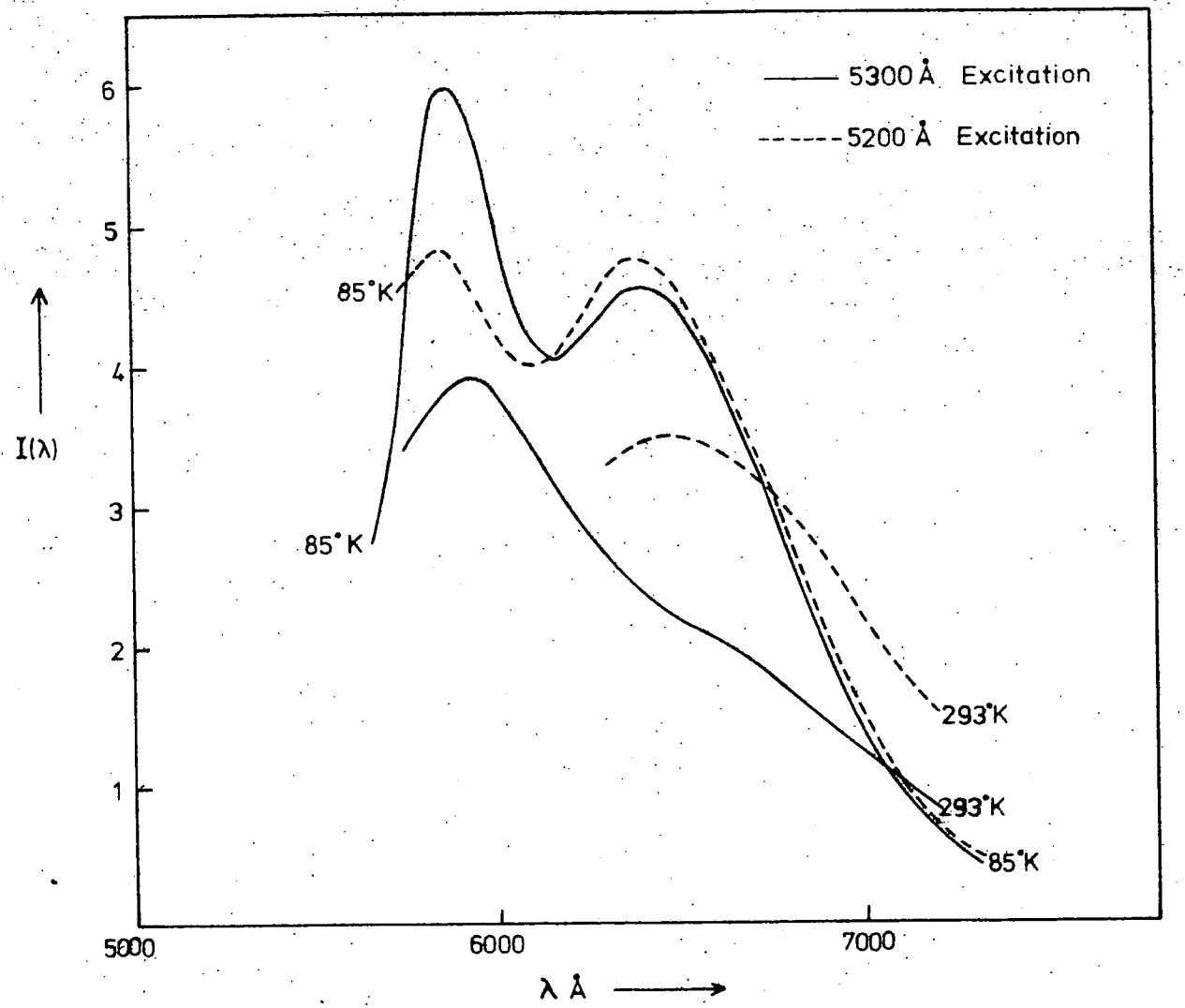

Fig. 6-3. Emission Spectrum of ZnSe:Mn 213 under 5200 Å and 5300 Å Excitation.

with 0·1% manganese chloride were sublimed to produce a yellow polycrystal, SS.3. The excitation spectrum of this crystal is illustrated in figure 6.1. The manganese bands are barely visible and the major excitation appears to occur across the bandgap. The crystal was later analysed and found to contain only 20 p.p.m. manganese. This estimate of the manganese content agrees quite well with the observed excitation spectrum. Zinc selenide mixed with 1% manganese chloride did not transport along the tube and instead the charge sintered to a deep red and orange mass (sample SS.4). The excitation spectrum of this material revealed prominent manganese peaks but the crystals were too non-uniform to be accurately analysed and were extremely polycrystalline.

(e) Finally boule 902 was produced using the iodine transport method in which zinc selenide platelets plus 1% manganese metal were transported using iodine. The boule had a deep orange body colour and was of high crystalline quality. When excited by 3650 Å light at 293°K it emitted a broad red band at 6550 Å with a halfwidth of 0·36 eV. When cooled to 85°K the band narrowed to 0.31 eV and shifted to 6250 Å (figure 6.4). The excitation spectrum of this crystal revealed once more the prominent manganese excitation bands (figure 6.1). There was no evidence of a band to band excitation peak although there was a small peak at 4670 A°. This did not appear to be the same band that was responsible for the shoulder observed in the spectra of crystals SS.3 and 170. This shoulder was probably associated with the S.A. and chlorine excitation bands which can be seen in figure 5.9. The peak at 4670 Å therefore is probably another manganese excitation band. At 293°K the excitation spectrum of crystal 902 was almost identical to that of crystal 213 (figure 6.2). The two manganese bands were again unresolved and displaced to longer wavelengths compared with their positions at 85°K.

When light chopped at 10 cps was used to excite crystal 165, it

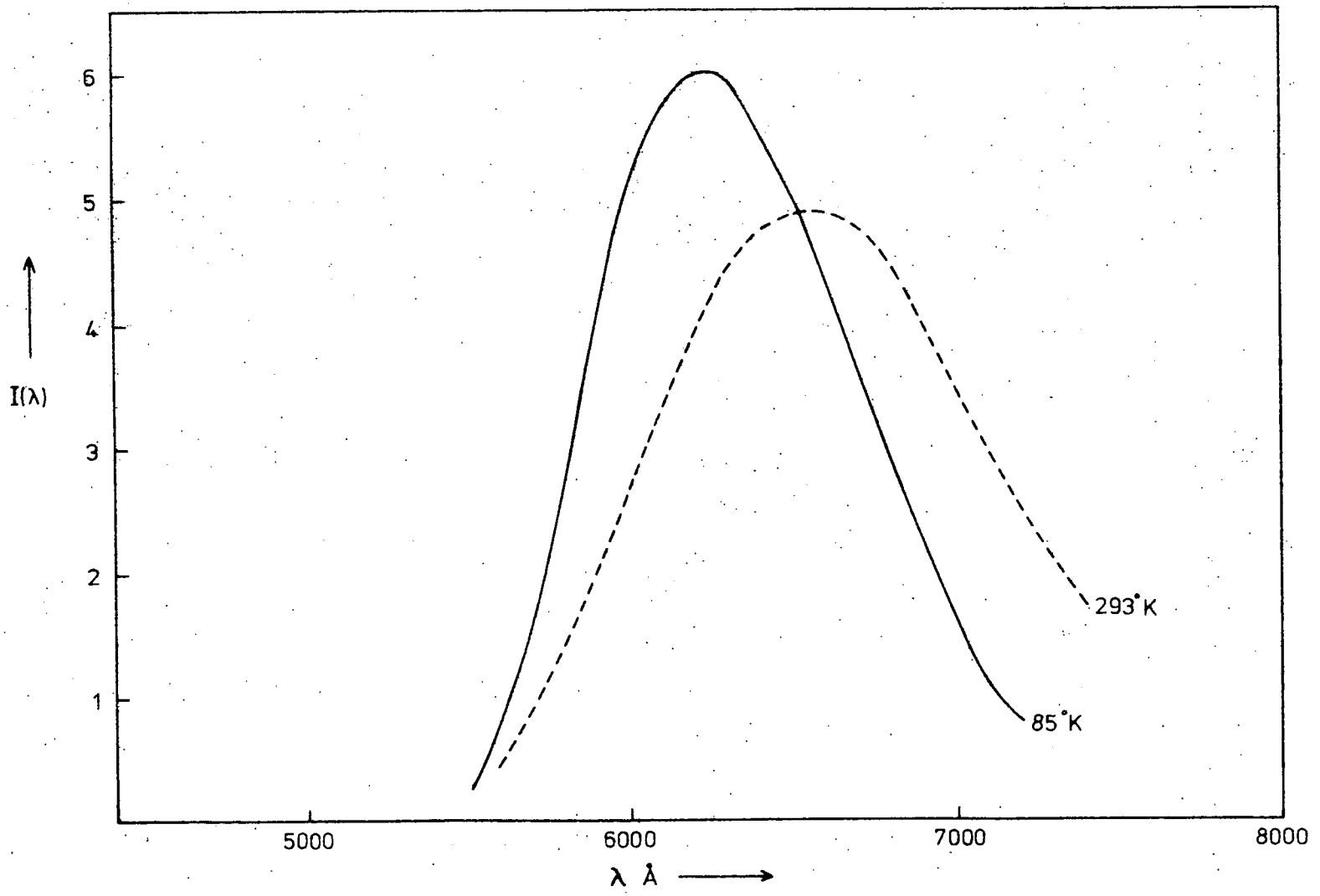

Fig. 6-4. Emission Spectrum under 3650 Å Excitation of ZnSe:Mn 902.

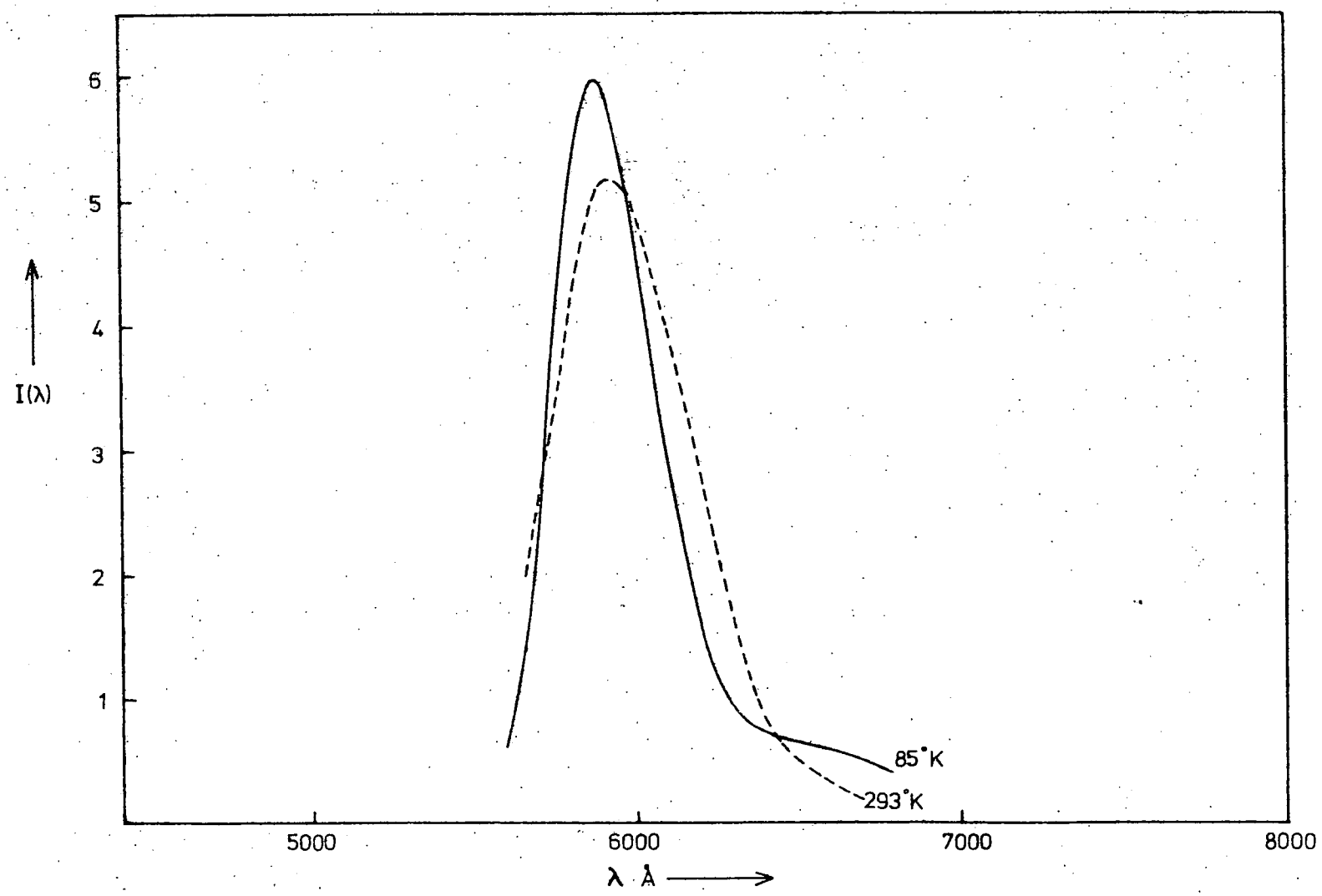

Fig. 6-5. Emission Spectrum under 5300 Å Excitation of ZnSe:Mn 902.

was found that the excitation peak at the bandgap and the shoulder at 4700 Å increased almost tenfold relative to the manganese peaks. Chopping frequencies higher than 200 c.p.s. did not appear to produce any further changes. The manganese bands were therefore resolved most easily when the exciting light was chopped at 200 c.p.s. and consequently this frequency was used to obtain the excitation spectra of all manganese doped crystals.

When crystal 902 was excited by 5300 Å light the narrow band shown in figure 6.5 was observed. At 293°K the band lay at 5920 Å and had a halfwidth of 0·18 eV. When the crystal was cooled to 85°K the band narrowed to 0·13 eV and shifted slightly to higher energy, finally lying at 5870 Å. The 6400 Å copper band was present only as a long wavelength shoulder. By comparison with figure 6.3 it is clear that the manganese content of crystal 902 is much higher than that of 213 in relation to the copper content. Chemical analysis showed that crystal 902 contained 1% manganese and hence all the manganese added prior to growth had entered the crystal. The halfwidth of the manganese emission band (figure 6.6) is considerably smaller than that of the S.A. emission and of the copper band, (figure 5.11). The width was found to vary by $3{\cdot}1 \times 10^{-4}$ eV/°K and was therefore less temperature dependent than that of the S.A. and copper bands. A plot of the position of the emission band maximum versus temperature (figure 6.6) shows that the manganese band shifts by $5{\cdot}6 \times 10^{-5}$ eV/°K which is practically negligible.

6.3 MEASUREMENTS AT LIQUID HELIUM TEMPERATURES

The emission from crystals 213 and 902 under 5300 Å excitation was also measured at temperatures down to approximately 15°K using an Optica spectrometer. Measurements of halfwidths down to 15°K showed that the width remained constant at approximately 0·14 eV at temperatures below 100°K. This is the result of all the excited electrons being confined

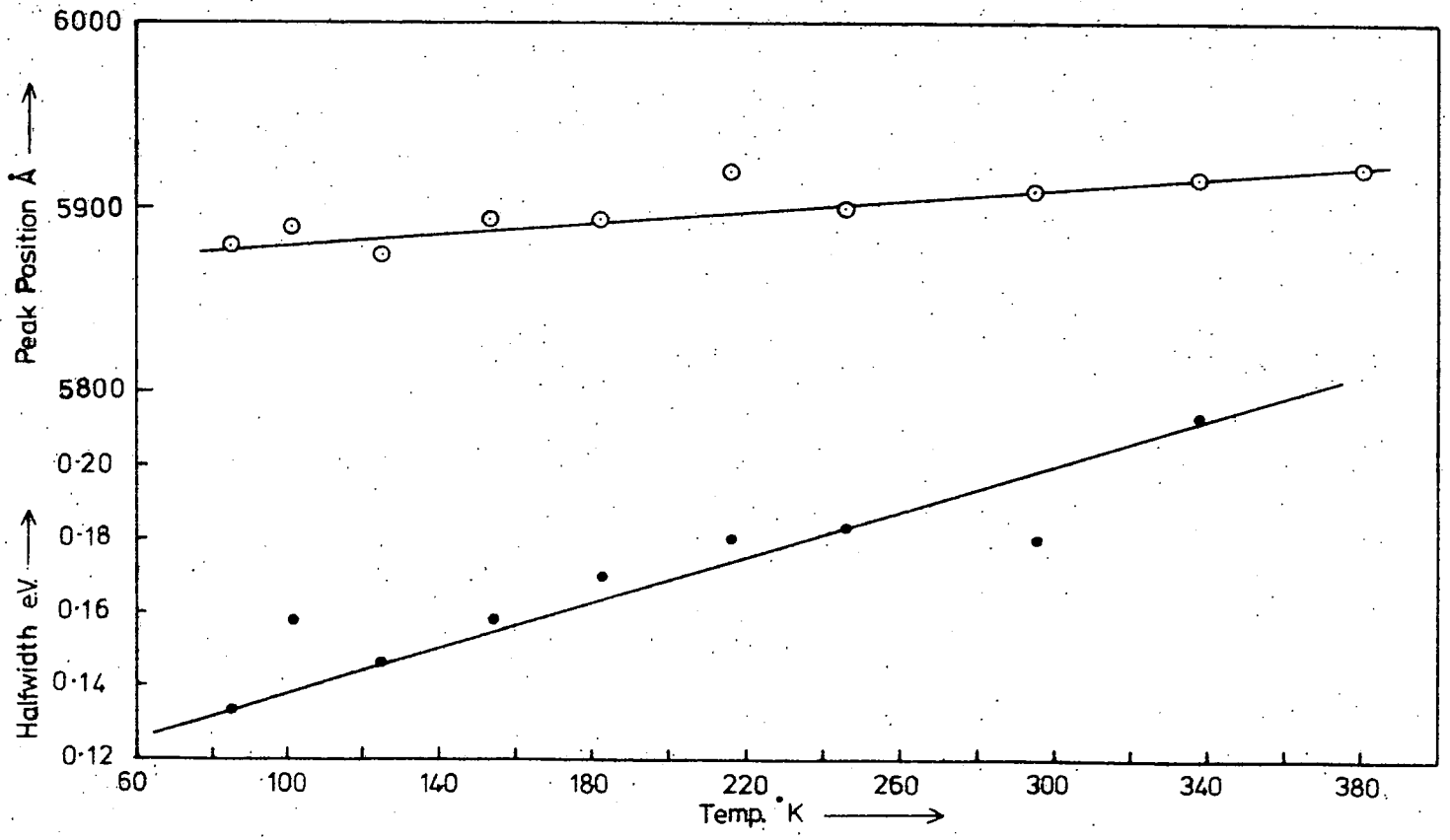

Fig.6-6. Change in Emission Band Position and Halfwidth as a function of Temperature for ZnSe:Mn 902 under 5300 Å Excitation.

to the zero point energy level in the configurational coordinate model as described in Chapter 1. The energy of the phonon which interacts in the excited state can therefore be obtained by applying equation 1.1.

$$W_T = Wo\left[\coth \frac{h\nu}{2kT}\right]^{\frac{1}{2}}$$

if $Z = \frac{h\nu}{2kT}$ $$W_T = Wo\left[\coth Z\right]^{\frac{1}{2}}$$

when expanded $$\coth Z = \frac{1}{Z} + \frac{Z}{3} - \frac{Z^3}{45} + \frac{2Z^5}{945}$$

At low T, Z is large and $\coth Z \longrightarrow 1$ $\therefore W_T \longrightarrow Wo$

At high T, Z is small so that terms after $\frac{1}{Z}$ can be neglected

$$\therefore \quad W_T = Wo\left(\frac{1}{Z}\right)^{\frac{1}{2}}$$

$$\therefore \quad W_T = Wo\left[\frac{2kT}{h\nu}\right]^{\frac{1}{2}} \qquad (6.1)$$

Thus if the square of the halfwidth is plotted as a function of temperature, the phonon energy $h\nu$ can be obtained from the slope of the straight line portion of the plot if Wo is known. From a plot of the square of the halfwidth versus temperature for the manganese emission from crystal 902 a value of 0·032 eV or 258 cm^{-1} was obtained for the energy of the phonon involved.

In the emission spectrum of crystal 213, two sharp lines at 5545 Å and 5565 Å were observed at 15°K. They could not be clearly resolved however because of overlap of the excitation and the emission bands. The higher energy line may well have been the zero phonon line of emission with the 5565 Å line a phonon replica although it is possible that any lines of higher energy still may have been swamped by the exciting light. No lines were observed in the emission from crystal 902.

6.4 TREATMENT IN ZINC OR SELENIUM

Since, in order to produce electroluminescent diodes, the resistivity of zinc selenide must be reduced by heating it in molten zinc, the effects of this zinc treatment upon the manganese luminescence processes were studied using crystals 213 and 902. The emission, under 3650 Å excitation from both crystals after they had been heated in molten zinc was identical to that from all other crystals treated similarly whether they originally contained manganese or not. That is to say, one band only was observed at room temperature with a maximum at 6050 Å which shifted to 6150 Å when cooled to 85°K. The excitation spectrum of crystal 213 following the zinc treatment is shown in figure 6.7. The two manganese excitation bands have been completely removed and the spectrum is very similar to that of the chlorine doped crystal 122 after heating in zinc (figure 5.12). The 4800 Å band characteristic of chlorine is again present. No manganese excitation bands either could be found with crystal 902 after it had been heated in zinc. In fact its spectrum was almost identical to that of the undoped crystal 909 grown by iodine transport after it had been subjected to the zinc treatment (figure 5.19). Analysis of crystal 902 after it had been heated in zinc showed, however, that it still contained the same amount of manganese as before that treatment. Samples of crystal 902 which had been heated in zinc, were subsequently heated in vacuum or in selenium. As a result the manganese excitation bands reappeared and an excitation spectrum identical to that prior to the zinc treatment was obtained. However, excitation by 5300 Å light did not resolve the manganese emission band as well as before the zinc treatment and excitation of the selenium treated crystal at 85°K by 3650 Å light produced a band at 6440 Å with a halfwidth of 0·24 eV. This is much narrower and at a longer wavelength than the emission from untreated material and seems to agree with the previously observed effect that the copper emission increases after heat treatment in vacuum or selenium.

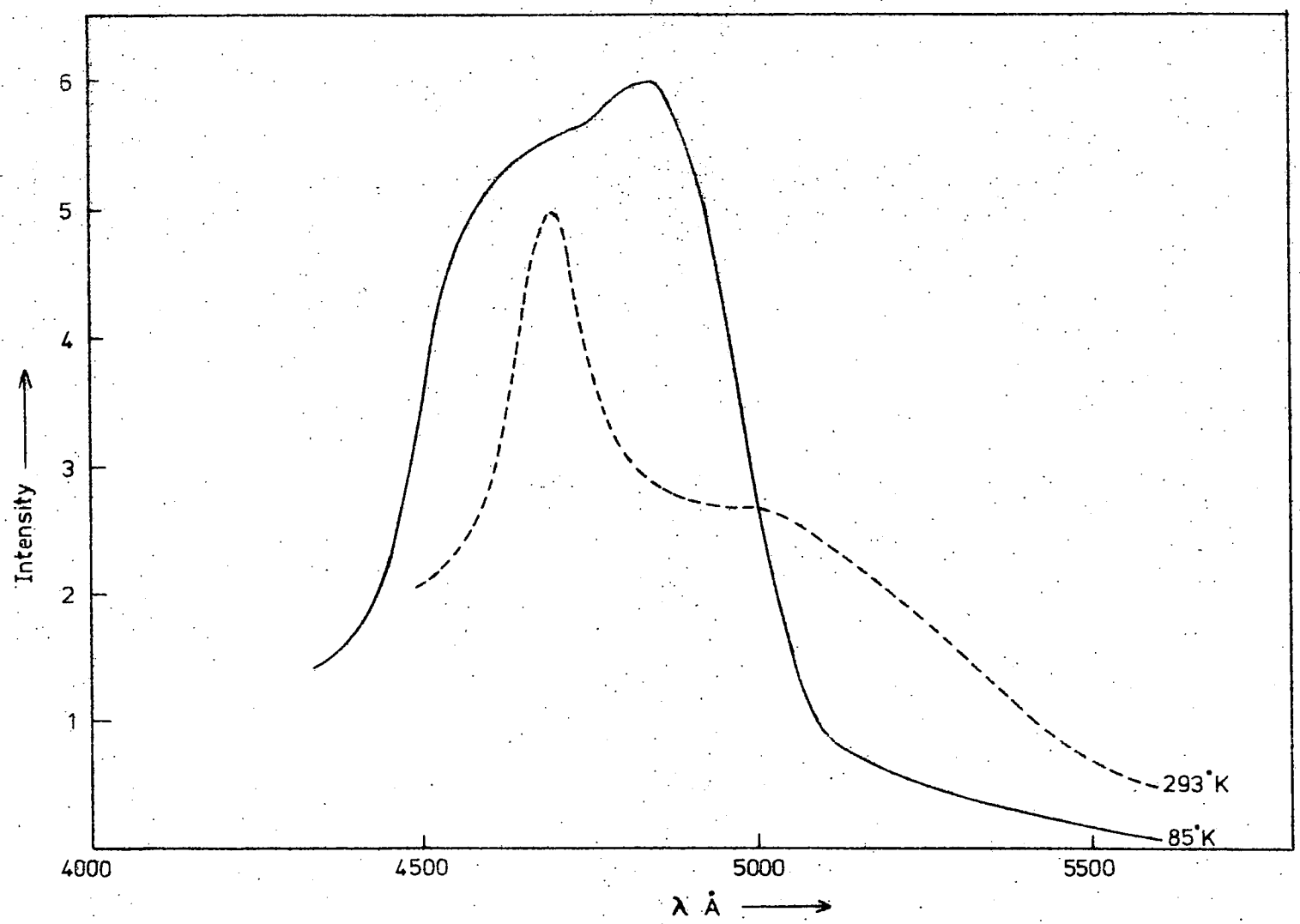

Fig.6-7 Excitation Spectrum of ZnSe:Mn 902 heated in Zn.

6.5 PHOTOCONDUCTIVITY

The photoconductivity of crystal 902 (figure 6.8) was studied in order to discover whether excitation within the two manganese bands led to photoconductivity. The apparatus used was virtually identical to that used to obtain the luminescent excitation spectra. That is, a chopped light source was passed through the monochromator onto the sample which had 100 V D.C. applied across it. The current through the crystal was taken through a 1 megohm resistor and the voltage produced across this resistor was fed to the phase sensitive detector. Therefore the signal being monitored was characteristic of the actual photocurrent and did not include the background dark current due to thermal excitation. Currents of the order of 10^{-9} amps could be measured.

At 85°K, with a chopping frequency of 200 c.p.s., a single peak at 4450 Å dominated the spectral response of the photoconductivity of crystal 902 (figure 6.8). With 10 c.p.s. excitation a small photocurrent was observed at longer wavelengths but it was still negligible in comparison with that at the bandgap. At 293°K the spectrum consisted of two shoulders at approximately 5300 Å and 4900 Å superimposed on the maximum response at the bandgap. When the temperature was raised to 360°K the 5350 Å and 4900 Å bands became more prominent and at 400°K they completely dominated the photoconductivity spectrum. The positions of these two longer wavelength bands do not coincide with those of the manganese bands at the same temperature (figure 6.2) and it is felt that they are more likely to be associated with the copper and the iodine impurity bands described in the previous chapter. The absence of the manganese bands from the photoconductivity spectrum at 85°K indicates that the excitation process responsible for the manganese emission is not associated with photoconductivity so that no electrons are excited from the ground state of the manganese ions into the conduction band.

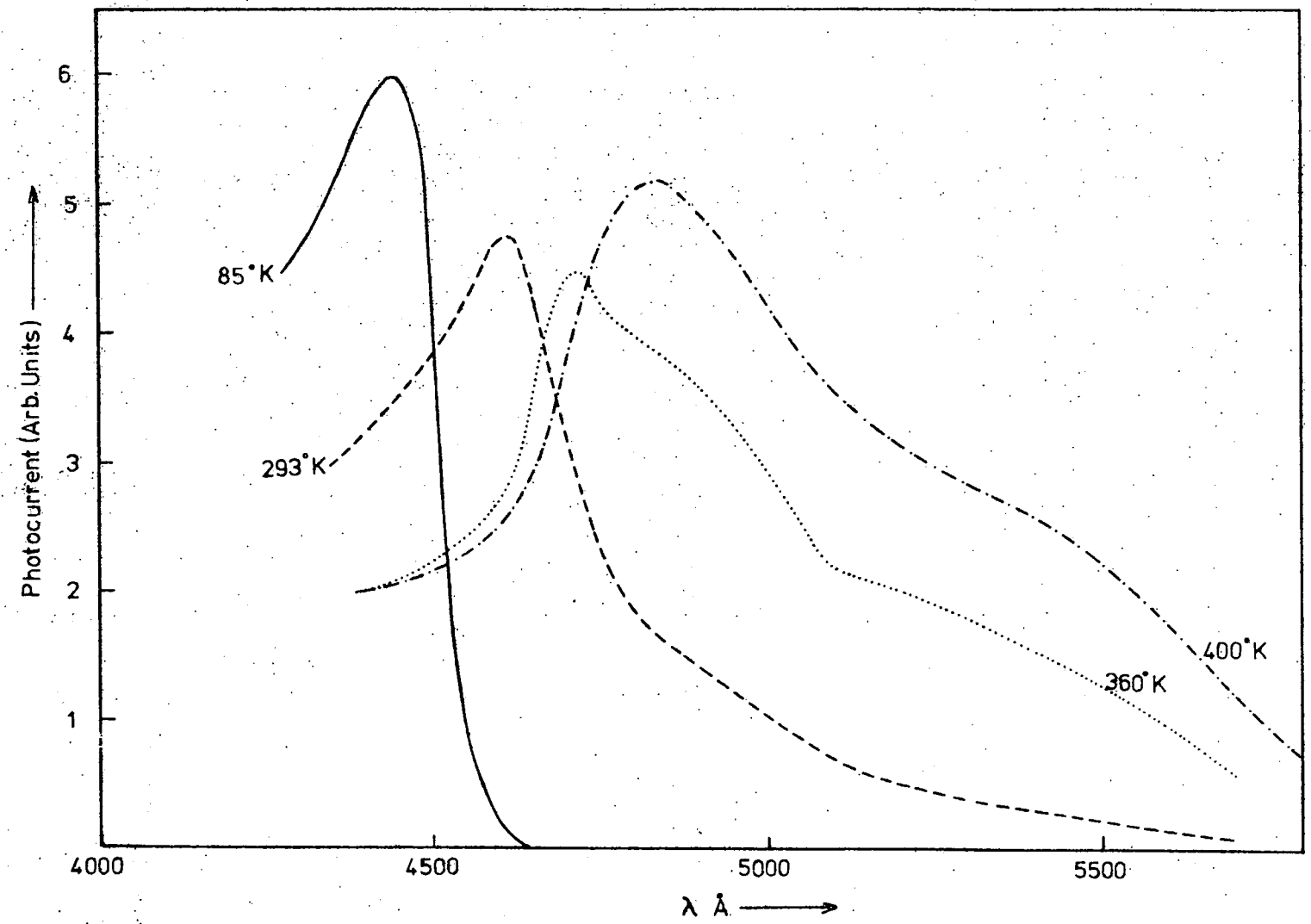

Fig. 6-8. Photoconductive Spectral Response of ZnSe:Mn 902.

The appearance of the excitation bands attributed to copper and iodine, as the temperature is raised, can be explained as follows. If an electron is excited to the iodine donor level, at low temperatures it will tend to recombine directly with a hole. The electron will therefore take no part in conduction processes. As the temperature is raised, however, the electron will be more likely to be excited into the conduction band and will therefore contribute towards the conductivity until it recombines. Therefore at low temperatures only hole photoconduction will occur whereas at higher temperatures the electron will also take part. The same argument can be applied to an electron excited from the copper level to the conduction band when hole conduction will only assist electronic conduction at higher temperatures. In both cases the temperature at which the conductivity begins to rise is associated with the temperature at which thermal quenching of the luminescence begins.

6.6 COMPARISON WITH MANGANESE CHLORIDE

In order to ensure that the emission associated with manganese in zinc selenide was not, in fact, due to precipitated manganese chloride or manganese iodide, a sample of manganese chloride was examined. Since the chloride is luminescent only when anhydrous, the sample was first melted in a silica tube and sealed off from the air.

When excited by 3650 Å radiation at room temperature, the sample emitted an asymmetric band at 6400 Å with a halfwidth of 0·29 eV (figure 6.9). When cooled to 85°K this band was gradually replaced by a longer wavelength band at 6800 Å with a halfwidth of 0·26 eV. Very similar bands were seen under 5300 Å excitation. The excitation spectrum at 293°K revealed broad bands at approximately 5600 Å, 4600 Å and 4200 Å (figure 6.10). When cooled to 85°K, bands were seen at 5550 Å, 4600 Å, 4150 Å, 3700 Å and 3650 Å. These bands again correspond to transitions within the manganese ion but they do not coincide with those obtained for the manganese ion in zinc selenide (figure 6.1). Furthermore

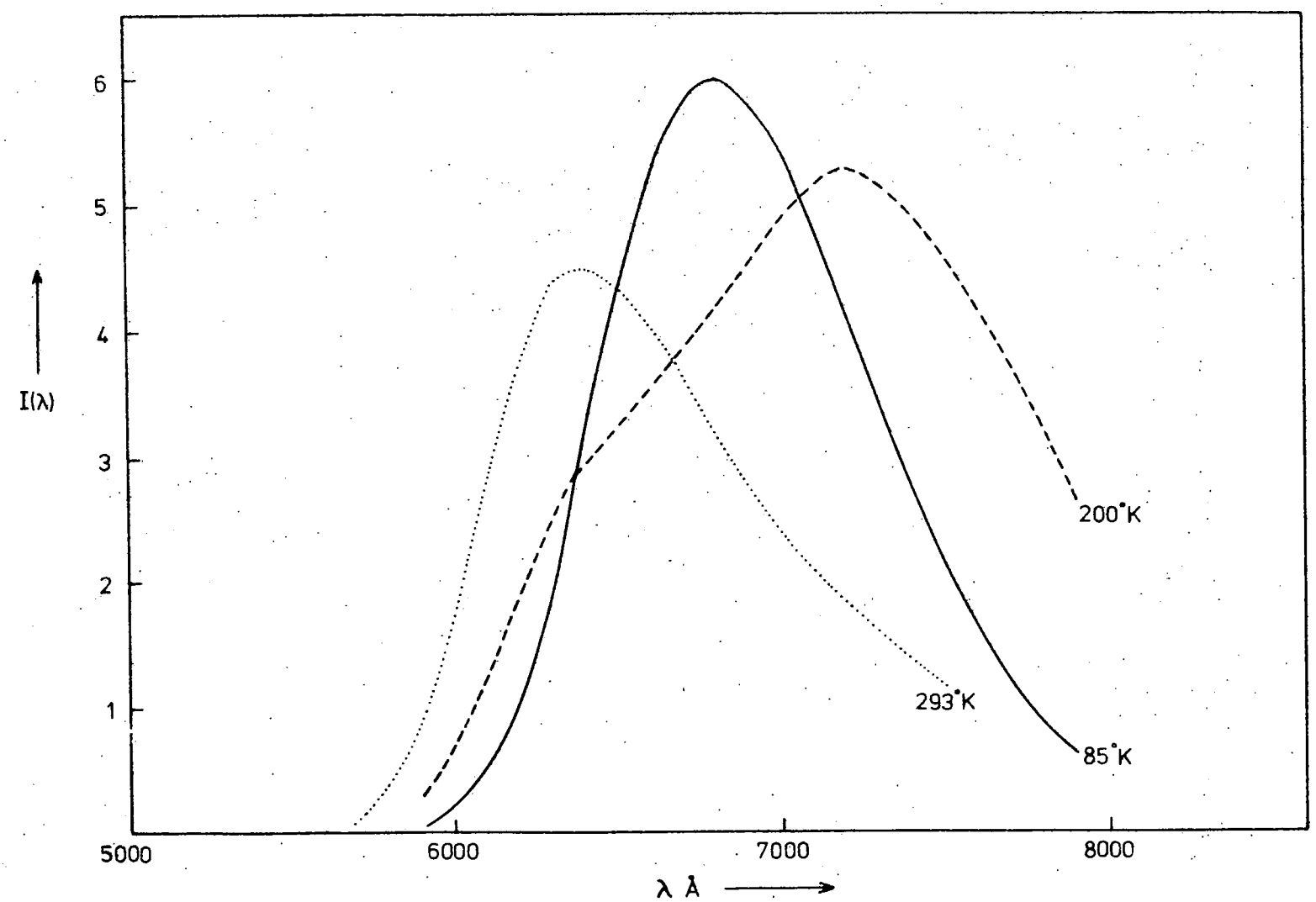

Fig. 6-9. Emission Spectrum under 3650 Å Excitation of $MnCl_2$.

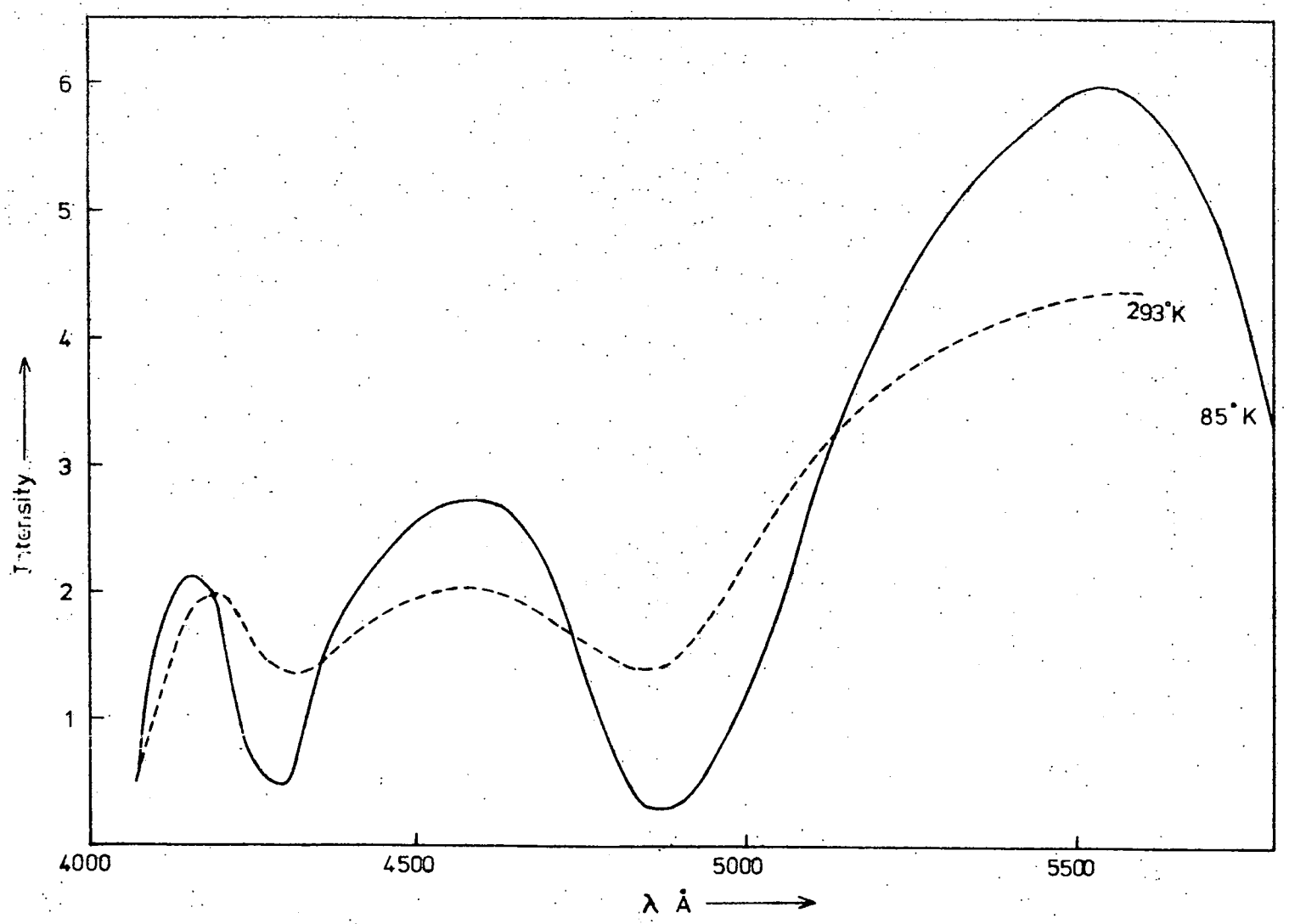

Fig. 6-10. Excitation Spectrum of $MnCl_2$.

the emission bands are also dissimilar, differing by almost 1000 Å at 85°K and 500 Å at room temperature.

The fact that two emission bands were observed might suggest that a substance other than manganese chloride was present within the tube, perhaps formed when the chloride was melted. This may have been responsible for the slight discrepancies observed between present results and those of Klick and Schulman (1952). Although the higher energy bands observed by Klick and Schulman correspond quite well to those observed in the present study, the longest wavelength excitation band they observed lay at 5200 Å not 5550 Å. The two emission bands may alternatively have been associated with recombination from two separate manganese levels, the lower energy transition being quenched at room temperature.

However, since neither the results of Klick and Schulman nor those obtained in the present study of manganese chloride agree with the results obtained from manganese activated zinc selenide, it can safely be assumed that the results reported in this chapter are in fact those of manganese activated zinc selenide.

6.7 THERMAL QUENCHING

As described in section 5.10, suitable excitation must be used to isolate the required manganese emission. Although light with a wavelength of 5300 Å was used this also excited the copper band in most samples and hence only crystal 902, with a negligible copper band, could be studied with confidence. Light with a wavelength of 5300 Å was also satisfactory since it lay within the low energy excitation band at all temperatures used (figure 6.2).

The curve which illustrates the quenching produced in crystal 902 is shown in figure 6.11. There is a gradual decline from 85°K to approximately room temperature whereupon the intensity begins to fall off more rapidly. This is very similar to the behaviour of the S.A. emission

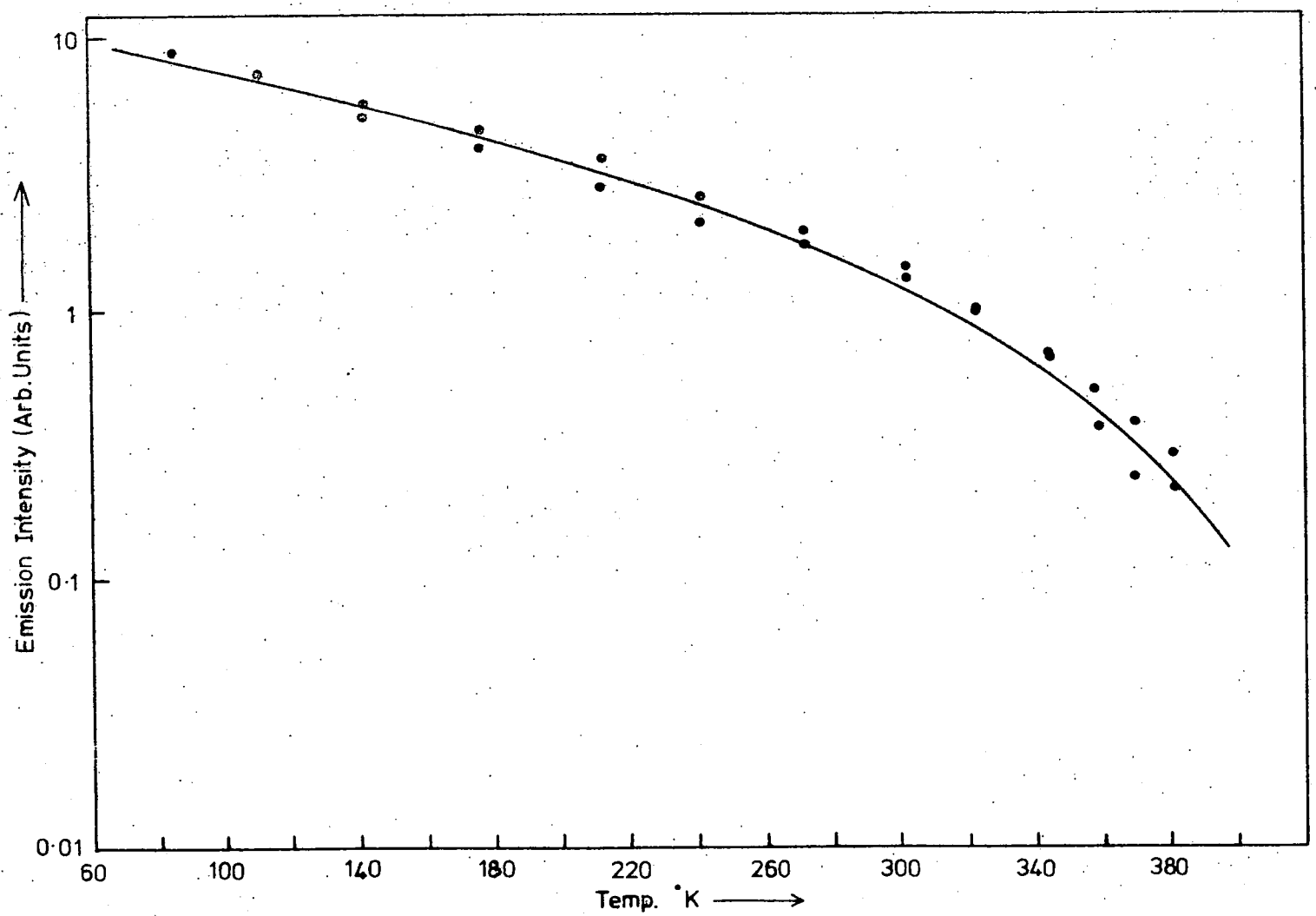

Fig. 6-11. Curve illustrating Thermal Quenching of Mn Emission for ZnSe:Mn 902.

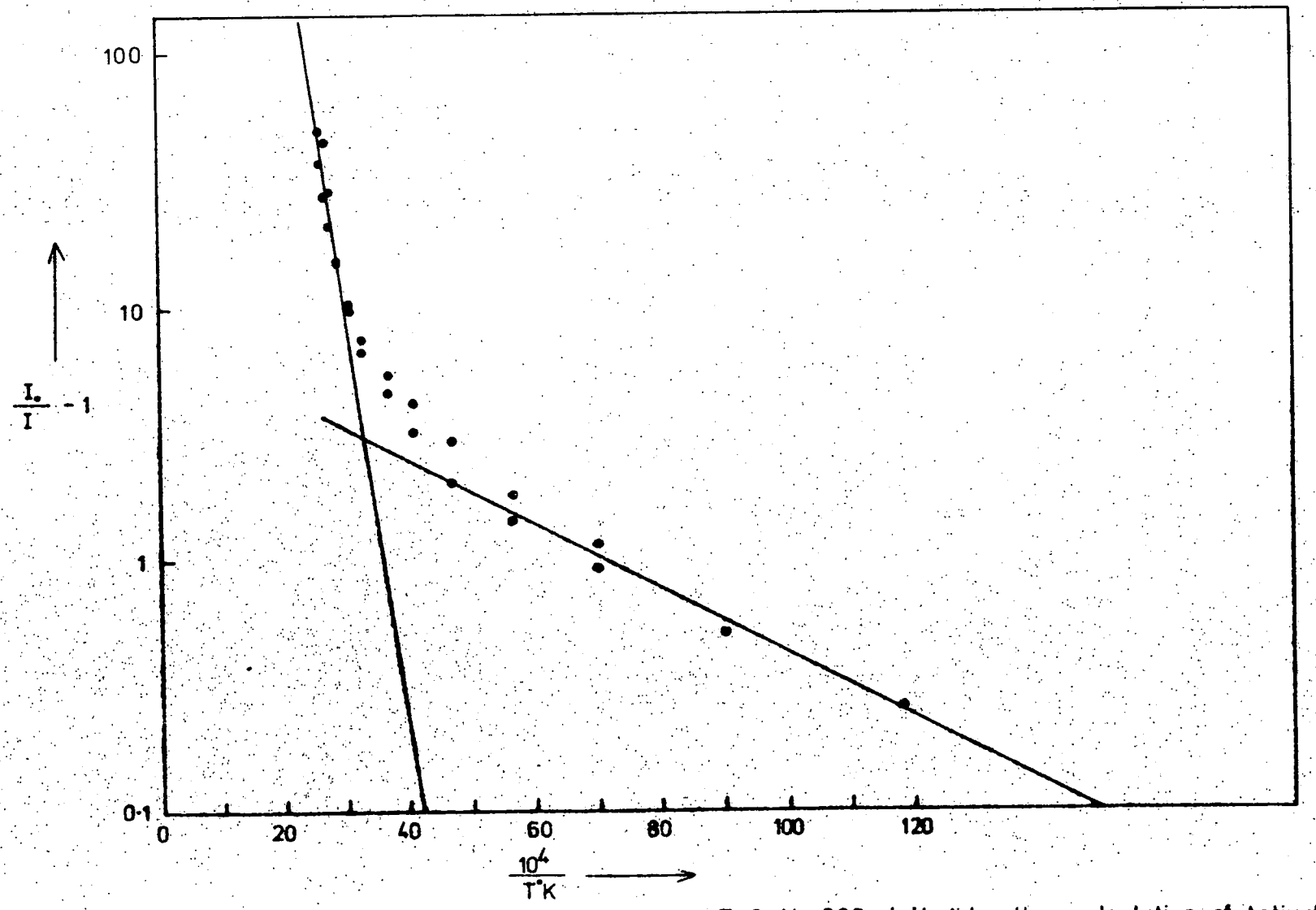

Fig. 6-12. Thermal Quenching Data for Mn Emission of ZnSe:Mn 902 plotted to allow calculation of Activation Energy.

(figure 5.33) and indeed, when the resulting curve was plotted in the form $\log\left(\frac{I_o}{I} - 1\right)$ versus $\frac{1}{T}$ (figure 6.12), two quenching energies of 0·025 eV and 0·33 eV were obtained. These are similar to the values obtained for the S.A. material. Once again the lower energy effect may be associated with some incidental process such as a shift of the low energy excitation band or it may be an actual low efficiency quenching process.

6.8 DISCUSSION

All the crystals which contained manganese emitted in a broad orange-red band when 3650 Å excitation was employed (figure 6.4). Measurement of the excitation spectra of this emission for all such crystals, however, revealed a common feature, namely the two sharp peaks in the green region (figure 6.1). At 85°K these lay at approximately 5040 Å and 5370 Å and increased with increasing manganese content (figure 6.1). A higher energy peak at 4660 Å was also observed in the crystal containing 1% manganese. Excitation with light with wavelengths within the two green excitation bands, either at 5300 Å or 5000 Å resulted in the emission of a narrow orange band at 5870 Å (figures 6.3, 6.5). This band broadened from 0·13 eV at 85°K to approximately 0·20 eV at room temperature and was clearly much narrower than typical emission bands reported in the previous chapter. At 293°K the band lay at 5910 Å and hence had only a slight temperature dependence. This emission is clearly associated with the manganese impurity within the crystal. The luminescence observed under 3650 Å excitation is broadened by the additional S.A. and copper bands which obscure the manganese emission.

The majority of previous workers on the emission of manganese activated zinc selenide appear to associate manganese with a red emission band in the region of 6400 Å at 293°K, (Leverenz 1950, Asano et al 1965, 1968 a, Apperson et al 1967). Such an emission is very similar to that

observed under 3650 Å excitation in the present crystals (figure 6.5) and is almost certainly affected to a considerable extent by the 6500 Å copper band reported in the previous chapter. Asano et al (1968 a) studied the excitation spectra of mixed zinc sulphide-selenide phosphors activated with manganese chloride. They observed sharp manganese excitation bands in the sulphur rich samples but these disappeared as the selenium content was increased until in zinc selenide a shoulder only was observed at approximately 5200 Å. This probably corresponded to the copper excitation band (figure 5.7). When 5300 Å excitation was used the red copper band, not the manganese band, was produced. It therefore appears that there was either considerable copper contamination in their samples, perhaps due to the flux employed, or the manganese (approximately 1%) was not entering the selenide. Apperson et al (1967) obtained an excitation band at approximately 5050 Å and a shoulder at 5500 Å at 85°K which may have been associated in some way with manganese. However the emission was again reported to be at 6300 Å although the wavelength of the exciting light was not given. This emission was probably again affected by copper impurities although no details of crystal preparation were given and thus no explanation is possible. Early cathodoluminescence measurements by Larach (1953) may have revealed the manganese emission at 5940 Å at room temperature although the addition of chlorine appears to have introduced S.A. emission centres.

Langer and Richter (1966) carried out optical absorption measurements at 4·2°K on melt grown zinc selenide containing 0·1% manganese. They observed two absorption bands at 4995 Å and approximately 5300 Å. A zero phonon line at 4737 Å corresponded to an unresolved third band at somewhat shorter wavelength. These three absorption bands almost certainly correspond to the excitation bands observed at 5040 Å, 5370 Å and 4660 Å in the present work, the slight shift being attributable to temperature differences. They also reported that the corresponding emission band lay at approximately 5815 Å although no further details were given.

The present results, therefore, are in agreement only with those of Langer and Richter. The three excitation bands are probably associated with transitions from the ground $6A_1$ state to three excited levels within the manganese ion, and are $6A_1 \longrightarrow 4T_1$, $6A_1 \longrightarrow 4T_2$ and $6A_1 \longrightarrow 4A_1, 4E$ in order of increasing energy (figure 1.6). Transitions to higher levels are not observed because of the onset of excitation across the bandgap as shown in figure 6.2. The orange emission band is due to the transition from the lowest excited state to the ground state, that is $4T_1 \longrightarrow 6A_1$, as in zinc sulphide.

The thermal quenching measurements led to a quenching energy of the order of 0·33 eV. This probably corresponds to the energy required to excite the electron from the minimum of the excited state in the configurational coordinate model to the point at which the ground state curve intersects it (figure 1.10a). Photocapacitance measurements by Braun et al (1973) place the manganese ion ground state 0·6 eV above the valence band. This would put the $4T_1$ level very close to the conduction band and the quenching energy of 0·025 eV may be associated with the transfer of electrons from the $4T_1$ level to the conduction band.

From the temperature dependence of the halfwidth of the manganese emission, a value of 258 $cm.^{-1}$ was obtained for the energy of the phonon which coupled with the manganese ion in the excited state. This is in the region of the energy of the longitudinal optical phonon of zinc selenide which has been reported to be 242 $cm.^{-1}$ from edge emission studies (Reynolds et al 1961) and 250 $cm.^{-1}$ from infra-red reflection measurements (Aven et al 1961). Langer and Richter also concluded that the manganese ions were coupled to the lattice phonons and obtained a maximum energy of 242 $cm.^{-1}$ from the separation of phonon replicas. It therefore seems most likely that the longitudinal optical phonon is responsible for the dominant interaction with the manganese ion.

The mechanism by which the manganese emission disappears after

crystals have been heated in zinc is not clear. The excitation bands reappear with their original intensity when the crystal is subsequently heated in vacuum or selenium and therefore the manganese is not removed from the crystal into the melt. This conclusion is also supported by atomic absorption analysis before and after zinc treatment. It seems unlikely that the manganese was precipitated in a similar manner to indium and gallium since no second phase was visible even in the 1% manganese sample after zinc treatment. A suggestion by Allen et al (1973) is that, because of the high concentration of free electrons after zinc treatment, the energy released by the manganese ion produces hot electrons by an Auger process rather than visible emission. Absorption measurements on a sample of boule 213 heated in zinc support this view since the zero phonon absorption line is still visible, showing that the manganese ion must remain in its original state (Jones and Woods 1973).

It is clear from the present results that up to 1% manganese can be successfully incorporated into zinc selenide crystals during growth. Growth from the vapour phase, in the presence of manganese chloride, can be used, but with the iodine transport method, a higher concentration of manganese can be introduced. The excitation and emission processes have been unambiguously identified and are ascribed to internal transitions within the manganese ion.

CHAPTER 7

RESULTS OF HALL EFFECT MEASUREMENTS

7.1 INTRODUCTION

The majority of crystals, whose transport properties have been studied, have already been discussed in Chapter 5 and details of their growth conditions and doping levels were given in Table 5.1. In the present chapter interest is concentrated mainly on samples containing group III impurities and the effect that heating in zinc has on their properties, although some mention of chlorine doped material is made towards the end of the chapter.

7.2 UNDOPED MATERIAL

As pointed out in Chapter 2, undoped zinc selenide has a very high resistivity and the majority of work has been carried out on crystals heated in molten zinc. Boule number 7 was investigated and a sample from the end which exhibited green luminescence, that is the end which was formed last, was found to have a room temperature conductivity of 5×10^{-13} ohm^{-1}.cm.$^{-1}$ in the dark. This is totally unsuitable for Hall effect measurements. However, when strongly illuminated by white light, passed through a copper sulphate filter, the conductivity was found to increase to 5×10^{-5} ohm.$^{-1}$cm.$^{-1}$. This enabled the Hall effect to be observed and values of the carrier density of 2×10^{12} cm.$^{-3}$ and mobility of 200 cm.^{2}/v.sec. were obtained. These figures are only intended to give an estimate of the transport properties since both the mobility and carrier density were strongly dependent on the light intensity and many

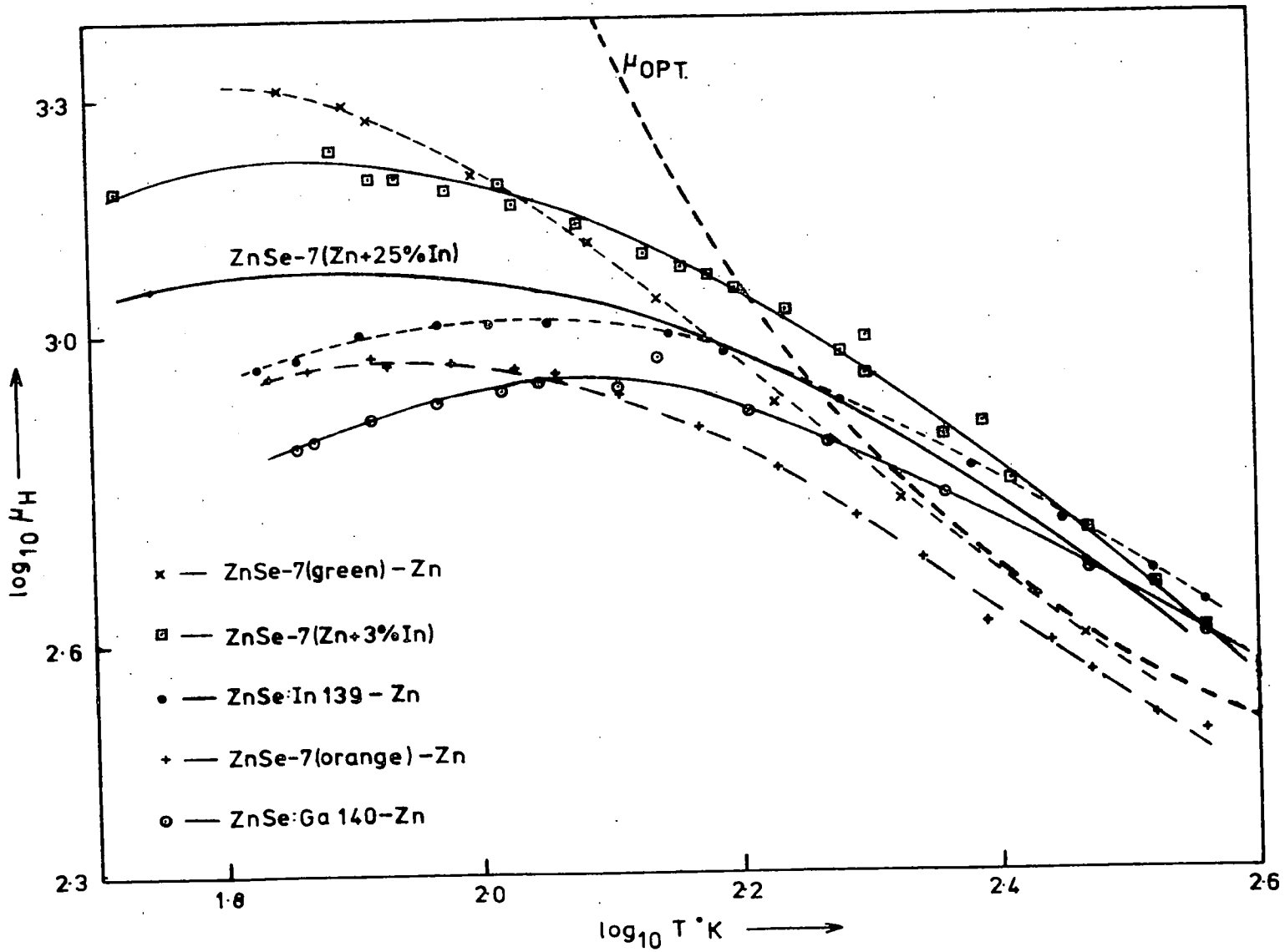

Fig. 7-1 Temperature Variation of Hall Mobility μ_H in Various Zn Treated Samples of ZnSe.

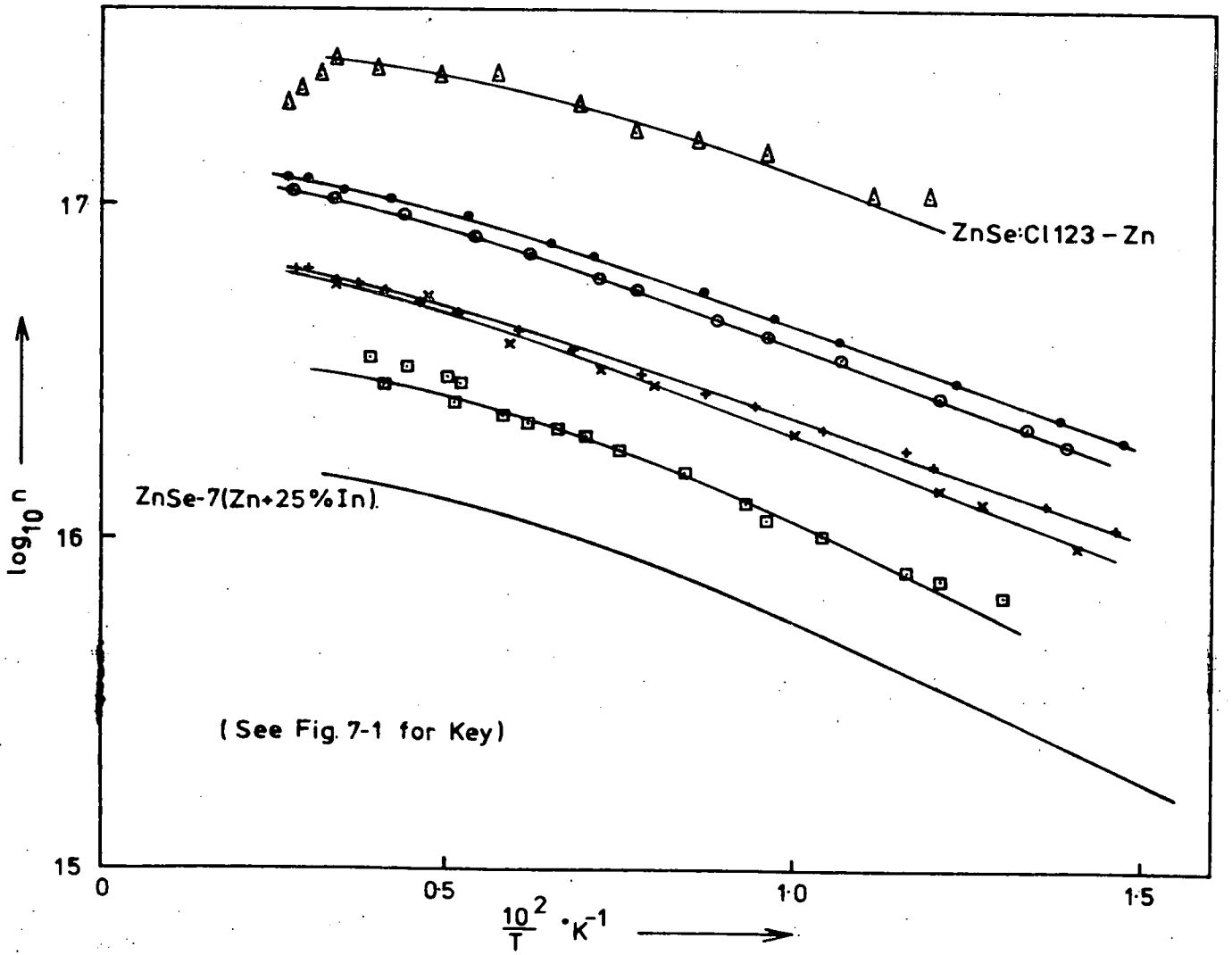

Fig. 7-2. Temperature Variation of Carrier Density n in various Zn treated Samples of ZnSe. (not corrected for r)

secondary effects such as hole conduction and quenching phenomena may have been present simultaneously.

In order to reduce the dark resistivity, samples from both ends of boule 7 were heated in molten zinc at 850°C for a week. In both cases the room temperature conductivity was found to have increased to approximately 3·5 ohm.$^{-1}$cm.$^{-1}$ and the transport properties were easily measured. At room temperature both samples had a mobility of approximately 400 cm.^{2}/v.sec. and a carrier density of 6 x 10^{16} cm.$^{-3}$. On cooling to 70°K the carrier densities fell gradually to 1 x 10^{16} cm.$^{-3}$ but whereas the mobility of the originally orange luminescent sample reached a maximum of 900 cm.^{2}/v.sec. in the region of 90°K, that of the originally green luminescent sample reached 2000 cm.^{2}/v.sec. at 70°K and was still increasing as the temperature was lowered even further. It will be shown in the next section that the most likely explanation for this behaviour is that neutral impurity scattering was acting as a mobility limiting process in the former sample. The temperature variation of the mobilities and carrier densities of these samples can be seen in figures 7.1 and 7.2, together with the results from several other samples which will be considered later.

7.3 INDIUM DOPED MATERIAL

(a) Doping from solution

Undoped zinc selenide samples were heated in molten zinc plus different amounts of indium at 850°C for a week in a similar manner to the luminescent samples described in Chapter 5, in an attempt to diffuse indium into the crystals. Samples from the green luminescent portion of boule 7 were again used as the basic material and two indium concentrations were used, 3 mole % and 25 mole %. The resistivity was reduced considerably and the room temperature mobilities of the 3% and 25% indium samples were 550 cm.^{2}/v.sec. and 500 cm.^{2}/v.sec. Corresponding carrier

densities of $3{\cdot}5 \times 10^{16}$ cm.$^{-3}$ and $1{\cdot}6 \times 10^{16}$ cm.$^{-3}$ were obtained. In both samples the mobility reached a maximum at about 60°K and then fell as the temperature was lowered further. The maximum mobilities were of the order of 2400 cm.^{2}/v.sec. and 1400 cm.^{2}/v.sec. respectively. The temperature variation of the carrier density was found to be identical for each sample down to 50°K although only the 25% indium doped sample was studied below this temperature. Figures 7.1 and 7.2 show how the mobilities and carrier densities of the two samples varied with temperature down to 65°K and figures 7.3 and 7.4 show the extension of this variation down to 17°K for the 25% indium sample.

According to equation 2.44 the value of n obtained directly from measurements of the Hall voltage should be multiplied by the scattering factor r to give the true carrier density. Down to approximately 100°K the scattering process will be shown to be associated with optical phonons and hence the value of r should be taken to be unity (see Table 2.1). However, below 100°K ionized impurity scattering seems to predominate. For this scattering process r has a value of 2 and therefore the true carrier density is a factor of 2 greater than the value obtained experimentally. When corrections for the scattering factor were applied to the variation in carrier density with temperature, the less steep curve, shown dotted in figure 7.4, was obtained. By fitting equation 2.15 to several points of the straight line portion of this curve it was possible to obtain values for the donor and acceptor impurity concentrations together with the donor ionization energy. A value of 0·17 m was chosen for the electron effective mass (Marple 1964) and this led to a value for the effective density of states N_C of $0{\cdot}34\ T^{1{\cdot}5} \times 10^{15}$ cm.$^{-3}$. $N_D - N_A$ was taken to be 2×10^{16} cm.$^{-3}$, this being the carrier density at high temperatures with all the donor levels empty. The best fit to the curve shown in figure 7.4 was obtained with values of

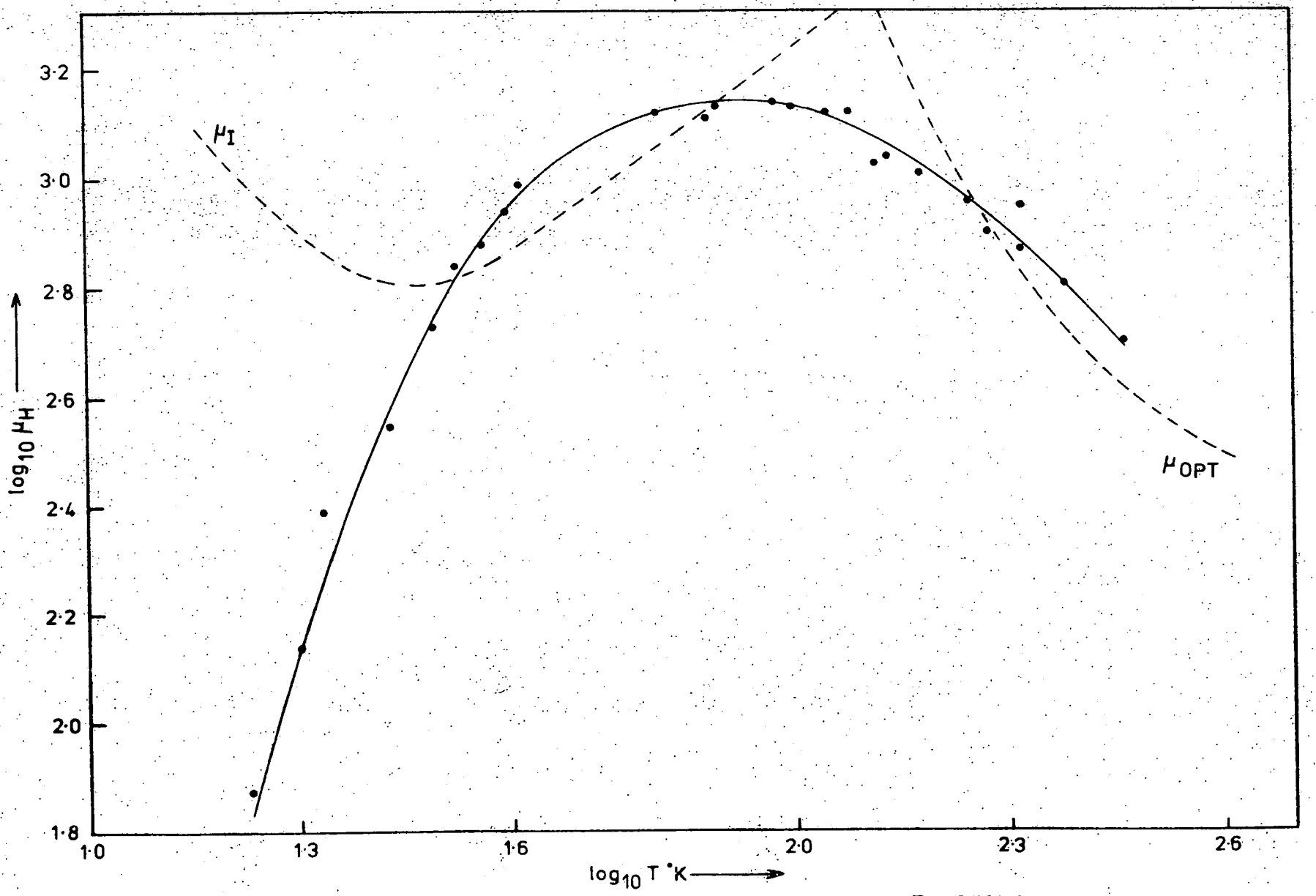

Fig. 7·3. Temperature Variation of Hall Mobility μ_H in ZnSe-7 heated in Zn+25% In.

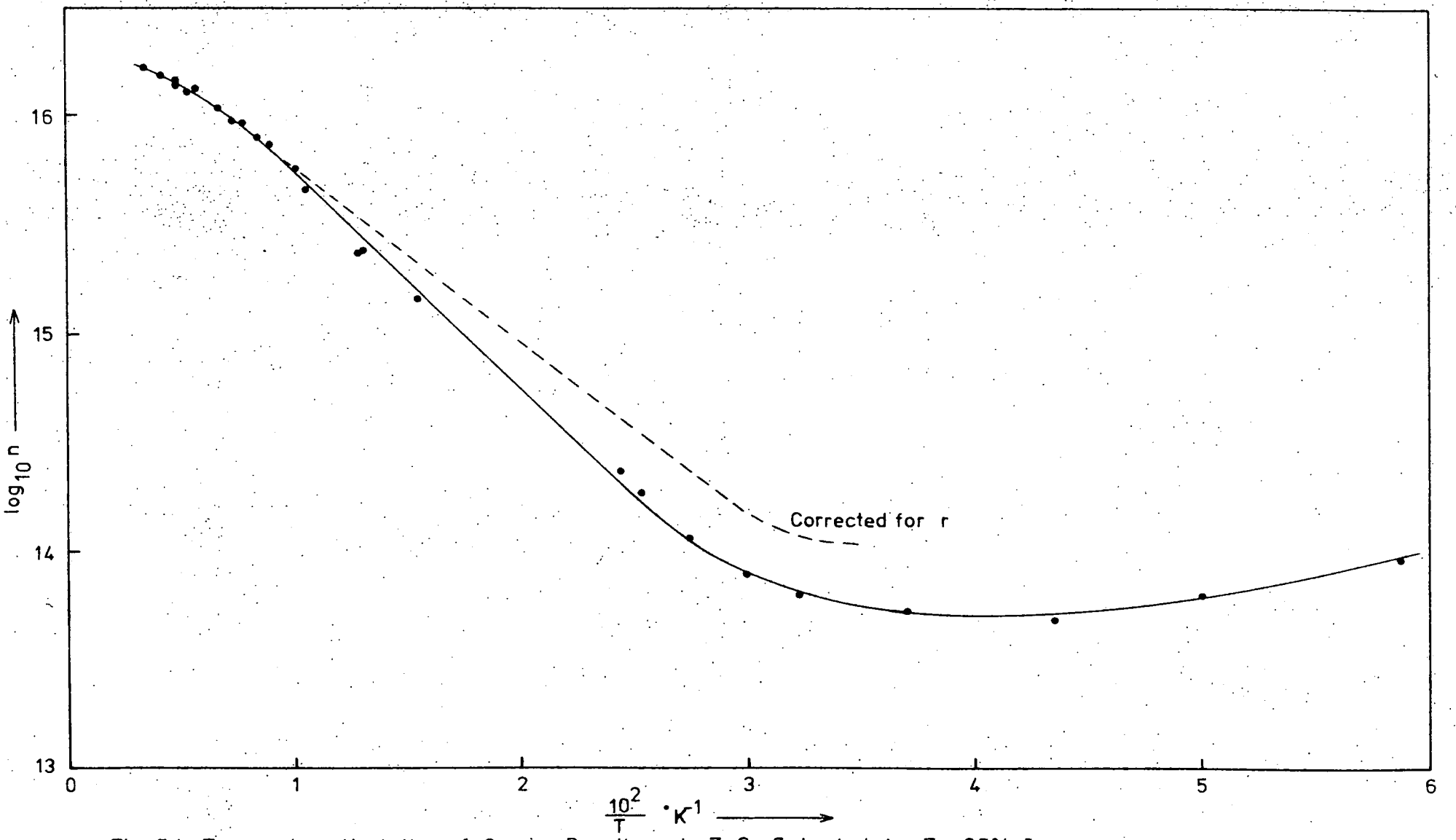

Fig. 7·4. Temperature Variation of Carrier Density n in ZnSe-7 heated in Zn+25% In.

$$E_d = 0{\cdot}012 \text{ eV}$$
$$N_D = 1{\cdot}05 \times 10^{17} \text{ cm.}^{-3}$$
$$N_A = 8{\cdot}5 \times 10^{16} \text{ cm.}^{-3}$$

The following values were obtained from measurements on the sample heated in zinc plus 3% indium

$$E_d = 0{\cdot}013 \text{ eV}$$
$$N_D = 1{\cdot}23 \times 10^{17} \text{ cm.}^{-3}$$
$$N_A = 8{\cdot}3 \times 10^{16} \text{ cm.}^{-3}$$

Because of the similarity of all the curves shown in figure 7.2 it seemed very probable that the same donor level was present in all the samples heated in molten zinc whether or not indium was present in the melt and that the indium was playing no part in the process and did not diffuse into the zinc selenide. This fact was in agreement with the apparent inability to introduce indium into zinc selenide as shown during the luminescence studies (see Chapter 5), and atomic absorption analysis, although not conclusive, showed that the indium concentration was below the limit of detection which was 70 p.p.m. It was therefore concluded that the same donor level was responsible for the low resistivities of all samples mentioned so far and the donor ionization energy of the samples heated in zinc alone was taken to be an average of the values obtained above, that is 0·0125 eV. The corresponding impurity concentrations in the sample of boule 7 heated in zinc alone were found to be

$$N_D = 1{\cdot}35 \times 10^{17} \text{ cm.}^{-3}$$
$$N_A = 6{\cdot}5 \times 10^{16} \text{ cm.}^{-3}$$

It is interesting to note that despite the fairly low resistivities obtained

in these crystals, there was still a high degree of compensation present.

For the crystal heated in zinc plus 25% indium, below approximately 30°K the carrier density ceased to fall off as a function of temperature and flattened off at a value just less than 10^{14} cm.$^{-3}$ (figure 7.4). As the temperature was reduced further there appeared to be a slight increase in carrier density. This behaviour is similar to that observed in cadmium sulphide (Crandall 1968) and can be explained by a non-metallic impurity conduction process in which the electrons frozen into the donor levels can hop between successive unoccupied donor levels without the need to be excited into the conduction band (Mott and Twose 1961). There were always sufficient unoccupied donor centres available for the hopping process to occur even at these low temperatures, because of the high degree of compensation present in the material.

In order to understand the variation of mobility with temperature of the sample heated in zinc plus 25% indium (figure 7.3) it is necessary to obtain some order of magnitude values for the mobility as limited by the various scattering mechanisms described in Chapter 2.

(1) Acoustic mode phonon scattering

Assume $\rho C_L^2 = 1{\cdot}06 \times 10^{12}$ dynes/cm.^{2} (Aven and Segall 1963)

$E_1 = 4$ eV (Aven and Segall 1963)

$m^* = 0{\cdot}17\ m$ (Marple 1964)

Equation 2.20 can be rewritten as

$$\mu_A = 1{\cdot}74 \times 10^8\ T^{-\frac{3}{2}}\ \text{cm.}^2/\text{v.sec.} \qquad (7.1)$$

This process would therefore result in a mobility much higher than that observed in the present work, for example, even at 400°K the mobility

would be over 20,000 $cm.^2/v.sec.$, and this mechanism can be ignored.

(2) Piezoelectric scattering

Assume ϵ_s = 9·1 at approximately room temperature (Berlincourt et al 1963)

$C = 1{\cdot}5 \times 10^4$ stat.coul./$cm.^2$ (Berlincourt et al 1963)

Equation 2.23 would therefore reduce to

$$\mu_{PZ} = 5{\cdot}8 \times 10^6 \, T^{-\frac{1}{2}} \; cm.^2/v.sec. \qquad (7.2)$$

At 300°K this equation would lead to a mobility of over 200,000 $cm.^2/v.sec.$, several orders of magnitude higher than values shown in figure 7.3 and hence this process can also be ignored.

(3) Neutral impurity scattering

Simplification of equation 2.25 leads to

$$\mu_N = 2{\cdot}7 \times \frac{10^{20}}{N} \; cm.^2/v.sec. \qquad (7.3)$$

It seems possible that neutral impurities might therefore be a factor determining the mobility. For example, it would only need approximately 100 p.p.m. of some impurity to restrict the mobility to values below 270 $cm.^2/v.sec.$ Because of the difficulty in obtaining a value for the density of neutral impurities this equation is rather limited in use but the process might be quite an important limiting factor in some cases.

(4) Optical mode scattering

A value of 0·54 can be obtained for α the polaron coupling constant from equation 2.22 using values of 5·75 for ϵ_∞ (Aven, Marple

and Segall 1961) and 9·0 for ϵ_s . The latter was obtained by interpolating between the room temperature result of 9·12 obtained by Berlincourt et al (1963) and a value of 8·66 obtained at 4°K by Roberts and Marple (see M. Aven 1971). The temperature variation of ϵ_s mentioned by Aven (1971) has negligible effect over the range 100°K to 300°K. If 0·54 is substituted for α in the equation proposed by Howarth and Sondheimer (equation 2.22) and a value of 4·8 x 10^{13}/sec. is taken for ω , the following simplified equation is obtained

$$\mu_{OPT} = 300\,\Psi_z(\exp z - 1)\; Z^{-\frac{1}{2}} \text{ cm.}^2\text{/v.sec.} \qquad (7.4)$$

where $Z = \frac{\theta_D}{T} = \frac{364}{T}$, (see for example Aven, Marple and Segall 1961 for energy of L.O. phonon). If the mobility is calculated using this equation the curve shown in figure 7.3 rising from 300 cm.^{2}/v.sec. at 400°K to 1600 cm.^{2}/v.sec. at 140°K is obtained. This is in quite good agreement with the experimentally obtained results. Optical mode scattering also appears to be the most important scattering mechanism above approximately 140°K in all the samples heated in zinc (figure 7.1).

(5) Ionized impurity scattering

As the curves in figure 7.3 demonstrate, the mobility variation above 140°K can be explained on the basis of scattering by optical mode phonons. However, at lower temperatures some other process appears to take over and cause the mobility to fall quite rapidly with decreasing temperature. This is the region in which ionized impurity scattering would be expected to become dominant. If the relevant constants are substituted into equation 2.24, the Brooks-Herring formula, the following simplified equation is obtained

$$\mu_I = 6{\cdot}1 \times 10^{17}\; \frac{T^{\frac{3}{2}}}{N_I}\left[\log_e \; 1{\cdot}94 \times 10^{14}\; \frac{T^2}{n'\,(2 - \frac{n'}{N_I})}\right]^{-1} \qquad (7.5)$$

where n' is obtained as described in Chapter 2.

It must be remembered that equations 7.1 to 7.5 give values for the conductivity mobility μ_C described in Chapter 2. When optical mode phonon scattering is the limiting process, the scattering factor r = 1 and therefore the Hall mobility $\mu_H \simeq \mu_C$. However, in the present case the scattering factor r has a value of 2 and the mobility obtained from equation 7.5 must be multiplied by this factor to obtain the Hall mobility shown in figure 7.3.

If values obtained for N_D, N_A and n in crystal 7 heated in zinc plus 25% indium, are substituted into equation 7.5, the curve illustrated in figure 7.3 is obtained. The centres are assumed to be singly charged. This curve can be seen to provide quite good agreement above 30°K but below this temperature the equation appeared to break down due to a rapid increase in the logarithmic term, since a rapid increase in mobility was predicted. Even the simpler Conwell-Weisskopf equation, which does not take into account the screening of scattering centres by the carriers, broke down at a similar temperature and there does not appear to be a suitable equation for this low temperature region. Below 30°K the mobility fell much more rapidly as the temperature was reduced than would be expected from ionized impurity scattering. When the mobility was plotted in the form $\log \mu \propto \frac{1}{T}$, it was found that below approximately 50°K the plot was linear (figure 7.5). This variation can be represented by an equation of the form

$$\mu = A \exp -\frac{W}{kT} \qquad (7.6)$$

where A and W are constants.

This type of behaviour is typical of a hopping process such as that which occurs in non-metallic impurity band conduction. The term W represents the energy barrier which the electrons must overcome in order

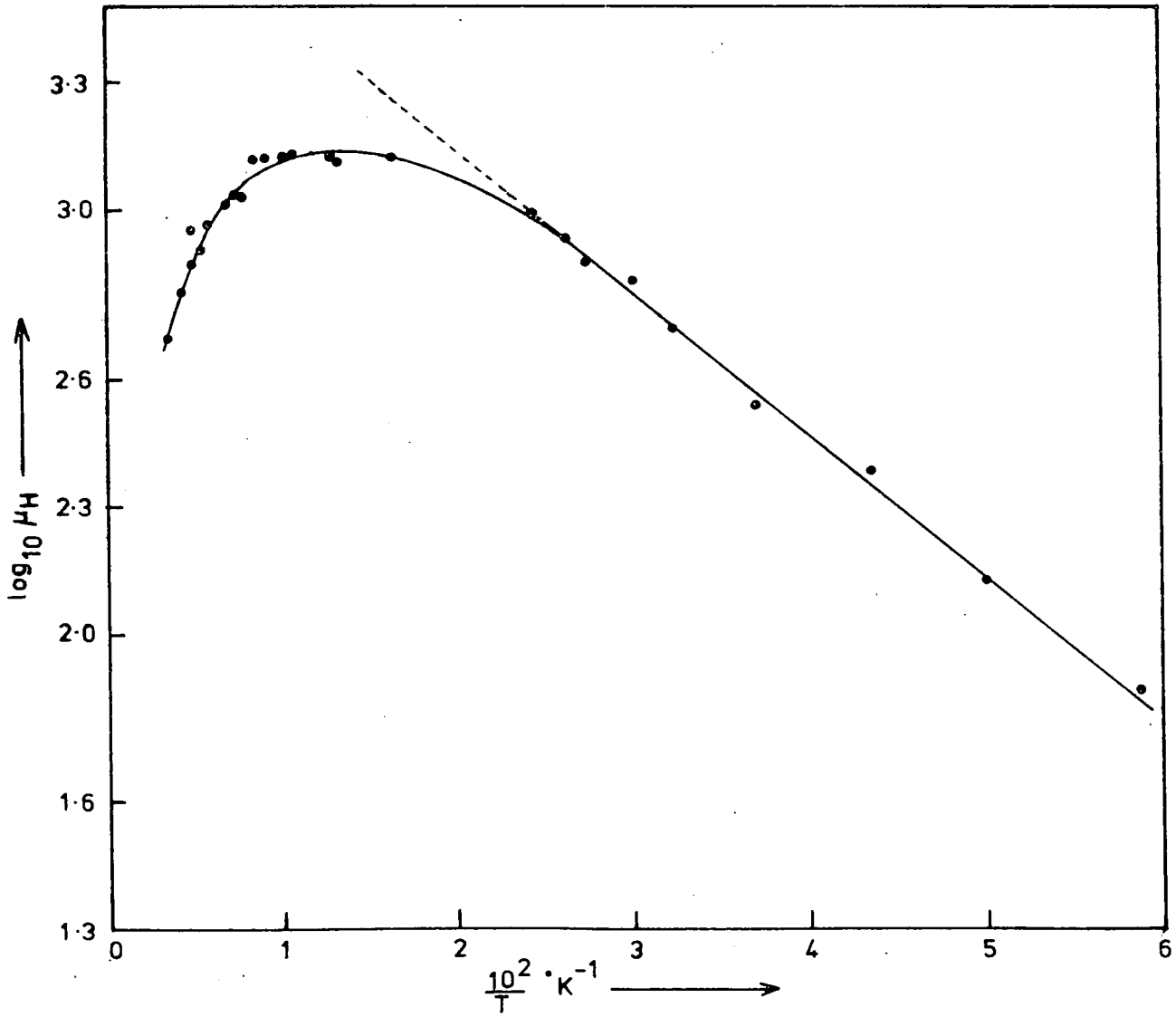

Fig. 7-5. Diagram to Illustrate Influence of Hopping Mechanism at Low Temperatures.

to hop from centre to centre. The gradient of the linear portion of figure 7.5 is equal to $-\frac{W}{k} \times 2{\cdot}303$, the latter factor introduced to convert $\log_{10} \mu$ to $\log_e \mu$. This allowed a value of 0·007 eV to be obtained for the barrier height.

It is therefore clear that the mobility of the sample heated in zinc plus 25% indium, which can be considered identical to a sample heated in zinc alone, can be explained on a basis of optical phonon interaction above approximately 150°K and ionized impurity scattering from about 30°K to 100°K. The intervening region from 100°K to 150°K is accounted for simply by a combination of the two scattering processes adding in the manner

$$\frac{1}{\mu} = \frac{1}{\mu_I} + \frac{1}{\mu_{OPT}} \qquad (7.7)$$

Below 30°K the mobility was limited by a hopping process associated with a barrier height of 0·007 eV. Such behaviour is typical of non-metallic impurity band conduction and is in agreement with the conclusions drawn from the carrier density measurements.

The various samples whose mobilities are plotted in figure 7.1 can be seen to behave very similarly to the 25% indium treated sample, the mobility of which is shown as a continuous line obtained from figure 7.3. The results agree quite well with the optical phonon scattering theory at high temperatures but there is a considerable spread at lower temperatures, with the mobilities lying between 700 $cm.^2/v.sec.$ and 2000 $cm.^2/v.sec.$ at 80°K. This spread is almost certainly due to the different concentrations of ionized impurity centres. In fact, if the mobility predicted by the Brooks-Herring formula at 70°K is calculated for the green luminescent sample of boule 7 heated in zinc alone, a value of 2000 $cm.^2/v.sec.$ is obtained. This is almost double the mobility of the crystal heated in zinc plus 25% indium and is in good agreement with the experimentally

observed value. The orange luminescent sample of crystal 7 after being heated in zinc, was found to contain the same donor and acceptor densities as the green luminescent sample heated in zinc and hence the same concentration of ionized impurities at any temperature. However, the maximum mobility was a factor of 2 lower and it seems likely that neutral impurity scattering may have been acting as a limiting process since only 10 p.p.m. of a neutral impurity would have produced such an effect. The reasons for the lower mobilities of indium and gallium doped crystals 139 and 140 will be dealt with later.

(b) Doping during growth

When indium metal was introduced into zinc selenide boules during growth the resulting boule was found to have a conductivity high enough to enable transport measurements to be made. For example, sample 3 of boule 139 had a conductivity of 2·0 $ohm.^{-1}cm.^{-1}$ at room temperature, which fell to 0·17 $ohm.^{-1}cm.^{-1}$ at 70°K. This was in fact the most highly conducting sample studied apart from samples heated in molten zinc. The second sample studied, number 4, had a room temperature conductivity of 0·1 $ohm.^{-1}cm.^{-1}$ which fell to 5×10^{-4} $ohm.^{-1}cm.^{-1}$ when cooled to 70°K. The amount of indium in boule 139 could not be determined although atomic absorption analysis showed it to be less than 50 p.p.m. Measurements were made on two samples from boule 139 as stated and the results were found to be somewhat different. The variation of carrier density with temperature of the two samples is shown in figure 7.6. There is a considerable difference between the values of carrier density of the two samples, sample 3 having approximately three times more free electrons than sample 4. The plot of carrier density in sample 3 shown in figure 7.6 was modified as shown to allow for the variation in scattering factor whilst that of sample 4 was multiplied by two, since ionized impurity scattering appeared dominant over the whole range (figure 7.7). When

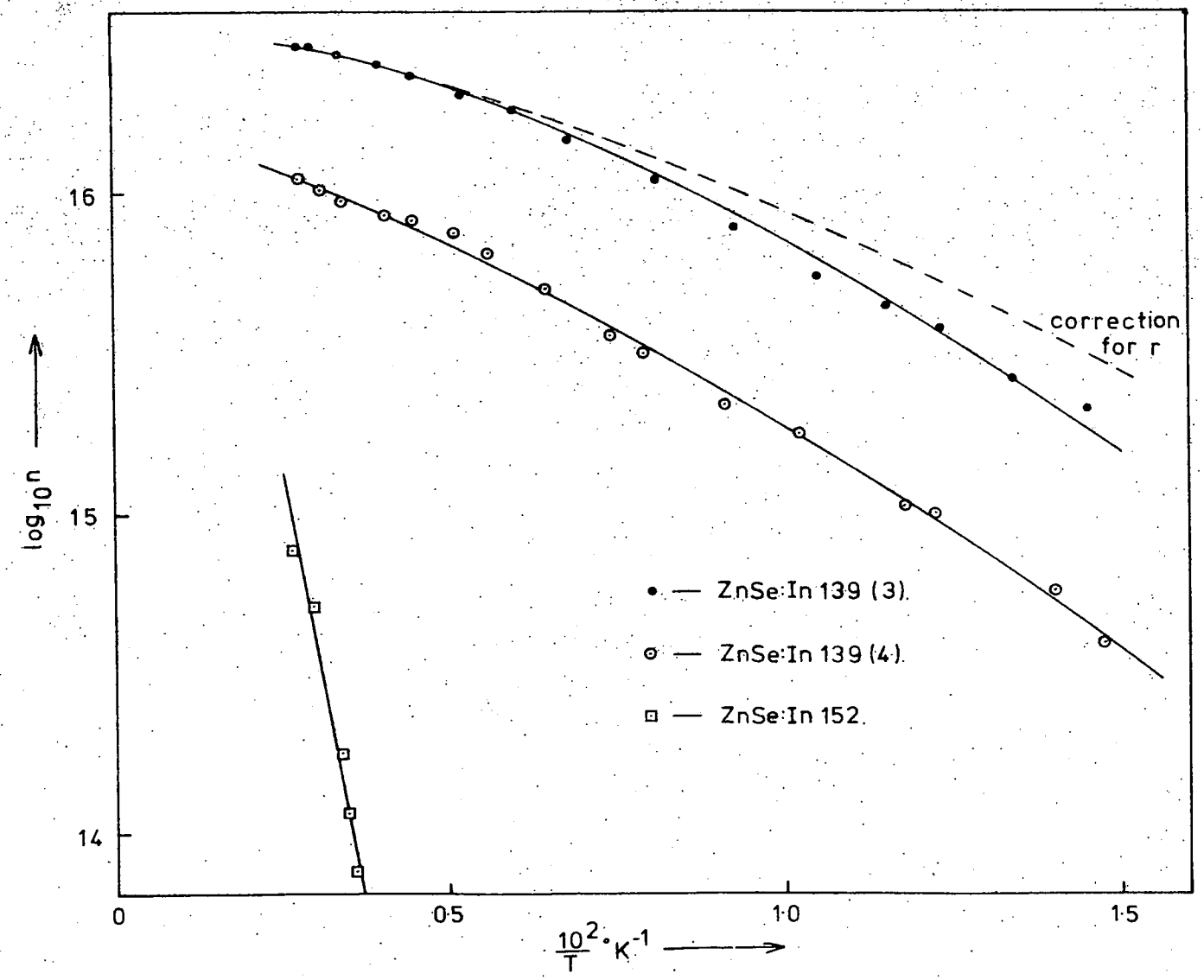

Fig. 7-6. Temperature Variation of Carrier Density n in three ZnSe:In Samples (corrected for r).

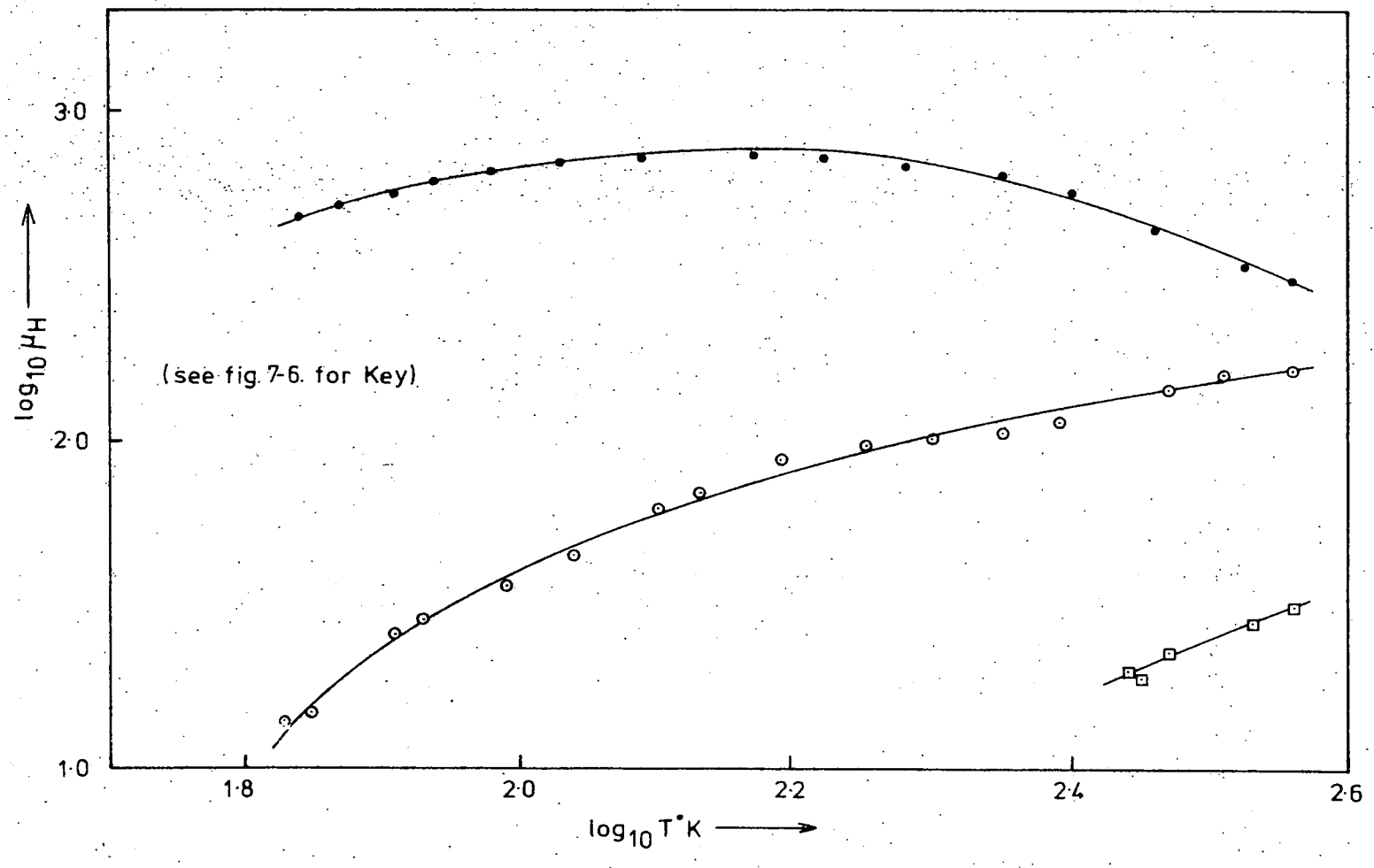

Fig. 7-7 Temperature Variation of Hall Mobility μ_H in three ZnSe:In Samples.

the curves in figure 7.6 were analysed using equation 2.15, the following values were obtained

Sample 3	Sample 4
E_d = 0·021 eV	E_d = 0·021 eV
N_D = 5·6 x 10^{16} $cm.^{-3}$	N_D = 1·24 x 10^{17} $cm.^{-3}$
N_A = 2·4 x 10^{16} $cm.^{-3}$	N_A = 1·06 x 10^{17} $cm.^{-3}$

Some error may be present in these values because of the restricted temperature range over which the measurements were made but the fact that the values for E_d are the same seems promising. The difference in donor impurity density is only a factor of two and would correspond to indium concentrations of roughly 5 p.p.m. and 10 p.p.m. These values would tend to agree with the atomic absorption analysis and the difference could easily be the result of uneven distribution of indium within the boule during growth.

Figure 7.7 shows the mobility variation with temperature for the two samples and clearly there is a difference between the scattering processes involved. The mobility of sample 3 behaved in a similar manner to that of the crystals studied previously although the maximum mobility of 750 is lower than that of the undoped zinc treated samples. The mobility of sample 4 behaved in a completely different manner, falling from a room temperature value of 160 $cm.^2$/v.sec. to less than 15 $cm.^2$/v.sec. at 70°K. These values are considerably smaller than previously reported mobility values in zinc selenide.

If the donor and acceptor impurity densities are substituted into the Brooks-Herring equation values of 4200 $cm.^2$/v.sec. and 1000 $cm.^2$/v.sec. are obtained for the mobilities at 75°K of samples 3 and 4 respectively. Although these values are greater than the experimentally observed values,

the theoretical value for the mobility of sample 4 is considerably less than that of 3 because of the higher degree of compensation and this is in agreement to a certain extent with experiment. It seems likely, however, that there is a further scattering process present which is reducing the mobilities to these low values. The only likely process is neutral impurity scattering. Since these crystals had not been heated in molten zinc it is very likely that they should contain a considerable number of impurity atoms, including those such as carbon, silicon or oxygen which could either have been present in the starting materials, including the indium, or introduced during growth. A total concentration of only 100 p.p.m. impurities would be sufficient to produce the sort of mobility seen in sample 4. Such a concentration of the stated impurities, which would tend to have little effect electrically, is not really excessive considering the source of silicon and oxygen with which the crystal is in contact during growth, and indeed of two boules analysed mass spectrographically, one was found to contain 200 p.p.m. silicon and the other 90 p.p.m. Neither carbon, nor oxygen could be measured by this method because of (a) contamination from the graphite used to bind the sample and so prevent it becoming charged, and (b) the unavoidable presence of oxygen in the system. Similarly, atomic absorption analysis was incapable of measuring carbon and oxygen concentrations because of the nitrous oxide plus acetylene flame used to vapourize the samples, and the minimum detectable silicon concentration was over 200 p.p.m. The two crystals reported above therefore remain the only ones analysed for silicon and no crystals were measured after they had been heated in zinc. A further possibility is that some of the indium present in the boule was interstitial and that irrespective of whether the centres were charged or neutral, the resultant scattering may have been more than that from an equivalent number of substitutional ions.

A second indium doped boule, number 152, grown in the presence of 100 p.p.m. indium, was also studied. Atomic absorption analysis showed that all the indium had entered the boule but it was found to have a low conductivity of 3×10^{-4} ohm.$^{-1}$cm.$^{-1}$ at room temperature which fell to approximately 7×10^{-6} at 170°K and hence restricted measurements to within a limited temperature range. The room temperature value of the carrier density was 4×10^{14} cm.$^{-3}$ when corrected for the scattering factor, considerably less than that of the previous sample despite the higher indium content. The carrier density fell off rapidly with temperature as shown in figure 7.6. Since the saturation carrier density $N_D - N_A$ could not be obtained, that is all the donor levels could not be emptied, an approximate value for the donor ionisation energy was obtained by assuming the slope of the curve $\log n \propto \frac{1}{T}$ to be equal to $\frac{E_d}{k} \times 2{\cdot}303$. The value obtained was 0·2 eV. Although there may be considerable error in this value, it is obviously different from that obtained from measurements on boule 139. Attempts were made to calculate values for N_D and N_A using equation 2.15, but a slight variation in E_d produced a large variation in these parameters and no reliable figures could be obtained. A value could therefore not be obtained for the theoretical mobility associated with ionized impurity scattering. However, the experimentally observed values were extremely low, falling from 30 cm.^{2}/v.sec. at 360°K to less than 20 cm.^{2}/v.sec. at just below room temperature. This variation is again characteristic of ionized impurity scattering although the value of 30 cm.^{2}/v.sec. is much too low to be explained using the Brooks-Herring equation. Even 100 p.p.m. of active indium, that is 10^{18} cm.$^{-3}$, almost completely compensated by 9×10^{17} cm.$^{-3}$ acceptors would only result in a mobility of 700 cm.^{2}/v.sec. at room temperature, which is considerably greater than that observed. It therefore seems as if there is another major scattering process present or that the Brooks-Herring formula ceases to work under these conditions

of high doping levels and high temperatures. A similar calculation using the Conwell-Weisskopf formula gives a value of around 1100 $cm.^2/v.sec.$

From the results of the carrier density measurements on crystals 139 and 152 it appears that indium can form two donor levels, a shallow one at 0·021 eV, and a much deeper one at approximately 0·2 eV. In the case of the heavily doped crystal a large number of compensating acceptor levels could have been introduced with the indium thus emptying the shallow levels and allowing only the deeper level to play any part in the electrical properties. Thermal excitation of electrons from the deeper level in crystal 139 would be negligible in comparison with the number of free electrons excited from the shallow level and hence the influence of the deeper level would not be expected to be seen. The deeper level, approximately 0·2 eV below the conduction band could either be associated with some form of indium complex, perhaps involving a native defect, or it could correspond to the ionization energy of a second electron from the indium which could act as a double donor. The very low mobility cannot be explained by ionized impurity scattering theories and there must either be a high density of neutral impurities present or the scattering theories must break down under these conditions.

(c) Treatment in Zinc

Indium doped boules were also investigated after being heated in molten zinc. This had a profound effect on the physical appearance as well as the electrical properties. The crystals which were originally a transparent brown in colour became either darkened, in the case of boule 139, or completely blackened in the case of crystals containing larger quantities of indium. A Hall sample after such treatment is shown in figure 7.8. This can be compared with the as grown sample shown in figure 4.5. When slices of the blackened sample were studied using a transmission optical microscope dark precipitates could be seen. These were assumed

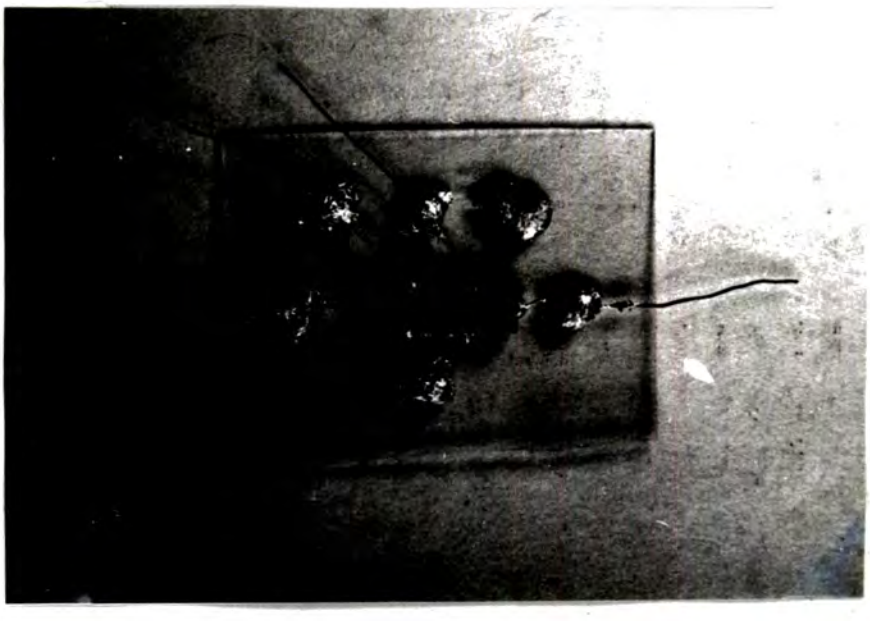

Fig. 7-8. ZnSe:In(Zn) Hall Effect Sample showing Black Precipitate produced after heating in Zn. (×2)

to be indium metal and this precipitation of the dopant as a second phase was in agreement with the results reported previously during the luminescence studies. This behaviour is also similar to that seen when crystals of zinc selenide grown from indium and gallium solution were treated in molten zinc, although no details of the precipitates themselves were given (Wagner and Lorenz 1966). More will be said about the nature of the precipitates in the next section.

The electrical properties of crystal 139 after it had been heated in zinc were found to be very similar to those of the undoped crystals heated in zinc as is shown in figure 7.1 and figure 7.2. The conductivity was increased by a factor of two due to an increase in both mobility and carrier density and the slopes of the curves shown in figure 7.2 seem to suggest that the donor level involved is the same as that present in the undoped zinc treated crystals, that is the level with an ionization energy of 0·012 eV. It thus appears that, as in the luminescence measurements, the effects of the indium are completely removed due to the precipitation. A sample doped with 100 p.p.m. indium, number 150, was also heated in zinc. A plot of log n v $\frac{1}{T}$ was again found to be similar to that of crystal 139 heated in zinc with a room temperature carrier density of 10^{17} $cm.^{-3}$ although the maximum mobility was only 820 $cm.^2$/v.sec. A possible explanation for this lower mobility is a combination of optical phonon and ionized impurity scattering as before, plus some effect from the indium precipitate.

It therefore seems that although the carrier density of indium doped samples is increased by heating in zinc, this is solely a result of the precipitation of the indium as a second phase and the introduction of the shallow 0·012 eV donor level as seen in undoped material. The mobility increase is probably due to a combination of the removal of neutral impurities and ionized impurities consisting of indium donors and compensating acceptors, although the indium precipitate when dense did seem to cause some scattering.

7.4 GALLIUM DOPED MATERIAL

(a) Doping during growth

Two gallium doped boules were investigated, number 140 containing 1000 p.p.m. gallium and 188 containing 100 p.p.m. Room temperature conductivities were approximately 5×10^{-3} ohm.$^{-1}$cm.$^{-1}$ falling to around 2×10^{-5} ohm.$^{-1}$cm.$^{-1}$ at 150°K. This again restricted measurements to a narrow temperature range. These low values of conductivity agree with the report by Wagner and Lorenz (1966) that zinc selenide containing 5×10^{19} cm.$^{-3}$ gallium atoms had a resistivity of 300 ohm.cm. at room temperature and led to their conclusion that the material was highly compensated.

The variation of carrier density with temperature is shown in figure 7.9 Since once again the carrier density did not saturate at high temperatures and hence a value of $N_D - N_A$ could not be obtained, an estimate of the donor ionization energy was obtained from the slope of the curves in figure 7.9. Values for the donor ionization energy of samples 3 and 4 of boule 140 and a sample from boule 188 were 0·13 eV, 0·065 eV and 0·07 eV respectively. As for the indium doped samples, the crystal containing the least amount of impurity, that is 188, possessed the highest carrier density which was 4×10^{15} cm.$^{-3}$ at room temperature when a scattering factor of 2 was assumed. This is probably the result of lower compensation in the more lightly doped sample. The mobilities of all the samples were very low and fell very rapidly with decreasing temperature (figure 7.10). The room temperature values were all below 100 cm.^{2}/v.sec. and that of sample 4 fell to below 2 cm.^{2}/v.sec. at 150°K. Once again this temperature dependence, approximately a T^4 variation, and the very low values of the mobility cannot be explained simply on a basis of ionized impurity scattering unless the formulae are incorrect and some other scattering process such as neutral impurity scattering must be present. The mobility

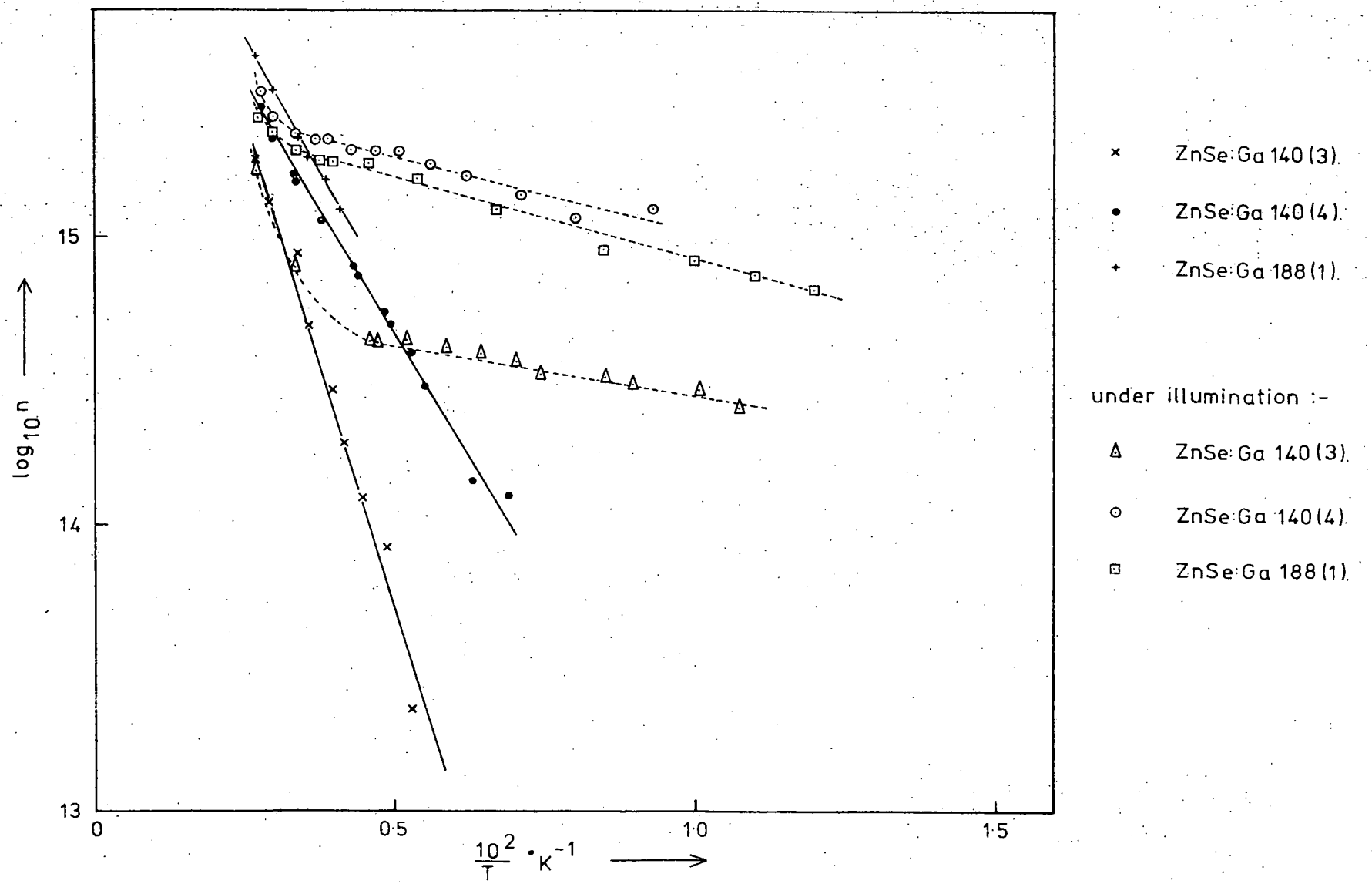

Fig. 7-9. Temperature Variation of Carrier Density n in three ZnSe:Ga Samples.(corrected for r).

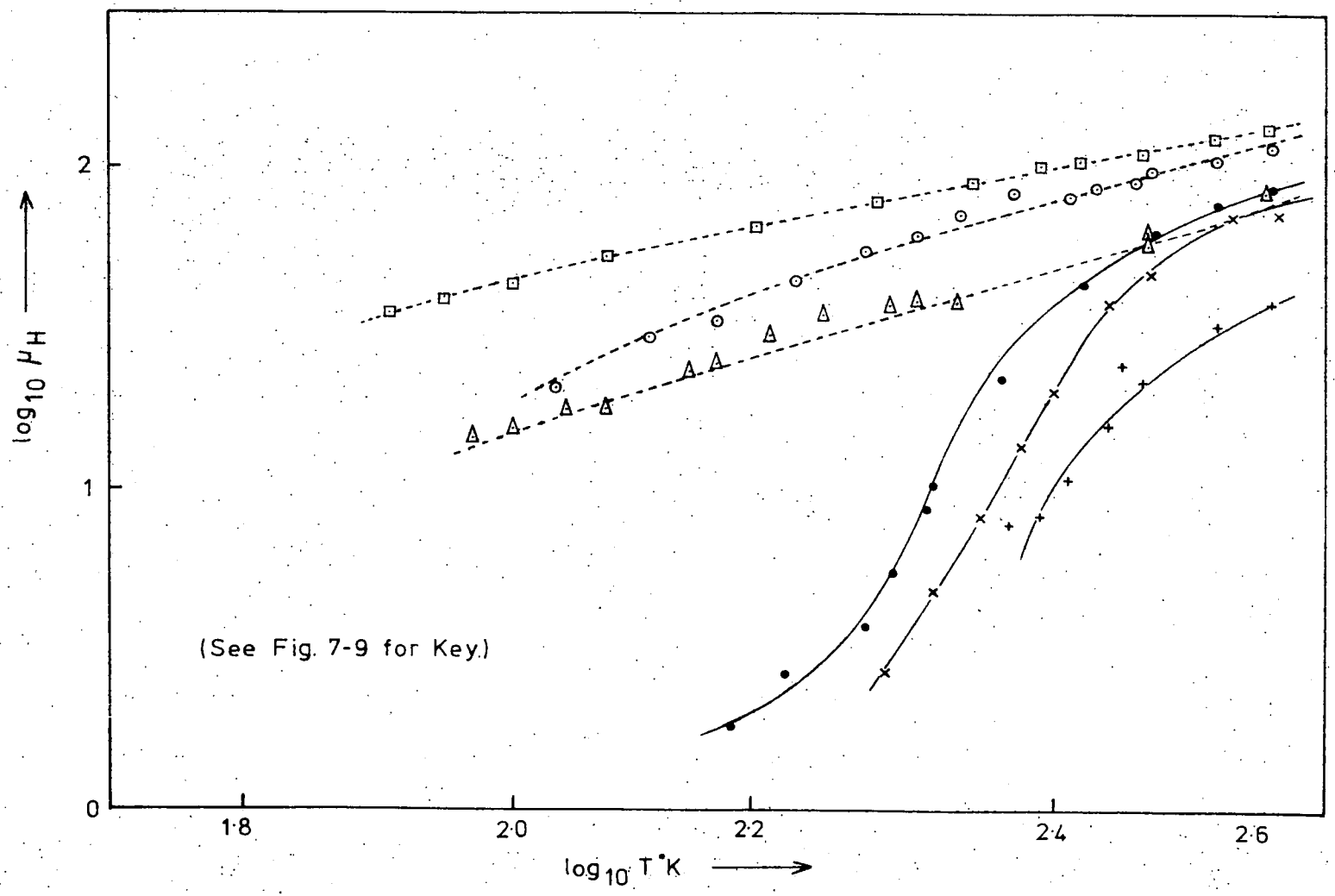

Fig. 7-10. Temperature Variation of Hall Mobility μ_H in three ZnSe:Ga Samples.

Fig. 7-11. Transmission Photomicrograph of ZnSe:In 139 heated in Zn. (×350)

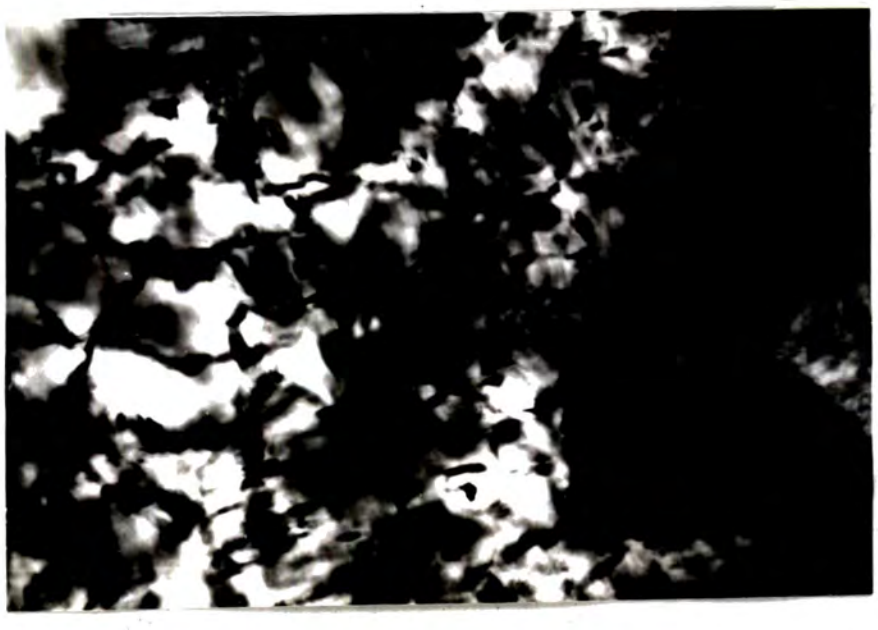

Fig. 7-12. Transmission Photomicrograph of ZnSe:In 152 heated in Zn. (×350)

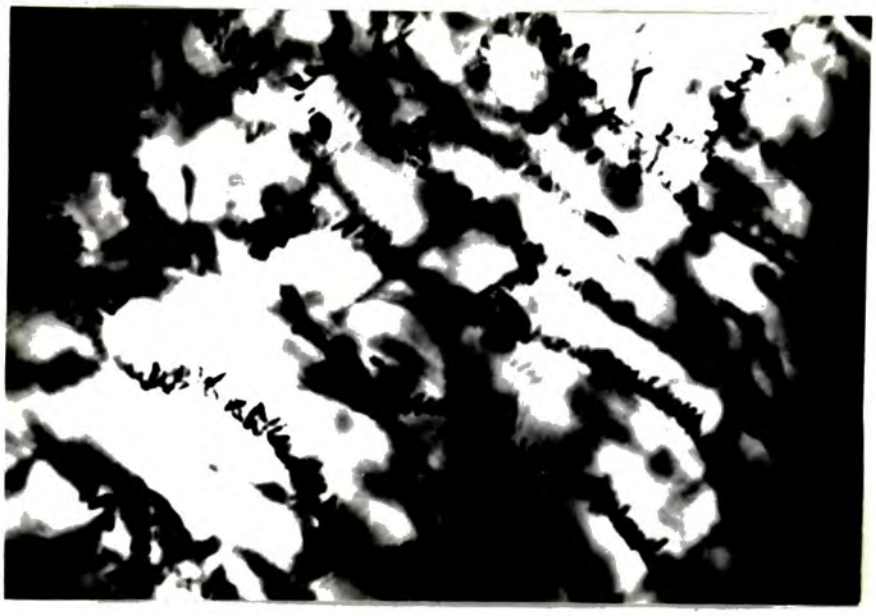

Fig. 7-13. (×350)

Fig. 7-14. (×1600)

Spiral Precipitates seen in ZnSe:In 152 after heating in Zn.

Fig.7-15. (×350)

Fig.7-16. (×1600)

Triangular Precipitates seen in ZnSe: In 150 after heating in Zn.

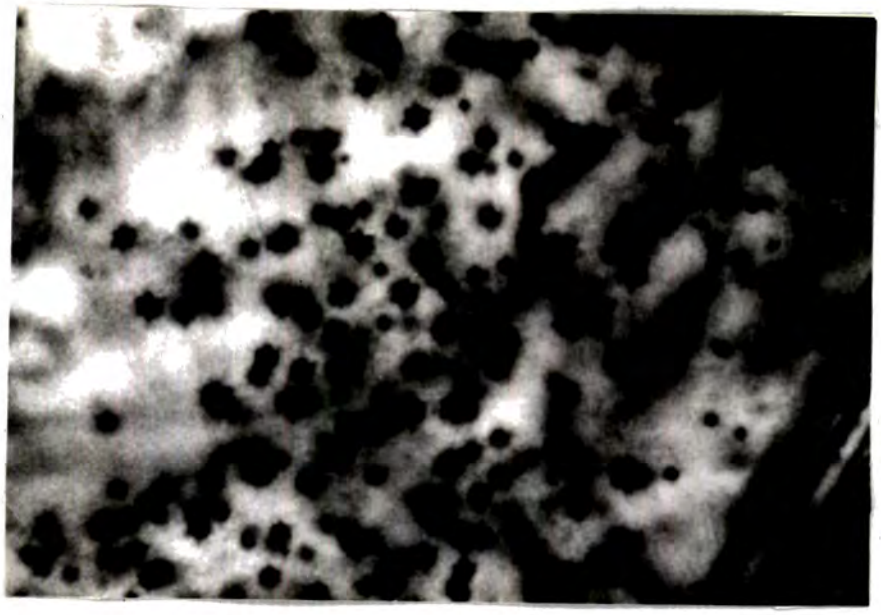

Fig. 7-17. (×350)

Fig 7-18 (×1600)

Star Shaped Precipitates seen in ZnSe:In 142 after heating in Zn.

The most likely reason for the precipitation of the metal would be to maintain charge neutrality when acceptor impurities were leached out into the zinc. Alternatively the zinc may simply have displaced the group III atoms from the zinc sites, although this seems less likely, since the zinc would need to diffuse completely into the crystal, removing zinc vacancies as well as displacing the indium or gallium, and this would not seem to agree with the conclusion from the luminescence studies that the S.A. emission is associated with zinc vacancies. Further work, especially on single crystals aligned in known directions is necessary to understand the reasons behind the various precipitate shapes.

7.5 ALUMINIUM DOPED MATERIAL

As grown aluminium doped zinc selenide was found, in general, to have a very low conductivity, of the order of 10^{-10} ohm.$^{-1}$cm.$^{-1}$ which prevented any transport measurements being made. Even the higher conductivity material which was used for luminescent measurements, of which only small samples were available, had a dark conductivity of 2×10^{-6} ohm.$^{-1}$cm.$^{-1}$ at room temperature and was unsuitable. A sample of boule 153 which was grown in the presence of 1000 p.p.m. aluminium plus 100 p.p.m. manganese selenide was studied after it had been heated in molten zinc in order to reduce its resistivity. The manganese selenide can be considered to have had no effect on the properties of the boule (see Chapter 6). The room temperature conductivity was increased to 1·2 ohm.$^{-1}$cm.$^{-1}$ after the treatment but the properties appeared to be dominated by the shallow donor level approximately 0·012 eV below the conduction band, as in the case of the indium and gallium doped samples (figure 7.2). Since no precipitate was visible it seems probable that the aluminium was leached out of the sample into solution in the zinc.

An aluminium doped sample was prepared, however, by heating a piece of boule 171 for a week at 850°C in a melt of zinc plus 10% mole aluminium.

This treatment was carried out in the same tube as the sample used for the luminescence measurements. This aluminium doped sample was found to have a conductivity of 2·7 $ohm.^{-1}cm.^{-1}$ at room temperature which fell to approximately 0·4 $ohm.^{-1}cm.^{-1}$ at 70°K. This high conductivity was mainly the result of a high carrier density of 1·2 x 10^{18} $cm.^{-3}$. This value was obtained by assuming that ionized impurity scattering was dominant and that the scattering factor was equal to 2. The temperature variation of the carrier density was very interesting, since it remained constant down to at least 70°K (figure 7.19). This would suggest a value of zero for the donor ionization energy. This behaviour is typical of crystals with a very high concentration of carriers. The value of carrier density above which zinc selenide can be considered degenerate is approximately 10^{18} $cm.^{-3}$. At this concentration the energy level produced by the donor impurity can be considered to have broadened into a band due to the overlap of the wave functions of the donor electrons and have in fact merged with the conduction band. This behaviour is known as metallic impurity band conduction (Mott and Twose 1961), and is not the same process as that which was observed at very low temperatures in the undoped zinc selenide (section 7.3a). In this process charge transport occurs by normal conduction methods within the impurity band not a hopping mechanism. The mobility of the samples was again fairly low and fell from a value of about 30 $cm.^2/v.sec.$ to 4 $cm.^2/v.sec.$ at about 70°K (figure 7.20). A mobility of 30 $cm.^2/v.sec.$ at room temperature would be produced, according to the Brooks-Herring equation, by a density of 5 x 10^{19} $cm.^{-3}$ donor centres almost completely compensated by 4·8 x 10^{19} acceptor centres. This concentration of impurities, about 5000 p.p.m., is not excessive considering the high concentration of aluminium in which the crystal was heated and the degenerate behaviour observed. Values could not be calculated at low temperatures because of the breakdown of the Brooks-Herring equation although the experimentally observed mobility varied approximately as

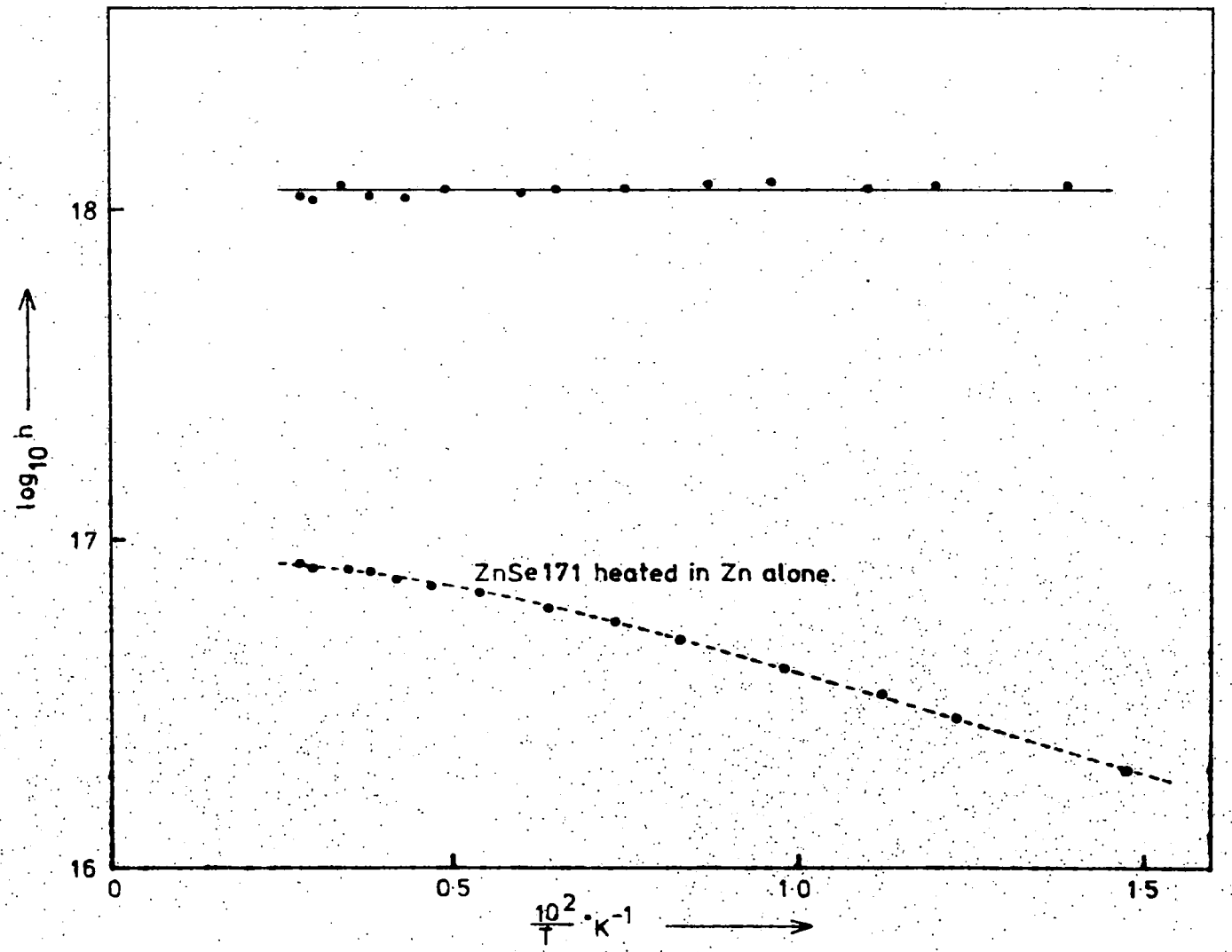

Fig. 7-19. Temperature Variation of Carrier Density n. in ZnSe 171 heated in Zn+10%Al. (corrected for r)

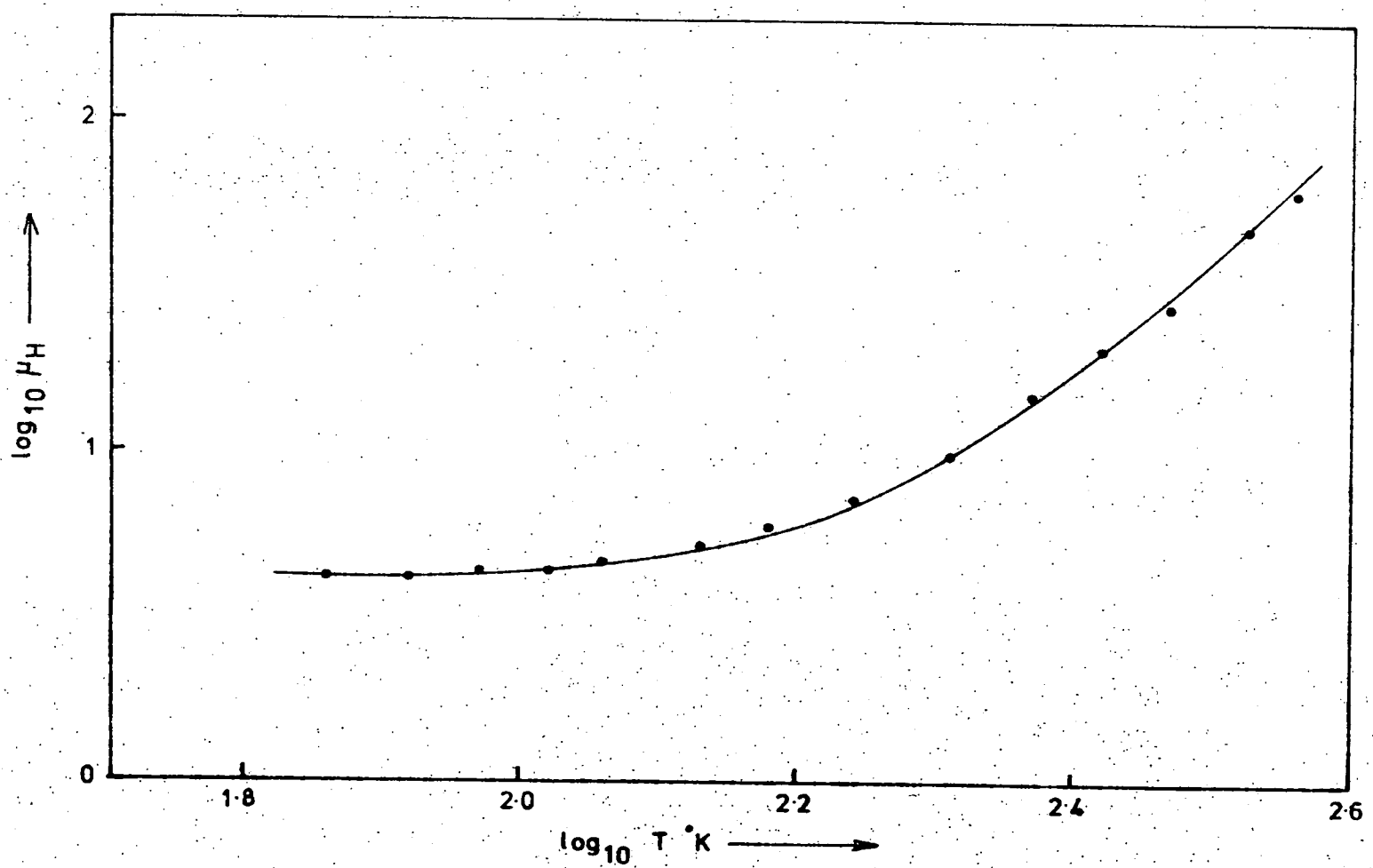

Fig. 7-20. Temperature Variation of Hall Mobility μ_H in ZnSe 171 heated in Zn+10% Al.

a $T^{3/2}$ power as would be expected if ionized impurity scattering were dominant. The behaviour of this aluminium doped crystal is the same as that seen by Aven and Segall (1963) who also found the carrier density to be independent of temperature although the mobility they reported was that of a much more lightly doped sample containing only 10^{16} $cm.^{-3}$ carriers and was very similar to that of undoped zinc treated material with a maximum of 700 $cm.^2/v.sec.$ at 100°K.

7.6 CHLORINE DOPED MATERIAL

Boule 123, which appeared from luminescence measurements to contain very little chlorine, was the only chlorine doped crystal studied, as it was available in large enough pieces for Hall samples and was of fairly low resistance. Two samples from the boule were studied. At room temperature the conductivity of sample 2 was found to be 3×10^{-4} $ohm.^{-1}cm.^{-1}$ and this fell to 10^{-5} $ohm.^{-1}cm.^{-1}$ when cooled to around 190°K. The room temperature carrier density was approximately 10^{14} $cm.^{-3}$ and from figure 7.21 a value of 0·33 eV was obtained for the donor ionization energy. No corrections have been made for the scattering factor r, since the scattering processes are not clear. The behaviour of the sample was strange since below 250°K the carrier density appeared to rise. This behaviour also occurred when the crystal was measured under illumination. The carrier density was over an order of magnitude higher but again began to rise on cooling below 250°K and saturated at approximately 2×10^{14} $cm.^{-3}$ at lower temperatures. The resistivity of sample 3 in the dark was several orders of magnitude higher than that of sample 2 and hence measurements were only possible under illumination. However, the carrier density behaved identically to that of sample 2 upon cooling, reaching a minimum at about the same temperature and remaining constant at about 2×10^{14} $cm.^{-3}$ at low temperatures (figure 7.21). This would tend to suggest that the behaviour is a function of the chlorine impurity and not some form of contact behaviour, for example. The mobility variation in sample 2 (figure 7.22)

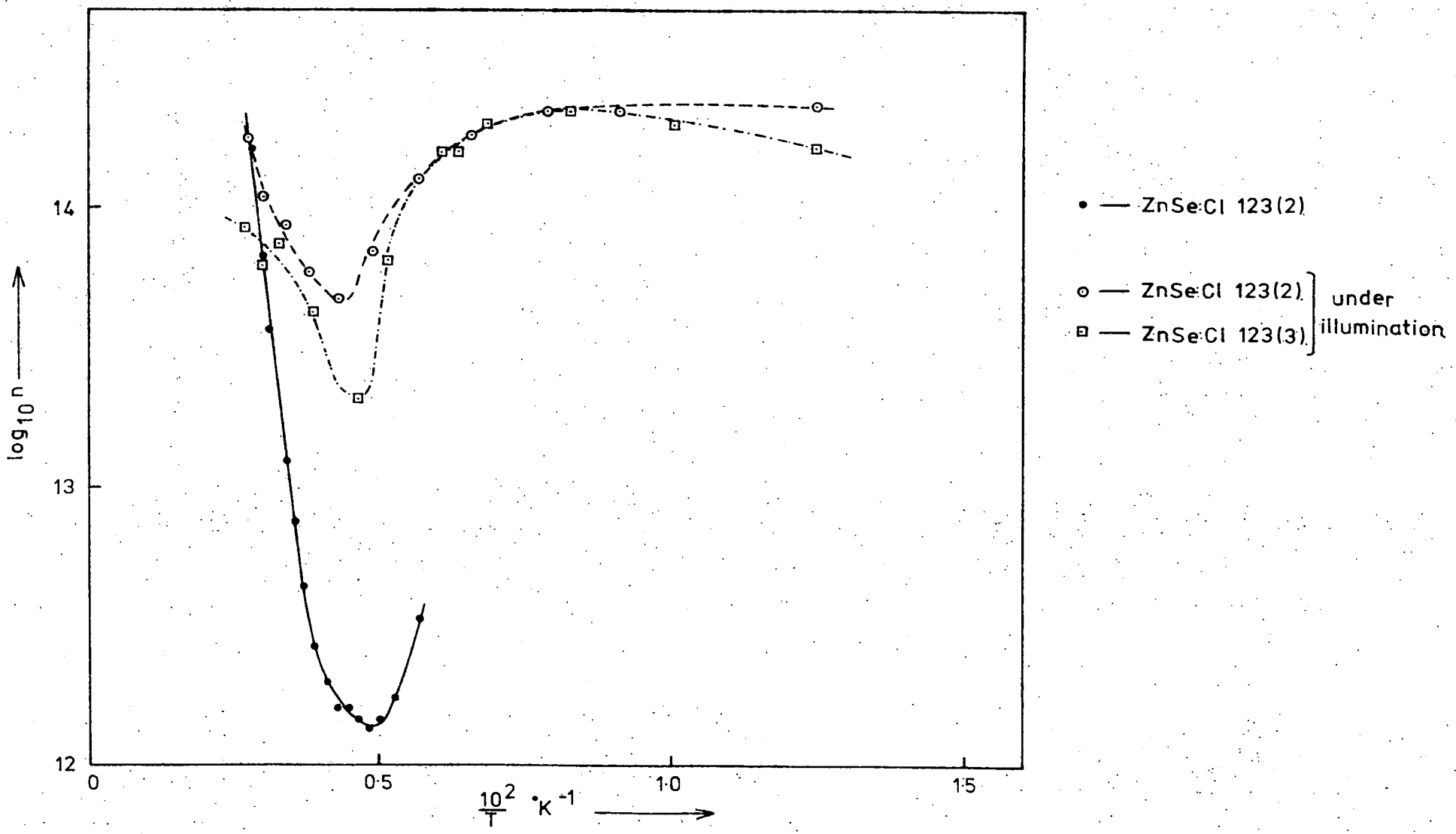

Fig. 7-21. Temperature Variation of Carrier Density n in two ZnSe:Cl Samples. (not corrected for r)

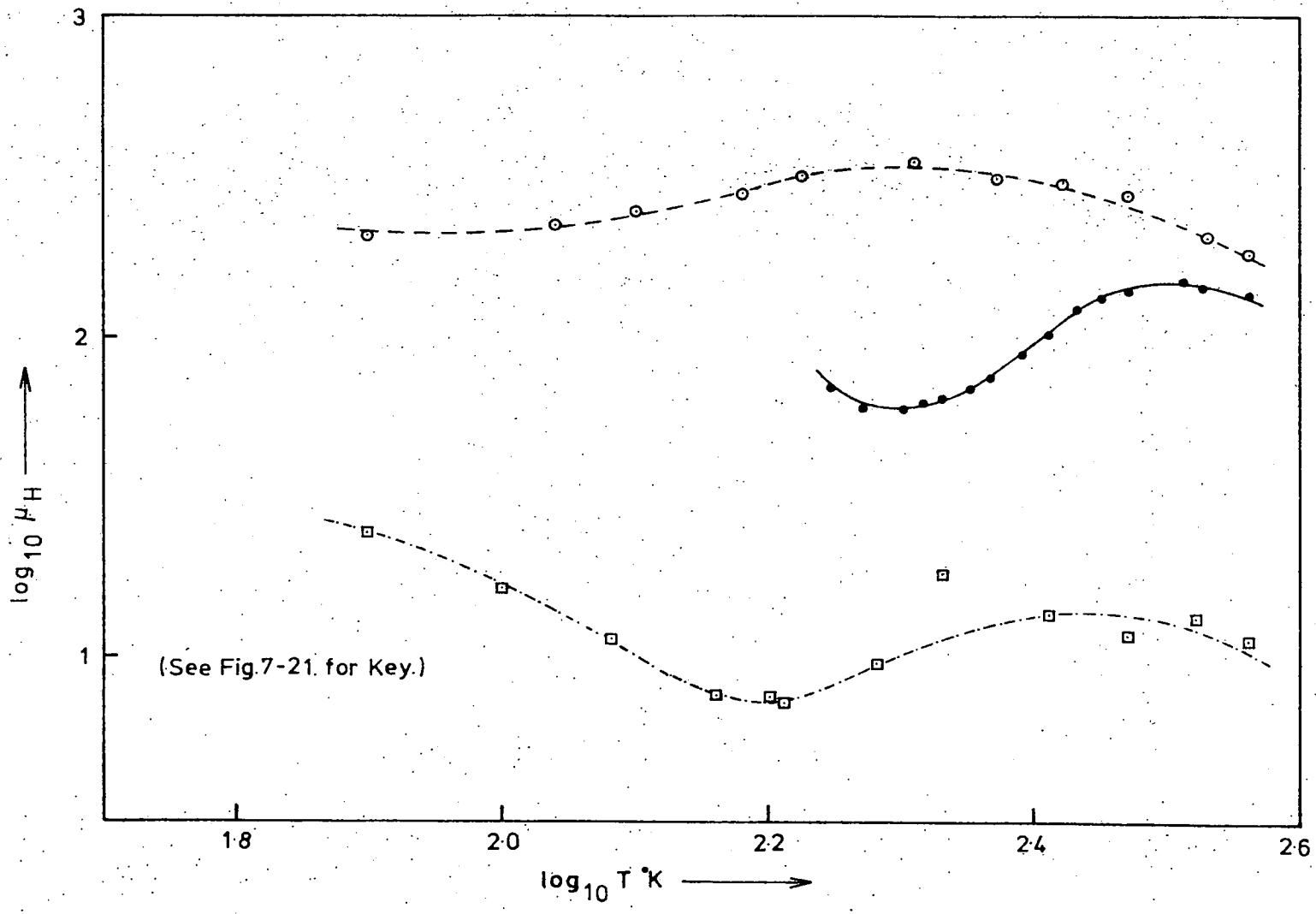

Fig. 7-22. Temperature Variation of Hall Mobility μ_H in two ZnSe:Cl Samples.

is interesting since μ falls from 150 $cm.^2/v.sec.$ at room temperature to 60 $cm.^2/v.sec.$ at about 200°K, but then begins to rise again as the temperature is reduced below 250°K. Under illumination the mobility of sample 2 rose to a maximum of 350 $cm.^2/v.sec.$ at about 200°K and then appeared to approach a constant value of about 200 $cm.^2/v.sec.$ on cooling further. The mobility of sample 3 under illumination was approximately an order of magnitude lower (figure 7.22). When cooled below room temperature the mobility fell gradually, but below approximately 160°K it rose from about 8 $cm.^2/v.sec.$ to 25 $cm.^2/v.sec.$ The behaviour of the carrier density and mobility suggests that some other conduction process may occur below approximately 200°K. This may be related in some way to the high density of compensated donors present, although the actual reason is unclear. Once again there is no clear reason for the low mobility of sample 3, since it is too low to be accounted for by ionized impurity scattering and mechanisms similar to those seen in the gallium and indium doped crystals must be present.

When a sample of boule 123 was studied after it had been heated in zinc, the results were once again unclear. The carrier density at room temperature was 3×10^{17} $cm.^{-3}$ and this appeared to decrease upon cooling as if the same shallow donor level encountered in all previous zinc treated samples was once again present (figure 7.2). It was shown in Chapter 5 that chlorine is not removed from a crystal subjected to a zinc extraction and hence the level 0·33 eV below the conduction band must still have been present. However, the number of electrons ionized from this level would be negligible in comparison with those from the shallow level and hence only the shallow level would appear to have any effect. The mobility of the sample was extremely low, in the region of 2 to 3 $cm.^2/v.sec.$ and remained constant down to 85°K. This behaviour once again cannot be explained although the high density of donor centres may be relevant.

7.7 SUMMARY

(a) The crystals heated in molten zinc had properties similar to those of crystals studied by the majority of previous workers (see Chapter 2). That is, the mobility was limited by optical phonon interaction at temperatures greater than about 100°K, leading to a room temperature value of 400 $cm^2/v.sec$. Below 100°K ionized impurity scattering caused the mobility to decrease. The mobility in this temperature region has received very little attention from other workers and no satisfactory explanations have been given. The mobility below 100°K varies much more rapidly than $T^{3/2}$ which would be expected if ionized impurity scattering were active over the whole range, although the Brooks-Herring equation predicts the mobility down to about 40°K. Below this temperature the mobility falls exponentially and is limited by a hopping process associated with a non-metallic impurity band type of conduction.

A value of 0·012 eV was obtained for the ionization energy of the donor level involved. Although this is less than the depth of a hydrogenic donor (approx. 0·03 eV) it is similar to previously reported values even though most workers do not take into account the scattering factor. A degree of impurity banding is almost certainly responsible for the small value of the donor energy and in fact the isolated level would appear to be simple hydrogen-like. In the discussion of luminescence it appeared that the S.A. emission was associated with donor impurities remaining after the zinc extraction and forming deep donor levels approximately 0·3 eV below the conduction band, perhaps associated with a complex centre. Two levels are therefore involved, and the shallow level revealed by measurements of the Hall coefficient could be the hydrogenic level of the same unremoved impurity. This would agree with the results of Smith (1969) concerning low resistance crystals treated in zinc. The chlorine might also be acting as a double donor with two electrons capable of being ionized.

The shallow level would again be hydrogen-like whilst the deeper level would correspond to ionization of the second electron. Present samples were found to be highly compensated with average values of 10^{17} cm.$^{-3}$ and 8×10^{16} cm.$^{-3}$ for the donor and acceptor concentrations. This high degree of compensation led to fairly low maximum mobilities in the region of 2000 cm.^{2}/v.sec. Crystals containing indium or gallium, after being heated in zinc, behaved identically to undoped, zinc treated crystals as regards the magnitudes of the donor energies and mobilities. The metal dopant was apparently completely precipitated and tended to decorate what were probably crystalline imperfections. The electrical properties thus appeared to be controlled by the same donor level as in the nominally undoped crystals.

(b) Before they were heated in zinc, the crystals containing indium or gallium possessed very low mobilities, sometimes as low as 20 cm.^{2}/v.sec. This behaviour is very difficult to explain on the basis of ionized impurity scattering as described by the Brooks-Herring equation and this equation may not be valid at the high impurity concentrations and high temperatures involved. Alternatively some other scattering process, perhaps due to neutral impurities leached out in the zinc treatment, may be present.

There appeared to be donor levels in two distinct regions. The two lightly indium doped samples gave values of 0·021 eV for the donor depth whereas the more heavily doped samples gave values ranging from 0·065 eV to 0·13 eV for gallium impurities and 0·2 eV for indium. The effect of light on the gallium doped samples was to increase both the mobility and carrier density considerably, and this behaviour was very similar to that reported by Lorenz et al (1963) and Woodbury and Aven (1964). They found that chlorine doping tended to favour the production of the deeper of two levels and explained a level 0·1 eV below the conduction band on a

basis of a doubly negatively charged level of a native acceptor together with a chlorine ion, known as a V_X centre. The deeper level found in the indium and gallium doped samples may well have been analogous to this level although a double donor model for the indium and gallium would also explain the two levels. The centre responsible for the 0·021 level may have been the hydrogenic level associated with substitutional indium in addition to the level associated with the residual impurities as in the undoped zinc selenide. It seems likely that the two levels were present in both the indium doped boules but that the additional indium led to the production of extra compensating acceptor centres which then emptied the shallow donor levels.

(c) Aluminium was the only group III element which could be introduced from a zinc melt. This was fortunate since as-grown aluminium doped samples had very high resistivities and were unsuitable for transport measurements. The crystal doped from a zinc solution was found to be degenerate with a carrier density of $1{\cdot}2 \times 10^{18}$ cm.$^{-3}$ and a mobility of 30 cm.^{2}/v.sec. at room temperature. The degeneracy was probably the result of considerable impurity banding of the hydrogenic level. The mobility appeared to be limited by ionized impurity scattering and fell to a value of 4 cm.^{2}/v.sec. at 80°K. These results are similar to those of Aven and Segall (1963) although they gave no mobility values for their highly doped sample.

(d) The behaviour of chlorine doped zinc selenide was very unusual and cannot be satisfactorily explained. From approximately 400°K down to 250°K the carriers appeared to be excited from a donor level about 0·3 eV below the conduction band. This is of the same order as the depth of the bromine level below the conduction band reported by Bube and Lind (1958) from the temperature variation of the dark conductivity, and probably corresponds to the level involved in the S.A. emission and discussed in section 7.7a. The mobility was once again fairly low with an average

value of 150 $cm.^2/v.sec.$ in this temperature range. Below 250°K the behaviour altered completely and the reason for the increase in mobility and carrier density with decreasing temperature is unknown. Although some form of thermal quenching may have been responsible for the variation observed under illumination, this would not account for the behaviour in the dark.

The electrical properties of chlorine doped zinc selenide heated in zinc were also dominated by a shallow donor level similar to that at 0·012 eV in the other zinc treated crystals. However the carrier density was considerably higher with a room temperature value of 3×10^{17} $cm.^{-3}$. The shallow level is probably the hydrogenic donor level associated with chlorine which, as the luminescence studies show, might well be the impurity present in undoped material after zinc extractions. This would imply that chlorine is responsible for the S.A. emission as well as the low resistivity which results from the zinc treatment. The value of donor ionization energy differs from that found by Aven and Segall (1963) who obtained a value of 0·19 eV in similar material, but agrees with measurements by Lorenz et al (1963) and Woodbury and Aven (1964). The material studied by Aven and Segall might well have been more highly compensated, with the shallow donor level substantially empty. However, the value of the mobility obtained from the present work was extremely low and is difficult to explain, although it may have been associated with the high carrier density, which almost certainly produced considerable impurity banding.

CHAPTER 8

CONCLUSIONS

8.1 SUMMARY OF RESULTS

The main aim of the research reported in this thesis was to investigate zinc selenide grown in this department with special reference to obtaining a material for use in fabricating electroluminescent diodes.

Various possible ways of introducing manganese were studied and it appeared that the two techniques which allowed manganese to be incorporated in useful amounts were (1) vapour phase transport in the presence of manganese chloride and (2) chemical transport using iodine vapour in the presence of manganese metal. The latter method resulted in the better quality crystals with higher possible manganese concentrations but only small boules could be produced. The vapour phase transport method however, enabled fairly large boules to be grown.

The emission band associated with manganese ions in zinc selenide, although masked by other impurity bands, was unambiguously identified as lying at 5910 Å at room temperature. On cooling to 85°K it shifted to 5870 Å and was reduced in width from 0·20 eV to 0·13 eV. This is much narrower than most other emission bands which were observed. From the halfwidth variation with temperature it was deduced that longitudinal optical phonons were responsible for the main lattice interaction with the manganese ion. The excitation processes were shown to occur within the manganese ion itself since transitions between the $^6A_1$ ground state and the three higher energy levels could be observed in the green region

of the excitation spectrum and thus no resonance transfer, for example, was present.

When manganese doped zinc selenide was heated in molten zinc in order to reduce its resistivity for the production of electroluminescent diodes, the photoluminescence associated with the manganese disappeared. The manganese was not removed from the boule or precipitated as a second phase, and the most plausible explanation seems to be that the high density of free electrons allows Auger de-excitation of the manganese ion in preference to photon emission. However it appears that photon emission still occurs in electroluminescent diodes, since the concentration of electrons near the contact is so low in the depletion region that the Auger process fortunately does not occur (Allen et al 1973).

It is therefore clear that the emission associated with manganese is fairly well understood and good quality zinc selenide containing high concentrations of manganese can now be produced quite easily.

After zinc selenide was heated in zinc, the only emission band which was then visible was the S.A. band. When the group VII elements, chlorine and iodine, were present the emission at 85°K consisted of a broad band at 6150 Å which shifted to 6050 Å on heating to room temperature. The halfwidth of this band at room temperature was 0·40 eV. When the group III element aluminium was present as coactivator the band was found to be displaced to longer wavelengths by approximately 200 Å in a similar manner to the S.A. emission from zinc sulphide. Indium appeared to act in the same way as aluminium. Undoped crystals behaved similarly to material containing group VII atoms, after zinc extraction, and it is reasonable to assume that small quantities of residual impurities of group VII elements, probably chlorine, are responsible for the emission. The presence of residual donor impurities was also suggested by Smith (1969) who attributed the low resistivity of zinc treated material to the presence of donor impurities left in the crystal. A pair recombination model has been assumed

for the S.A. emission, recombination occurring between a donor level in the region of 0·3 eV below the conduction band and a zinc vacancy approximately 0·4 eV above the valence band. The 0·3 eV level may be related to the deeper donor level revealed by Hall effect measurements and may be the result of either a donor complex or the doubly ionized state of the donor atom.

The S.A. emission band was observed in some zinc selenide samples prior to zinc extraction although this treatment did help to enhance the resolution of the band. This was probably because the number of zinc vacancies was increased slightly on removal of the copper impurity. The major factor, however, was the removal of the red emission band which lay at 6400 Å at 85°K and tended to swamp the S.A. band. The long wavelength red band could be produced by heating zinc selenide in melts of zinc plus copper and also by heating in selenium. It was observed in almost every crystal and was excited preferentially by 5300 Å light. The emission was attributed to the presence of substitutional copper which may have been introduced from a variety of sources such as the starting materials or from the silica-ware during growth. Thermal quenching was not apparent until the temperature reached 300°K. In consequence the copper red band tended to dominate the emission spectra of most crystals at and above room temperature when 3650 Å excitation was employed. The luminescence mechanism would seem to be of the Schön-Klasens type although pair recombination can not be ruled out.

It is not possible to offer an explanation for many of the emission bands which lay in the green region of the spectrum, for example those observed in undoped zinc selenide, and it proved difficult to distinguish between those associated with native defects and those caused by impurities.

A major problem encountered when constructing an energy level diagram for a particular luminescent process in this material is the difficulty

in obtaining an accurate value for the energy gap. This is complicated by the fact that the peak in the excitation spectrum corresponding to bandgap excitation is often displaced by contributions from surface effects (Gergely 1963) and this also causes difficulties in distinguishing bandgap transitions from those involving shallow donors. There is also a problem of deciding whether to take the transition energy as corresponding to the maximum of an emission or excitation band or whether to consider the energy of the threshold. In all cases the band maximum was chosen although this may have led to errors especially where the conduction or valence band was involved in transitions.

The most satisfactory means by which low resistivity zinc selenide was produced was to subject undoped material to the zinc extraction process. This resulted in crystals with conductivities in the region of 1 ohm.cm. which is very satisfactory for the production of light emitting diodes. The low resistance results from shallow donors with a level approximately 0·012 eV below the conduction band. In untreated zinc selenide this level would have been present but emptied by compensating acceptors. The zinc treatment simply removes some of the acceptor centres although the material remains fairly well compensated. The 0·012 eV level is probably also associated with residual impurities as suggested by Smith (1969) and is probably a simple hydrogenic donor level. Further support for this assumption is the value of around 0·027 eV obtained optically by Merz et al (1972) for the ionization energies of various substitutional donors such as the halogens and group III elements. The lower energy obtained in present results is probably the result of impurity banding of the donor level.

When zinc selenide was grown with donor impurities added deliberately the conductivity was found to be lower than that of material simply heated in zinc although much higher than that of as-grown undoped crystals. Impurities, especially when introduced in high concentrations encouraged

the introduction of compensating levels, as demonstrated by luminescence studies, and these again compensated the shallow donor levels. Levels in the region of 0.2 eV below the conduction band were found in such material and these may have been associated with the V_X donor complex or the double donor nature of the impurities, and are probably involved in the S.A. emission processes. Although heating crystals in zinc plus aluminium resulted in a higher donor density than heating in zinc alone, in fact the material became degenerate while the mobility was reduced so that the resulting conductivity was almost identical. Attempts to remove compensating centres from indium and gallium doped material by zinc treatments were unsuccessful because of the precipitation of the dopant as a second phase.

The mobility of samples heated in zinc was clearly limited by three processes. At temperatures greater than about 100°K, optical phonon interaction appeared to be dominant. The room temperature mobility was approximately 400 $cm^2/v.sec$. Below 100°K scattering by ionized impurities became more important and the mobility began to fall as the temperature was reduced further. The maximum mobility was within the range 1000 to 2000 $cm^2/v.sec$. Below 50°K the conduction mechanism changed to a hopping process involving compensated donor centres and the mobility began to decrease exponentially with reduction in temperature. Before crystals were heated in zinc their mobilities were very low. No explanation of this result has been found.

8.2 FUTURE WORK

In order to understand the mechanisms involved in the luminescent processes, several additional techniques would be of use. In order to identify definitely pair recombination processes such as the S.A. emission and to clarify the copper red emission, time resolved spectroscopy would be invaluable. A pair recombination process is recognised by a wavelength

shift of the emission band with time after the excitation pulse. If the photoconductive and luminescent excitation spectra of samples were obtained simultaneously this would also help to identify pair recombination and localised transitions. Chopped excitation, such as that used when studying the manganese doped samples, should enable the photoconductive response to be obtained even for reasonably low resistivity material.

Infra-red quenching of the various luminescent emission processes would enable the optical depths of the luminescent centres to be obtained very accurately and at fixed temperatures as opposed to the method of thermal quenching. Thermal quenching is fairly inaccurate, gives the thermal as opposed to optical depth and is an average value over a range of temperatures. The Barr and Stroud monochromator could easily be used for such a purpose if a different prism material, for example sodium chloride, were substituted and interference filters were used to excite and monitor the emission of interest.

Although the manganese emission has been fairly well understood it might be of interest to carry out excitation and emission spectra measurements down to $4^{\circ}K$ in order to resolve the phonon structure. Electron spin resonance measurements perhaps under photoexcitation might also provide further information concerning the ionic transitions.

With the Hall effect measurements, the energies of the deeper levels observed in the doped crystals prior to zinc treatment could be obtained much more accurately if measurements were extended to lower temperatures. This would involve much more sensitive measurement techniques since the resistivity increases considerably at low temperatures and perhaps an A.C. method involving phase sensitive detection would be more suitable. Use of single crystal samples and boules prepared from zinc selenide produced from semiconductor grade elements might lead to a better understanding of some of the phenomena observed.

In all the work carried out on zinc selenide, the results would

undoubtedly be much more readily understood if a sensitive means of analysing the material chemically were available. Although mass spectrographic analysis would be more sensitive than the atomic absorption technique used during part of this work, neutron activation analysis would appear to be the ideal means by which the presence or absence of low impurity concentrations of such as copper and chlorine and their effects could finally be verified. Such an analytical technique would assist the understanding of the properties of zinc selenide much more than all the previous suggestions in this section.

REFERENCES

J.W. Allen, M.D. Ryall and E.M. Wray (1973) To be published

J. Apperson, Y. Vorobiov and G.F.J. Garlick (1967) Brit. J. App. Phys. Vol. 18. P.389

S. Asano, Y. Nakao and K. Omori (1965) J. Phys. Soc. Japan. Vol.20. No.7. P.1120

S. Asano, N. Yamashita and M. Oishi (1968 a) J. Phys. Soc. Japan. Vol. 24. No.6. P.1302

S. Asano, K. Omori and T. Sumimoto (1968 b) Sov. Phys. Sol. State. Vol. 10. No.4. P.891

M. Aven (1962) Ext. Abstracts. Electrochem. Soc. Vol. 11. P.46

M. Aven (1964) Bull. Am. Phys. Soc. Vol. 9. P.248

M. Aven (1971) Phys. Rev. Vol. 42. No.3 P.1204

M. Aven and R.E. Halsted (1965) Phys. Rev. Vol. 137 No.1A. P.228

M. Aven, D.T.F. Marple and B. Segall (1961) J. App. Phys. Vol. 32. No.10. P.2261

M. Aven and B. Segall (1963) Phys. Rev. Vol. 130 No.1 P.81

M. Aven and H.H. Woodbury (1962) App. Phys. Letters. Vol. 1 No.3 P.53

J. Bardeen and W. Shockley (1950) Phys. Rev. Vol. 80 P.72

D. Berlincourt, H. Jaffe and L.R. Shiozawa (1963) Phys. Rev. Vol. 129 P.1009

J.L. Birman (1960) J. Electrochem. Soc. Vol. 107. No.5 P.409

J.L. Birman (1961) Phys. Rev. Vol. 121. No.1 P.144

R. Bowers and N.T. Melamed (1955) Phys. Rev. Vol. 9. No.6 P.1781

S. Braun, H.G. Grimmeiss and J.W. Allen (1973) Phys. Stat. Sol. A. Vol. 14. No.2 P.527

H. Brooks (1955) Advances in Electronics and Electron Phys. Vol. 7. P.156

I. Broser, R. Broser - Warminsky, G. Klipping, R. Rass and H.J. Schulz (1961) J. Phys. Chem. Sols. Vol. 22. P.213

I. Broser and K.H. Franke (1965) J. Phys. Chem. Sols. Vol. 26. P.1013

I. Broser and H.J. Schulz (1961) J. Electrochem. Soc. Vol. 108. P.545

F.J. Bryant and A.F.J. Cox (1965) Brit. J. App. Phys. Vol. 16. P.463

R.H. Bube and E.L. Lind (1958) Phys. Rev. Vol. 110. No.5 P.1040

K.F. Burr and J. Woods (1971) J. Cryst. Growth. Vol. 9. P.183

L. Clark and J. Woods (1968) J. Cryst. Growth. Vol. 3, 4. P.127

E.M. Conwell and V.F. Weisskopf (1950) Phys. Rev. Vol. 77. P.388

R.S. Crandall (1968) Phys. Rev. Vol. 169. P.577

G. and D. Curie (1960) J. Phys. Rad. Vol. 21. P.127

P.J. Dean and J.L. Merz (1969) Phys. Rev. Vol. 178. No.3. P.1310

R.M. Detweiler and B.A. Kulp (1966) Phys. Rev. Vol. 146. No.2 P.513

D.L. Dexter, C.C. Klick and G.A. Russell (1955) Phys. Rev. Vol. 100. No.2. P.603

D.L. Dexter and F. Seitz (1952) Phys. Rev. Vol. 86. No.6. P.964

J. Dieleman, S.H. De Bruin, C.Z. van Doorn and J.H. Haanstra (1964) Philips Res. Reports. Vol. 19. P.311

A. Dreeben (1966) J. Electrochem. Soc. Vol. 113. No.12. P.1275

C. Erginsoy (1950) Phys. Rev. Vol. 79. No.6 P.1013

J. Ewles (1938) Proc. Roy. Soc. A. Vol. 167. P.34

A.G. Fischer (1959) J. Electrochem. Soc. Vol. 106. No.9. P.838

S. Fujiwara and M. Fukai (1966) J. Phys. Soc. Japan. Vol. 21. P.1463

S. Fujiwara and M. Fukai (1967) J. Phys. Soc. Japan. Vol. 23. P.657

S. Fujiwara and M. Fukai (1967) J. Phys. Soc. Japan. Vol. 23. P.669

Y. Fukuda and M. Fukai (1967) J. Phys. Soc. Japan. Vol. 23. P.902

G.Y. Gergely (1963) J. Phys. Chem. Sols. Vol. 24. P.681 and P.687

S. Gezci and J. Woods (1972) J. Mat. Sci. Vol. 7. P.603

O. Goede and E. Gutsche (1966) Phys. Stat. Sol. Vol. 17. P.911

E.F. Gross and L.G. Suslina (1963) Sov. Phys. Sol. State Vol. 4. No.12 P.2689

J.H. Haanstra and J. Dieleman (1965) Ext. Abstracts Electrochem. Soc. Vol. 14. P.2

R.E. Halsted, M. Aven and H.D. Coghill (1965) J. Electrochem. Soc. Vol. 112. P.177

W.A. Harrison (1956) Phys. Rev. Vol. 101. No.3. P.903

J.L. Heaton, E.H. Hammond and R.B. Goldner (1972) App. Phys. Letters. Vol. 20. No.9. P.333

N. Hemmat and M. Weinstein (1967) J. Electrochem. Soc. Vol. 114. P.851

C.H. Henry, R.A. Faulkner and K. Nassau (1969). Phys. Rev. Vol. 183. No.3. P.798

W.C. Holton, M. de Wit and T.L. Estle (1965) Int. Symposium on Luminescence (Karl Theimig K.G., Munich) P.454

J.J. Hopfield, D.G. Thomas and M. Gershenzon (1963) Phys. Rev. Letters. Vol. 10. No.5. P.162

D.J. Howarth and E.H. Sondheimer (1953) Proc. Roy. Soc. Vol. 219. P.53

S. Ibuki, H. Komiya, A. Mitsuishi, A. Manabe and H. Yoshinaga (1967) Proc. Int. Conf. on II - VI Semiconducting Compounds. Providence. R.I. (Benjamin N.Y.). P.1140

S. Iida (1968) J. Phys. Soc. Japan. Vol. 25, No.1. P.177

S. Iida (1969) J. Phys. Soc. Japan. Vol. 26. No.5. P.1140

S. Iida and M. Toyama (1971) J. Phys. Soc. Japan. Vol. 31. No.1. P.190

G. Jones and J. Woods (1973) J. Phys. D. Vol. 6. No.13. P.1640

H.A. Klasens (1953) J. Electrochem. Soc. Vol. 100. No.2. P.72

C.C. Klick (1952) Phys. Rev. Vol. 85. No.1. P.154

C.C. Klick (1953) Phys. Rev. Vol. 89. No.1. P.274

C.C. Klick and J.H. Schulman (1952) J. Opt. Soc. Am. Vol. 42. No.12. P.910

F.A. Kröger (1940) Physica Vol. 7. P.1

F.A. Kröger and J. Dikhoff (1950) Physica Vol. 16. No.3. P.297

F.A. Kröger and J.E. Hellingman (1949) J. Electrochem. Soc. Vol. 95. P.68

F.A. Kröger and H.J. Vink (1954) J. Chem. Phys. Vol. 22. No.2. P.250

B.A. Kulp and R.M. Detweiler (1963) Phys. Rev. Vol. 129. No.6. P.2422

B.A. Kulp and R.H. Kelley (1960) J. App. Phys. Vol. 31. No.6. P.1057

J. Lambe (1955) Phys. Rev. Vol. 98. No.4. P.985

Phys. Rev. Vol. 100. No.6. P.1586

J. Lambe and C.C. Klick (1955) Phys. Rev. Vol. 98. No.5. P.909

D.W. Langer and S. Ibuki (1965) Phys. Rev. Vol. 138. No.3A. P.809

D.W. Langer and H.J. Richter (1966) Phys. Rev. Vol. 146. No.2. P.554

S. Larach (1953) J. Chem. Phys. Vol. 21. P.756

W. Lehmann (1966) J. Electrochem. Soc. Vol. 113. No.5. P.449

W. Lehmann (1967) J. Electrochem. Soc. Vol. 114. No.1. P.83

H.W. Leverenz (1950) An Introduction to Luminescence of Solids. (Wiley N.Y.)

W.Y. Liang and A.D. Yoffe (1967a) Phil. Mag. Vol. 16. P.1153

W.Y. Liang and A.D. Yoffe (1967b) Proc. Roy. Soc. A. Vol. 300. P.326

M.R. Lorenz, M. Aven and H.H. Woodbury (1963) Phys. Rev. Vol. 132. No.1 P.143

G.W. Ludwig and M. Aven (1967) J. App. Phys. Vol. 38. No.13. P.5326

L.Ya. Markovskii, I.A. Mironov and Yu.S. Ryzhkin (1969a) Bull. Acad. Sci. U.S.S.R. Phys. Ser. (U.S.A.) Vol. 33. No.6 P.887

L.Ya. Markovskii, I.A. Mironov and Yu.S. Ryzhkin (1969b) Optics and Spectroscopy Vol. 27. No.1. P.84

L.Ya. Markovskii and R.I. Smirnova (1961) Optics and Spectroscopy Vol. 10. P.98

D.T.F. Marple (1964) J. App. Phys. Vol. 35. No.6. P.1879

D.S. McClure (1963) J. Chem. Phys. Vol. 39. No.11. P.2850

J.L. Merz, H. Kukimoto, K. Nassau and J.W. Shiever (1972) Phys. Rev. B. Vol. 6. No.2. P.545

I.A. Mironov and L.Ya. Markovskii (1965) Sov. Phys. Sol. Stat. Vol. 6. No.8. P.1779

F.F. Morehead (1963) J. Phys. Chem. Sols. Vol. 24. P.37

N.F. Mott (1940) Electronic Processes in Ionic Crystals. N.F. Mott and R.W. Gurney (Oxford Univ. Press) 2nd. Ed. 1957 P.221

N.F. Mott and W.D. Twose (1961) Advances in Phys. Vol. 10. P.107

Y. Nakao (1965) Jap. J. App. Phys. Vol. 4. No.4 P.311

R. Nitsche (1960) J. Phys. Chem. Sols. Vol. 17. P.163

L.E. Orgel (1955) J. Chem. Phys. Vol. 23. No.6. P.1004

Y.S. Park and C.H. Chung (1971) App. Phys. Letters. Vol. 18. No.3. P.99

Y.S. Park and J.R. Schneider (1968) Phys. Rev. Letters. Vol. 21. No.12. P.798

L.S. Pedrotti and D.C. Reynolds (1960) Phys. Rev. Vol. 120. No.5. P.1664

J.S. Prener and D.J. Weil (1959) J. Electrochem. Soc. Vol. 106. P.409

J.S. Prener and F.E. Williams (1956a) J. Electrochem. Soc. Vol. 103. P.342

J.S. Prener and F.E. Williams (1956b) J. Chem. Phys. Vol. 25. No.2. P.361

A. Reinberg, W.C. Holton, M. de Wit and R.K. Watts (1971) Phys. Rev. B. Vol. 3. No.2. P.410

D.C. Reynolds, L.S. Pedrotti and Larson (1961) J. App. Phys. Vol. 32. No.10. P.2250

A.N. Rushby and J. Woods (1970) J. Phys. E. Vol. 3. P.726

A. Sagar, W. Lehmann and J.W. Faust (1968a) J. App. Phys. Vol. 39. No.11. P.5336

A. Sagar, M. Pollak and W. Lehmann (1968b) Phys. Rev. Vol. 174. No.3. P.859

J. Schneider, A. Räuber, N. Dischler, T.L. Estle and W.C. Holton (1965) J. Chem. Phys. Vol. 42. P.1839

M. Schon (1942) Z. Physik. Vol. 119. P.463

F. Seitz (1939) Trans Faraday Soc. Vol. 35. P.74

S. Shionoya, K. Era and Y. Washizawa (1966) J. Phys. Soc. Japan. Vol. 21. P.1624

S. Shionoya, T. Koda, K. Era and H. Fujiwara (1962) Proc. Int. Conf. on Lum. of Organic and Inorganic Materials. New York. (J. Wiley. N.Y.) P.355

S. Shionoya, T. Koda, K. Era and H. Fujiwara (1964) J. Phys. Soc. Japan. Vol. 19. P.1157

F.T.J. Smith (1969) Sol. Stat. Comms. Vol. 7. P.1757

R.A. Smith (1961) Semiconductors (Cambridge Univ. Press) P.118

G.B. Stringfellow and R.H. Bube (1968) Phys. Rev. Vol. 171. No.3. P.903

J. App. Phys. Vol. 39. No.8. P.3657

Y. Tsujimoto, Y. Onodera and M. Fukai (1966) Jap. J. App. Phys. Vol. 5. P.636

F.G. Ullman and J.J. Dropkin (1961) J. Electrochem. Soc. Vol. 108. P.154

C.C. Vlam (1949) Physica Vol. 15. P.609

A. Vecht, N.J. Werring, R. Ellis and P.J.F. Smith (1970) J. Phys. D. Vol. 3. L.65

P. Wagner and M.R. Lorenz (1966) J. Phys. Chem. Sols. Vol. 27. P.1749

G.D. Watkins (1971) Rad. Effects. Vol. 9. P.105

F.E. Williams (1951) J. Chem. Phys. Vol. 19. No.4. P.457

F.E. Williams (1953) J. Phys. Chem. Vol. 57. P.776

H.H. Woodbury and M. Aven (1964) 7th. Int. Conf. Phys. Semicon. (Rad. Damage) Paris. P.179

J.D. Zook (1964) Phys. Rev. Vol. 136. No.3A. P.869